Implications of a changing Arctic on microbial communities

Following the effects of thawing permafrost from land to sea

Oliver Müller

Thesis for the Degree of Philosophiae Doctor (PhD)
University of Bergen, Norway
2018

UNIVERSITY OF BERGEN

Implications of a changing Arctic on microbial communities

Following the effects of thawing permafrost from land to sea

Oliver Müller

Thesis for the Degree of Philosophiae Doctor (PhD)
at the University of Bergen

2018

Date of defence: 14.06.2018

Year: 2018

Title: Implications of a changing Arctic on microbial communities

Name: Oliver Müller

Print: Skipnes Kommunikasjon / University of Bergen

Contents

SCIENTIFIC ENVIRONMENT **5**
ACKNOWLEDGEMENTS **6**
LIST OF ABBREVIATIONS **7**
SUMMARY **8**
LIST OF PUBLICATIONS **11**
1. INTRODUCTION **12**
2. AIMS **17**
3. THE STUDY AREA - THE ROLE OF MICROBES IN THE ARCTIC **18**
3.1 SAMPLING SITES 18
3.2 PERMAFROST: THE FROZEN SOIL 20
Box 1 | Arctic permafrost - Consequences of thawing *21*
Permafrost research site: *22*
3.3 FJORDS: THE INTERPLAY BETWEEN LAND AND OCEAN 23
Box 2 | tDOM - Terrigenous dissolved organic matter *24*
Box 3 | Planktonic food web - The role of bacteria *26*
Fjord systems: *27*
3.4 ARCTIC OCEAN: CHANGING SEASONS AND WATER MASSES 28
Box 4 | Changing seasons - Microbial life in the surface and the deep Arctic Ocean *30*
Arctic Ocean research cruises: *32*
4. RESULTS AND DISCUSSION **33**
4.1 COMMUNITY COMPOSITION PATTERNS IN THE ARCTIC AND ECOSYSTEM FUNCTION 33
4.1.1 Community changes along environmental gradients *34*
4.1.2 Bacteria as sentinels of climate change *42*
4.2 MICROBIAL RESPONSE TO THAW 45
4.2.1 Experimentally induced permafrost thaw *45*
4.2.2 Microbial response to DOM in fjord microcosms *47*
4.3 METHODOLOGICAL CHALLENGES 51
5. CONCLUSION AND FUTURE PERSPECTIVE **53**
REFERENCES **55**
PAPER I - V

Scientific environment

This Ph.D. was carried out at the Faculty of Mathematics and Natural Sciences of the University of Bergen, at the Department of Biological Sciences in the Marine Microbiology group. The work was part of the two projects “Microorganisms in the Arctic: Major drivers of biogeochemical cycles and climate change” (RCN 227062) and “MicroPolar [µP]: Processes and Players in Arctic Marine Pelagic Food Webs” (RCN 225956), funded by the Research Council of Norway, in close collaboration with the project CarbonBridge (RCN 226415). Research in Greenland was additionally supported by the Danish Research Council for Independent Research (DFF 1323–00336).

UNIVERSITY OF BERGEN

Microorganisms in the Arctic
Major drivers of biogeochemical cycles
And climate change

MicroPolar [µP]
Processes and Players in Arctic
Marine Pelagic Food Webs

CENPERM
Center for Permafrost

Acknowledgements

First of all I want to thank my supervisors for this opportunity and all the support I received throughout the entire PhD-time. I was so lucky to be part of not just one, but two amazing research projects and grateful for the many possibilities for travelling and field work in the Arctic. Thank you Lise, for letting me take part in your fantastic permafrost project, helpful guidance in becoming a better scientist and introducing me to all your fascinating colleagues from labs all around the world. To Gunnar, thank you for including me in the MicroPolar project, which showed me all the fun of working in and being part of a large research community and for always finding a solution. To Janet, thank you for the opportunity to visit your inspiring group in the US and all the great collaborations that started from there. And thank you to all the Danish collaborators at CENPERM, where I was always welcomed with open arms and learned a lot.

A big thank you to the entire Marine Microbiology group for many enjoyable moments and making going to work something I was looking forward to (even on weekends). Especially thank you to Evy, Hilde and Hilde and Ela for taking care of everything in the labs. Big thank you to all the amazing colleagues and friends I could share the office with during the last years. Alejandro and Eliana thanks for the relaxed Spanish vibe and Julia thank you for representing wonderfully the young Norwegians. Berna thank you for all your help with getting started, answering my many questions and introducing me to all the fun Norwegian outdoor activities and teaching me how to (successfully) brew beer. Pia thank you for always taking the time to help with anything, for all the fun at work and all the nice beers you brought from your many travels. Bryan thank you for your funny stories, bioinformatics tricks and some very memorable conferences together. And a huge thank you to Maria, without you I would not have ended up here and seen so many beautiful parts of the world. I am really glad that we can work together on so many projects and that you are an important part of my thesis. And thank you to all the very helpful post-docs, Tanya, Selina and Antonio who always had time to talk and discuss. A final thank you to Tommy, for being an excellent PhD-coordinator and many fun football games during the last years.

Finally I want to thank my family and friends in Germany! Vor allem ein riesen großes Dankeschön an meine Eltern Ulrike und Wolfgang, meine Großeltern Ruth und Heinrich und meiner Schwester Katja die alle immer für mich da sind, mich immer unterstützen (selbst hier in Norwegen) und mir geholfen haben meine eigene Wege zu gehen. Til min kjæreste Johanne, takk for å gjøre meg den lykkeligste personen i verden hver dag og at Norge føler som en ekte hjem.

List of Abbreviations

OTU	Operational taxonomic unit (97% sequence similarity)
AL	Active layer
TZ	Transition zone
PL	Permafrost layer
CO_2	Carbon dioxide
CH_4	Methane
SOM	Soil organic matter
---	---
POM	Particulate organic matter
DOM	Dissolved organic matter
tDOM	terrestrial derived DOM
DCM	Deep chlorophyll maximum
YS	Young Sound (Fjord in north-east Greenland)
---	---
SW	Surface Water
AW	Atlantic Water
cAW	cold Atlantic Water
IW	Intermediate Water
ArW	Arctic Water
AOA	Ammonia oxidizing Archaea
NH_4^+	Ammonium

Summary

Climate change has severe impacts in the Arctic, where permafrost is thawing, glaciers are retreating and sea ice is melting. These physical changes are not only affecting large predators like polar bears, but also microscopic organisms such as Bacteria and Archaea. The impacts on microbes are far more concerning, as they are the main drivers of global biogeochemical cycles. Microbial-driven degradation of recently thawed permafrost organic matter is causing the release of critical greenhouse gases, including methane (CH_4) and carbon dioxide (CO_2). Parts of this formerly preserved organic carbon pool is upon thaw transported into marine systems, affecting the structure and dynamics of marine microbial communities. This thesis addresses the extensive implications of thawing permafrost on Arctic microbes. I investigated not only the microbial community composition and processes directly within the soil, but also the indirect effects of permafrost derived carbon run-off on the marine microbial structure, function and activity.

By analyzing the microbial community composition, using high-throughput 16S rRNA gene sequencing, new insights on how microbial communities are structured in permafrost **(Paper I)**, in a run-off affected fjord system **(Paper II)** and the Arctic Ocean **(Paper IV and V)** were revealed. 16S rRNA gene sequencing was also used to elucidate how permafrost derived organic matter affected the community structure and activity of coastal microbial communities **(Paper III)**. Together, these results improve our understanding on how microbial community patterns can be used to explain biochemical processes like carbon degradation **(Paper I, II, III and IV)**. We analyzed shifts in community composition due to climate change processes like permafrost thawing **(Paper I)** and carbon run-off **(Paper III)**, thereby providing insights on which organisms and processes will be sensitive to the changes in a warmer Arctic.

Permafrost is increasingly thawing, which will stimulate microbial activity, and subsequently cause the release of greenhouse gases to the atmosphere. In **Paper I**, we analyzed the microbial community composition every 3 cm along a 2-meter

permafrost core, in order to better understand the connection between the active layer and the permafrost layer. The microbial community in the active layer was diverse and gradually shifting until a distinctive transition zone, where the phylum Bacteroidetes dominated. This short transition zone was followed by a different permafrost layer, which was dominated by a single Actinobacteria family (*Intrasporangiaceae*). We also performed activity measurements along the various layers, where we tested the implications of thaw. These experiments demonstrated a quick change in community composition together with an increase of genes coding for proteins involved in carbon degradation, which was leading to increased CO_2 production.

Terrestrial dissolved organic matter (tDOM), originating from thawing permafrost and melting glaciers, is increasingly entering the Arctic Ocean. Yet, the understanding of which fraction of tDOM is bioavailable and how fjord microbial communities respond to increases in tDOM is limited. In **Paper II** we investigated the DOM bioavailability in a glacial run-off affected high Arctic fjord system over time. Different DOM compounds correlated to community changes and specific indicator species, including various taxa from the order Alteromonadales were identified. The effects of permafrost derived tDOM on an Arctic fjord microbial community was tested experimentally in **Paper III** and we documented significant growth of one specific genus (*Glaciecola*) within the order Alteromonadales, due to this carbon input. This increase of *Glaciecola* was tightly connected with an increase of bacterial grazers, highlighting an important, yet often neglected link in the Arctic microbial food web when predicting the impact of climate change on the carbon cycle.

The dynamics of microbial changes in the Arctic Ocean over a polar year was the focus of **Paper IV and V**. We were especially interested in the seasonal interplay between processes during the light summer and dark winter period, as this is an important driver of community composition that might be disturbed by climate change. The relative abundance of several taxa in the surface waters was found to

vary with season and was associated to phytoplankton dynamics, while communities in deeper waters remained relatively unchanged. With global warming, changing surface phytoplankton growth dynamics will affect associated surface microbial communities. This will inevitably have an impact on microbial groups in the deep ocean, that are dependent on nutrients from above. One of those groups is the Thaumarchaeota, which are recognized as major contributors to marine ammonia oxidation, a crucial step in the biochemical cycling of nitrogen. The remineralization of nitrogen in the deep ocean is an important process to support the life in the surface layers. Thaumarchaeota were abundant in winter surface and deep waters throughout the year, but nearly not detectable in summer surface samples. Besides the seasonal dynamics we identified water mass to be the predominant factor in defining Thaumarchaeota community composition and not solely depth or ammonium concentration as suggested in most studies. Since their abundance is linked to water masses, a freshening of the Arctic Ocean or increased Atlantification, due to climate change, will affect Thaumarchaeota distribution.

The studies included in this thesis underline the importance of microbes as the main drivers of processes that determine the balance of carbon storage and release in the Arctic and contribute to a better understanding of their role in a drastically changing environment. The results highlight the necessity of detailed microbial community analyses in order to understand how different microbes are distributed, how they interact and how they function in a globally important and changing Arctic.

List of publications

The thesis is based on the following five papers, referred to in the text by their Roman numerals and additional data, which is connected to these papers but not published.

Paper I: **Müller O**, Bang-Andreasen T, White III RA, Elberling B, Taş N, Kneafsey T, Jansson JK, Øvreås L (2018). Disentangling the complexity of permafrost soil by using high resolution profiling of microbial community composition, key functions and respiration rates. (*Manuscript under review in Environmental Microbiology*)

Paper II: Paulsen ML, **Müller O**, Larsen A, Møller EF, Sejr MK, Middelboe M, and Stedmon CA (2018). Biological transformation of Arctic dissolved organic matter in a NE Greenland fjord. (*Manuscript under review in Limnology and Oceanography*)

Paper III: **Müller O**, Seuthe L, Bratbak G, Paulsen ML (2018) Bacterial response to permafrost derived organic matter input in an Arctic fjord. (*Manuscript under review in Frontiers in Marine Science*)

Paper IV: Wilson B, **Müller O**, Nordmann E-L, Seuthe L, Bratbak G and Øvreås L (2017). Changes in marine prokaryote composition with season and depth over an Arctic polar year. Front. Mar. Sci. 4:95. doi: 10.3389/fmars.2017.00095

Paper V: **Müller O**, Wilson B, Paulsen ML, Rumińska A, Armo HR, Bratbak G, Øvreås L (2018). Spatiotemporal dynamics of ammonia-oxidizing Thaumarchaeota in distinct Arctic water masses. Front. Microbiol. 9:24. doi: 10.3389/fmicb.2018.00024

1. Introduction

With the increasing melting in the Arctic, the description of this area as the eternal ice seems like a long forgotten tale. At nearly twice the global rate, warming is especially affecting the Arctic ecosystems (Trenberth and Josey, 2007; Screen and Simmonds, 2010; Vincent, 2010). Permafrost, soil that has been consecutively frozen for at least two years, is thawing, which leads to increased greenhouse gas emissions and to increased carbon loads in run-off from land into coastal areas (**Figure 1**). The increased availability of carbon and nutrients changes the dynamics within the planktonic food web, which will inevitably affect processes in the deep Arctic Ocean. Processes on land and in the ocean are both causing increased carbon emissions, which is further heating up the atmosphere (Vonk and Gustafsson, 2013). Microorganisms, involved in various biochemical cycles, form a central part in the processes that are causing this climate change feedback loop. Even though changes in seasons are immense and temperatures are low, microbes developed strategies to thrive under these extreme conditions and are the key players in a hidden, biologically diverse and active environment.

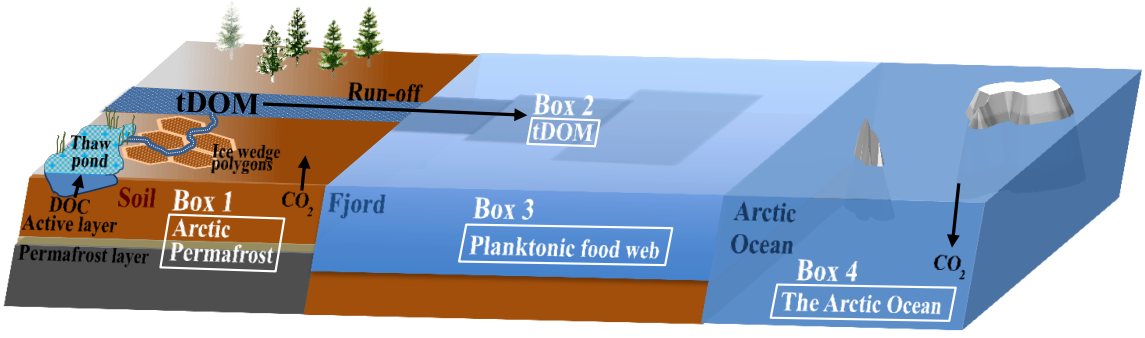

Figure 1: Illustration of an Arctic landscape showing the land-to-ocean carbon fluxes. The four boxes highlight relevant topics covered in this thesis and are each explained in detail in chapter 3. In short, thawing permafrost soil (Box 1) releases tDOM (Box 2) via rivers into the coastal Arctic, where it influences the dynamics in the microbial food web (Box 3), with cascading effects on higher trophic levels, possibly changing microbial dynamics in the entire Arctic Ocean (Box 4).

Microbes are found in high abundances in Arctic soils, fjord systems and the open ocean. This has consequences for the Arctic carbon budget, as organic matter that is currently locked away in the frozen soil becomes increasingly available due to the rising temperatures, and is thereby vulnerable to degradation by microbes. This is especially concerning, considering that permafrost stores 50% of earth`s below ground carbon (Tarnocai *et al.,* 2009).

Significant advances in permafrost microbial ecology research have put the focus on microbes as the main drivers of processes that determine the balance of the terrestrial carbon cycle in the Arctic (**Box 1, p. 21**). Analyzing the microbial community structure and its functions are central in order to understand the processes in thawing permafrost that are contributing to greenhouse gas release (Romanovsky *et al.,* 2010; Mackelprang *et al.,* 2011). Still, much is unknown and several questions remain unanswered. One important question is how the microbial community composition and activity will change with increasing permafrost thaw. With overall increasing CO_2 concentration in the atmosphere, understanding the controls of microbial turnover of permafrost carbon is crucial in predicting the extent of additional greenhouse gas emissions in a warmer future.

Not all permafrost carbon that becomes available after thaw will be directly degraded. A large part of the organic material will, as riverine discharge, be washed out into the Arctic Ocean and potentially influence the marine carbon cycle and ecosystem as illustrated in **Figure 1** (Serreze *et al.,* 2000; Fichot *et al.,* 2013; Feng *et al.,* 2013; Holmes *et al.,*, 2013). This continental run-off introduces vast amounts of freshwater, nutrients and tDOM into the Arctic Ocean (**Box 2, p. 24**). It is estimated that mobilization of tDOM has increased by three to six percent from 1985 to 2004 (Feng *et al.,* 2013) and will continue to increase under current warming climate conditions (Amon *et al.,* 2012). Yearly, about 3,300 km^3 of freshwater stream into the Arctic Ocean and influence stratification, light absorption, surface temperatures, gas exchange, productivity and carbon sequestration (Rachold *et al.,* 2004). Various factors play together and influence how increased tDOM loads will alter the microbial life in Arctic coastal ecosystems. Firstly, the colored fraction of the organic matter has shading effects and thereby affects the productivity of the phytoplankton.

Secondly, to influence growth of heterotrophic bacteria the tDOM has to be available for degradation. The organic matter that enters the Arctic Ocean has been described to be mainly refractory (Opsahl *et al.,* 1999; Dittmar and Kattner, 2003; Xie *et al.,* 2012), while other studies showed that up to 40% can be bioavailable, even on shorter time scales of a few days (Hansell, 2004; Holmes *et al.,* 2008; Vonk *et al.,* 2013; Sipler *et al.,* 2017). This suggests that tDOM derived from Arctic rivers can represent a food source for bacteria and indirectly grazers that feed on bacteria. It has been shown that increased tDOM concentrations caused a shift in the bacterial community composition based on the capabilities of certain species to degrade complex organic matter (Sipler *et al.,* 2017). There is the need to further investigate how this community shift and potential respiration of tDOM might affect higher trophic levels in order to better understand climate change impacts on the marine Arctic ecosystem. A higher bacterial activity due to the degradation of tDOM might cause a higher turnover within the microbial loop, which could cause an increased CO_2 production (**Box 3, p. 26**). Increased carbon availability might also affect the competition between bacteria and phytoplankton for inorganic nutrients and indirectly disadvantage larger phytoplankton (Thingstad *et al.,* 2008; Sipler *et al.,* 2017). If even a small part of the community adapts to the increased carbon run-off and degrades the additional carbon sources, it would have enormous consequences for the entire marine carbon cycle. On a global scale, an increase in bacterial respiration of just 1% would cause a higher CO_2 release than all anthropogenic sources combined (Hedges, 2002).

Not only the Arctic coastal areas are affected by increased fresh water run-off, also the entire Arctic Ocean is expected to become fresher due to this terrestrial run-off in addition to sea ice melting (Dutkiewicz *et al.,* 2005). Together this can lead to increased thermal and haline stratification with reduced deep mixing, which is in turn causing a lower nutrient supply from the deep ocean up to the surface layer (Li *et al.,* 2009). This can have widespread consequences for the marine food web structure and carbon cycling in the Arctic Ocean (**Box 3, p. 26**). Nutrients that are depleted during phytoplankton growth in summer might not be replaced due to decreased upwelling,

which will cause a less productive summer season in the following year that inevitably will affect higher trophic levels (**Box 4, p. 30**). Chemolithotrophic Thaumarchaeota have an important role in the nutrient cycle in the deep ocean. They are a major contributor to marine ammonia oxidation, which is a crucial step in the biogeochemical cycling of nitrogen (Könneke *et al.,* 2005; Wuchter *et al.,* 2006). Thaumarchaeota oxidize ammonium, which is predominantly originating from zooplankton feeding on phytoplankton. This shows how these groups in the Arctic Ocean are connected and highly depend on each other. It is thus necessary to better understand the dynamic connections between surface and deep waters in the Arctic Ocean in order to predict how climate change will affect the marine food web and consequently the marine carbon cycle.

Even though great advances in Arctic research have put the focus on the importance of microbial processes, many uncertainties remain due to logistic sampling difficulties and small study sizes. Necessary investments in travel, equipment and security are enormous and are causing temporal and spatial study limitations. This makes Arctic samples highly unique. However, it also is the reason for two tremendous drawbacks of current Arctic research, replicability and generalization. For example, even though permafrost is known to be highly heterogeneous, measurements of greenhouse gas production from only a few study sites are extrapolated to predict potential emissions from the entire permafrost region. The heterogeneity of permafrost is not only occurring horizontally, but also vertically. Still many studies are based on broad scale sampling, comparing surface with deep samples and knowledge regarding fine-scale shifts throughout the soil core is still scarce. In order to obtain an in depth study of the various layers of the permafrost core, we used an unprecedented high vertical sampling resolution to gain novel insights into the structure and function of permafrost microbial communities. Such information is crucial for understanding how microbial communities are shaped and which mechanisms are important drivers for the activity of the microbes. We further wanted to monitor permafrost greenhouse gas emissions upon thaw and relate these fluxes to microbial activity.

Sampling strategies were also regarded important in our other studies in which different aquatic environments were analyzed, which are as well known to exhibit strong heterogeneity. We thus attempted to improve the understanding of the structure and function of microbial communities in: 1) Arctic waters around Svalbard during a full annual cycle; 2) a high Arctic fjord system in north-east Greenland during the ice-free period and 3) incubation experiments where we investigated the effects of tDOM run-off. The research presented in this PhD thesis highlights the necessity of studies including both community composition analyses and environmental factors, which are based on a high sampling resolution in order to elucidate drivers of changes in the microbial community due the warming in the Arctic.

2. Aims

This PhD project aims to contribute to the understanding of effects of climate change on Arctic microbial life by integrating descriptive field observations with experimental studies of community structures and metabolic processes. I particularly aimed to emphasize the need of studies that are linking terrestrial and marine environments and the microbial processes within.

Thawing permafrost will not only result in the release of large amounts of greenhouse gases, but also set additional complex organic carbon compounds free that might wash out into the fjords and ocean, where, if degraded, it has the potential to change microbial-based food web structures. To highlight the importance of microbial processes in the Arctic and the consequences of climate change on the microbes, the following three main objectives are addressed in my thesis:

1. To describe microbial communities in Arctic permafrost (**Paper I**), coastal waters (**Paper II and III**) and open ocean (**Paper IV and V**) and determine how they may respond to climate change.

2. To investigate to what degree the microbial community composition can provide information about how carbon is processed in the Arctic (**Paper I, II, III and IV**).

3. To assess the effects of terrestrial derived carbon on marine microbial ecosystems and in particular on microbial growth and community composition (**Paper II and III**).

3. The study area - The role of microbes in the Arctic

Extreme seasonality and general low temperatures characterize Arctic environments. These environments foster, despite the harsh conditions, a biologically diverse and active environment. As microbes have evolved to thrive under these conditions, they are important mediators for several biochemical cycles, including carbon and nitrogen cycling and are key players in Arctic terrestrial and marine environments, (**Box 1, Box 3 and Box 4**). The studies presented in this PhD-thesis, in which we have investigated and assessed microbial community composition and their interactions in Arctic environments, represent an important record for the state of the art of the microbial life in these rapidly changing habitats. With this information, we could further test how specific effects of climate warming, such as permafrost thawing or tDOM run-off, will potentially affect these microbial communities, and thereby gain insights about the future of the Arctic ecosystem.

3.1 Sampling sites

For this thesis, samples were taken at different Arctic sites (**Figure 2, A**). Samples originated from various marine and terrestrial sites on and around Svalbard, including five cruises west and north of Svalbard over an entire year (**Figure 2**, **B**), a fjord in north-west Svalbard (**Figure 2**, **C**) and an ice-wedge polygon permafrost site in Adventdalen (**Figure 2**, **D**). Another fjord system was studied in north-eastern Greenland (**Figure 2**, **E**).

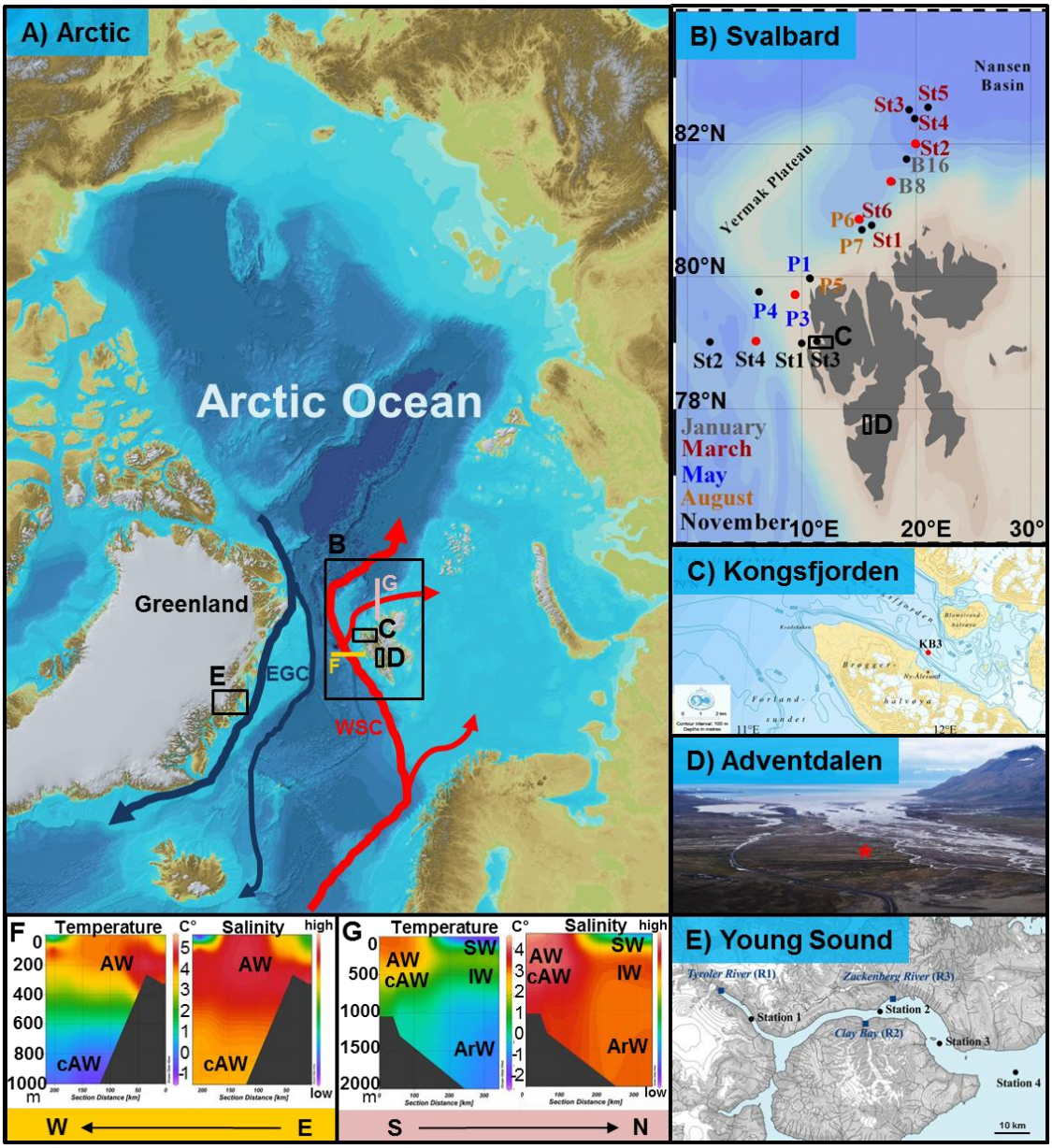

Figure 2: A) Map of the Arctic, including the four study sites (B, C, D and E). The red arrows indicate the transport of warm and saline Atlantic water up the Norwegian coast and branching into the West Spitsbergen Current (WSC). The flow of cold and less saline Arctic water is indicated by blue arrows and includes the major branch called East Greenland Current (EGC) (based on Blindheim and Østerhus, 2005). The dots on B) mark the sampling stations and colors indicate sampling months. C) and E) illustrate the two fjord systems where the microbial community under influence of terrestrial run-off was tested experimentally C) or monitored E). D) shows a photograph of the permafrost sampling site, which is marked with a red asterisk. F) and G) illustrate two cross sections, where temperature and salinity are indicators of the different water masses in the study area (AW=Atlantic Water; cAW=cold Atlantic Water; IW=Intermediate Water; SW=Surface Water; ArW= Arctic Water).

3.2 Permafrost: The frozen soil

Permafrost is continuously frozen soil and stores vast amounts of buried, ancient carbon, equaling about half of the global belowground soil organic matter (SOM) pool (Hugelius *et al.,* 2014). Covering the permafrost is a so called active layer (AL). The AL can reach down to a maximum of 1.5 m and experiences seasonal freeze-thaw cycles, while the permafrost layer (PL) can extend several meters and contains SOM that has been frozen for thousands of years.

While microbial community composition can vary substantially from site to site, microbial structures in the AL and PL can be distinguished by certain universal differences (Yergeau *et al.,* 2010; Frank-Fahle *et al.,* 2014; Hultman *et al.,* 2015). The AL communitiy is more diverse, including bacteria belonging to the phyla Acidobacteria, Proteobacteria, Planctomycetes, candidate phylum WPS-2, Bacteroidetes, Chloroflexi, Gemmatimonadetes, and candidate phylum AD3. PL samples show a lower alpha diversity and include bacterial taxa belonging to the phyla of Actinobacteria, Proteobacteria, Verrucomicrobia, Chloroflexi, Bacteroidetes and Firmicutes (Hansen *et al.,* 2007; Yergeau *et al.,* 2010; Mackelprang *et al.,* 2011; Yang *et al.,* 2012).

The current warming in the Arctic is of special concern, as this may trigger an increased microbial activity leading to faster decomposition of formerly preserved SOM and release of greenhouse gases, including CO_2 and CH_4 as illustrated in **Box 1** (Schuur *et al.,* 2009; Grosse *et al.,* 2011; Mackelprang *et al.,* 2011; Xue *et al.,* 2016). How microbes contribute to greenhouse gas emissions is still not understood in detail, partly because of the heterogeneous character of soil (Elberling *et al.,* 2004; McCalley *et al.,* 2014). Therefore it is important to capture the changes throughout the permafrost profile in detail by using a high resolution community composition analysis to address the future implications and consequences of thawing permafrost.

Box 1 | Arctic permafrost - Consequences of thawing

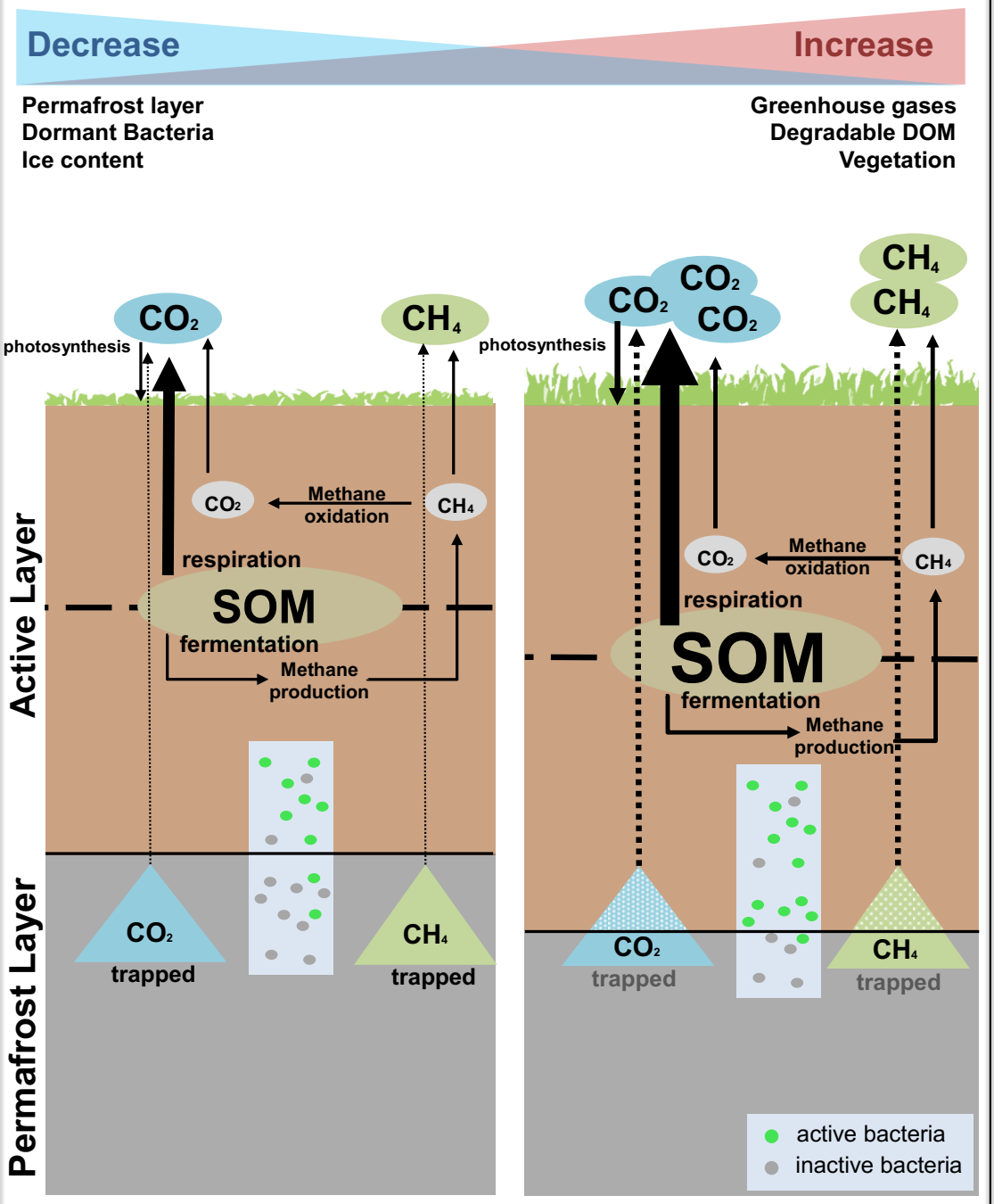

When permafrost thaws, becomes previously frozen soil organic matter (SOM) available for microbial degradation in the expanded active layer. The SOM is decomposed and either respired as carbon dioxide (CO_2) in the aerobic parts or as methane (CH_4) in the anaerobic parts of the soil. Additionally, formerly trapped CO_2 and CH_4 are released into the atmosphere.

Permafrost research site:

The soil samples were taken in 2011 and 2014 from a site located in the valley Adventdalen on Svalbard (Figure 2 D; 78.186N, 15.9248E), an archipelago at the entrance to the Arctic Ocean. The valley is 35 km long and 3 km wide and has a characteristic U-shape caused by glacial erosion. The site is covered with Late Holocene loess deposits and is characterized by high silt/sand content, resulting in a relatively well-drained soil. The soil profile can be divided into an AL, seasonally thawing in summer, with a thickness of up to 100 cm and a continuously frozen PL below extending to greater than 100 m (Humlum *et al.,* 2003). Adventdalen is one of the driest parts of Svalbard, averaging 190 mm of annual precipitation. The mean annual air temperature is approximately -6°C and ground temperatures range from -3˚C to -6˚C. Strong winds from the south-east dominate during winter and cause a thin snow cover. Adventdalen is a dynamic landscape, with changing periglacial landforms, such as ice-wedge polygons, typically covered by grasses and mosses in the central parts and sparse vegetation on the ramparts.

3.3 Fjords: The interplay between land and ocean

Fjords are long, narrow oceanic inlets, largely influenced by terrestrial run-off. They are characterized by mainly three water masses, including surface water, intermediate water and basin water (Stigebrandt, 2012). These water masses are, due to density gradients generally highly stratified and water circulation consists mainly of two opposing currents, one surface layer current, fueled by the freshwater run-off moving out of the fjord and one current below, transporting water into the fjord (Stigebrandt *et al.,* 1989). Seasonal mixing processes as observed in open water are far less common in fjord ecosystems and sources for resupply of nutrients are predominantly entering as run-off from land (Gutiérrez *et al.,* 2015). This run-off from lands introduces not only nutrients and carbon, but also microbes, such as Cyanobacteria, Proteobacteria and Actinobacteria and thereby influences the dynamics of fjord microbial communities (Gutiérrez *et al.,* 2015).

With increasing temperatures in the Arctic this discharge of organic material into fjord systems has the potential to alter the carbon cycle and the marine ecosystem (Serreze *et al.,* 2000; Holmes *et al.,* 2012; Feng *et al.,* 2013; Fichot *et al.,* 2013). The continental run-off introduces vast amounts of freshwater, nutrients and tDOM via fjords into the Arctic Ocean. Microorganisms can use this organic carbon source as a food supply and its uptake depends on the composition of bioavailable compounds (Middelboe and Lundsgaard, 2003). Various optical methods can be used to differentiate between refractory DOM (resistant to biological degradation) and bioavailable DOM. As illustrated in **Box 2**, the refractory DOM is characteristic for an increase in aromaticity, conjugation and carbon to hydrogen ratio and can be measured on a spectrofluorometer (fluorescent dissolved organic matter) (Álvarez-Salgado and Stedmon 2011). The bioavailable part of DOM remains colorless in these measurements.

Box 2 | tDOM - Terrigenous dissolved organic matter

DOM is including different types of carbon compounds that are categorized, based on their degradability, into labile (light green), semi-labile (darker green) and refractory (black) groups.

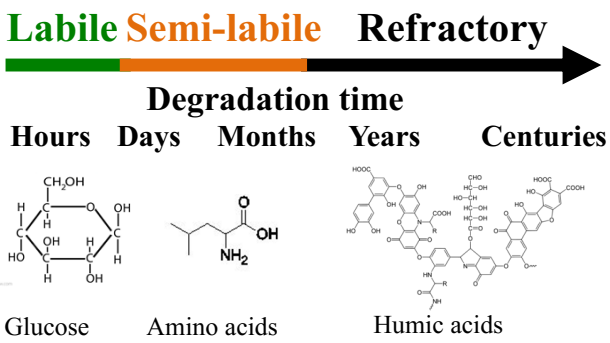

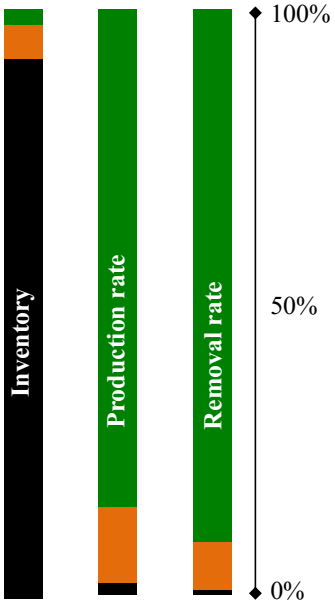

Global distribution, production and removal of marine DOM components (adapted with data from Hansell, 2013)

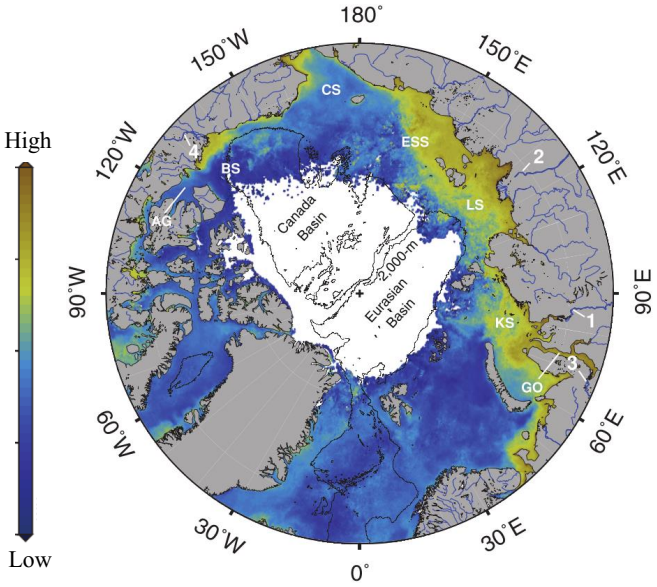

Fluorescence of humic acid-like DOM components in the Arctic Ocean (Fichot *et al.,* 2013)

tDOM in the Arctic

Terrigenous DOM (tDOM) has relatively high concentrations of refractory components from remnants of plant materials like lignin. Fluorescence signals of humic acid-like substances in the Arctic Ocean show the transport of tDOM from land into the coastal areas. The tDOM that eventually enters the Arctic Ocean is even more refractory, as it has been abiotically (UV-rays) and biotically (microbes) degraded in ponds and rivers where it originated.

Changes in the balance of available organic material, bacterial respiration of DOC and ocean CO_2 release will eventually have a great effect on the global carbon cycle and atmospheric CO_2 concentrations. The role of bacteria in processing different DOC sources is complex and yet not well investigated. However, experiments which were conducted in two different locations in the Arctic, hint towards a positive influence of both temperature and concentration of labile carbon sources on bacterial growth rates (Middelboe and Lundsgaard 2003; Kritzberg *et al.,* 2010). It is of high importance to understand these processes induced by climatic changes, since bacteria comprise the largest biomass and are responsible for most respiration in the ocean.

The concentration of DOM does not only affect bacteria, but the entire marine ecosystem by influencing nutrient and light availability (Urtizberea *et al.,* 2013). Further, with DOM affecting microbial community structure, cascading effects higher up the trophic level are expected (Thingstad *et al.,* 2008; Sipler *et al.,* 2017). Specific predator-prey relations between bacteria and heterotrophic nanoflagellates (HNF) might be an important link in the microbial food web of Arctic fjord systems, affecting higher trophic levels, including ciliates, copepods and reaching up to top level predators. How these food web structures are connected and link to the carbon cycle is illustrated in **Box 3** (Azam and Malfatti, 2007; Worden *et al.,* 2015).

There is a need to understand how increased tDOM might change the fjord microbial community composition and thereby also higher trophic levels in order to better predict climate change impacts on the marine Arctic ecosystem. To gain a better understanding, it is necessary to add detailed knowledge about the structure and activity of the microbial community under the influence of increased tDOM run-off.

Box 3 | Planktonic food web - The role of bacteria

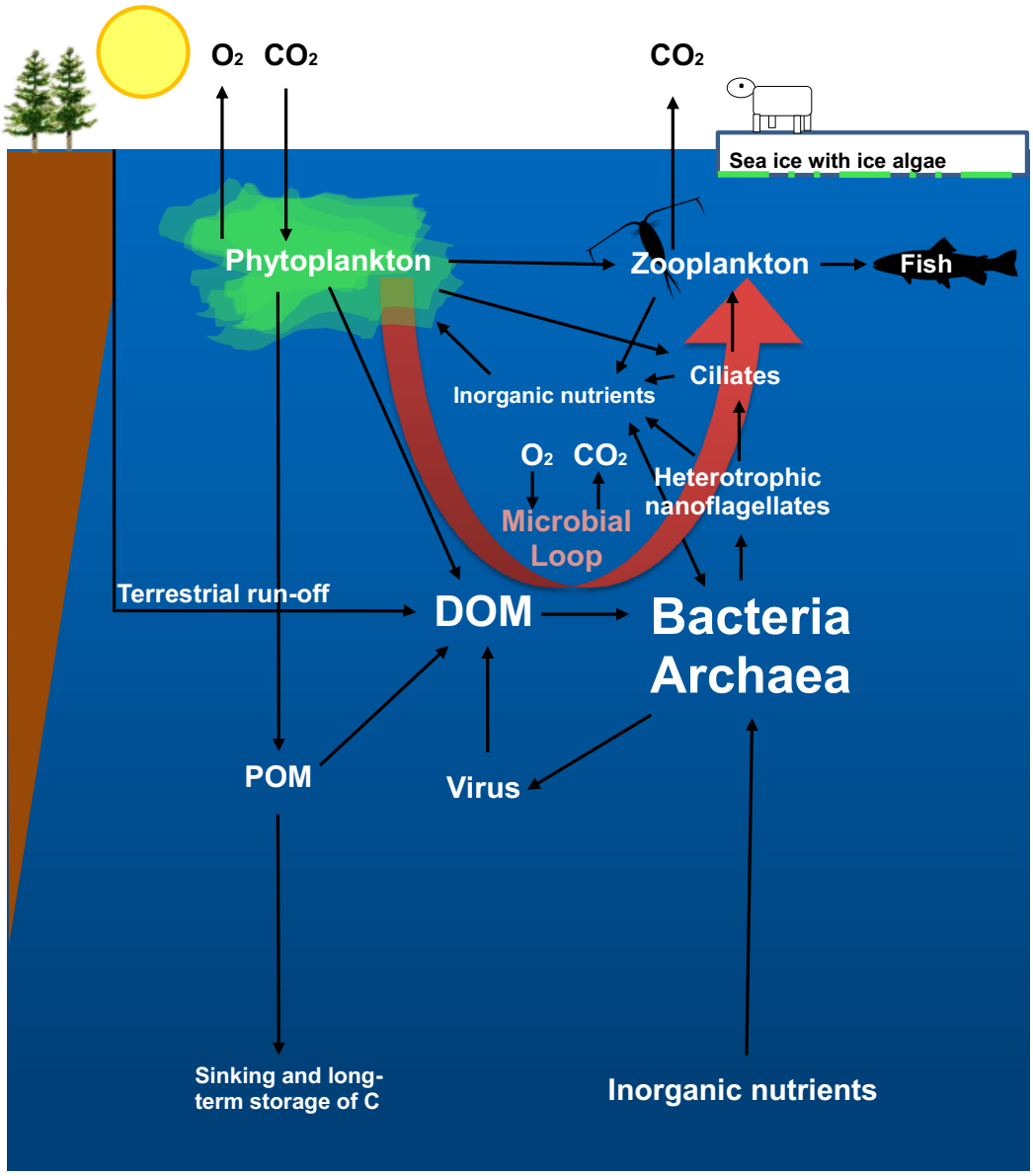

A schematic view of the marine microbial food web and carbon cycling in the Arctic Ocean (based on Azam and Malfatti *et al.,* 2007 and Worden *et al.,* 2015). One key process is photosynthesis, the conversion of inorganic carbon (CO_2) to organic carbon by phytoplankton. This phytoplankton derived organic carbon build the basic resource for heterotrophic organisms. The organic carbon is either directly used by zooplankton (e.g. copepods) or indirectly, via the microbial loop, transported from prokaryotes (Bacteria and Archaea) which are eaten by nanoflagellates and ciliates up to zooplankton, which are eventually eaten by fish.

Fjord systems:

We chose Young Sound, a fjord in north-eastern Greenland (Figure 2 E), for the long term study as there is in a clear gradient of allochthonous sources of both organic matter and silt throughout the fjord (Murray *et al.,* 2015). Young Sound receives most of its run-off from the Greenland Ice Sheet via land terminating glaciers (Citterio *et al.,* 2017). The organic carbon sources in the fjord comprise the autochthonous phytoplankton production, allochthonous carbon from the rivers (with diverse vegetation and soil catchments) and allochthonous organic carbon that enters the fjord via entrance of coastal waters, which contain DOM from the Arctic Ocean that are transported in the East Greenland current (Amon, 2003).

The other fjord system, where tDOM experiments were conducted, is situated in the western part of Svalbard (Figure 2 C; 79.0 °N, 11.4 °E). Kongsfjord is 26 km long, 6 to 14 km wide and two glaciers, Kronebreen and Kongsvegen, terminate at the head of the fjord. This fjord is well characterized and was chosen for the incubation experiments, since tDOM extracts were produced from local permafrost samples. This provided an optimal setting to simulate and study future scenarios of increased tDOM concentrations in fjord systems.

3.4 Arctic Ocean: Changing seasons and water masses

The Arctic Ocean comprises the water masses around the North Pole and undergoes therefore extreme seasonal changes during an annual cycle. It switches from a dark, ice-covered winter to light, more open water conditions in the summer (**Box 4**). Despite these extreme periodic shifts, biodiversity is high in the Arctic. But climate warming is altering the conditions microbes have adapted to. The Arctic is currently undergoing the warmest period since the last 40,000 years, causing a lengthening of the melt season and dramatic decline of sea-ice (**Figure 3**) (Stroeve *et al.,* 2014).

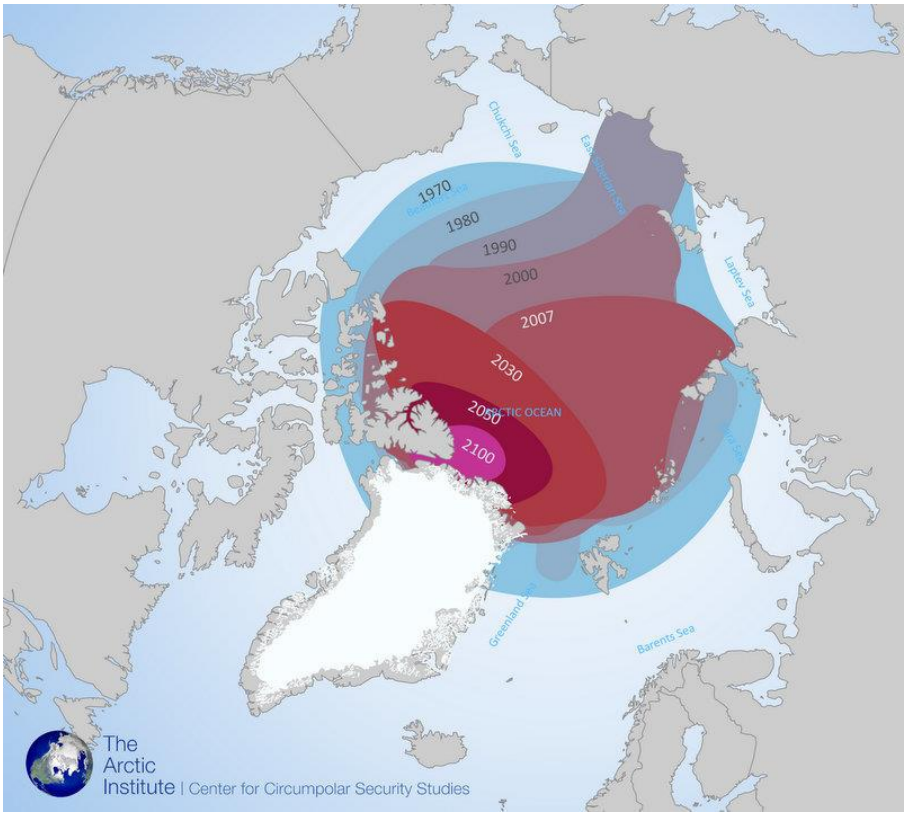

Figure 3: Extent of Arctic summer sea ice (based on historical satellite records and climate models) showing the retreat over the last centuries and the predicted future decline (Figure: Yale University).

Despite the increased melting, sea-ice covers the ocean surface through much of the year and limits vertical mixing, which leads to a strong stratification of water masses (Stein and Macdonald, 2004). The cold surface layer spans approximately 0-30m and is influenced by river run-off and melting sea ice. Below that is a nutrient rich intermediate layer (30-250m) comprised of Pacific waters. Finally, a warm Atlantic layer spans 250-1500m above the isolated deep water (**Figure 4**). The upper cold freshwater rich layer sustains a perennial halocline, which acts as an isolation from the warmer, saline Atlantic waters (Aagaard and Carmack, 1989; Shimada *et al.,* 2006).

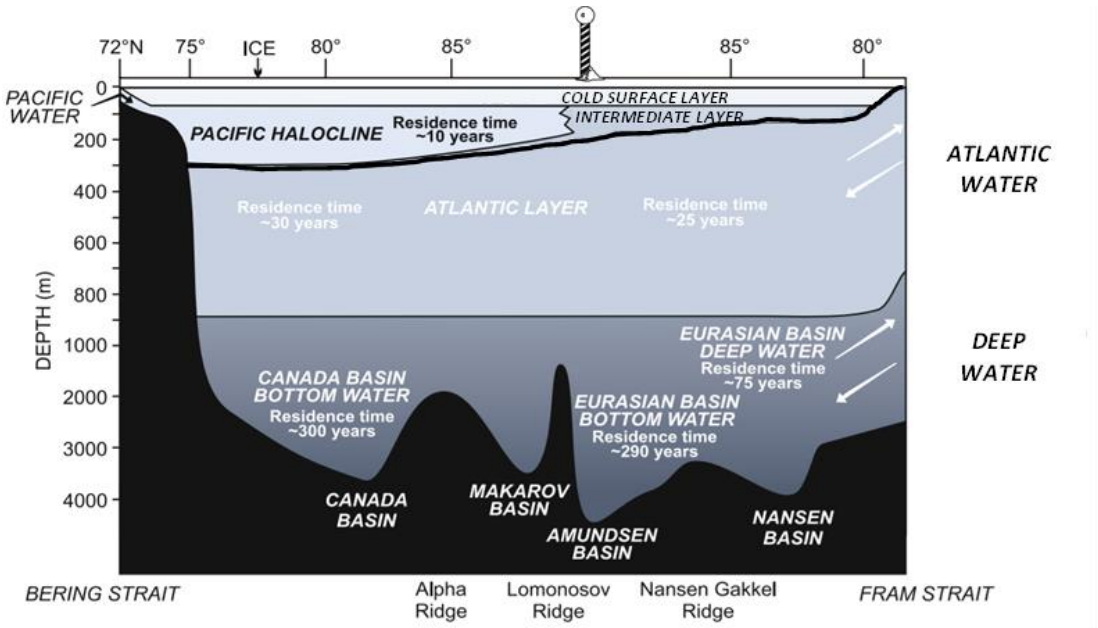

Figure 4: Schematic diagram showing the stratification of the Arctic Ocean (modified from Macdonald and Bewers, 1996).

The transport of water masses, their history and mixing are important regulators of mesopelagic microbial community structures (Galand *et al.,* 2010; Reinthaler *et al.,* 2010). Due to the extreme differences between summer and winter, microbial life has adapted and developed different strategies to thrive under both conditions (**Box 4**).

Box 4 | Changing seasons - Microbial life in the surface and the deep Arctic Ocean

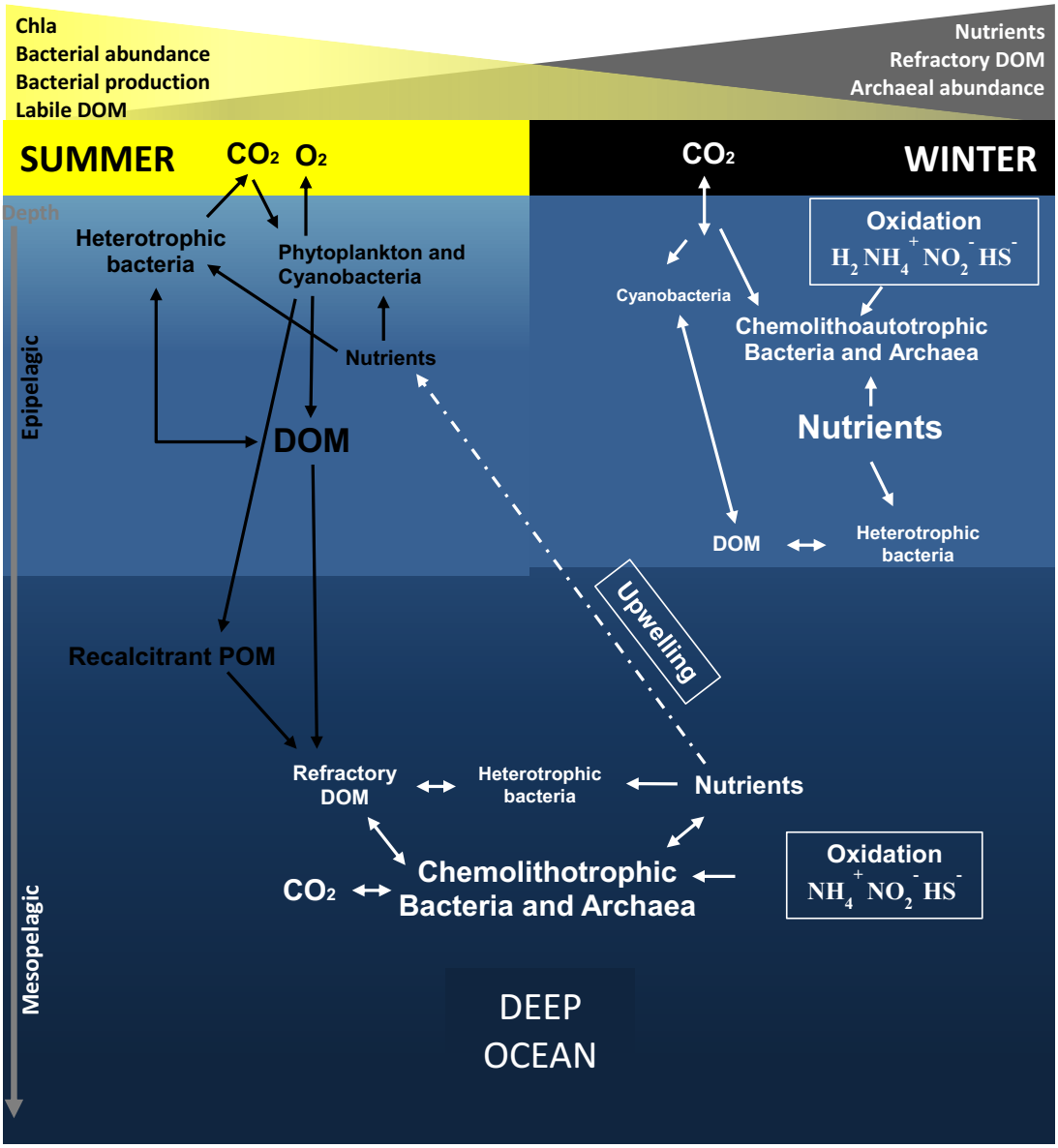

Illustration of plankton-driven processes in Arctic Ocean surface and deep layers during summer and winter (based on Grzymski *et al.,* 2012). The summer surface water has higher bacterial activity associated with light-driven processes and heterotrophic bacteria that degrade labile phytoplankton derived DOM. The winter surface water is dominated by chemolithoautotrophic processes, where predominantly Archaea oxidize substrates like ammonium and fix CO_2. In the deep ocean, microbial processes are similar to the winter surface situation, including the dominance of chemolithotrophic Bacteria and Archaea. Upwelling in spring transports nutrients like nitrate (as product of microbial nitrification) to the surface layer where it sustains phytoplankton growth in the upcoming summer season.

Especially in the surface during the dark winter and in the deep waters all year round, where phytoplankton cannot grow, chemolithotrophic microorganisms, such as ammonia oxidizing Thaumarchaeota that remineralize nutrients and fix CO_2, are the dominant organisms (Murray *et al.,* 1998; Alonso-Sáez *et al.,* 2008; Grzymski *et al.,* 2012). Thaumarchaeota are key players in the nitrification process and oxidize ammonium to nitrite, which is then further oxidized to nitrate by, among others, members of the family *Nitrospinaceae* (Levipan *et al.,* 2014). Thus, nitrate is accumulating in the deep ocean and transported via upwelling to the surface, where it supports phytoplankton growth in the summer season (Zehr and Ward, 2002). Despite the important role of Thaumarchaeota in the marine nitrogen cycle, little is known about how these Archaea change over an annual cycle and what factors drive their distribution in the Arctic Ocean.

Arctic Ocean research cruises:

Samples were collected during five cruises in 2014 north-west of Svalbard (Figure 2 B), following several transects along the West Spitsbergen Current (WSC) at the eastern part of the Fram Strait up to the Arctic Ocean. Sampling periods extended over an entire polar year with cruises in January (06.01-15.01), March (05.03-10.03), May (15.05-02.06), August (07.08-18.08) and November (03.11-10.11). Depth profiles of temperature, salinity and fluorescence were recorded using a SBE 911plus CTD system, to identify water masses and to collect water for downstream analyses. Samples (25-50 L) for molecular analyses were taken between depths of 1 to 1000 m , filtered onto 0.22 µm pore size Millipore® Sterivex filters (Merck-Millipore, MA, USA) and immediately frozen at -80°C.

The sampling area is hydrographically characterized by three Atlantic water masses, including Atlantic Water (AW), cold Atlantic Water (cAW) and Intermediate Water (IW), having salinity >34.9 and temperatures >2°C, 0-2°C and <0°C, respectively; and also, by two Arctic water masses, Surface Water (SW) and Arctic Water (ArW), having salinity <34.92 and a density (σ_t) of <27.7 kg m^{-3} and >27.7 kg m^{-3} respectively (Cokelet *et al.,* 2008; de Steur *et al.,* 2014; Randelhoff *et al.,* 2015). The WSC at the eastern part of the Fram Strait transports Atlantic water into the Arctic Ocean. This Atlantic water can also be found in deeper mesopelagic zones as cAW and IW. The water masses classified as Arctic Water do not necessarily originate from the Arctic Ocean interior, but have undergone similar freshening and cooling processes and have the same physical characteristics as Arctic Ocean water masses.

4. Results and Discussion

4.1 Community composition patterns in the Arctic and ecosystem function

In ecology, the first step to understand processes and functions in the environment is to identify patterns in time, space and at different scales, as the distribution of organisms in nature, is neither random nor uniform. What are able to observe are distribution patterns, most often as a result of multiple ecological processes (Legendre and Fortin, 1989). Various ecological processes, together with species responses are generally causing pattern structures, including gradients, patches or noise (Fortin *et al.,* 2002). While gradients describe steady directional distributional change, patch structures are more homogenous distributions that are separated from each other. Variations in patterns that cannot be explained are categorized as noise and are most likely caused by processes that act on more than one spatial scale.

In microbial ecology, community composition is most often driven by environmental factors and processes (Baas-Becking, 1934; de Wit and Bouvier, 2006). By analyzing patterns of community composition, the magnitude of the effect of environmental factors can be revealed and ecosystem functions understood. Defining the magnitude and importance of environmental factors driving community composition changes can be difficult when spatiotemporal variations occur (Borcard *et al.,* 1992). Consequently, correlations of community patterns with environmental factors can only be meaningful if spatiotemporal variations are not disregarded.

Recent advances in next-generation sequencing opened the possibility to investigate community composition patterns at a much higher sampling resolution and thereby enabled better elucidation between spatiotemporal factors and environmental drivers. We used this method in all our studies and were thereby able to discover novel community composition patterns, their environmental relevance in different Arctic environments, and how they might be affected by climate change.

4.1.1 Community changes along environmental gradients

Temperature, pH, salinity, carbon concentration, nutrients and oxygen, are only few examples of environmental factors that can gradually change and thereby create gradients that influence the microbial community composition. We identified a gradually changing community composition in both terrestrial (**Paper I**) and marine Arctic (**Paper II, III, IV and V**) study sites. While the community composition differs greatly, similar environmental gradients might be important in the different ecosystems. We were therefore interested to what degree environmental factors (**Table 1**) can inform about changes in microbial community composition in permafrost (**Paper I**), in an Arctic fjord system (**Paper II**) and further in the Arctic Ocean (**Paper IV and V**). In order to detect gradual changes in community composition, several factors, including scale, time, distance and sample grouping have to be considered (Borcard *et al.,* 1992; Torsvik *et al.,* 2002). When studying different environments the complexity becomes even greater.

Table 1: Different environmental factors that influenced the microbial communities analyzed in three studies included in this PhD-thesis. ++: important; +: moderate; -: minor/no role

Environmental gradient	Permafrost core	Fjord transect	Arctic Ocean
Depth	++	+	++
Water content	+	-	-
pH	+	-	-
DOC-content/quality	++	++	+
Salinity	-	++	+
Nutrients	+	+	++
Light	+	+	++
Water mass	-	++	++
Sampling resolution	++	+	-

During the last decade, permafrost studies began to describe environmental factors which are driving the microbial community composition. But until now, microbial community structures in permafrost have most often been characterized as a two layer system, divided in AL and PL (Yergeau *et al.,* 2010; Wilhelm *et al.,* 2011; Frank-

Fahle *et al.,* 2014; Gittel *et al.,* 2014; Koyama *et al.,* 2014; Taş *et al.,* 2014; Deng *et al.,* 2015).

In **Paper I** we investigated the microbial community composition in a permafrost core from Svalbard and applied an unprecedented high sampling resolution of every 3-4 cm over the two-meter soil core and identified small scale changes as a consequence of environmental gradients (**Figure 5**).

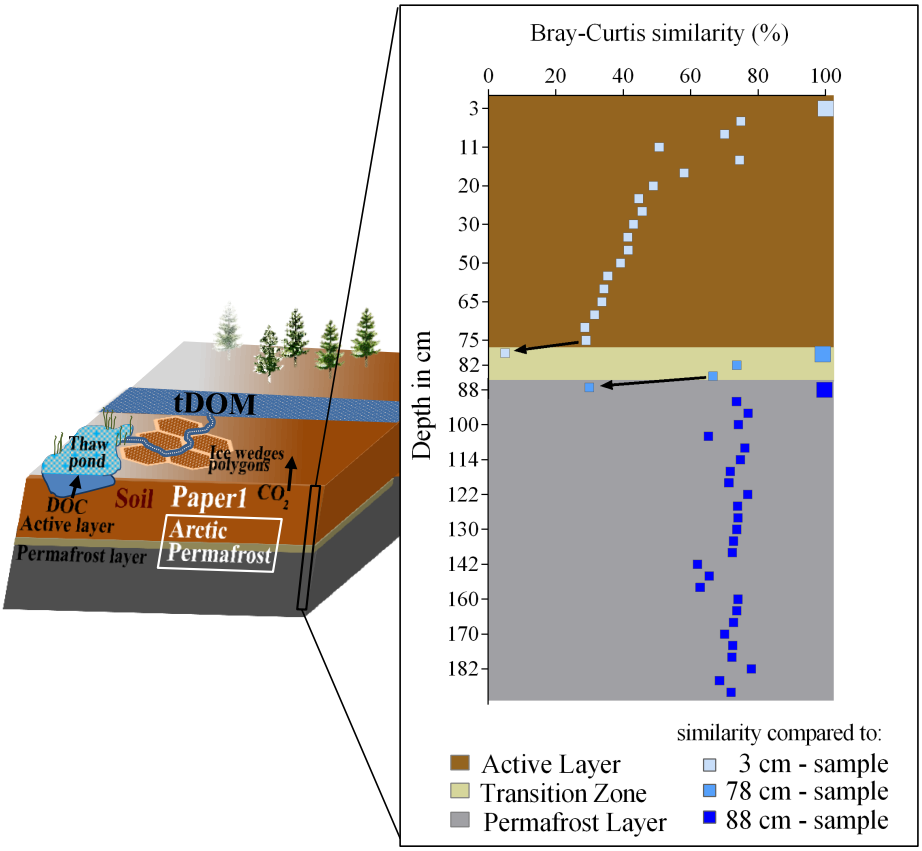

Figure 5*:* Bray-Curtis values illustrating sample similarities based on 16S rRNA gene sequences in a two-meter permafrost core. Sample similarity revealed three distinctive groups; Active Layer, Transition Zone and Permafrost Layer and shifts in sample similarity between these layers are indicated by the black arrows. Three samples (larger symbols) were therefore used to compare sample similarity (light blue: 3 cm; medium blue: 78 cm; dark blue: 88 cm).

Analysis of similarities (ANOSIM) of the distinctive microbial community patterns revealed a significant difference between the three layers. While we identified clear gradual changes in the upper AL, both the TZ and PL showed a homogenous community composition. The TZ and PL were dominated by just one bacterial family each, belonging to Bacteriodetes and Actinobacteria, respectively.

Even though carbon plays an especially important role in this system, the changes can only partly be explained by carbon concentration differences and are more likely associated with carbon quality characteristics, which were not assessed in this study. Especially the dominance of copiotrophic Bacteroidetes above the frozen above the frozen permafrost table might be due to their metabolic flexibility and their ability to respond fast to a variety of easy available carbon and nutrients that can accumulate in the TZ (Padmanabhan *et al.,* 2003; Fierer *et al.,* 2007). As we identified such distinct characteristics in the TZ for the first time, the question if this zone deepens with increasing AL thaw and how fast the microbial community in the PL might change remains.

Carbon availability is undoubtedly an important factor for microbial life, not only in permafrost, but also in aquatic Arctic ecosystems. In **Paper II** we investigated the influence of different carbon sources on the fjord microbial community with the specific aim to identify the different microbial drivers during the productive ice-free period. Changes in community composition over time or distance appeared random at first (**Figure 6**) and are a result of various different environmental parameters interacting with each other, as well as a matter of scale regarding taxonomical classification (**Paper II**).

The high Arctic fjord that was investigated, Young Sound, is a rather complex fjord system, with three adjoining rivers. The three rivers all have a different origin and catchment area; river 1 (R1) has a close connection (0.5 km) to the Greenland Ice Sheet, river 2 (R2) a longer distance (2 km) to a smaller local glacier, and river 3 (R3) runs through lowland rich vegetation with a lake connection. The difference in origin is very important in shaping the bacterial communities in the rivers, which were

highly specific to each of them. The other stations showed community differences between surface and deeper samples, which refers to the physical water mass characteristics they were sampled from. Both surface and deep samples showed gradually community changes from inner to outer fjord stations, with specific taxa at family level either decreasing or increasing, respectively.

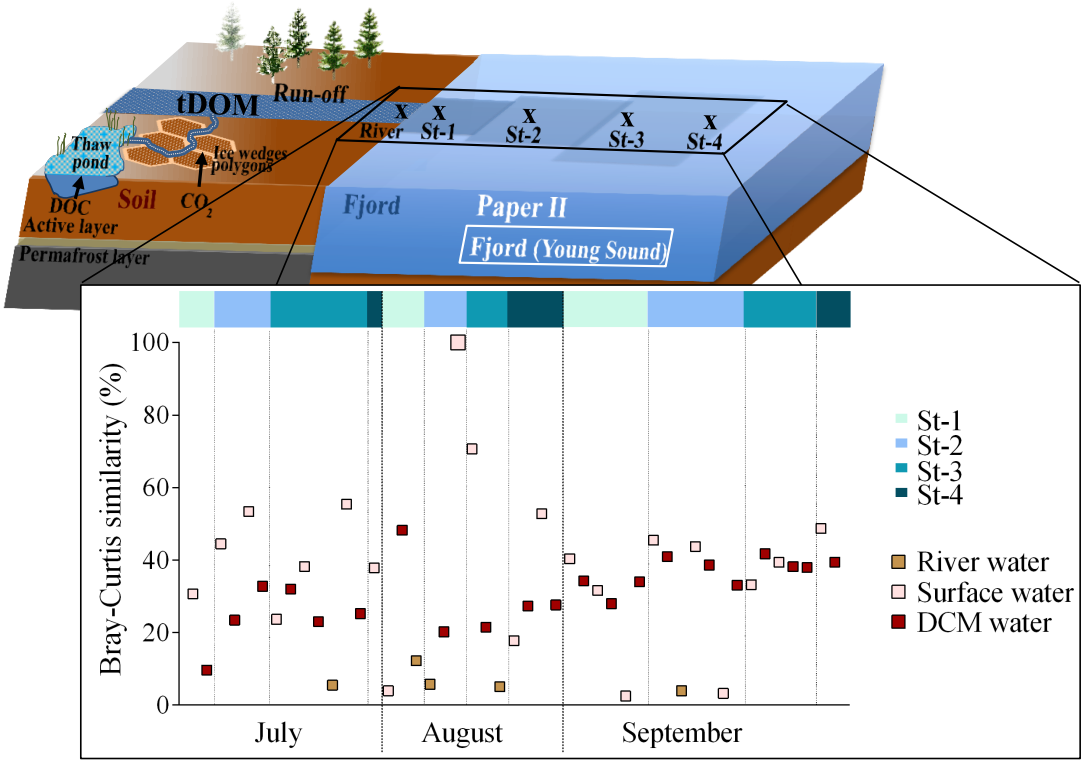

Figure 6: Bray-Curtis values based on 16S rRNA gene sequences from fjord profiles showing sample similarities in Young Sound over time (July until September) and at four stations and including additional river samples, schematic indicated as "x" in illustration above. A surface sample taken in August at station St-2 was used as reference to compare sample similarity. Samples were grouped according to the station where they were taken (varying between one and three sampling occasions per month and station). DCM=Deep chlorophyll maximum

Depending on the spatiotemporal constrains, different environmental factors influenced community composition. For example while no measured environmental parameter correlated with community composition of samples from all stations over the entire sampling period, some parameters, including salinity and carbon concentrations correlated for the period when run-off from land was strongest and the fjord was stratified. These conditions also enabled the communities found in glacial

river run-off to persist. It has been suggested that such bacteria, residing in glacial meltwater have the competitive advantage of tolerating the colder and fresher conditions of the fjord surface water (Gutiérrez *et al.,* 2015). The differences between surface and subsurface communities were only evident as long as fresh water was supplied by the rivers and were not detected when thermal stratification stopped towards the end of the sampling period (**Figure 6**).

Interestingly, only at the lowest taxonomic level (OTUs), some correlations became evident. Especially carbon seemed to affect only some OTUs over a range of different species, while others remain unchanged. This might be due to intraspecific specializations to degrade specific carbon compounds (**Paper III and V** and Sipler *et al., 2017)*. The overall structuring was based on water sources and along freshwater gradients, common for coastal environments (Bouvier and del Giorgio, 2002; Gutiérrez *et al.,* 2015). It will be important to understand these processes in fjord systems, in order to predict how hydrology changes, such as increased freshwater run-off might affect the microbial community in the future.

Freshening and increased terrestrial carbon inputs have also been predicted for the entire Arctic Ocean (Kwok and Cunningham, 2010; Comeau *et al.,* 2011; Fichot *et al.,* 2013). We analyzed the microbial community structure repeatedly in the Arctic Ocean north-west of Svalbard during five cruises distributed over an entire year (**Figure 7**). This dataset revealed the main drivers of community change in epi- and mesopelagic waters over the course of an Arctic polar year (**Paper IV**) and provided new insights towards the importance of water masses in defining marine microbial community structures (**Paper V**). Both, the influence of seasonal factors and water mass on community composition became evident when comparing Bray-Curtis sample similarities (**Figure 7**). Highest were similarities between winter surface and summer deep samples, indicating that light and light associated processes, including phytoplankton growth causing nutrient depletions and competition, greatly affects the Arctic Ocean surface microbial community structure (Giovannoni and Stingl, 2005). Associated with the observed patterns of community similarities were patterns of general alpha diversity. We observed a lower diversity in summer surface samples,

even though prokaryotic abundance was highest. In winter surface and mesopelagic waters all year round, where prokaryotic abundances are lower, we observed a higher diversity. These diversity differences are tightly connected to concentrations and quality of carbon and nutrients. In summer, the increase of labile carbon compounds following phytoplankton blooms is favoring a few specific bacterial groups and thereby decreasing the diversity (Buchan *et al.,* 2014). On the contrary, in winter surface and deep waters the labile DOM sources are deprived and only rather complex and diverse recalcitrant DOM compounds remain as energy sources (Hansell, 2013). This substrate complexity fosters a mix of different specialized bacteria to proliferate and results in higher diversity (Alonso-Sáez *et al.,* 2008).

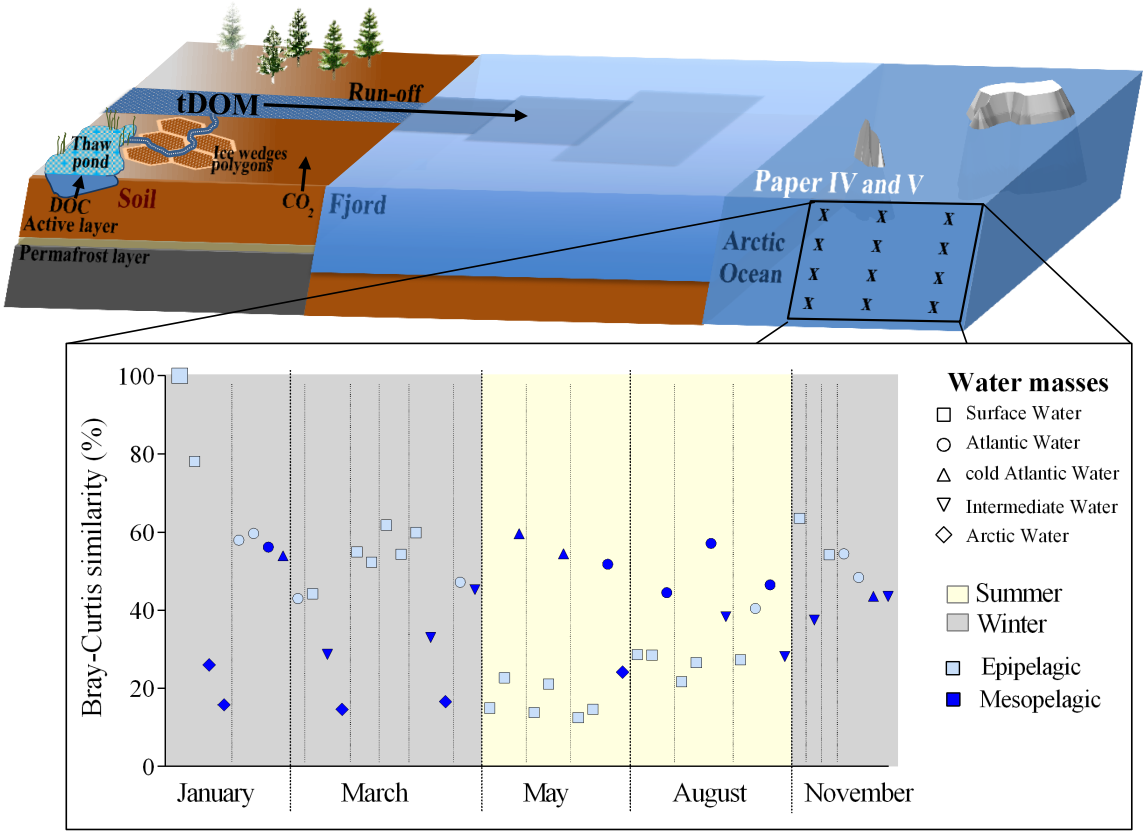

Figure 7: Bray-Curtis values based on 16S rRNA gene sequences from Arctic Ocean profiles (sampling points are shown schematically as "x") showing sample similarities over time (January until November), different stations and different depths. Different stations are separated by a dotted line. The 1 m sample taken in January at station B-16 was used as reference to compare sample similarity.

One important functional microbial group in the deep waters and winter surface waters are Thaumarchaeota. We described the distribution and dispersal limitations of this important group of ammonia oxidizers in **Paper V**. Thaumarchaeota abundance varied with season and depth, with highest numbers in deep and winter surface samples. Photoinhibition of ammonia oxidation has been widely suggested to cause this cyclical decline in abundance (Guerrero and Jones, 1996; Murray *et al.,* 1998; Mincer *et al.,* 2007; Merbt *et al.,* 2012).

Besides the overall seasonal differences, we also identified a pattern of different Thaumarchaeota ecotypes that were distributed according to water masses found around Svalbard (**Paper V**). This is in contrast to the common perception of depth or ammonium concentration as main drivers of Thaumarchaeota distribution (Kirchman *et al.,* 2007; Christman *et al.,* 2011; Sintes *et al.,* 2013, 2015, 2016; Santoro *et al.,* 2017). Further, this might have great ecological implications in the future, when water masses in the Arctic Ocean might change, due to increased sea ice melting (Comeau *et al.,* 2011) or "Atlantification" (Polyakov *et al.,* 2005; Holland *et al.,* 2006; Walczowski and Piechura, 2006).

Interestingly, not only Thaumarchaeota abundance but also the distribution of other taxa was associated with water masses. This is illustrated in **Figure 7**, where community similarity between the surface sample and the 1000 m samples was either below 20% or between 40 and 60%. The 1000 m samples in which similarities were below 20% originated all from the Nansen Basin and were associated with a deep Arctic water mass (ArW), while the other 1000 m samples with higher similarities to the surface sample were associated with water masses that are transformed Atlantic water masses (cAW or IW). Depending on their origin, the water masses acted either as barriers or promoters of microbial dispersal, causing distinct biogeographical patterns. This supports the general theory that water mass history to a great extent defines the marine microbial community composition (Galand *et al.,* 2010; Reinthaler *et al.,* 2010).

We identified different microbial patterns in all the investigated environments with different drivers causing the observed distributions. While comparing samples based

on Bray-Curtis similarities is an effective way to identify community patterns, it is necessary to include environmental information in order to explain the observed distribution when different scales, both temporal and spatial are applied. Scale is also important regarding taxonomical resolution. Some ecologically important patterns, such as correlations with DOM compounds, only become evident when comparing samples at the OTU level, while other distribution patterns can be informative already at phylum or class level, as shown for the Thaumarchaeota pattern.

Following the changes in these patterns can furthermore highlight consequences of disturbances in the ecosystem, including the changes associated to climate warming. We can only report on the consequences of climate change effects on the microbial community if we have detailed records of their current state and can identify ecologically important patterns. It is therefore crucial to identify bacteria that are sensitive to climate change and to further test experimentally if certain stressors can affect these sentinels of change.

4.1.2 Bacteria as sentinels of climate change

Prokaryotes are sensitive to climate change processes and can thus serve as sentinels to detect and monitor climate change effects on ecosystems in different Arctic environments (Blaud *et al.,* 2015; Oliverio *et al.,* 2017; Rofner *et al.,* 2017; Sipler *et al.,* 2017). In order to identify new prokaryotes that can be used as sentinels of climate change, we have to understand their function and identify distribution patterns. Especially species that show gradually changing abundances to certain environmental parameters that can be associated with climate change, including carbon and freshwater run-off, are suitable candidates. The taxonomic level is also important to define such sentinels. We identified environmental gradients causing abundance patterns already on phylum or class level (**Paper I, Paper II and Paper IV**) or patterns that were only detectable at the species or OTU level (**Paper II and Paper III**).

Of all phylogenetic groups, Proteobacteria appeared particular useful to follow climate change related trends and we observed gradual abundance changes of members of this group in all three environments that we investigated (**Paper I, Paper II and Paper IV**). Throughout the permafrost soil profile that we analyzed in **Paper I**, we identified gradual changes for the different Proteobacterial classes. The relative abundance of Alphaproteobacteria and Gammaproteobacteria was decreasing and the relative abundance of Betaproteobacteria was increasing with soil depth in the AL. It has been speculated that such abundance differences correlate with carbon and nutrient availability (Koyama *et al.,* 2014; Kim *et al.,* 2016). As we analyzed a mineral permafrost core with throughout low carbon concentrations, we concluded that other parameters which can directly be associated with increasing depth, like oxygen availability, redox conditions or carbon quality, might be more important in controlling the abundance of Alphaproteobacteria and Gammaproteobacteria and can explain the observation of similar patterns both in mineral and carbon rich Arctic soils. This makes the group of Proteobacteria especially suitable as sentinel for changes in permafrost environments. The TZ represents formerly frozen PL and is therefore the layer experiencing extreme physical changes. We identified significant increases in relative abundance of Betaproteobacteria in samples from the transition

zone after 16 days of incubation under thawing conditions. Due to this change in community composition thawed TZ samples became more similar to AL samples. In regard to climate change, Betaproteobacteria might therefore serve as sentinels to identify recently thawed permafrost soils.

Betaproteobacteria also became the focus of our search for sentinels of climate change in marine systems, as they can be indicators for freshwater influences in both Arctic fjords and the Arctic Ocean. Their increase in relative abundance in marine systems has therefore been associated with either increased run-off from land (Garneau *et al.,* 2009) or melting sea-ice (Brinkmeyer *et al.,* 2004). In Young Sound their abundance was highest in the river samples and the surface samples of the stations nearest to river inflow (**Figure 8** and **Paper II**).

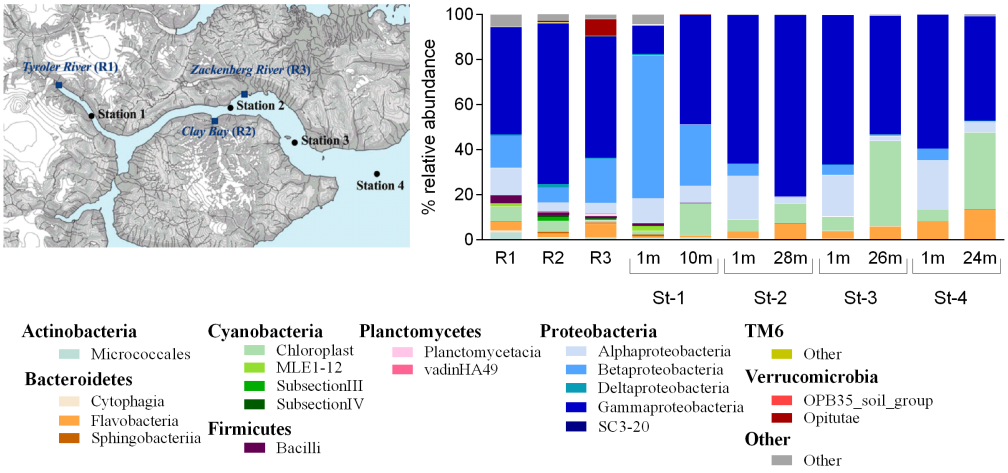

Figure 8: Relative abundance of the most abundant prokaryotic groups at class level in Young Sound shown for samples taken in the beginning of August.

We also observed a decrease in relative abundance of Betaproteobacteria in surface water samples with increasing distance either from the coast or from the sea-ice (**Paper IV**). With increasing run-off from land and sea-ice melt, we hence expect an increase of Betaproteobacteria in marine Arctic systems, which therefore can be used to indicate the extent of these climate change effects.

Some microbes can also serve as sentinels of climate change in regard to much more specific environmental parameters, such as tDOM. With increasing permafrost thaw and run-off from land, more tDOM is entering the Arctic Ocean (Holmes *et al.,* 2012;

Feng *et al.,* 2013; Fichot *et al.,* 2013). With the potential to affect the entire marine food web and carbon cycle, increase in tDOM may have huge impacts on the Arctic ecosystem (**Paper III** and Thingstad *et al.,* 2008; Sipler *et al.,* 2017). It is therefore important to closely follow the distributions of tDOM as well as the microbes that are able to process this carbon source. We identified one particular species, *Glaciecola*, in association with increased tDOM concentrations, both *in situ* in Young Sound (**Paper II**) and in experiments in Young Sound (**Paper II**) and Ny Ålesund (**Paper III**). Interestingly, not all *Glaciecola* OTUs responded similarly to the input of tDOM and different OTUs dominated in the different studies. It remains unclear whether the differences are caused by OTU dependent substrate specificities or their abundance at *in situ* conditions.

With the current changes in the Arctic it is important to have records of the microbial state to be able to identify how the Arctic microbes react to the warming climate. By identifying microbial sentinels of climate change we can go one step further and detect specific environmental climate change effects using molecular tools. Experiments that especially target such sentinels and test their function can further help to predict the consequences on the local microbial community and even on entire biogeochemical cycles, such as the carbon cycle.

4.2 Microbial response to thaw

Global warming is affecting the Arctic cryosphere, causing the decline in annual sea ice, glaciers and permafrost extent. In this scenario, Arctic microbes can serve both as sentinels and amplifiers of the ongoing changes. With Arctic microbial ecosystems shifting towards new states, changing microbial processes have implications on important biogeochemical fluxes, including the carbon cycle. Some microbes become more active with a longer growth season, others can inhabit newly available areas and in some cases entire microbial communities might change (Schuur *et al.,* 2008; Kirchman *et al.,* 2009). In **Paper I, II** and **III** we performed different experiments in different Arctic environments in order to test the effects and predict the consequences of climate warming on the microbial level.

4.2.1 Experimentally induced permafrost thaw

Being one of the most significant potential carbon feedbacks to the atmosphere, permafrost is central for all climate related changes in the Arctic. The carbon locked away in the frozen ground becomes available for degradation upon thaw, but may also be washed out in aquatic systems. In the end, microbial degradation processes in both environments are fueling greenhouse gas emissions, which in turn causes warmer temperatures and lead to even faster thaw. Studies measuring permafrost gas fluxes have shown that plant related carbon uptake cannot keep up with microbial CO_2 production (Schuur *et al.,* 2009). Permafrost environments might thus become a large carbon source to the biosphere. Research simulating future scenarios of warmer climate is needed to increase our knowledge about the microbial role in permafrost carbon processing.

We incubated subsamples from five segments of the Svalbard permafrost core at 4(±1) °C to simulate thawing conditions to different permafrost layers and document greenhouse gas fluxes thoroughly over 19 days (**Paper I**). CO_2 production rates were found to be high, but we did not detect any release or production of CH_4 or N_2O. Independent of the soil layer, respiration rates were higher, with up to four times

more produced CO_2, under aerobic than anaerobic conditions. Similar results have been obtained with permafrost incubations from different sites, which together shows that permafrost carbon from aerobic soil systems might have a greater effect on climate change than anaerobic environments (Lee *et al.,* 2012; Elberling *et al.,* 2013). This is especially important when data from such experiments is used to scale up and represent entire landscapes to predict future greenhouse gas release.

Such predictions are often based on results which compare gas fluxes based on broad scales, for example comparing surface (AL) with deep (PL) samples. This implies that greenhouse gas release is comparable within these layers. We showed that between the different layers, CO_2 production rates varied with changing community structure and incubation time. The highest within-layer difference was measured in the AL, where AL-1 samples released 60 µg C-CO_2 per gram soil, while samples from AL-2 released three times less during 19 days of incubation. This became especially evident when production rates were used to integrate CO_2 release over depth, as illustrated in **Figure 9**.

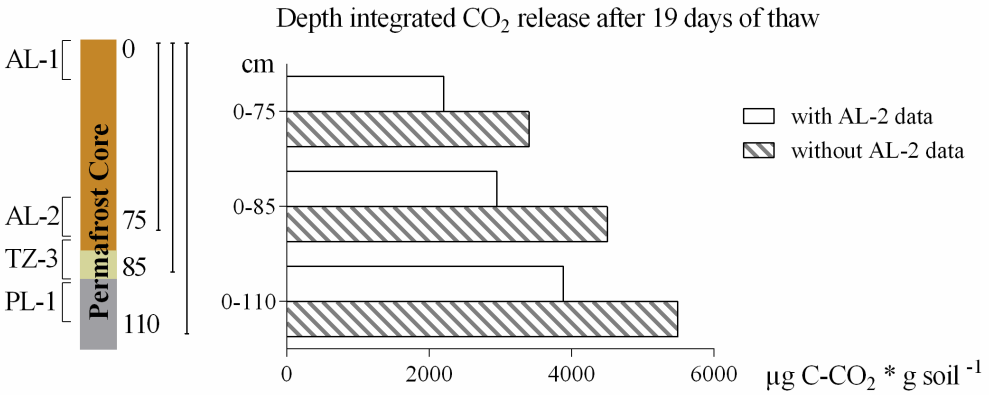

Figure 9: Depth integrated CO_2 production per gram soil differences of permafrost samples based on two AL sampling points (green bars) or only one AL sampling point (red bars).

Considering the different responses in the different permafrost layers, there is a need for further detailed gas flux studies in order to improve our understanding of the microbial response to permafrost thawing.

4.2.2 Microbial response to DOM in fjord microcosms

Arctic marine environments are experiencing increased inputs of terrestrial DOM sources fueled by permafrost thaw. However, the understanding of what fraction of tDOM is bioavailable and how fjord microbial communities will respond to increased tDOM is limited. In **Paper II** we investigated the DOM bioavailability in a high Arctic fjord system (Young Sound) over time and tested the bacterial uptake of the different DOM compounds experimentally, which correlated with the abundance of specific species. In **Paper III** we then tested the direct effects of tDOM input on the bacterial community composition in Kongsfjorden.

The natural sources of organic carbon in the Young Sound fjord system are; (1) local phytoplankton production; (2) runoff from land-terminating glaciers and a lowland river and (3) inflow from the ocean shelf. Bioavailability was up to six times higher in river samples. However, which DOM compounds dominated in the different rivers depended on their origins. The rivers fed by glacial run-off transported significantly lower humic DOM compounds than the river running through a vegetated permafrost landscape. We used three experiments at different time points and different *in situ* conditions to evaluate what role the bacterial community plays in processing different DOM compounds. Bacteria within the class Gammaproteobacteria, especially of the order Alteromonadales (genera *Glaciecola*, *Colwellia, Pseudoalteromonas* and the SAR92 clade) can occur at high concentrations in coastal environments, where humic DOM compounds can be found in high abundances (Sosa *et al.,* 2015; Paulsen *et al.,* 2017; Sipler *et al.,* 2017). They are also known to be able to degrade a great variety of carbon sources, including humic like compounds. Interestingly, we found highest *in situ* abundances of these taxa in the fjord in July, when run-off was highest and in the first two experiments, with increased abundance at the end of the incubation (**Figure 10**). Likewise, only in these two first experiments, humic DOM compounds decreased over the course of the incubation, indicating that only a specific part of the residing bacterial community was able to degrade humic DOM (**Figure 10**).

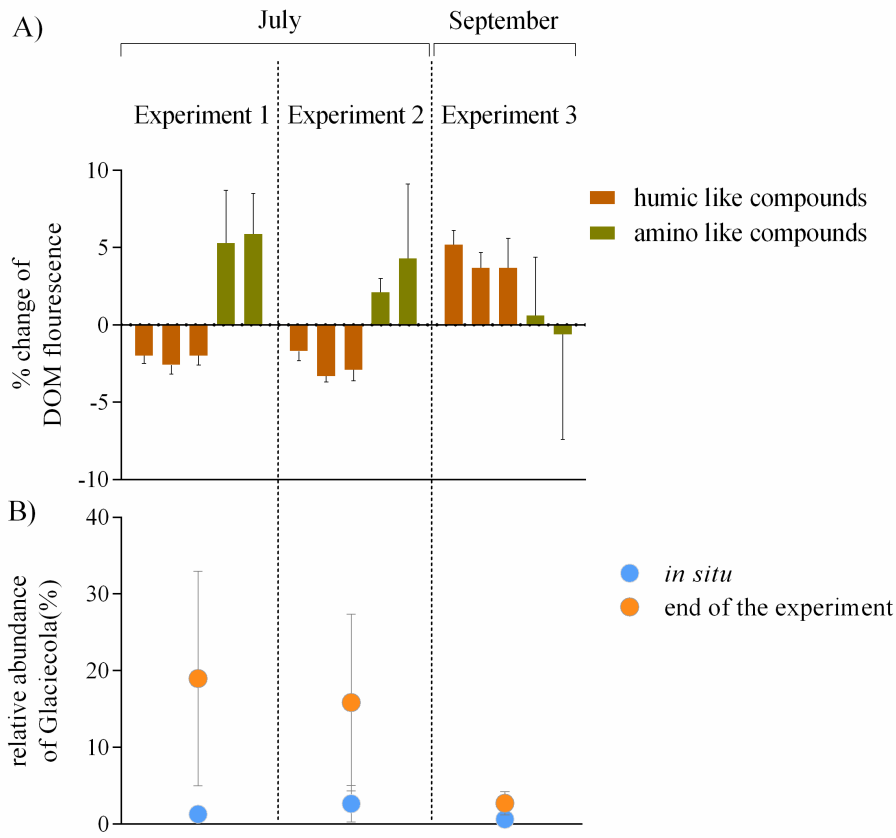

Figure 10: Changes observed in the incubation experiments performed at different time points in Young Sound regarding **A)** fluorescent DOM compounds and **B)** relative abundance of *Glaciecola*.

The relative abundance of OTUs correlated significantly with humic DOM components, both positively (e.g. *Balneatrix, Glaciecola* and SAR92 clade) and negatively (e.g. *Litoricola* and SAR86 clade). Especially the abundance of the genus *Glaciecola* was higher when natural humic DOM concentrations were elevated (**Paper II**) and in experiments in association with a decrease in humic DOM compounds (**Paper III** and **Figure 10**). Interestingly, correlations between taxa and DOM compounds were often only detectable at the OTU level. This indicates that strains within the same genus might have different functions.

We therefore focused in **Paper III** on identifying the taxa and OTUs that are capable to degrade humic compounds originating from permafrost and how they respond to increased inputs of this material in an experiment performed with an Arctic fjord microbial community from Kongsfjorden. This is especially relevant if the bacterial carbon uptake of humic DOM, via bacterial grazing, also affects higher trophic levels (Thingstad *et al.,* 2008; Sipler *et al.,* 2017).

We found an immediate response in diversity and activity upon tDOM addition, as the growth of predominantly large bacteria was increased, thereby contributing to more than 77% of the total bacterial abundance after five days of incubation (**Figure 11**). The growth of large bacteria corresponded to a change in the community composition caused by the rise of the genus *Glaciecola* which increased 2-fold within the first 12 hours and up to 138-fold after four days (**Figure 11**).

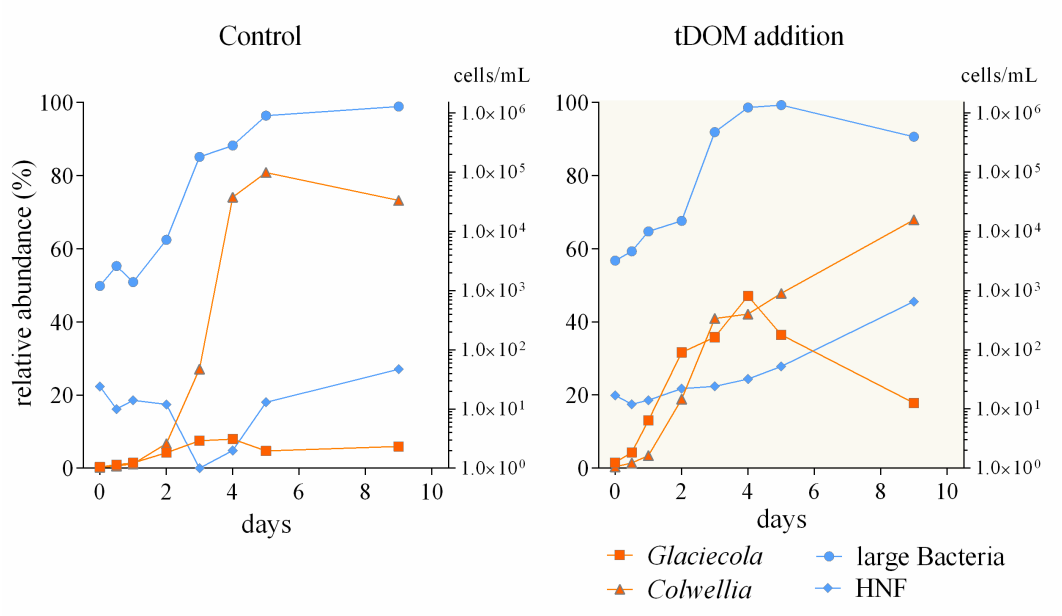

Figure 11: Change in absolute abundance of large bacteria and HNF (blue symbols) and relative abundance of the two most abundant taxa *Glaciecola* and *Colwellia* (orange symbols) over 9 days of incubation under A) control settings and B) after addition of tDOM.

Glaciecola and other genera of the family *Alteromonadaceae* are not known to initially dominate marine or coastal communities, but have shown rapid responses upon phytoplankton-derived DOM input (Eilers *et al.,* 2000; McCarren *et al.,* 2010;

Gómez-Consarnau *et al.,* 2012; Beier *et al.,* 2015). They have also experimentally been shown to increase in abundance due to the addition of terrestrial derived DOM (Sipler *et al.,* 2017). Besides *Glaciecola*, other taxa known to degrade complex organic matter, such as *Marinomonas* and *Colwellia* showed growth upon tDOM addition. They have both been associated with the breakdown of high molecular-weight organic compounds (Huston *et al.,* 2004; Methé *et al.,* 2005; Chandra *et al.,* 2015; Gontikaki *et al.,* 2015).

Interestingly, the abundance of *Glaciecola* declined towards the end of the experiment by 84%. At the same time there was a substantial increase of a group of bacterial grazers (**Figure 11**). Size-selective predator-prey interactions have been shown for *Glaciecola*, which first became abundant upon rapid utilization of phytoplankton derived DOM and were subsequently grazed, which caused a decline in their abundance (von Scheibner *et al.,* 2017). HNF did not increase in control incubations, where absolute abundance of bacteria was comparable high, but *Glaciecola* abundance was low (**Figure 11**). This suggests a specific predator-prey relation between *Glaciecola* and HNF in our experiment, which might be an important link in the microbial food web of Arctic fjord systems, with cascading effects on higher trophic levels, including ciliates, copepods and up to the top level predators.

Our results indicate that tDOM has various effects on the structure and activity of fjord microbial communities and that it can quickly be utilized by some marine taxa. We further observed that the different DOM compounds can shape the microbial community composition and that these responses could affect higher trophic levels and biogeochemical cycles. Increases in land-to-ocean tDOM fluxes will, therefore, be important to the overall productivity of the Arctic Ocean.

4.3 Methodological challenges

The studies presented in this PhD-thesis were part of two large projects and only possible because of years of planning behind these projects, long before I even started my PhD. Thus, I could benefit from well-organized sampling strategies, sample collection and sample processing plans. Details, for example, whether DNA or RNA should be used to analyze community composition, were decided based on first test results throughout the projects. While sequencing of DNA enables to capture the entire potential of the community, RNA, which is less stable than DNA, is better suitable to catch the more metabolically-active fraction of the community. We used DNA in **Paper I** and **Paper V**, and RNA in **Paper II, III** and **IV** for various molecular methods, including PCR, qPCR, cloning and sequencing.

In molecular microbiology, basically all methods have different distinctive independent limitations, which can affect final interpretations of the data. Every step, from sampling and biomass collection to sample processing, DNA and RNA extraction and sequencing, harbors risks. Permafrost samples, like those we used in **Paper I**, are due to the drilling process sensitive for contamination, as nucleic acid concentrations are low (Juck *et al.,* 2005). We therefore removed large parts of the outer layer of the permafrost core samples and due to the high sample resolution and replication rate, we were confident that contamination was avoided. Another aspect is that DNA has, due to the constant frozen conditions, a very long lifetime in permafrost and can keep its structural integrity even outside of bacterial cells (Willerslev *et al.,* 2004). Still, due to low amounts of nucleic acids in the samples, extraction of DNA was challenging and extraction of RNA was not possible.

Extraction of DNA and RNA from the marine water samples used in **Paper IV** and **V** was also complicated. Especially the samples taken at 1000 m depth had very low nucleic acid concentrations, which were sometimes below the detection limit. In contrast, summer surface sample had RNA concentrations of up to 1.4 µg/L sea water, since total biomass, including phytoplankton, was collected on the filters. This however, caused different problems during the analysis part, as over 90% of

sequences of these summer surface samples were from phytoplankton chloroplast 16S rRNAs and thereby reduced the sequencing coverage of the targetted prokaryotes. These chloroplast sequences were simply removed, since high-throughput sequencing produces a high read output. Rarefaction curve analysis showed that the remaining prokaryotic sequences were sufficient to cover the diversity in summer, while winter samples were more diverse and sequencing efforts were undersaturated.

Also the amplification of nucleic acids is sensitive to bias, as primer selection can influence specific population abundances. For example, the 16S rRNA gene primer used to characterize the marine microbial community in **Paper II, III, IV and V**, had a low affinity for the SAR11 cluster and therefore the relative abundance of other groups was slightly overestimated (Apprill *et al.,* 2015). Still, changes in community dynamics observed over the changing seasons were not affected, as also recently confirmed in a study testing the influence of different primer combinations on community dynamics of coastal marine bacteria (Wear *et al.,* 2018). Additionally, by acknowledging the methodological biases and combing several different methods, like quantitative PCR, cloning and sequencing as in **Paper V**, or 16S rRNA gene sequencing and metagenomics in **Paper I**, the individual biases can be reduced and the interpretations be strengthened.

However, some methodological biases cannot be avoided, simply because alternative methods have not been successfully established. For example, the incubations in **Paper III**, are as all incubation studies biased due to a so called “bottle effect” (Lee and Fuhrman, 1991; Massana *et al.,* 2001; Stewart *et al.,* 2012). Because of this bottle effect, the growth of certain bacteria is enhanced due to a combination of factors, including biofilm formation and binding of nutrients to the surface of the incubation container (Fogg and Calvario-Martinez, 1989; Fletcher, 1996). Also larger incubation volumes (>1000 L) can be affected (Calvo-Díaz *et al.,* 2011; Hosia *et al.,* 2014). We therefore decided to use shorter incubation times, followed the changes in growth and community composition daily and were thereby able to distinguish between bottle effects and tDOM effects in **Paper III**.

5. Conclusion and future perspective

The studies presented in this PhD-thesis address the extensive implications of climate change on Arctic microbial communities. The effects of climate change were evident in all analyzed environments, making descriptive studies that can be used as a historic record of the current microbial state, as presented in **Paper I, II, IV and V**, highly necessary in order to indicate how the Arctic is changing. We add substantial new insights in regard of community composition and drivers determining these structures in permafrost, fjord systems and the Arctic Ocean.

Our results indicate that permafrost microbial communities are much more complex than previously thought and that in future projects sampling strategies have to be adapted to resolve this complexity. Especially the discovery of the distinctively different community composition in the TZ and small scale changes over the depth of the AL highlight the necessity of a higher sampling resolution in order to understand the processes in permafrost soil. Future research should also focus on investigating environmental drivers, like carbon quality, that might cause this complex structuring, in more detail.

The descriptive and experimental analyses of the different marine systems also shed light on the central role of permafrost carbon in the entire Arctic ecosystem. Soil microbes are, especially under aerobic conditions, capable of quickly processing the carbon, available upon thaw, into CO_2, which is then released into the atmosphere. We followed the fate of permafrost derived carbon in marine environments and showed that, against the common perception, a large part of this carbon source is bioavailable and identified microbes, predominantly belonging to the genus *Glaciecola*, that are capable of degrading it. As this permafrost derived carbon caused a dramatic shift in the microbial community, which in turn affected higher trophic levels due to grazing, further research is needed to investigate this unexplored link in the microbial food web of Arctic marine systems.

We also showed that community structures in Arctic marine environments are highly affected by seasonal changes, but that additionally, regardless of season, water mass and history are crucial to explain abundance pattern, such as shown for ammonia oxidizing Thaumarchaeota. In future studies it will be important to identify the parameters behind the group of factors that collectively describe water masses, which are driving the distribution observed by us and whether this Thaumarchaeota niche separation is associated with different functional strategies.

Descriptive studies, as presented here, represent the first step to understand largely unexplored systems as the Arctic. Especially by identifying microbial patterns, we get one step closer to understand the players behind important biogeochemical cycles. We also need more research investigating the environmental drivers behind the observed pattern and the functions of the microbes. The latest technological advances allow for such analyses. For example, with Fourier transform-ion cyclotron resonance mass spectrometry (FT-ICR MS) carbon composition can be described with a much higher sensitivity (Nebbioso and Piccolo, 2013). The highly improved resolution of this important environmental parameter together with the in depth functional analysis using metagenomics and metatranscriptomics can provide new insights into how the environment influences microbial communities and how they functionally cope under different conditions (Ward *et al.,* 2017).

This study clearly shows that climate change has various impacts on the different Arctic ecosystems and that the microbial community responds to these changes. We have documented community changes by identifying abundance patterns and sentinels that are sensitive to the changes in their environment. When such community profiles are combined with functional analyses and connected to interdisciplinary studies, yet more information can be obtained, that gets us closer to grasp how these ecosystems function. We observed that climate change is altering the microbial community, predominantly in association with functional changes that causes increased CO_2 release into the atmosphere. This demonstrates that these results are not only relevant for the Arctic, but the entire global ecosystem and shows the importance of further research, along the line presented in this work.

References

Aagaard, K. and Carmack, E.C. (1989) The role of sea ice and other fresh water in the Arctic circulation. *J. Geophys. Res.* **94**: 14485.

Alonso-Sáez, L., Sánchez, O., Gasol, J.M., Balagué, V., and Pedrós-Alio, C. (2008) Winter-to-summer changes in the composition and single-cell activity of near-surface Arctic prokaryotes. *Environ. Microbiol.* **10**: 2444–2454.

Amon, R.M.W. (2003) Dissolved organic carbon distribution and origin in the Nordic Seas: Exchanges with the Arctic Ocean and the North Atlantic. *J. Geophys. Res.* **108**: 3221.

Amon, R.M.W., Rinehart, A.J., Duan, S., Louchouarn, P., Prokushkin, A., Guggenberger, G., *et al.,* (2012) Dissolved organic matter sources in large Arctic rivers. *Geochim. Cosmochim. Acta* **94**: 217–237.

Apprill, A., McNally, S., Parsons, R., and Weber, L. (2015) Minor revision to V4 region SSU rRNA 806R gene primer greatly increases detection of SAR11 bacterioplankton. *Aquat. Microb. Ecol.* **75**: 129–137.

Azam, F. and Malfatti, F. (2007) Microbial structuring of marine ecosystems. *Nat. Rev. Microbiol.*

Baas-Becking, L.G.M. (1934) Geobiologie of inleiding tot de milieukunde.

Beier, S., Rivers, A.R., Moran, M.A., and Obernosterer, I. (2015) The transcriptional response of prokaryotes to phytoplankton-derived dissolved organic matter in seawater. *Environ. Microbiol.* **17**: 3466–3480.

Blaud, A., Lerch, T.Z., Phoenix, G.K., and Osborn, A.M. (2015) Arctic soil microbial diversity in a changing world. *Res. Microbiol.* **166**: 796–813.

Borcard, D., Legendre, P., and Drapeau, P. (1992) Partialling out the Spatial Component of Ecological Variation. *Ecology* **73**: 1045–1055.

Bouvier, T.C. and del Giorgio, P.A. (2002) Compositional changes in free-living bacterial communities along a salinity gradient in two temperate estuaries. *Limnol. Oceanogr.* **47**: 453–470.

Brinkmeyer, R., Glöckner, F.-O., Helmke, E., and Amann, R. (2004) Predominance of ß-proteobacteria in summer melt pools on Arctic pack ice. *Limnol. Oceanogr.* **49**: 1013–1021.

Buchan, A., LeCleir, G.R., Gulvik, C.A., and González, J.M. (2014) Master recyclers: features and functions of bacteria associated with phytoplankton blooms. *Nat. Publ. Gr.* **12**:.

Calvo-Díaz, A., Díaz-Pérez, L., Suárez, L.Á., Morán, X.A.G., Teira, E., and Marañón, E. (2011) Decrease in the autotrophic-to-heterotrophic biomass ratio of picoplankton in oligotrophic marine waters due to bottle enclosure. *Appl. Environ. Microbiol.* **77**: 5739–46.

Chandra, R., Chowdhary, P., Ibarra, D., Rencoret, J., Romero, J., Speranza, M., *et al.,* (2015) Properties of bacterial laccases and their application in bioremediation of industrial wastes. *Environ. Sci. Process. Impacts* **17**: 326–342.

Christman, G.D., Cottrell, M.T., Popp, B.N., Gier, E., and Kirchman, D.L. (2011) Abundance, diversity, and activity of ammonia-oxidizing prokaryotes in the coastal Arctic ocean in summer and winter. *Appl. Environ. Microbiol.* **77**: 2026–34.

Citterio, M., Sejr, M.K., Langen, P.L., Mottram, R.H., Abermann, J., Larsen, S.H., *et al.,* (2017) Towards quantifying the glacial runoff signal in the freshwater input to Tyrolerfjord – Young Sound , NE Greenland. *Ambio* **46**: 146–159.

Cokelet, E.D., Tervalon, N., and Bellingham, J.G. (2008) Hydrography of the West Spitsbergen Current, Svalbard Branch: Autumn 2001. *J. Geophys. Res.* **113**: C01006.

Comeau, A.M., Li, W.K.W., Tremblay, J.-É., Carmack, E.C., and Lovejoy, C. (2011) Arctic Ocean Microbial Community Structure before and after the 2007 Record Sea Ice Minimum. *PLoS One* **6**: e27492.

Deng, J., Gu, Y., Zhang, J., Xue, K., Qin, Y., Yuan, M., *et al.,* (2015) Shifts of tundra bacterial and archaeal communities along a permafrost thaw gradient in Alaska. *Mol. Ecol.* **24**: 222–234.

Dittmar, T. and Kattner, G. (2003) The biogeochemistry of the river and shelf ecosystem of the Arctic Ocean: a review. *Mar. Chem.* **83**: 103–120.

Dutkiewicz, S., Sokolov, A.P., Scott, J., and Stone, P.H. (2005) A three-dimensional ocean-seaice-carbon cycle model and its coupling to a two-dimensional atmospheric model: uses in climate change studies.

Eilers, H., Pernthaler, J., and Amann, R. (2000) Succession of pelagic marine bacteria during enrichment: a close look at cultivation-induced shifts. *Appl. Environ. Microbiol.* **66**: 4634–40.

Elberling, B., Jakobsen, B.H., Berg, P., Søndergaard, J., and Sigsgaard, C. (2004) Influence of Vegetation, Temperature, and Water Content on Soil Carbon Distribution and Mineralization in

Four High Arctic Soils. *Arctic, Antarct. Alp. Res.* **36**: 528–538.

Elberling, B., Michelsen, A., Schädel, C., Schuur, E.A.G., Christiansen, H.H., Berg, L., *et al.,* (2013) Long-term CO2 production following permafrost thaw. *Nat. Clim. Chang.* **3**: 890–894.

Feng, X., Vonk, J.E., van Dongen, B.E., Gustafsson, Ö., Semiletov, I.P., Dudarev, O. V, *et al.,* (2013) Differential mobilization of terrestrial carbon pools in Eurasian Arctic river basins. *Proc. Natl. Acad. Sci. U. S. A.* **110**: 14168–73.

Fichot, C.G., Kaiser, K., Hooker, S.B., Amon, R.M.W., Babin, M., Bélanger, S., *et al.,* (2013) Pan-Arctic distributions of continental runoff in the Arctic Ocean. *Sci. Rep.* **3**: 1053.

Fierer, N., Bradford, M.A., and Jackson, R.B. (2007) TOWARD AN ECOLOGICAL CLASSIFICATION OF SOIL BACTERIA. *Ecology* **88**: 1354–1364.

Fletcher, M. (1996) Bacterial Adhesion: Molecular and Ecological Diversity Wiley.

Fogg, G.E. and Calvario-Martinez, O. (1989) Effects of bottle size in determinations of primary productivity by phytoplankton. *Hydrobiologia* **173**: 89–94.

Fortin, M.J., Dale, M.R.T., and Hoef, J. (2002) Spatial analysis in ecology. *Encycl. Environmetrics* **4**: 2051–2058.

Frank-Fahle, B.A., Yergeau, É., Greer, C.W., Lantuit, H., Wagner, D., Kuhry, P., *et al.,* (2014) Microbial Functional Potential and Community Composition in Permafrost-Affected Soils of the NW Canadian Arctic. *PLoS One* **9**: e84761.

Galand, P.E., Potvin, M., Casamayor, E.O., and Lovejoy, C. (2010) Hydrography shapes bacterial biogeography of the deep Arctic Ocean. *ISME J.* **4**: 564–576.

Garneau, M.È., Vincent, W.F., Terrado, R., and Lovejoy, C. (2009) Importance of particle-associated bacterial heterotrophy in a coastal Arctic ecosystem. *J. Mar. Syst.* **75**: 185–197.

Giovannoni, S.J. and Stingl, U. (2005) Molecular diversity and ecology of microbial plankton. *Nature* **437**: 343–348.

Gittel, A., Bárta, J., Kohoutová, I., Schnecker, J., Wild, B., Capek, P., *et al.,* (2014) Site- and horizon-specific patterns of microbial community structure and enzyme activities in permafrost-affected soils of Greenland. *Front. Microbiol.* **5**: 541.

Gómez-Consarnau, L., Lindh, M. V., Gasol, J.M., and Pinhassi, J. (2012) Structuring of

bacterioplankton communities by specific dissolved organic carbon compounds. *Environ. Microbiol.* **14**: 2361–2378.

Gontikaki, E., Thornton, B., Cornulier, T., Witte, U., Cox, M., and Joint, I. (2015) Occurrence of Priming in the Degradation of Lignocellulose in Marine Sediments. *PLoS One* **10**: e0143917.

Grosse, G., Romanovsky, V., Jorgenson, T., Anthony, K.W., Brown, J., and Overduin, P.P. (2011) Vulnerability and feedbacks of permafrost to climate change. *Eos, Trans. Am. Geophys. Union* **92**: 73.

Grzymski, J.J., Riesenfeld, C.S., Williams, T.J., Dussaq, A.M., Ducklow, H., Erickson, M., *et al.,* (2012) A metagenomic assessment of winter and summer bacterioplankton from Antarctica Peninsula coastal surface waters. *ISME J.* **6**: 1901–1915.

Guerrero, M.A. and Jones, R.D. (1996) Photoinhibition of marine nitrifying bacteria. I. Wavelength-dependent response. *Mar. Ecol. Prog. Ser.* **141**: 183–192.

Gutiérrez, M.H., Galand, P.E., Moffat, C., and Pantoja, S. (2015) Melting glacier impacts community structure of Bacteria, Archaea and Fungi in a Chilean Patagonia fjord. *Environ. Microbiol.* **17**: 3882–3897.

Hansell, D.A. (2004) Degradation of Terrigenous Dissolved Organic Carbon in the Western Arctic Ocean. *Science (80-.).* **304**: 858–861.

Hansell, D.A. (2013) Recalcitrant Dissolved Organic Carbon Fractions. *Ann. Rev. Mar. Sci.* **5**: 421–445.

Hansen, A.A., Herbert, R.A., Mikkelsen, K., Jensen, L.L., Kristoffersen, T., Tiedje, J.M., *et al.,* (2007) Viability, diversity and composition of the bacterial community in a high Arctic permafrost soil from Spitsbergen, Northern Norway. *Environ. Microbiol.* **9**: 2870–2884.

Hedges, J.I. (2002) Sedimentary Organic Matter Preservation and Atmospheric O2 Regulation. In, Gianguzza,A., Pelizzetti,E., and Sammartano,S. (eds), *Chemistry of Marine Water and Sediments SE - 4*. Springer Berlin Heidelberg, pp. 105–123.

Holland, M.M., Finnis, J., Serreze, M.C., Holland, M.M., Finnis, J., and Serreze, M.C. (2006) Simulated Arctic Ocean Freshwater Budgets in the Twentieth and Twenty-First Centuries. *J. Clim.* **19**: 6221–6242.

Holmes, R.M., Coe, M.T., Fiske, G.J., Gurtovaya, T., Mcclelland, J.W., Shiklomanov, A.I., *et al.,* (2012) Climate Change Impacts on the Hydrology and Biogeochemistry of Arctic Rivers. In,

Climatic Change and Global Warming of Inland Waters: Impacts and Mitigation for Ecosystems and Societies., pp. 1–26.

Holmes, R.M., McClelland, J.W., Raymond, P.A., Frazer, B.B., Peterson, B.J., and Stieglitz, M. (2008) Lability of DOC transported by Alaskan rivers to the Arctic Ocean. *Geophys. Res. Lett.* **35**: L03402.

Hosia, A., Augustin, C.B., Dinasquet, J., Granhag, L., Paulsen, M.L., Riemann, L., *et al.,* (2014) Autumnal bottom-up and top-down impacts of Cyanea capillata: A mesocosm study. *J. Plankton Res.* **37**: 1042–1055.

Hugelius, G., Strauss, J., Zubrzycki, S., Harden, J.W., Schuur, E.A.G., Ping, C.-L., *et al.,* (2014) Estimated stocks of circumpolar permafrost carbon with quantified uncertainty ranges and identified data gaps. *Biogeosciences* **11**: 6573–6593.

Hultman, J., Waldrop, M.P., Mackelprang, R., David, M.M., McFarland, J., Blazewicz, S.J., *et al.,* (2015) Multi-omics of permafrost, active layer and thermokarst bog soil microbiomes. *Nature* **521**: 208–212.

Humlum, O., Instanes, A., and Sollid, J.L. (2003) Permafrost in Svalbard: a review of research history, climatic background and engineering challenges. *Polar Res.* **22**: 191–215.

Huston, A.L., Methe, B., and Deming, J.W. (2004) Purification, characterization, and sequencing of an extracellular cold-active aminopeptidase produced by marine psychrophile Colwellia psychrerythraea strain 34H. *Appl. Environ. Microbiol.* **70**: 3321–3328.

Jihao, N., Azam, F., Sanders, S. (2011) Microbial Carbon Pump in the Ocean Jiao,N., Azam,F., and Sean,S. (eds) Science.

Juck, D.F., Whissell, G., Steven, B., Pollard, W., Mckay, C.P., Greer, C.W., *et al.,* (2005) Utilization of fluorescent microspheres and a GFP-marked strain for assessing microbiological contamination of permafrost and ground ice core samples from the Canadian High Arctic. *Appl. Environ. Microbiol.* **71**: 1035–1041.

Kim, H.M., Lee, M.J., Jung, J.Y., Hwang, C.Y., Kim, M., Ro, H.-M., *et al.,* (2016) Vertical distribution of bacterial community is associated with the degree of soil organic matter decomposition in the active layer of moist acidic tundra. *J. Microbiol.* **54**: 713–723.

Kirchman, D.L., Elifantz, H., Dittel, A.I., Malmstrom, R.R., and Cottrell, M.T. (2007) Standing stocks and activity of Archaea and Bacteria in the western Arctic Ocean. *Limnol. Oceanogr.* **52**:

495–507.

Kirchman, D.L., Morán, X.A.G., and Ducklow, H. (2009) Microbial growth in the polar oceans - Role of temperature and potential impact of climate change. *Nat. Rev. Microbiol.* **7**: 451–459.

Könneke, M., Bernhard, A.E., De La Torre, J.R., Walker, C.B., Waterbury, J.B., and Stahl, D.A. (2005) Isolation of an autotrophic ammonia-oxidizing marine archaeon. *Nature* **437**: 543–546.

Koyama, A., Wallenstein, M.D., Simpson, R.T., and Moore, J.C. (2014) Soil bacterial community composition altered by increased nutrient availability in Arctic tundra soils. *Front. Microbiol.* **5**: 516.

Kritzberg, E.S., Duarte, C.M., and Wassmann, P. (2010) Changes in Arctic marine bacterial carbon metabolism in response to increasing temperature. *Polar Biol.* **33**: 1673–1682.

Kwok, R. and Cunningham, G.F. (2010) Contribution of melt in the Beaufort Sea to the decline in Arctic multiyear sea ice coverage: 1993-2009. *Geophys. Res. Lett.* **37**: 1023–1035.

Lee, H., Schuur, E.A.G., Inglett, K.S., Lavoie, M., and Chanton, J.P. (2012) The rate of permafrost carbon release under aerobic and anaerobic conditions and its potential effects on climate. *Glob. Chang. Biol.* **18**: 515–527.

Lee, S. and Fuhrman, J.A. (1991) Species composition shift of confined bacterioplankton studies at the level of community DNA. *Mar Ecol Prog Ser* **79**: 195–201.

Legendre, P. and Fortin, M.J. (1989) Spatial pattern and ecological analysis. *Vegetatio* **80**: 107–138.

Levipan, H.A., Molina, V., and Fernandez, C. (2014) Nitrospina-like bacteria are the main drivers of nitrite oxidation in the seasonal upwelling area of the Eastern South Pacific (Central Chile ~36°S). *Environ. Microbiol. Rep.* **6**: 565–573.

Li, W.K.W., McLaughlin, F.A., Lovejoy, C., and Carmack, E.C. (2009) Smallest algae thrive as the arctic ocean freshens. *Science (80-.).* **326**: 539.

Mackelprang, R., Waldrop, M.P., DeAngelis, K.M., David, M.M., Chavarria, K.L., Blazewicz, S.J., *et al.,* (2011) Metagenomic analysis of a permafrost microbial community reveals a rapid response to thaw. *Nature* **480**: 368–371.

Massana, R., Pedros-Alio, C., Casamayor, E.O., and Gasol, J.M. (2001) Changes in marine bacterioplankton phylogenetic composition during incubations designed to measure biogeochemically significant parameters. *Limnol. Oceanogr.* **46**: 1181–1188.

McCalley, C.K., Woodcroft, B.J., Hodgkins, S.B., Wehr, R.A., Kim, E.-H., Mondav, R., *et al.,* (2014) Methane dynamics regulated by microbial community response to permafrost thaw. *Nature* **514**: 478–481.

McCarren, J., Becker, J.W., Repeta, D.J., Shi, Y., Young, C.R., Malmstrom, R.R., *et al.,* (2010) Microbial community transcriptomes reveal microbes and metabolic pathways associated with dissolved organic matter turnover in the sea. *Proc. Natl. Acad. Sci. U. S. A.* **107**: 16420–7.

Merbt, S.N., Stahl, D.A., Casamayor, E.O., Martí, E., Nicol, G.W., and Prosser, J.I. (2012) Differential photoinhibition of bacterial and archaeal ammonia oxidation. *FEMS Microbiol. Lett.* **327**: 41–46.

Methé, B.A., Nelson, K.E., Deming, J.W., Momen, B., Melamud, E., Zhang, X., *et al.,* (2005) The psychrophilic lifestyle as revealed by the genome sequence of Colwellia psychrerythraea 34H through genomic and proteomic analyses. *Proc. Natl. Acad. Sci. U. S. A.* **102**: 10913–8.

Middelboe, M. and Lundsgaard, C. (2003) Microbial activity in the Greenland Sea : role of DOC lability, mineral nutrients and temperature. *Aquat. Microb. Ecol.* **32**: 151–163.

Mincer, T.J., Church, M.J., Taylor, L.T., Preston, C., Karl, D.M., and DeLong, E.F. (2007) Quantitative distribution of presumptive archaeal and bacterial nitrifiers in Monterey Bay and the North Pacific Subtropical Gyre. *Environ. Microbiol.* **9**: 1162–1175.

Murray, A.E., Preston, C.M., Massana, R., Taylor, L.T., Blakis, A., Wu, K., and DeLong, E.F. (1998) Seasonal and spatial variability of bacterial and archaeal assemblages in the coastal waters near Anvers Island, Antarctica. *Appl. Environ. Microbiol.* **64**: 2585–95.

Murray, C., Markager, S., Stedmon, C.A., Juul-Pedersen, T., Sejr, M.K., and Bruhn, A. (2015) The influence of glacial melt water on bio-optical properties in two contrasting Greenlandic fjords. *Estuar. Coast. Shelf Sci.* **163**: 72–83.

Nebbioso, A. and Piccolo, A. (2013) Molecular characterization of dissolved organic matter (DOM): a critical review. *Anal. Bioanal. Chem.* **405**: 109–124.

Oliverio, A.M., Bradford, M.A., and Fierer, N. (2017) Identifying the microbial taxa that consistently respond to soil warming across time and space. *Glob. Chang. Biol.* **23**: 2117–2129.

Opsahl, S., Benner, R., and Amon, R.M.W. (1999) Major flux of terrigenous dissolved organic matter through the Arctic Ocean. *Limnol. Oceanogr.* **44**: 2017–2023.

Padmanabhan, P., Padmanabhan, S., DeRito, C., Gray, A., Gannon, D., Snape, J.R., *et al.,* (2003)

Respiration of 13C-labeled substrates added to soil in the field and subsequent 16S rRNA gene analysis of 13C-labeled soil DNA. *Appl. Environ. Microbiol.* **69**: 1614–22.

Paulsen, M.L., Nielsen, S.E.B., Müller, O., Møller, E.F., Stedmon, C.A., Juul-Pedersen, T., *et al.,* (2017) Carbon Bioavailability in a High Arctic Fjord Influenced by Glacial Meltwater, NE Greenland. *Front. Mar. Sci.* **4**: 176.

Polyakov, I. V., Beszczynska, A., Carmack, E.C., Dmitrenko, I.A., Fahrbach, E., Frolov, I.E., *et al.,* (2005) One more step toward a warmer Arctic. *Geophys. Res. Lett.* **32**: 1–4.

Randelhoff, A., Sundfjord, A., and Reigstad, M. (2015) Seasonal variability and fluxes of nitrate in the surface waters over the Arctic shelf slope. *Geophys. Res. Lett.* **42**: 3442–3449.

Reinthaler, T., van Aken, H.M., and Herndl, G.J. (2010) Major contribution of autotrophy to microbial carbon cycling in the deep North Atlantic's interior. *Deep Sea Res. Part II Top. Stud. Oceanogr.* **57**: 1572–1580.

Rofner, C., Peter, H., Catalán, N., Drewes, F., Sommaruga, R., and Pérez, M.T. (2017) Climate-related changes of soil characteristics affect bacterial community composition and function of high altitude and latitude lakes. *Glob. Chang. Biol.* **23**: 2331–2344.

Romanovsky, V.E., Smith, S.L., and Christiansen, H.H. (2010) Permafrost thermal state in the polar Northern Hemisphere during the international polar year 2007-2009: a synthesis. *Permafr. Periglac. Process.* **21**: 106–116.

Santoro, A.E., Saito, M.A., Goepfert, T.J., Lamborg, C.H., Dupont, C.L., and DiTullio, G.R. (2017) Thaumarchaeal ecotype distributions across the equatorial Pacific Ocean and their potential roles in nitrification and sinking flux attenuation. *Limnol. Oceanogr.* **62**: 1984–2003.

von Scheibner, M., Sommer, U., and Jürgens, K. (2017) Tight Coupling of Glaciecola spp. and Diatoms during Cold-Water Phytoplankton Spring Blooms. *Front. Microbiol.* **8**: 27.

Schuur, E.A.G., Bockheim, J., Canadell, J.G., Euskirchen, E., Field, C.B., Goryachkin, S. V., *et al.,* (2008) Vulnerability of Permafrost Carbon to Climate Change: Implications for the Global Carbon Cycle. *Bioscience* **58**: 701–714.

Schuur, E.A.G., Vogel, J.G., Crummer, K.G., Lee, H., Sickman, J.O., and Osterkamp, T.E. (2009) The effect of permafrost thaw on old carbon release and net carbon exchange from tundra. *Nature* **459**: 556–559.

Screen, J.A. and Simmonds, I. (2010) The central role of diminishing sea ice in recent Arctic

temperature amplification. *Nature* **464**: 1334–1337.

Serreze, M., Walsh, J., and Iii, F.C. (2000) Observational evidence of recent change in the northern high-latitude environment. *Clim. Change* 159–207.

Shimada, K., Kamoshida, T., Itoh, M., Nishino, S., Carmack, E., McLaughlin, F., *et al.,* (2006) Pacific Ocean inflow: Influence on catastrophic reduction of sea ice cover in the Arctic Ocean. *Geophys. Res. Lett.* **33**: L08605.

Sintes, E., Bergauer, K., De Corte, D., Yokokawa, T., and Herndl, G.J. (2013) Archaeal *amo* A gene diversity points to distinct biogeography of ammonia-oxidizing *Crenarchaeota* in the ocean. *Environ. Microbiol.* **15**: 1647–1658.

Sintes, E., De Corte, D., Haberleitner, E., and Herndl, G.J. (2016) Geographic Distribution of Archaeal Ammonia Oxidizing Ecotypes in the Atlantic Ocean. *Front. Microbiol.* **7**: 77.

Sintes, E., De Corte, D., Ouillon, N., and Herndl, G.J. (2015) Macroecological patterns of archaeal ammonia oxidizers in the Atlantic Ocean. *Mol. Ecol.* **24**: 4931–4942.

Sipler, R.E., Baer, S.E., Connelly, T.L., Frischer, M.E., Roberts, Q.N., Yager, P.L., and Bronk, D.A. (2017) Chemical and photophysiological impact of terrestrially-derived dissolved organic matter on nitrate uptake in the coastal western Arctic. *Limnol. Oceanogr.* **62**: 1881–1894.

Sipler, Kellogg, C.T.E., Connelly, T.L., Roberts, Q.N., Yager, P.L., and Bronk, D.A. (2017) Microbial community response to terrestrially derived dissolved organic matter in the coastal Arctic. *Front. Microbiol.* **8**: 1018.

Sosa, O.A., Gifford, S.M., Repeta, D.J., and Delong, E.F. (2015) High molecular weight dissolved organic matter enrichment selects for methylotrophs in dilution to extinction cultures. *ISME J* **9**: 2725–2739.

Stein, R. and Macdonald, R.W. (2004) Organic Carbon Budget: Arctic Ocean vs. Global Ocean. In, Stein,R. and MacDonald,R. (eds), *The Organic Carbon Cycle in the Arctic Ocean SE - 8*. Springer Berlin Heidelberg, pp. 315–322.

de Steur, L., Hansen, E., Mauritzen, C., Beszczynska-Möller, A., and Fahrbach, E. (2014) Impact of recirculation on the East Greenland Current in Fram Strait: Results from moored current meter measurements between 1997 and 2009. *Deep Sea Res. Part I Oceanogr. Res. Pap.* **92**: 26–40.

Stewart, F.J., Dalsgaard, T., Young, C.R., Thamdrup, B., Revsbech, N.P., Ulloa, O., *et al.,* (2012) Experimental Incubations Elicit Profound Changes in Community Transcription in OMZ

Bacterioplankton. *PLoS One* **7**: e37118.

Stigebrandt, A. (2012) Hydrodynamics and Circulation of Fjords. In, *Encyclopedia of Lakes and Reservoirs*. Springer, Dordrecht, pp. 327–344.

Stigebrandt, A., Aure, J., Stigebrandt, A., and Aure, J. (1989) Vertical Mixing in Basin Waters of Fjords. *J. Phys. Oceanogr.* **19**: 917–926.

Stroeve, J.C., Markus, T., Boisvert, L., Miller, J., and Barrett, A. (2014) Changes in Arctic melt season and implications for sea ice loss. *Geophys. Res. Lett.* **41**: 1216–1225.

Tarnocai, C., Canadell, J.G., Schuur, E.A.G., Kuhry, P., Mazhitova, G., and Zimov, S. (2009) Soil organic carbon pools in the northern circumpolar permafrost region. *Global Biogeochem. Cycles* **23**: n/a-n/a.

Taş, N., Prestat, E., McFarland, J.W., Wickland, K.P., Knight, R., Berhe, A.A., *et al.,* (2014) Impact of fire on active layer and permafrost microbial communities and metagenomes in an upland Alaskan boreal forest. *ISME J.* **8**: 1904–1919.

Thingstad, T.F., Bellerby, R.G.J., Bratbak, G., Børsheim, K.Y., Egge, J.K., Heldal, M., *et al.,* (2008) Counterintuitive carbon-to-nutrient coupling in an Arctic pelagic ecosystem. *Nature* **455**: 387–390.

Torsvik, V., Øvreås, L., and Thingstad, T.F. (2002) Prokaryotic diversity - Magnitude, dynamics, and controlling factors. *Science (80-.).* **296**: 1064–1066.

Trenberth, K.E. and Josey, S.A. (2007) Observations: surface and atmospheric climate change. *Changes* **164**: 235–336.

Urtizberea, A., Dupont, N., Rosland, R., and Aksnes, D.L. (2013) Sensitivity of euphotic zone properties to CDOM variations in marine ecosystem models. *Ecol. Modell.* **256**: 16–22.

Vincent, W.F. (2010) Microbial ecosystem responses to rapid climate change in the Arctic. *ISME J.* **4**: 1087–1090.

Vonk, J.E. and Gustafsson, Ö. (2013) Permafrost-carbon complexities. *Nat. Geosci.* **6**: 675–676.

Vonk, J.E., Mann, P.J., Davydov, S., Davydova, A., Spencer, R.G.M., Schade, J., *et al.,* (2013) High biolability of ancient permafrost carbon upon thaw. *Geophys. Res. Lett.* **40**: 2689–2693.

Walczowski, W. and Piechura, J. (2006) New evidence of warming propagating toward the Arctic

Ocean. *Geophys. Res. Lett.* **33**: L12601.

Ward, C.P., Nalven, S.G., Crump, B.C., Kling, G.W., and Cory, R.M. (2017) Photochemical alteration of organic carbon draining permafrost soils shifts microbial metabolic pathways and stimulates respiration. *Nat. Commun.* **8**:.

Wear, E.K., Wilbanks, E.G., Nelson, C.E., and Carlson, C.A. (2018) Primer selection impacts specific population abundances but not community dynamics in a monthly time-series 16S rRNA gene amplicon analysis of coastal marine bacterioplankton. *Environ. Microbiol.*

Wilhelm, R.C., Niederberger, T.D., Greer, C., and Whyte, L.G. (2011) Microbial diversity of active layer and permafrost in an acidic wetland from the Canadian High Arctic. *Can. J. Microbiol.* **57**: 303–315.

Willerslev, E., Hansen, A.J., and Poinar, H.N. (2004) Isolation of nucleic acids and cultures from fossil ice and permafrost. *Trends Ecol. Evol.* **19**: 141–147.

de Wit, R. and Bouvier, T. (2006) "Everything is everywhere, but, the environment selects"; what did Baas Becking and Beijerinck really say? *Environ. Microbiol.* **8**: 755–758.

Worden, A.Z., Follows, M.J., Giovannoni, S.J., Wilken, S., Zimmerman, A.E., and Keeling, P.J. (2015) Rethinking the marine carbon cycle: Factoring in the multifarious lifestyles of microbes. *Science (80-.).* **347**:.

Wuchter, C., Abbas, B., Coolen, M.J.L., Herfort, L., van Bleijswijk, J., Timmers, P., *et al.,* (2006) Archaeal nitrification in the ocean. *Proc. Natl. Acad. Sci. U. S. A.* **103**: 12317–22.

Xie, H., Bélanger, S., Song, G., Benner, R., Taalba, A., Blais, M., *et al.,* (2012) Photoproduction of ammonium in the southeastern Beaufort Sea and its biogeochemical implications. *Biogeosciences* **9**: 3047–3061.

Xue, K., M. Yuan, M., J. Shi, Z., Qin, Y., Deng, Y., Cheng, L., *et al.,* (2016) Tundra soil carbon is vulnerable to rapid microbial decomposition under climate warming. *Nat. Clim. Chang.* **6**: 595–600.

Yang, S., Wen, X., Jin, H., Wu, Q., and Chavarria, K. (2012) Pyrosequencing Investigation into the Bacterial Community in Permafrost Soils along the China-Russia Crude Oil Pipeline (CRCOP). *PLoS One* **7**: e52730.

Yergeau, E., Hogues, H., Whyte, L.G., and Greer, C.W. (2010) The functional potential of high Arctic permafrost revealed by metagenomic sequencing, qPCR and microarray analyses. *ISME*

J. **4**: 1206–1214.

Zehr, J.P. and Ward, B.B. (2002) Nitrogen cycling in the ocean: New perspectives on processes and paradigms. *Appl. Environ. Microbiol.* **68**: 1015–1024.

I

Disentangling the complexity of permafrost soil by using high resolution profiling of microbial community composition, key functions and respiration rates

Running title:

High resolution permafrost microbial profile

Authors:

Oliver Müller[a], Toke Bang-Andreasen[b,c], Richard Allen White III[f], Bo Elberling[d], Neslihan Taş[e], Timothy Kneafsey[e], Janet K. Jansson[f], Lise Øvreås[a,g]

Author Affiliation:

[a]Department of Biology, University of Bergen, Norway, [b]Department of Environmental Science, Aarhus University, DK-4000 Roskilde, Denmark, [c]Department of Biology, University of Copenhagen, DK-2100 Copenhagen, Denmark, [d]Center for Permafrost (CENPERM), Department of Geosciences and Natural Resource Management, University of Copenhagen, DK-1350 Copenhagen, Denmark, [e]Lawrence Berkeley National Laboratory, US, [f]Pacific Northwest National Laboratory, US, [g]University Center in Svalbard, UNIS

Corresponding author:

Oliver Müller

University of Bergen, Department of Biology, Marine Microbiology Research Group

Thormøhlensgt. 53B, 5006 Bergen, Norway

e-mail: oliver.muller@uib.no

Originality-Significance Statement:

The work presented here is addressing one of the most pressing aspects regarding global warming, the fate of carbon currently locked in permafrost. Organic matter immobilized in the frozen soil is increasingly available due to temperature rises in the Arctic and thereby exposed to degradation by microbes. We used state of the art next-generation sequencing techniques to identify the responsible microbial communities and revealed, by using an unprecedented high vertical sampling resolution, novel insights into the structure and diversity of permafrost microbial communities. We further linked community composition, gene function and respiration measurements to address if and how they are connected. This work provides valuable new knowledge within the field of permafrost microbiology and further strengthens the general importance of microbes as the main drivers of processes that determine the balance of carbon storage and release in the Arctic. Our sampling strategy highlights the importance of high resolution microbial profiling of permafrost soils, in order to identify the highly variable communities which ultimately respond differently in regard to CO_2 production under thawing conditions. This information is of utter importance for projecting permafrost greenhouse gas emissions related to microbial activity.

Summary:

Thawing permafrost can stimulate microbial activity, leading to faster decomposition of formerly preserved organic matter and CO_2 release. Detailed knowledge about the vertical distribution of the responsible microbial community that is changing with increasing soil depth is limited. In this study, we determined the microbial community composition from cores sampled in a HighArctic heath at Svalbard, Norway; spanning from the active layer (AL) into the permafrost layer (PL). A special aim has been on identifying a layer of recently thawed soil, the transition zone (TZ), which might provide new insights into the fate of thawing permafrost. A unique sampling strategy allowed us to observe a diverse and gradually shifting microbial community in the AL, a Bacteroidetes dominated community in the TZ, and throughout the PL, a community strongly dominated by a single Actinobacteria family (*Intrasporangiaceae*). The contrasting abundances of these two taxa caused a community difference of about 60%, just within three centimeters from TZ to PL. We incubated sub-samples at about 5°C and measured highest CO_2 production rates under aerobic incubations, yet contrasting for five different layers and correlating to the microbial community composition. This high resolution strategy provides new insights on how microbial communities are structured in permafrost and a better understanding of how they respond to thaw.

Introduction:

Permafrost constitutes 25% of Earth's terrestrial surface and stores a vast amount of buried, ancient carbon (C) equaling about half of the global belowground soil organic matter (SOM) pool (Hugelius *et al.*, 2014). The current warming in the Arctic is therefore of special concern, as this may trigger increased microbial activity, leading to faster decomposition of formerly preserved organic matter and release of greenhouse gases such as carbon dioxide (CO_2) and methane (CH_4) (Schuur *et al.*, 2009; Grosse *et al.*, 2011; Mackelprang *et al.*, 2011; Xue *et al.*, 2016).

Permafrost thaw has expanded dramatically across the Arctic, as measured by the increasing extent of active layer thickness (ALT) in the soil (Jorgenson *et al.*, 2001; Åkerman and Johansson, 2008; Romanovsky *et al.*, 2010; Hayes *et al.*, 2014). The active layer (AL) is the upper part of the permafrost, undergoing seasonal freezing-thawing cycles, while the permafrost layer (PL) remains constantly frozen throughout the year. Together, this is the underlying reason for the microbial differences between those layers (Jansson and Taş, 2014).

Several studies of Arctic permafrost have shown a higher microbial diversity, biomass and activity in the AL, which is decreasing towards the PL (Yergeau *et al.*, 2010; Mackelprang *et al.*, 2011; Frank-Fahle *et al.*, 2014; Gittel, Bárta, Kohoutová, Schnecker, *et al.*, 2014; Taş *et al.*, 2014; Deng *et al.*, 2015). However, the impact of microbes on SOM degradation processes and greenhouse gas production remains unclear. Only a few studies have combined microbial community composition and activity measurements. Interestingly, experiments showed that microbial communities in the PL changed rapidly in structure and function upon thaw, indicating that the newly available SOM can be processed instantly (Mackelprang *et al.*, 2011; Deng *et al.*, 2015). Whether this degradation will result in increased CO_2 or CH_4 fluxes depends strongly on conditions at the permafrost site, including soil type, water content and if aerobic or anaerobic conditions are dominating (Lee *et al.*, 2012; Elberling *et al.*, 2013). Additionally, the microbial

contribution to greenhouse gas emissions is not fully understood (Elberling *et al.*, 2004; McCalley *et al.*, 2014).

One important challenge in all soil studies is the heterogeneous character of a soil profile (Elkateb *et al.*, 2003). Nevertheless, most permafrost studies compare microbial communities based on broad scales, comparing surface (AL) with deep (PL) samples and knowledge regarding fine-scale shifts throughout the soil core is still scarce. In this study we therefore investigated the changes in microbial community structure along a fine scaled depth profile, following, in a high resolution (every 3-4 cm), the transition from AL into the PL in a two-meter soil core from Svalbard. Sub-samples were thawed and incubated at 4 (±1) °C and microbial activity response was measured using gas flux analysis (CO_2, CH_4 and N_2O) over intervals of hours to months.

Our high resolution analysis therefore aims to precisely capture the microbial community composition throughout a permafrost core and to identify potential connections between community structure and greenhouse gas fluxes. This information is crucial to improve computational predictions of climate change effects that include microbial processes (Schwalm *et al.*, 2010). In order to better understand these processes we need detailed knowledge on how permafrost communities are structured and on their metabolic response to thaw.

Results:

Soil characteristics

The soil structure throughout the core was found to be homogenous (Figure 1a), as confirmed using X-ray Computer Tomography (Figure 1e), where estimated bulk densities ranged between 0.3-0.4 g cm^{-3}. The soil sampling site is covered with Late Holocene loess deposits and is characterized by a high silt/sand content of up to ~47% (Bang-Andreasen *et al.*, 2017). Due to the high silt/sand content the site is relatively well-drained. In this location, the combination of continuous sedimentation and freezing conditions resulted in thickening of the permafrost layer, where organic C surface layers were buried with

95 time and can be observed throughout the core in thin layers (Figure 1a). This is reflected in the

96 homogenous character of soil properties such as total carbon (TC), total nitrogen (TN) and pH (Figure 1f).

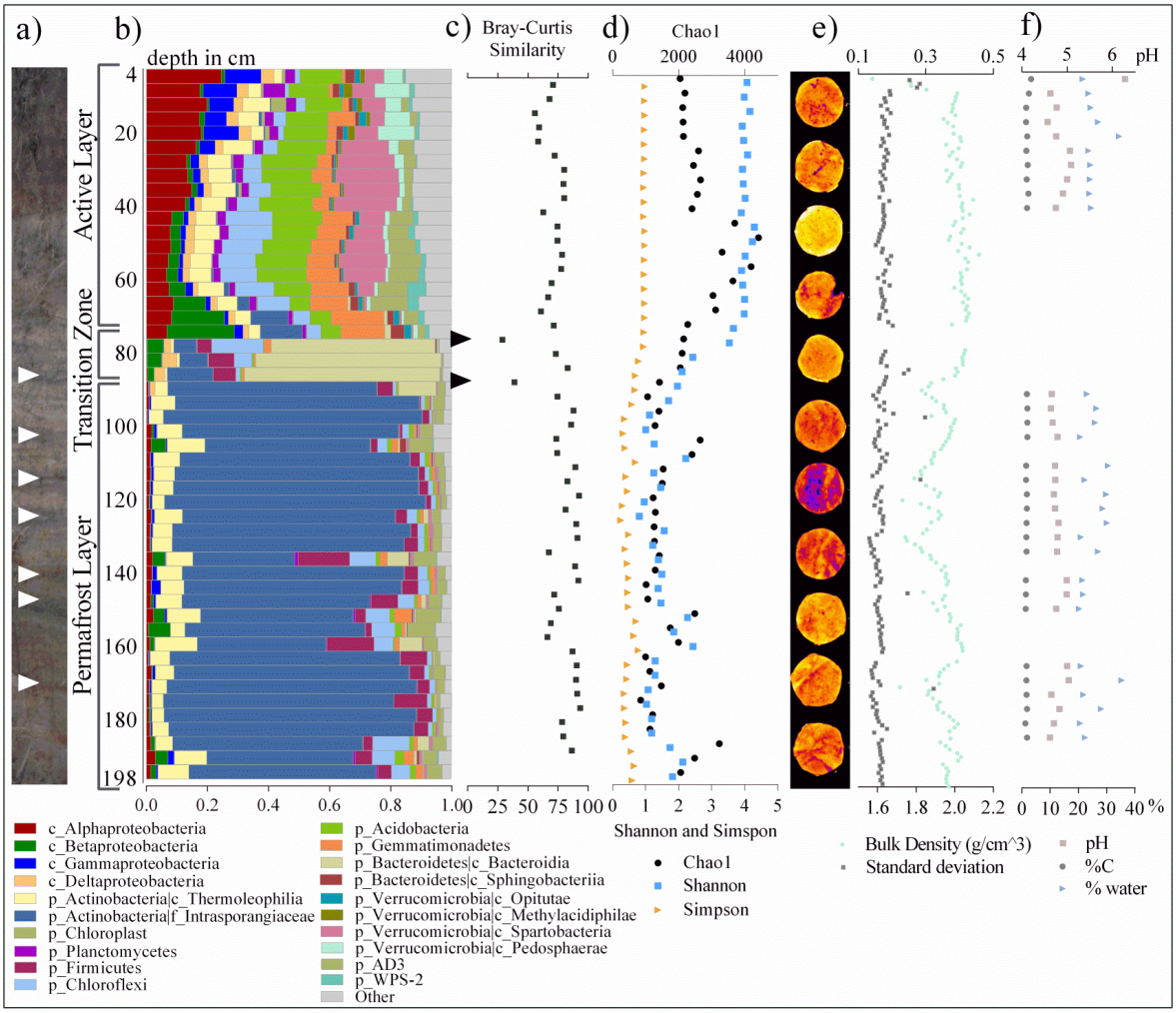

Figure 1: Permafrost soil profile illustrating:

a) The soil structure in Adventdalen. Photograph shows the sedimentation process with periods of low sedimentation rates (small darker organic rich layers, marked with white triangles) and periods with higher sedimentation rates (thicker more pale layers).

b) Relative abundance of the 20 most abundant taxa at different taxonomical levels based on 16S rRNA gene sequence data showing the taxonomic prokaryotic community composition of the permafrost core profile. When taxonomical classes within a phylum showed very contrasting trends, the most abundant classes were illustrated instead of the entire phyla. Taxonomical levels are indicated by a one-letter code (p=phylum; c=class; f=family). Taxa comprising <1% of the total number of sequences within a sample were summarized as "Other". Relative abundances for each sampling point are average values calculated from 2-6 replicates (Table S1). **c)** Bray-Curtis dissimilarity values calculated for 16S rRNA gene sequence data at OTU level. Black triangles mark the transition from AL to TZ and from TZ to PL.

d) Alpha diversity indices (Chao1, Shannon and Simpson). **e)** Bulk density measurement using X-ray CT scanning with measuring points for every centimeter (eleven example images illustrated on the left). **f)** Soil chemistry (n=1) showing in blue the water content, in grey the carbon content and in red the pH throughout the core. Note that data was not available between 30 and 80 cm.

Microbial Community Composition

We could identify characteristic differences in relative abundance of the predominant microbial groups originating from the AL and PL. In the AL the most abundant phyla were Acidobacteria (14% on average), Actinobacteria (9%), Proteobacteria (24%) and Verrucomicrobia (16%) (Figure 1b). Especially the relative abundance of different classes of the phylum Proteobacteria showed gradual fine-scale changes within the AL (Figure 1b and S1). The abundance of Alphaproteobacteria and Gammaproteobacteria decreased gradually from 24 to 7% and 11 to 1.5% respectively (Figure 1b). The decrease in relative abundance in the AL of those two classes correlated with depth (Alphaproteobacteria: r=-0.85, p<0.002 and Gammaproteobacteria: r=-0.89, p<0.001), while no significant correlations to C, pH or water content could be identified (Table 1).

Table 1: Statistical analysis using the Pearson correlation coefficient to identify linear correlations throughout the entire core (grey background) and the first 30 cm of active layer (white background) by comparing depth, and the soil properties carbon concentration, pH and water content with the relative abundance of the 20 most abundant taxa at class level.

	Depth						% Carbon						pH						% water					
	Entire core			First 30 cm			Entire core			First 30 cm			Entire core			First 30 cm			Entire core			First 30 cm		
	r	P (two-tailed)	P value summary	r	P (two-tailed)	P value summary	r	P (two-tailed)	P value summary	r	P (two-tailed)	P value summary	r	P (two-tailed)	P value summary	r	P (two-tailed)	P value summary	r	P (two-tailed)	P value summary	r	P (two-tailed)	P value summary
c_Alphaproteobacteria	-0.8	< 0.0001	****	-0.9	0.002	**	0.5	0.002	**	0.5	0.126	ns	0.4	0.015	*	0.6	0.079	ns	0.0	0.905	ns	-0.1	0.863	ns
c_Betaproteobacteria	-0.1	0.321	ns	0.5	0.123	ns	0.4	0.056	ns	0.0	0.99	ns	0.3	0.116	ns	0.1	0.849	ns	-0.1	0.709	ns	-0.3	0.384	ns
c_Gammaproteobacteria	-0.6	< 0.0001	****	-0.9	0.001	***	0.5	0.002	**	0.4	0.228	ns	0.4	0.030	*	0.3	0.495	ns	0.1	0.596	ns	0.3	0.405	ns
c_Deltaproteobacteria	-0.8	< 0.0001	****	-0.8	0.004	**	0.5	0.002	**	0.4	0.262	ns	0.3	0.063	ns	0.3	0.452	ns	0.1	0.743	ns	0.4	0.274	ns
p_Actinobacteria| c_Thermoleophilia	0.1	0.3554	ns	0.6	0.089	ns	-0.4	0.026	*	-0.7	0.016	*	-0.2	0.442	ns	-0.4	0.232	ns	-0.1	0.706	ns	-0.2	0.515	ns
p_Actinobacteria| f_Intrasporangiaceae	0.8	< 0.0001	****	0.6	0.046	*	-0.4	0.014	*	-0.5	0.175	ns	-0.3	0.079	ns	-0.4	0.299	ns	0.0	0.972	ns	0.1	0.727	ns
p_Chloroplast	-0.4	0.0017	**	-0.4	0.224	ns	0.1	0.637	ns	-0.2	0.51	ns	0.1	0.776	ns	-0.2	0.682	ns	0.1	0.767	ns	0.1	0.778	ns
p_Planctomycetes	-0.8	< 0.0001	****	-0.5	0.132	ns	0.5	0.003	**	0.4	0.302	ns	0.2	0.247	ns	-0.2	0.66	ns	0.0	0.967	ns	-0.2	0.661	ns
p_Firmicutes	0.6	< 0.0001	****	0.4	0.258	ns	-0.4	0.029	*	0.2	0.599	ns	-0.1	0.525	ns	-0.2	0.545	ns	-0.1	0.610	ns	-0.2	0.617	ns
p_Chloroflexi	-0.2	0.141	ns	0.9	0	***	0.0	0.844	ns	-0.4	0.295	ns	0.1	0.601	ns	-0.2	0.556	ns	-0.2	0.376	ns	-0.2	0.502	ns
p_Acidobacteria	-0.8	< 0.0001	****	0.9	0.002	**	0.4	0.015	*	-0.1	0.793	ns	0.3	0.099	ns	0.0	0.989	ns	0.0	0.898	ns	-0.1	0.753	ns
p_Gemmatimonadetes	-0.5	0.0009	***	0.6	0.089	ns	0.1	0.786	ns	-0.5	0.108	ns	0.0	0.928	ns	-0.4	0.229	ns	0.0	0.825	ns	0.1	0.742	ns
p_Bacteroidetes| c_Bacteroidia	0.0	0.797	ns	0.1	0.719	ns	0.0	0.904	ns	-0.4	0.265	ns	-0.1	0.491	ns	-0.2	0.652	ns	-0.1	0.633	ns	0.0	0.954	ns
p_Bacteroidetes| c_Sphingobacteriia	-0.5	0.0001	***	-0.8	0.003	**	0.7	< 0.0001	****	0.7	0.043	*	0.5	0.005	**	0.5	0.157	ns	0.1	0.602	ns	0.2	0.688	ns
p_Verrucomicrobia| c_Opitutae	-0.7	< 0.0001	****	-0.7	0.015	*	0.4	0.020	*	0.1	0.759	ns	0.3	0.143	ns	0.1	0.888	ns	0.1	0.583	ns	0.3	0.381	ns
p_Verrucomicrobia| c_Methylacidiphilae	-0.7	< 0.0001	****	-0.8	0.011	*	0.5	0.004	**	0.3	0.403	ns	0.2	0.334	ns	-0.1	0.75	ns	0.1	0.505	ns	0.4	0.319	ns
p_Verrucomicrobia| c_Spartobacteria	-0.7	< 0.0001	****	0.9	0	***	0.3	0.100	ns	-0.2	0.583	ns	0.2	0.221	ns	-0.1	0.836	ns	-0.1	0.801	ns	-0.3	0.453	ns
p_Verrucomicrobia| c_Pedosphaerae	-0.7	< 0.0001	****	-0.7	0.025	*	0.4	0.016	*	0.2	0.644	ns	0.1	0.487	ns	-0.2	0.61	ns	0.2	0.280	ns	0.6	0.083	ns
p_AD3	0.0	0.7589	ns	0.5	0.124	ns	-0.4	0.039	*	-0.6	0.067	ns	-0.1	0.586	ns	-0.2	0.606	ns	-0.1	0.715	ns	-0.3	0.424	ns
p_WPS-2	-0.4	0.0035	**	-0.7	0.028	*	0.3	0.071	ns	0.0	0.977	ns	0.1	0.799	ns	-0.3	0.371	ns	0.2	0.430	ns	0.4	0.285	ns

An opposite trend was observed for the class Betaproteobacteria, which was underrepresented down to 36 cm before their relative abundance increased from 4 to 22% down to 75 cm. Other phyla, like the Gemmatimonadetes and candidate phylum AD3 also increased in abundance from 42 cm down to 75 cm and 68 cm, respectively. A general decrease down to 75 cm could be observed for the phyla Acidobacteria, Verrucomicrobia, Chloroflexi and Planctomycetes. Throughout the entire core, an increase or decrease in relative abundance of certain taxa significantly correlated with depth, while correlations to C concentrations, pH and water content were predominantly not significant (Table 1).

We detected a major shift in microbial community composition at 75 - 78 cm depth in the AL. This was mainly driven by changes in relative abundance of Bacteroidetes (class Bacteroidia), which increased from 2 to 54% and Proteobacteria, which decreased from 34 to 8%. Bacteroidetes (class Bacteroidia) stayed abundant until 85 cm before decreasing to <0.5% within the next 7 cm of the soil core. We identified mayor differences in Bray-Curtis dissimilarity values at the transition from 75-78 cm with 29% and 85-88 cm with 39% (Figure 1c). Since community similarity between consecutive samples is on average about 78%, we interpreted those two shifts as the transition from AL to TZ and TZ to PL, respectively. Consequently, this change at 88 cm, where the microbial community composition shifted towards a dominance of Actinobacteria, can be interpreted as the beginning of the PL and the depths between 78-85 cm as the TZ. The PL is dominated by four OTUs belonging to *Intrasporangiaceae* (family) with an average relative abundance of 70% (±13%). An ANOSIM analysis on Bray-Curtis dissimilarities between the three layers showed that they are significantly different to each other and justifies the introduction of the TZ as a biological independent layer in the permafrost core (Table 2).

Table 2: ANOSIM analysis of Bray-Curtis dissimilarities for the three different permafrost zones AL (Active layer), TZ (Transition zone) and PL (Permafrost layer). R indicates the grade of dissimilarity (1=most dissimilar) and p the statistical probability.

Sample grouping	Global R	P
Active layer - Transition zone	0.997	0.002
Active layer - Permafrost layer	0.993	0.001
Transition zone - Permafrost layer	1	0.001

Archaea were generally underrepresented with a maximum relative abundance of 0.5% throughout the entire core and OTUs were predominantly assigned to Crenarchaeota (class MBGA) and Euryarchaeota (class Thermoplasmata).The three layers showed significant differences in richness (Chao1), evenness (Simpson) and diversity (Shannon), illustrated in Figure 2 (ANOVA, $p<0.0001$).

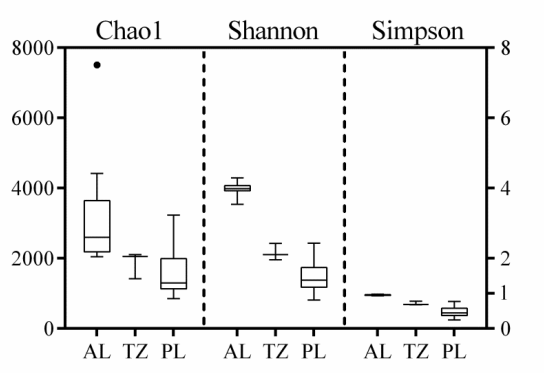

Figure 2: Richness and alpha diversity indices (Chao1, Shannon and Simpson). Pooled samples from the AL (n=19), TZ (n=3) and PL (n=27) were used to calculate alpha diversity indices.

All three alpha diversity indices were higher in the AL and decreased significantly with depth down to the PL (Pearson's r: Shannon [r=-0.8242] and Simpson [r=-0.7666] with $p<0.0001$ and Chao1 [r=-0.5121] with $p=0.0002$) (Figure 1d). Beta-diversity analysis confirmed these differences and is illustrated by a MDS plot (Figure 3).

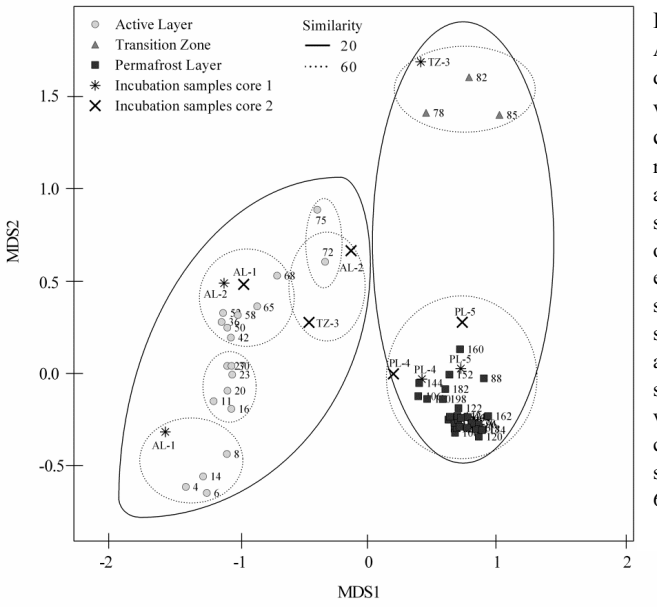

Figure 3: Multidimensional Scaling Analysis (MDS) plot of Bray-Curtis dissimilarity values illustrating the variation of bacterial community composition based on sequenced 16S rRNA gene fragments at OTU level. The analysis included the high resolution core samples and samples from the five layers of each core used for the incubation experiment. The soil type of each core sample is given by symbols and the sample depth and incubation segment is added as caption. Numbers correspond to sampling depths in core 1. The stress value for the MDS plot is 0.06. The black circles around clusters indicate similarities of 20% and the dotted circles 60% similarity.

All samples from the PL shared 60% similarity, while AL samples only shared 20% similarity. Furthermore, the AL, TZ and PL samples grouped separately, with AL samples showing the widest distribution with a clear, gradual clustering from surface to deeper AL samples. Community composition of sub-samples from core 2 was similar compared to the corresponding layers in core 1 (Figures 3 and 4c). One exception was the absence of a Bacteroidetes dominated TZ, instead, community composition in the TZ-3 sample from core 2 was more similar to the AL-2 sample from core 1 (Figure 3 and Table S3). The characteristic differences between AL and PL segments observed for core 1 were also present in core 2 and included the decrease of Alphaproteobacteria and increase of Betaproteobacteria with increasing AL depth and the dominance of *Intrasporangiaceae* in PL samples (Figure 4c).

Degradation potential of soil organic matter

From both cores, five segments were chosen as models to simulate thawing conditions in different permafrost layers and document CO_2 fluxes. These segments were from the AL (AL-1; AL-2), the TZ (TZ-3) and the PL (PL-4; PL-5). They were chosen based on differences in microbial community composition as described above and in order to confirm the expected differences for the five segments, 16S rRNA gene sequencing analysis was performed (Figure 4c). All five segments from core 1 revealed the characteristic community structure according to their depth and were similar to the community structure identified in the high resolution profile (Figure 3 and Table S3).

Sub-samples from the five segments were incubated for up to 122 days and CO_2 was measured regularly at eight time points for the first 19 days (Figure 4a). Overall CO_2 emissions were higher in core 1 than core 2, but showed similar trends for the different segments (Figure 4a). In core 1, highest CO_2 values were measured for PL-5 and lowest for AL-2 with 65 µg C-CO_2 g $soil^{-1}$ and 19 µg C-CO_2 g $soil^{-1}$ respectively. Differences could be observed when the 19 days were divided into three phases. The first 24h cover the release of trapped CO_2 (phase 1), the next five days mark the first CO_2 production phase (phase 2) and the last 12 days represent the later CO_2 production phase (phase 3). PL-5, PL-4 and TZ-3 had all high amounts of stored CO_2 which were released during the first 24h. AL-1 and AL-2 released

only small amounts during this first phase. The production during phase 2 was highest in PL-5 (29 µg C-CO_2 g $soil^{-1}$) and decreased towards AL-1 (12 µg C-CO_2 g $soil^{-1}$). The most contrasting rates between the five segments were observed during production phase 3, when AL-1 showed the highest CO_2 emissions with 47 µg C-CO_2 g $soil^{-1}$ making up for 78% of the total emissions within 19 days.

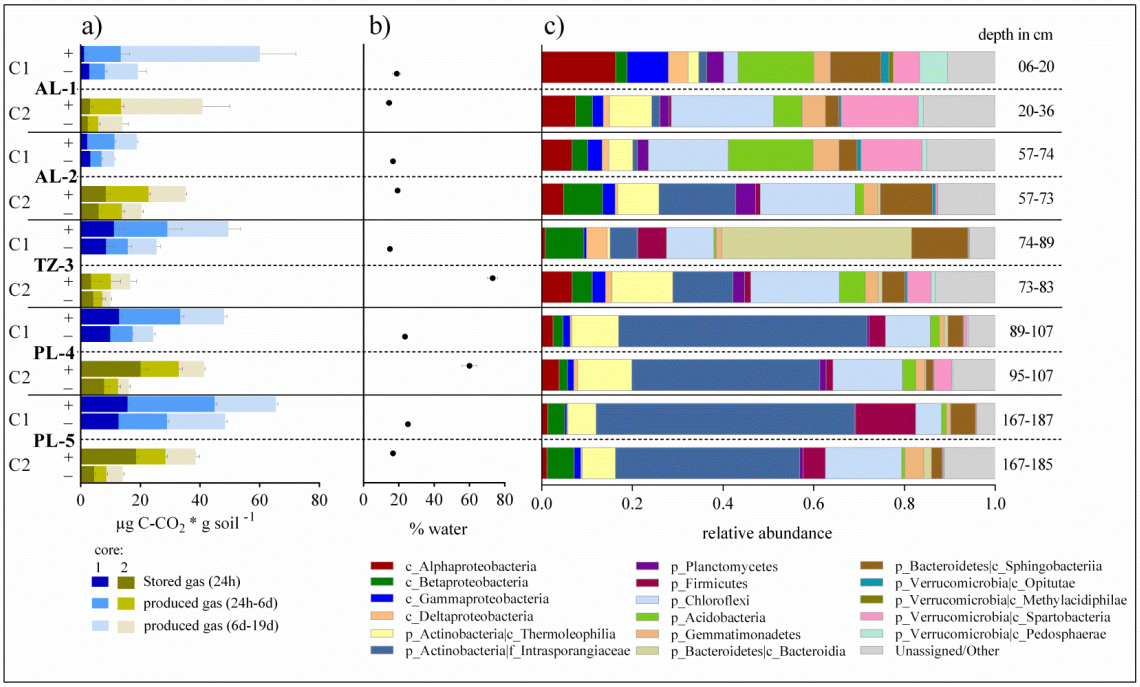

Figure 4: CO_2 emissions, water content and microbial community structure of five characteristic layers from two replicate permafrost cores. C1: Core 1 from 2011 and C2: Core 2 from 2014
a) CO_2 emissions of permafrost samples measured over 19 days and categorized in 3 phases which are indicated by the different shades of blue and green as stacked bars. Samples from five segments of the cores were incubated at 4 (±1) °C under aerobic (+) or anaerobic (-) conditions (n=3). **b)** Water content in % of weight for the five different layers (n=3). **c)** Microbial community composition of the five segments from the two permafrost cores used for the incubation experiment covering the AL, TZ and PL (n=1). Illustrated are the most abundant taxa at different taxonomical levels. Taxonomical levels are indicated by a one-letter code (p=phylum; c=class; f=family).

Overall similar trends, as described above, could be observed for the representative segments from core 2. By comparing both treatments, we found that CO_2 emissions were always higher under aerobic incubations, with up to 4.2 times more CO_2 produced for AL-1 in phase3 (Figure 4a). The last sampling point was after 122 days and during this 103 day period, AL-1 samples produced the most CO_2 with 1207

µg C-CO_2 g $soil^{-1}$ (Figure S4), while the segments TZ-3, PL-4 and PL-5 released around 800 µg C-CO_2 g $soil^{-1}$ and AL-2 produced only 330 µg C-CO_2 g $soil^{-1}$.

All layers released significant amounts of CO_2, thereby showing spatial (ANOVA, core 1: p=0.0369; core 2: p=0.007) and temporal (ANOVA, core 1: p=0.0032; core 2: p=0.0041) differences. These differences were compared to the community composition in the different layers and visualized in a redundancy analysis biplot (Figure 5).

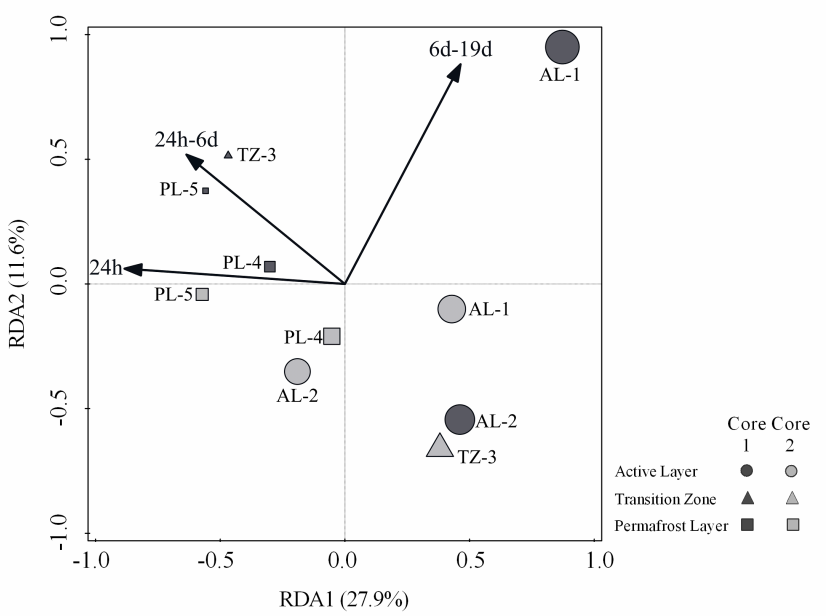

Figure 5: Redundancy analysis biplot summarizing the variation of bacterial community composition in the five segments from both cores used for the incubation experiment plotted in relation to CO_2 emission under aerobic conditions used as explanatory variables (black arrows). CO_2 emission was grouped into three periods covering the first 24h, 24h to 6d and 6d to 19d. The size of the symbols relates to the sample diversity (Shannon-Wiener index) at species level.

The RDA model included the OTU abundance matrix as response variables and CO_2 emission values for the three categories (24h; 24h-6d; and 6d-19d) as predictor variables, which explained 46.2% (p=0.016) of the total variance. For core 1, chemical parameters such as DOC, DTN, NH_4-N, pH and water content, before and after 19 days of incubation, were measured. The results showed no major differences between the two different treatments and incubation time (Figure S3).

Metagenomics analysis

We were interested in identifying functional differences in the different layers of the core as well as differences due to the induced thawing conditions of the incubation experiment (Figure 6). Firstly, differences between the four analyzed segments were greater than differences caused by incubation for up to 16 days (Figure S4). Changes in gene abundance over the course of the 16 days of incubation were more pronounced under aerobic conditions than in anaerobic treatments, where microbial communities remained relatively unchanged (data not shown). Overall, most reads (>60%) were assigned to genes involved in various metabolisms, of which the carbohydrate metabolism was most represented with 10-15% of all reads, but varying for each layer. Glycolysis, starch and sucrose metabolism and degradation of aromatic compounds were overrepresented in the PL, while the fructose metabolism and the pentose phosphate pathway were pronounced in the TZ (Figure 6).

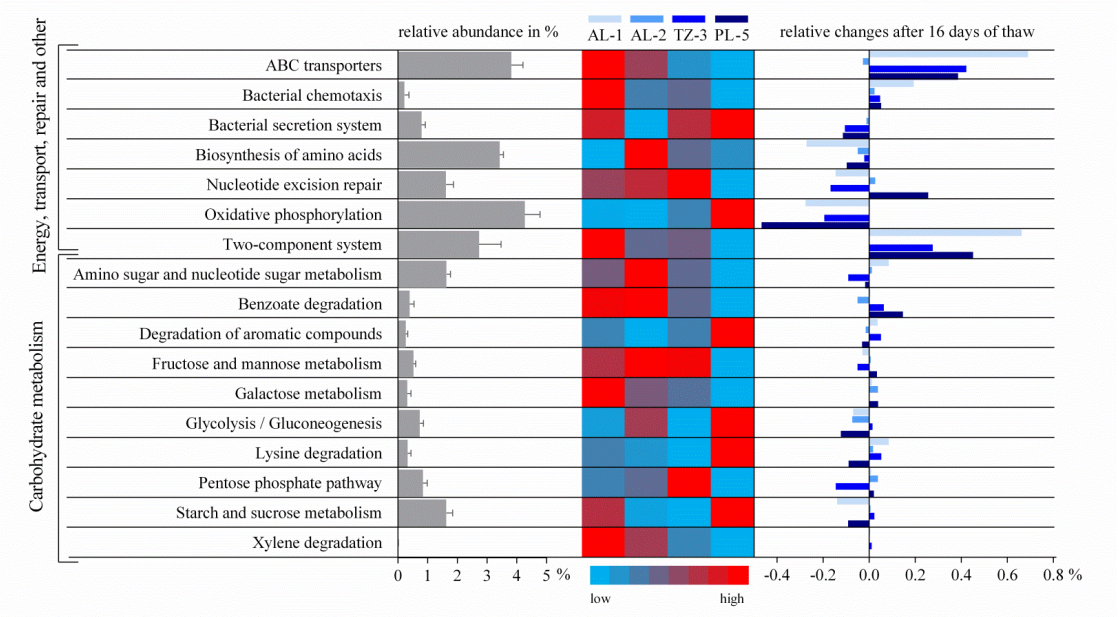

Figure 6: Heat map displaying the relative abundance of KEGG annotated metagenomics reads assigned to a selection of different metabolic pathways in four different layers of the permafrost core. The relative abundance of reads assigned to each pathway is displayed by the grey bar graph to the left and the changes in relative abundance for each layer after 16 days of incubation is indicated by the bar graph to the right.

In the AL, benzoate and xylene degradation and the galactose metabolism were overrepresented. After 16 days of thaw, the relative abundance of these KEGG pathways changed considerably in three of the four layers, only AL-2 samples showed no or minimal changes (Figure 6). Common for all layers was an increase in reads assigned to DNA repair mechanisms and decarboxylases. The most pronounced change after 16 days of thaw was an increase in relative abundance of genes connected to ABC transporters and the two-component system. Changes in the relative abundance of carbohydrate pathways were considerably less pronounced after 16 days of thaw. Additionally, the layers where a certain carbohydrate pathway was overrepresented compared to the other layers, also had the strongest reduction of the respective pathway after 16 days of thaw, for example the decrease in relative abundance of the starch and sucrose metabolism in AL-1 and PL-5 (Figure 6).

Discussion:

Fine-scale resolution

Numerous studies have characterized the microbial community structure of permafrost-affected soils, but mostly on broader scales (Yergeau *et al.*, 2010; Wilhelm *et al.*, 2011; Frank-Fahle *et al.*, 2014; Gittel, Bárta, Kohoutová, Schnecker, *et al.*, 2014; Koyama *et al.*, 2014; Taş *et al.*, 2014; Deng *et al.*, 2015; Schostag *et al.*, 2015). So far, only two studies characterized shifting microbial communities at a finer scale (Kim *et al.*, 2016; Tripathi *et al.*, 2018). They analyzed the AL of Alaskan organic rich tundra soils in steps of five centimeter and showed that a high resolution analysis of the soil profile can reveal unique changes in relative abundance of certain bacterial groups with depth.

Here a permafrost core from Svalbard was analyzed at three to four centimeter intervals to a depth of two meters. Due to the fine resolution we were able to identify microbial community shifts in the AL and the PL, and further to distinguish a structurally unique and different TZ between these layers. Throughout the entire core, bacteria were dominating over archaea, which could be detected at various depths, but did not exceed abundances of more than 0.5% of the total community. Low archaeal abundances have been reported before and especially the absence of methanogenic archaea has been associated with low water content, similar to the soil investigated in this study (Høj *et al.*, 2006; Yergeau *et al.*, 2010; Rivkina *et al.*, 2016). We identified similar trends as seen in Kim et al (2016) for the bacterial community in the AL, where the relative abundance of Alphaproteobacteria, Gammaproteobacteria and Acidobacteria decreased, whereas Betaproteobacteria, Gemmatimonadetes and candidate phylum AD3 increased with soil depth. The community shifts caused by the different abundances of Proteobacteria and the other phyla have to some extent been described before (Koyama *et al.*, 2014; Deng *et al.*, 2015; Kim *et al.*, 2016), and correlated with different soil horizons based on C turnover. Although those studies were based on organic soils, we could identify similar community shifts in our mineral soil core with <5% C content. The higher abundance of Alphaproteobacteria and Gammaproteobacteria in the upper AL has been speculated to correlate with higher C and nutrient availability (Koyama *et al.*, 2014; Kim *et al.*, 2016). However,

Alphaproteobacteria and Gammaproteobacteria were also more abundant in the upper AL of our core, despite the overall low C content in this mineral soil. This indicates that C availability alone might not be suitable to explain changes in the relative abundance of Alphaproteobacteria and Gammaproteobacteria in Arctic soils with both low and high carbon concentraions. The current study can, however, not discriminate whether the observed decline in abundance is related to carbon related factors like C quality or a combination of several factors, including oxygen availability and redox effects.

Betaproteobacteria and especially taxa belonging to the uncultured and uncharacterized order SBla14 and the order *Gallionellales* increased in abundance in the deeper AL. As *Gallionellales* are chemolithotrophic iron-oxidizers, their increase in relative abundance might be connected to an increase in available Fe(II), which they use as primary energy source (Emerson *et al.*, 2015). In mineral soils, Fe(II) is less likely to be bound to organic ligands and therefore available for oxidation by iron-oxidizing bacteria (Liang *et al.*, 1993). Other taxa that increased in relative abundance in the deeper AL belong to the phylum Gemmatimonadetes and the candidate phylum AD3 and have been detected in deeper soils before (Costello, 2007; Taş *et al.*, 2014; Deng *et al.*, 2015). It is unclear which environmental factors are causing their increase, as members of these phyla are largely uncharacterized. While dry soils and neutral pH have been associated with a higher abundance of Gemmatimonadetes (DeBruyn *et al.*, 2011), higher abundances of candidate phylum AD3 were associated with low carbon concentrations (Jansson and Taş, 2014). Interestingly, all phyla, independent of increasing or decreasing abundance towards the deeper AL, abruptly changed from 75 to 78 cm, due to the tremendous increase in relative abundance of Bacteroidetes (from 2 to 54%; Figure 1). The Bacteroidetes-dominated zone likely coincides with a geocryological defined transition zone, which, according to the three-layer conceptual model, describes a zone between the seasonally thawed AL and the stable PL, with sub-decadal freeze-thaw transitions (Shur *et al.*, 2005). The thickness of the AL is variable in Adventdalen and can range between 63-90cm within a 20m radius of our study site (field measurements in 2016 and Cable *et al.*, 2018). These AL maximum depths however suggest that a TZ above the permafrost table in core 1 might have been located where we also

identified the high Bacteroidetes abundance. It might also explain why we did not identify this zone of high Bacteroidetes abundance at similar depths in core 2. Since the community composition of the TZ-3 segment from core 2 was most similar to the AL-2 samples from core 1, the AL might have extended deeper in core 2 than in core 1 and hence might explain why we did not identify the actual TZ with high Bacteroidetes abundance in core 2. The current study can, however, not provide evidence whether the high Bacteroidetes abundance is associated to the effects of recent thawing in the transition zone. High Bacteroidetes abundances in general have been associated with their metabolic flexibility and their ability to quickly respond to the easy available C and nutrients (Padmanabhan *et al.*, 2003; Fierer *et al.*, 2007). Chemical analysis of the TZ-3 samples from core 1 however, showed neither elevated carbon nor nitrogen levels compared to the neighboring layers AL-2 and PL-4. It remains uncertain what factors caused this clear separation of the TZ or whether this layer might be a record of a particular condition in the past when it was formed and buried due to sedimentation processes. Interestingly, the dominance by one taxonomical group (unknown family; within the class Bacteroidia) in the TZ is followed by the dominance of another family (*Intrasporangiaceae*; within the phylum Actinobacteria) in the PL. The sharp community changes between the different layers, which we here demonstrate for the first time, are an indicator that community structures are highly flexible and might adapt quickly to distinct conditions.

Studies of permafrost layers from other Arctic regions have reported a high variability of bacteria belonging to the phyla of Actinobacteria, Proteobacteria, Verrucomicrobia, Chloroflexi, Bacteroidetes and Firmicutes (Hansen *et al.*, 2007; Yergeau *et al.*, 2010; Mackelprang *et al.*, 2011; Yang *et al.*, 2012; Jansson and Taş, 2014). In our study we observed a dominance of only four OTUs, belonging to the family of *Intrasporangiaceae*, which accounted for up to 80% of the entire community in the PL in core 1 (Figure 1b) and up to 42% in core 2 (Figure 4c). High dominance of this Actinobacteria family has been seen in permafrost soils before ((Gittel, Bárta, Kohoutová, Schnecker, *et al.*, 2014): Greenland up to 8%; (Gittel, Bárta, Kohoutová, Mikutta, *et al.*, 2014): Siberian Arctic up to 47%), but to our knowledge never been reported in such consistent high numbers throughout the entire PL. It has been discussed that these

Actinobacteria are globally successful in permafrost environments due to their adaptions to low C availability and capabilities to degrade complex C compounds, like cellulose, cellobiose and lignin (DeAngelis *et al.*, 2011; Giongo *et al.*, 2013; Gittel, Bárta, Kohoutová, Schnecker, *et al.*, 2014).

Greenhouse gas fluxes and functional genes

Although respiration takes place at sub-zero temperature, several studies have shown a rapid increase in respiration upon thaw, probably due to the availability of liquid water (Clein and Schimel, 1995; Larsen *et al.*, 2002; Elberling and Brandt, 2003; Mackelprang *et al.*, 2011). Nikrad and colleagues (2016) therefore suggested that several parameters, including temperature, C content and changes in the physical environment, should be included when comparing respiration rates. In our study we included the microbial community composition as an additional factor regarding respiration rates.

We were able to show in detail, that both incubation conditions and soil depth with associated differences in microbial community structure influence CO_2 fluxes during permafrost thaw (Figure 4a). Incubations with a different community structure showed different respiration rates. The highest difference was observed between AL-1 and AL-2 incubations from core 1. Within 19 days AL-1 samples release 60 µg C-CO_2 per gram soil, while samples from AL-2 release three times less (Figure 4a). Similar low CO_2 production rates were observed for samples from TZ-3 of core 2 (Figure 4a). The community composition of TZ-3 from core 2 was most similar to the AL-2 segment from core 1 (Figure 3 and Table S3), indicating that depth-dependent differences in community structure might be indicators for the CO_2 production potential (Figure 5). If these findings can be applied to longer term and field conditions requires further investigations as well as the identification of the active drivers of CO_2 production and their abundance in the different communities. Further, the correlation between community composition and CO_2 fluxes that we observed, might also be driven by substrate specific factors which we did not measure. Nevertheless, our results highlight the complexity of microbial driven respiration throughout a permafrost core and the necessity for further detailed gas flux studies considering the different responses in the different permafrost layers.

Independent of soil layer and community structure, respiration rates were highestunder aerobic than anaerobic conditions, with up to four times more produced CO_2 (Figure 4a). Similar results have been documented in a study with permafrost from Greenland, incubated for 12 years (Elberling *et al.*, 2013) and a comparative study investigating aerobic and anaerobic permafrost incubations from different locations in Alaska and Siberia (Lee *et al.*, 2012).

Under anaerobic conditions the release of CO_2 was with 50 µg C-CO_2 per gram soil twice as high in PL-5 as in PL-4 and TZ-3 and almost three times as high as in AL-1 and AL-2. This indicates that the fermentative potential is highest in the deepest PL layer, which also represents the only layer which has not been thawed at any point since the beginning of the Holocene. Even though TZ-3 has been thawed during the last 15 years, similar amounts of stored CO_2 were released during the first 24 hours compared to PL-5. This indicates that CO_2 is produced under freezing conditions and that CO_2 can be stored until it is released upon thawing (as previous documented by Elberling & Brandt 2003).

In contrast to other permafrost incubations, we could not detect CH_4 production in any of our treatments. The absence of methane production has been shown to be connected to iron and sulfate reduction processes, which energetically outcompete methanogenesis under anaerobic conditions (Patrick and Jugsujinda, 1992; Megonigal *et al.*, 2004). The metagenomics analysis confirmed that methanogenesis might not have been activated, as genes involved in methane production were at a very low level or absent throughout the entire soil core, while genes encoding iron transporter proteins and sulfoxide reductases, were widely expressed and abundant throughout the core.

This analysis also revealed that of all metabolisms, most genes were assigned to several carbohydrate pathways, varying for the different layers. The microbial community in the AL was involved in various carbohydrate degradation pathways, whereas communities in deeper layers depended on smaller organic substrates for energy conservation and degradation of complex aromatic compounds. Especially, transport and signaling genes were overrepresented in the AL and increased upon incubation. The abundance of certain genes changed in nearly all soil layers over the course of the incubation, with the exception of the

lower part of the AL (AL-2) (Figure S4). This was also the layer that, despite the genomic potential to degrade various carbon sources, produced the least amount of CO_2 during the incubation. It remains unclear why CO_2 production rates differed so substantially within the AL. These spatial and temporal differences in CO_2 production within the different layers indicate important implications for future climate change models which incorporate permafrost greenhouse gas release.

Conclusion:

In this study, high resolution profiling of the microbial community throughout an entire two-meter permafrost core from Svalbard allowed us to closely follow changes. It showed significant differences between the AL and the PL, with the latter being dominated by *Intrasporangiaceae* and revealed a ~8cm spanning TZ with a clearly different community, dominated by Bacteroidetes. Further, we showed that CO_2 release from our permafrost samples varied within the different layers and during different incubation periods. Together, our results indicate that the spatial and temporal variability of CO_2 is reflected in the fine-scale variations of microbial communities throughout the permafrost core, that can change dramatically even within 3 cm. Due to observed structural variability of permafrost soils we cannot expect our identified microbial and activity patterns to be universal. However, the results from our study strengthen the necessity of detailed high resolution microbial community permafrost profiles in order to understand how the different microbes are distributed, how they interact and how they function in this globally important and changing Arctic environment.

406 **Experimental Procedures:**

407 *Study site and sampling*

408 Soil samples were obtained from a characteristic low-centred ice-wedge polygon site in the valley
409 Adventdalen on Svalbard (78.186N, 15.9248E). Overall, two separate cores were drilled; the first core was
410 obtained in April 2011 and is referred to as "core 1" and a replicate core was drilled at the same
411 coordinates in July 2014 ("core 2"). The high resolution sequencing and chemical analyzes are based on
412 soil samples from core 1. Sub-samples (n=2-6) from each of the analyzed 50 sections of the core were
413 used as replicates for the 16S rRNA gene sequencing (Table S1). The incubation experiments included
414 samples from five representative segments from core 1 and at similar depths five segments from core 2
415 (Table S2). Samples from these five layers used in the incubation experiments were also used for 16S
416 rRNA gene sequencing. The incubation experiments and chemical analyzes included three to four
417 replicates.

418 *Soil processing and chemical properties*

419 To remove potential core surface contaminants, introduced during the drilling procedures, the outermost 2
420 cm were scraped off with sterile blades. The remaining inner part was kept frozen on dry ice and
421 transferred to a sterile thick plastic bag and homogenized by hammering. Characteristic soil properties,
422 such as pH, water content, dissolved organic carbon (DOC), NO_3 and NH^{4+} were measured for most of the
423 subsections of core 1 used for the high resolution profile and for all segments from both cores used for the
424 incubation experiments.

425 *X-ray CT scanning*

426 The core was X-ray CT scanned using a modified Siemens Somatom HiQ medical CT scanner at 133 kV.
427 To obtain bulk density, the CT scanner was calibrated by scanning a number of materials having known
428 density. The data were analyzed using imageJ (Schindelin *et al.*, 2015).

Soil incubations and gas-flux measurements

All preparations for soil incubations were performed in a -20 °C cold room. All incubation experiments included three replicates and covered five different segments (2 from AL, 1 from TZ and 2 from PL) from each of the two permafrost cores. Two gram of soil were added to sterilized glass vials (20 ml) and sealed with butyl rubber stoppers and aluminum crimps. Samples incubated under anaerobic conditions were flushed with nitrogen for 1 min. Three milliliters of headspace gas were collected from the vials immediately after the incubation was started and at 9 time points (4h, 12h, 24h, 2d, 4d, 6d, 16d, 19d, 122d) during incubation. After each gas collection, aerobic or anaerobic conditions were re-established. The gas samples were transferred into 3 ml Exetainer glass vials and analyzed for CO_2, CH_4 and N_2O on a SRI 8610C gas chromatograph. Measurements for CH_4 and N_2O were below the detection limit in all the segments and data was therefore not included. All samples were incubated at 4(±1) °C in the dark.

DNA extraction, 16S rRNA gene amplification and amplicon sequencing

Frozen soil from homogenized segments of the core was used for DNA extractions, following manufacturer's instructions of the PowerSoil® DNA Isolation Kit (Mobio, Carlsbad, USA) and performed in triplicates with minor modifications. Instead of 0.25 g, 0.3-0.4 g soil was used for the DNA extraction and an additional incubation step of 70°C for 5 min was included after solution C1 was added. Information regarding the sub-sample depth, the number of replicates, DNA concentration and the number sequences before and after processing is listed in Table S1. DNA amplification included a two-step nested PCR approach with primers 519F (CAGCMGCCGCGGTAA; (Øvreås *et al.*, 1997)) and 806R (GGACTACHVGGGTWTCTAAT; (Caporaso *et al.*, 2011)) targeting the bacterial and archaeal 16S rRNA gene V4 hypervariable region. Details can be found in (Wilson *et al.*, 2017). Libraries were send to the Yale Center for Genome analysis (Yale University, the W.M. Keck Biotechnology Resource Laboratory, CT, US) and the Norwegian Sequencing Centre (Oslo, Norway) for high-throughput

sequencing on a MiSeq platform (Illumina). Sequencing data is available at "The European Bioinformatics Institute" under study accession number PRJEB21759. (http://www.ebi.ac.uk).

Bioinformatic sequence analysis

Sequencing data was processed using different bioinformatic tools incorporated in the Qiime-processing platform using version 1.9.1. (Caporaso *et al.*, 2010). A total of 13,669,151 sequences were retrieved from 151 samples. Prokaryotic OTUs were selected at a sequence similarity threshold of 97% using a de novo uclust (Edgar, 2010) OTU clustering method with default parameters and taxonomy assigned, using the Greengenes reference database (DeSantis, 2006). OTUs with a taxonomic identification were assembled to an OTU table providing abundances for each sample excluding singletons and unassigned OTUs. After removal of singletons and unassigned OTUs, a total of 37,016 unique OTUs at 97% sequence identity were retrieved. Alpha diversity, including Shannon and Simpson indices (Shannon, 1948; Simpson, 1949) and Chao1 richness (Chao, 1984), was calculated using a rarefied sample set, standardized to the smallest read number of 3,500 sequences per sample. To test for multivariate environmental correlation with the prokaryotic community structure, the programs primer-e version 6 (Plymouth, UK) and Canoco 5 (ter Braak and Šmilauer, 2012) were used. Among others, Bray-Curtis resemblance, ANOSIM and principal component analyses were calculated using these programs. Multidimensional Scaling Analysis (MDS) plot was used to illustrate the variation of bacterial diversity based on Bray-Curtis dissimilarity values of sequenced 16S rRNA gene data. For the redundancy analysis (RDA), the OTU abundance matrix was log transformed and used as response variables, while CO_2 emission values for the three categories (24h; 24h-6d; and 6d-19d) were used as predictor variables.

Metagenomics analysis

Samples for metagenomics Illumina High-Seq sequencing were collected from four of the five different segments (2 from AL, 1 from TZ and 1 from PL) from core 1 used in the incubation experiment. Triplicate soil samples of 0.3 - 0.4 g were collected before the incubation started and after 16 days of thaw under

aerobic conditions, frozen immediately in liquid nitrogen and stored in at -80 °C. DNA was extracted using the PowerSoil® DNA Isolation Kit (Mobio, Carlsbad, USA) as described above. DNA was sent to WSU Genomics Core (Washington, Spokane) where DNA was quality checked and libraries prepared using 100 ng DNA per sample and the Illumina® TruSeq® Nano DNA Library Prep kit (Illumina), according to manufacturer`s instructions. Metagenomics shot sequencing data was analyzed using the ATLAS software package and standard settings (White III *et al.*, 2017). Raw paired-end Illumina reads (.fastq format) were extended for overlaps by using FLASH (Magoč and Salzberg, 2011), after which φX174 was removed using Bowtie2 (Langmead and Salzberg, 2012), the reads were trimmed with trimmomatic (Bolger *et al.*, 2014), and then quality control was performed with FastQC (Andrews, 2010). Overlapped paired-end reads (from FLASH) and unpaired reads were assembled using MEGAHIT (Li *et al.*, 2015). The resulting contigs were subsampled for lengths >1 kbp and translated to protein coding open reading frames (ORFs) using Prodigal (Hyatt *et al.*, 2010) in metagenome mode and annotated using DIAMOND (Buchfink *et al.*, 2015) blastp for protein-protein searching. DIAMOND blastp high-scoring pairs were filtered to user specified bitscore and e-value cut-offs (defaults >200 and $<1x10^{7}$, respectively). Functional annotation utilizes non-redundant RefSeq (O'Leary *et al.*, 2016) and obtains KEGG (Ogata *et al.*, 1999) (i.e., KO number) annotations from EggNOG reference database. KEGG reads were normalized to metagenome size and relative abundance differences between layers were normalized for each pathway. ATLAS uses RefSeq high-scoring pairs along with NCBI's taxonomy assignments reference tree via a modified majority voting-method (MMVM) that utilizes lowest common ancestor (LCA) (Hanson *et al.*, 2016), to determine the lowest common ancestor represented across all ORFs present within a single contig. Functional and taxonomic count data was obtained by mapping quality controlled reads to assembled contig annotations using Bowtie2, then parsed using featureCounts of the Subread package (Liao *et al.*, 2014). Sequencing details can be found in Table S4.

Statistical analysis

ANOSIM analysis comparing Bray-Curtis dissimilarities between samples for the three different permafrost zones was carried out using the program primer-e version 6 (Plymouth, UK). Calculations for ANOVA and the Pearson correlation coefficient (Pearson`s *r*) were carried out using GraphPad Prism v 6.01 for Windows (GraphPad Software, CA, USA). Differences in CO_2 emission in the different layers and for the three time periods (24h; 24h-6d; 6d-9d) during the incubation experiment were analyzed by one-way ANOVA with $p<0.05$ as threshold for statistical significance. To compare the differences of the three alpha diversity indices for the different layers one-way ANOVA was performed and Pearson`s *r* to indicate whether those indices decreased significantly with depth. Further, Pearson`s *r* linear correlations were carried out to investigate the significance of correlation between the 16S rRNA relative abundance data and depth and the soil properties C concentration, pH and water content.

Acknowledgments:

We would like to thank Graham Gilbert for obtaining the soil core from Adventdalen, Svalbard and Hanne Christiansen for relevant site information and UNIS for logistical support. We are grateful to be able to include data from the Circumpolar Active Layer Monitoring (CALM) program. We further like to thank Shi Wang and Yanhong Wang (Lawrence Berkeley National Laboratory), for laboratory assistance processing the soil core. We also like to thank CENPERM for excellent support regarding gas flux experiments and chemical analyzes. Thanks also to Bryan Wilson for discussion and help regarding bioinformatics analyzes. We further would like to thank Aviaja Lyberth Hauptmann, Jacob Bælum and Rachel Mackelprang for helpful discussions and ideas.

Funding:

This study is part of the project “Microorganisms in the Arctic: Major drivers of biogeochemical cycles and climate change” (RCN 227062) funded by the Norwegian Research Council. Lise Øvreås was awarded Fulbright Arctic chair 2012/2013 funded by the Fulbright foundation and Bo Elberling and Toke Bang-Andreasen were funded by the Danish National Research Foundation (CENPERM DNRF100). This

work was supported in part by the Office of Biological and Environmental Research, Office of Science, US Department of Energy (DOE) grants awarded to Lawrence Berkeley National Laboratory under contract number DE-AC02-05CH11231. The authors acknowledge additional financial support from the Microbiomes in Transition (MinT) Initiative at Pacific Northwest National Laboratory, under contract number DE-AC05-76LO1803 and the DOE Next Generation Ecosystem Experiment-Arctic (NGEE-Arctic) project.

Conflict of interest statement:

The authors declare no conflict of interest.

References:

Åkerman, H.J. and Johansson, M. (2008) Thawing permafrost and thicker active layers in sub-arctic Sweden. *Permafr. Periglac. Process.* **19**: 279–292.

Andrews, S. (2010) FastQC: A quality control tool for high throughput sequence data. *Http://Www.Bioinformatics.Babraham.Ac.Uk/Projects/Fastqc/* http://www.bioinformatics.babraham.ac.uk/projects/.

Bairoch, A. (2000) The ENZYME database in 2000. *Nucleic Acids Res.* **28**: 304–305.

Bang-Andreasen, T., Schostag, M., Priemé, A., Elberling, B., Jacobsen, C.S., and Douglas, T. (2017) Potential microbial contamination during sampling of permafrost soil assessed by tracers. *Sci. Rep.* **7**: 43338.

Bolger, A.M., Lohse, M., and Usadel, B. (2014) Trimmomatic: a flexible trimmer for Illumina sequence data. *Bioinformatics* **30**: 2114–20.

ter Braak, C. and Šmilauer, P. (2012) Canoco Reference Manual and User's Guide: Software for Ordination, Version 5.0 t.

Buchfink, B., Xie, C., and Huson, D.H. (2015) Fast and sensitive protein alignment using DIAMOND. *Nat. Methods* **12**: 59–60.

Cable, S., Elberling, B., and Kroon, A. (2018) Holocene permafrost history and cryostratigraphy in the High-Arctic Adventdalen Valley, central Svalbard. *Boreas* **47**: 423–442.

550 Caporaso, J.G., Kuczynski, J., Stombaugh, J., Bittinger, K., Bushman, F.D., Costello, E.K., et al. (2011)
551 NIH Public Access. **7**: 335–336.

552 Caporaso, J.G., Kuczynski, J., Stombaugh, J., Bittinger, K., Bushman, F.D., Costello, E.K., et al. (2010)
553 QIIME allows analysis of high-throughput community sequencing data. *Nat. Methods* **7**: 335–336.

554 Chao, A. (1984) Nonparametric Estimation of the Number of Classes in a Population. *Source Scand. J.*
555 *Stat.* **11177125**: 265–270.

556 Clein, J.S. and Schimel, J.P. (1995) Microbial activity of tundra and taiga soils at sub-zero temperatures.
557 *Soil Biol. Biochem.* **27**: 1231–1234.

558 Costello, E.K. (2007) Molecular phylogenetic characterization of high altitude soil microbial communities
559 and novel, uncultivated bacterial lineages.

560 DeAngelis, K.M., Allgaier, M., Chavarria, Y., Fortney, J.L., Hugenholtz, P., Simmons, B., et al. (2011)
561 Characterization of Trapped Lignin-Degrading Microbes in Tropical Forest Soil. *PLoS One* **6**:
562 e19306.

563 DeBruyn, J.M., Nixon, L.T., Fawaz, M.N., Johnson, A.M., and Radosevich, M. (2011) Global
564 biogeography and quantitative seasonal dynamics of Gemmatimonadetes in soil. *Appl. Environ.*
565 *Microbiol.* **77**: 6295–6300.

566 Deng, J., Gu, Y., Zhang, J., Xue, K., Qin, Y., Yuan, M., et al. (2015) Shifts of tundra bacterial and
567 archaeal communities along a permafrost thaw gradient in Alaska. *Mol. Ecol.* **24**: 222–234.

568 Edgar, R.C. (2010) Search and clustering orders of magnitude faster than BLAST. *Bioinformatics* **26**:
569 2460–1.

570 Elberling, B. and Brandt, K.K. (2003) Uncoupling of microbial CO2 production and release in frozen soil
571 and its implications for field studies of arctic C cycling. *Soil Biol. Biochem.* **35**: 263–272.

572 Elberling, B., Jakobsen, B.H., Berg, P., Søndergaard, J., and Sigsgaard, C. (2004) Influence of Vegetation,
573 Temperature, and Water Content on Soil Carbon Distribution and Mineralization in Four High Arctic
574 Soils. *Arctic, Antarct. Alp. Res.* **36**: 528–538.

575 Elberling, B., Michelsen, A., Schädel, C., Schuur, E.A.G., Christiansen, H.H., Berg, L., et al. (2013)
576 Long-term CO2 production following permafrost thaw. *Nat. Clim. Chang.* **3**: 890–894.

577 Elkateb, T., Chalaturnyk, R., and Robertson, P.K. (2003) An overview of soil heterogeneity:

quantification and implications on geotechnical field problems. *Can. Geotech. J.* **40**: 1–15.

Emerson, D., Scott, J.J., Benes, J., and Bowden, W.B. (2015) Microbial iron oxidation in the arctic tundra and its implications for biogeochemical cycling. *Appl. Environ. Microbiol.* **81**: 8066–8075.

Fierer, N., Bradford, M.A., and Jackson, R.B. (2007) TOWARD AN ECOLOGICAL CLASSIFICATION OF SOIL BACTERIA. *Ecology* **88**: 1354–1364.

Frank-Fahle, B.A., Yergeau, É., Greer, C.W., Lantuit, H., Wagner, D., Kuhry, P., et al. (2014) Microbial Functional Potential and Community Composition in Permafrost-Affected Soils of the NW Canadian Arctic. *PLoS One* **9**: e84761.

Giongo, A., Favet, J., Lapanje, A., Gano, K.A., Kennedy, S., Davis-Richardson, A.G., et al. (2013) Microbial hitchhikers on intercontinental dust: high-throughput sequencing to catalogue microbes in small sand samples. *Aerobiologia (Bologna).* **29**: 71–84.

Gittel, A., Bárta, J., Kohoutová, I., Mikutta, R., Owens, S., Gilbert, J., et al. (2014) Distinct microbial communities associated with buried soils in the Siberian tundra. *ISME J.* **8**: 841–853.

Gittel, A., Bárta, J., Kohoutová, I., Schnecker, J., Wild, B., Capek, P., et al. (2014) Site- and horizon-specific patterns of microbial community structure and enzyme activities in permafrost-affected soils of Greenland. *Front. Microbiol.* **5**: 541.

Grosse, G., Romanovsky, V., Jorgenson, T., Anthony, K.W., Brown, J., and Overduin, P.P. (2011) Vulnerability and feedbacks of permafrost to climate change. *Eos, Trans. Am. Geophys. Union* **92**: 73.

Hansen, A.A., Herbert, R.A., Mikkelsen, K., Jensen, L.L., Kristoffersen, T., Tiedje, J.M., et al. (2007) Viability, diversity and composition of the bacterial community in a high Arctic permafrost soil from Spitsbergen, Northern Norway. *Environ. Microbiol.* **9**: 2870–2884.

Hanson, N.W., Konwar, K.M., and Hallam, S.J. (2016) LCA∗: An entropy-based measure for taxonomic assignment within assembled metagenomes. *Bioinformatics* **32**: 3535–3542.

Hayes, D.J., Kicklighter, D.W., McGuire, A.D., Chen, M., Zhuang, Q., Yuan, F., et al. (2014) The impacts of recent permafrost thaw on land–atmosphere greenhouse gas exchange. *Environ. Res. Lett.* **9**: 45005.

Høj, L., Rusten, M., Haugen, L.E., Olsen, R.A., and Torsvik, V.L. (2006) Effects of water regime on

archaeal community composition in Arctic soils. *Environ. Microbiol.* **8**: 984–996.

Huerta-Cepas, J., Szklarczyk, D., Forslund, K., Cook, H., Heller, D., Walter, M.C., et al. (2016) EGGNOG 4.5: A hierarchical orthology framework with improved functional annotations for eukaryotic, prokaryotic and viral sequences. *Nucleic Acids Res.* **44**: D286–D293.

Hugelius, G., Strauss, J., Zubrzycki, S., Harden, J.W., Schuur, E.A.G., Ping, C.-L., et al. (2014) Estimated stocks of circumpolar permafrost carbon with quantified uncertainty ranges and identified data gaps. *Biogeosciences* **11**: 6573–6593.

Hyatt, D., Chen, G.L., LoCascio, P.F., Land, M.L., Larimer, F.W., and Hauser, L.J. (2010) Prodigal: Prokaryotic gene recognition and translation initiation site identification. *BMC Bioinformatics* **11**:.

Jansson, J.K. and Taş, N. (2014) The microbial ecology of permafrost.

Jorgenson, M.T., Racine, C.H., Walters, J.C., and Osterkamp, T.E. (2001) Permafrost Degradation and Ecological Changes Associated with a WarmingClimate in Central Alaska. *Clim. Change* **48**: 551–579.

Kim, H.M., Lee, M.J., Jung, J.Y., Hwang, C.Y., Kim, M., Ro, H.-M., et al. (2016) Vertical distribution of bacterial community is associated with the degree of soil organic matter decomposition in the active layer of moist acidic tundra. *J. Microbiol.* **54**: 713–723.

Koyama, A., Wallenstein, M.D., Simpson, R.T., and Moore, J.C. (2014) Soil bacterial community composition altered by increased nutrient availability in Arctic tundra soils. *Front. Microbiol.* **5**: 516.

Langmead, B. and Salzberg, S.L. (2012) Fast gapped-read alignment with Bowtie 2. *Nat. Methods* **9**: 357–359.

Larsen, K.S., Jonasson, S., and Michelsen, A. (2002) Repeated freeze–thaw cycles and their effects on biological processes in two arctic ecosystem types. *Appl. Soil Ecol.* **21**: 187–195.

Lee, H., Schuur, E.A.G., Inglett, K.S., Lavoie, M., and Chanton, J.P. (2012) The rate of permafrost carbon release under aerobic and anaerobic conditions and its potential effects on climate. *Glob. Chang. Biol.* **18**: 515–527.

Li, D., Liu, C.M., Luo, R., Sadakane, K., and Lam, T.W. (2015) MEGAHIT: An ultra-fast single-node solution for large and complex metagenomics assembly via succinct de Bruijn graph. *Bioinformatics* **31**: 1674–1676.

Liang, L., McNabb, J.A., Paulk, J.M., Gu, B., and McCarthy, J.F. (1993) Kinetics of iron(II) oxygenation at low partial pressure of oxygen in the presence of natural organic matter. *Environ. Sci. Technol.* **27**: 1864–1870.

Liao, Y., Smyth, G.K., and Shi, W. (2014) FeatureCounts: An efficient general purpose program for assigning sequence reads to genomic features. *Bioinformatics* **30**: 923–930.

Mackelprang, R., Waldrop, M.P., DeAngelis, K.M., David, M.M., Chavarria, K.L., Blazewicz, S.J., et al. (2011) Metagenomic analysis of a permafrost microbial community reveals a rapid response to thaw. *Nature* **480**: 368–371.

Magoč, T. and Salzberg, S.L. (2011) FLASH: Fast length adjustment of short reads to improve genome assemblies. *Bioinformatics* **27**: 2957–2963.

McCalley, C.K., Woodcroft, B.J., Hodgkins, S.B., Wehr, R.A., Kim, E.-H., Mondav, R., et al. (2014) Methane dynamics regulated by microbial community response to permafrost thaw. *Nature* **514**: 478–481.

Megonigal, J.P., Hines, M.E., and Visscher, P.T. (2004) Anaerobic Metabolism: Linkages to Trace Gases and Aerobic Processes.

Nikrad, M.P., Kerkhof, L.J., and Aggblom, M.M. (2016) The subzero microbiome: microbial activity in frozen and thawing soils. *FEMS Microbiol. Ecol.* **92**:.

O'Leary, N.A., Wright, M.W., Brister, J.R., Ciufo, S., Haddad, D., McVeigh, R., et al. (2016) Reference sequence (RefSeq) database at NCBI: Current status, taxonomic expansion, and functional annotation. *Nucleic Acids Res.* **44**: D733–D745.

Ogata, H., Goto, S., Sato, K., Fujibuchi, W., Bono, H., and Kanehisa, M. (1999) KEGG: Kyoto Encyclopedia of Genes and Genomes. *Nucleic Acids Res.* **27**: 29–34.

Øvreås, L., Forney, L., and Daae, F.L. (1997) Distribution of Bacterioplankton in Meromictic Lake Sælenvannet , as Determined by Denaturing Gradient Gel Electrophoresis of PCR-Amplified Gene Fragments Coding for 16S rRNA. *Appl. Environmantal Microbiol.* **63**: 3367–3373.

Padmanabhan, P., Padmanabhan, S., DeRito, C., Gray, A., Gannon, D., Snape, J.R., et al. (2003) Respiration of 13C-labeled substrates added to soil in the field and subsequent 16S rRNA gene analysis of 13C-labeled soil DNA. *Appl. Environ. Microbiol.* **69**: 1614–22.

662 Patrick, W.H. and Jugsujinda, A. (1992) Sequential Reduction and Oxidation of Inorganic Nitrogen,
663 Manganese, and Iron in Flooded Soil. *Soil Sci. Soc. Am. J.* **56**: 1071.

664 Quast, C., Pruesse, E., Yilmaz, P., Gerken, J., Schweer, T., Glo, F.O., and Yarza, P. (2013) The SILVA
665 ribosomal RNA gene database project : improved data processing and web-based tools. *nucleic acid*
666 *Res.* **41**: 590–596.

667 Rivkina, E., Petrovskaya, L., Vishnivetskaya, T., Krivushin, K., Shmakova, L., Tutukina, M., et al. (2016)
668 Metagenomic analyses of the late Pleistocene permafrost - Additional tools for reconstruction of
669 environmental conditions. *Biogeosciences* **13**: 2207–2219.

670 Romanovsky, V.E., Smith, S.L., and Christiansen, H.H. (2010) Permafrost thermal state in the polar
671 Northern Hemisphere during the international polar year 2007-2009: a synthesis. *Permafr. Periglac.*
672 *Process.* **21**: 106–116.

673 Schindelin, J., Rueden, C.T., Hiner, M.C., and Eliceiri, K.W. (2015) The ImageJ ecosystem: An open
674 platform for biomedical image analysis. *Mol. Reprod. Dev.* **82**: 518–529.

675 Schostag, M., Stibal, M., Jacobsen, C.S., Bælum, J., Taş, N., Elberling, B., et al. (2015) Distinct summer
676 and winter bacterial communities in the active layer of Svalbard permafrost revealed by DNA- and
677 RNA-based analyses. *Front. Microbiol.* **6**: 399.

678 Schuur, E.A.G., Vogel, J.G., Crummer, K.G., Lee, H., Sickman, J.O., and Osterkamp, T.E. (2009) The
679 effect of permafrost thaw on old carbon release and net carbon exchange from tundra. *Nature* **459**:
680 556–559.

681 Schwalm, C.R., Williams, C.A., Schaefer, K., Anderson, R., Arain, M.A., Baker, I., et al. (2010) A model-
682 data intercomparison of CO_2 exchange across North America: Results from the North American
683 Carbon Program site synthesis. *J. Geophys. Res.* **115**: G00H05.

684 Shannon, C.E. (1948) A mathematical theory of communication, bell System technical Journal 27: 379-
685 423 and 623–656. *Math. Rev. MR10, 133e*.

686 Shur, Y., Hinkel, K.M., and Nelson, F.E. (2005) The transient layer: implications for geocryology and
687 climate-change science. *Permafr. Periglac. Process.* **16**: 5–17.

688 Simpson, E.H. (1949) Measurement of diversity. *Nature*.

689 Taş, N., Prestat, E., McFarland, J.W., Wickland, K.P., Knight, R., Berhe, A.A., et al. (2014) Impact of fire

690 on active layer and permafrost microbial communities and metagenomes in an upland Alaskan boreal
691 forest. *ISME J.* **8**: 1904–1919.

692 Tatusov, R.L., Fedorova, N.D., Jackson, J.D., Jacobs, A.R., Kiryutin, B., Koonin, E. V., et al. (2003) The
693 COG database: An updated vesion includes eukaryotes. *BMC Bioinformatics* **4**:.

694 Tripathi, B.M., Kim, M., Kim, Y., Byun, E., Yang, J.-W., Ahn, J., and Lee, Y.K. (2018) Variations in
695 bacterial and archaeal communities along depth profiles of Alaskan soil cores. *Sci. Rep.* **8**: 504.

696 White III, R.A., Brown, J., Colby, S., Overall, C.C., Lee, J.-Y., Zucker, J., et al. (2017) ATLAS
697 (Automatic Tool for Local Assembly Structures) -a comprehensive infrastructure for assembly,
698 annotation, and genomic binning of metagenomic and metatranscriptomic data. *PeerJ Prepr.* 1–11.

699 Wilhelm, R.C., Niederberger, T.D., Greer, C., and Whyte, L.G. (2011) Microbial diversity of active layer
700 and permafrost in an acidic wetland from the Canadian High Arctic. *Can. J. Microbiol.* **57**: 303–315.

701 Wilson, B., Müller, O., Nordmann, E.-L., Seuthe, L., Bratbak, G., and Øvreås, L. (2017) Changes in
702 Marine Prokaryote Composition with Season and Depth Over an Arctic Polar Year. *Front. Mar. Sci.*
703 **4**:.

704 Xue, K., M. Yuan, M., J. Shi, Z., Qin, Y., Deng, Y., Cheng, L., et al. (2016) Tundra soil carbon is
705 vulnerable to rapid microbial decomposition under climate warming. *Nat. Clim. Chang.* **6**: 595–600.

706 Yang, S., Wen, X., Jin, H., Wu, Q., and Chavarria, K. (2012) Pyrosequencing Investigation into the
707 Bacterial Community in Permafrost Soils along the China-Russia Crude Oil Pipeline (CRCOP).
708 *PLoS One* **7**: e52730.

709 Yergeau, E., Hogues, H., Whyte, L.G., and Greer, C.W. (2010) The functional potential of high Arctic
710 permafrost revealed by metagenomic sequencing, qPCR and microarray analyses. *ISME J.* **4**: 1206–
711 1214.

712 Yin, Y., Mao, X., Yang, J., Chen, X., Mao, F., and Xu, Y. (2012) DbCAN: A web resource for automated
713 carbohydrate-active enzyme annotation. *Nucleic Acids Res.* **40**:.

714

Supplementary Information

Disentangling the complexity of permafrost soil by using high resolution profiling of microbial community composition, key functions and respiration rates

Oliver Müller[1], Toke Bang-Andreasen[2,3], Richard Allen White III[6], Bo Elberling[4], Neslihan Taş[5], Timothy Kneafsey[5], Janet K. Jansson[6], Lise Øvreås[1,7]

[1]Department of Biology, University of Bergen, Norway

[2]Department of Environmental Science, Aarhus University, DK-4000 Roskilde, Denmark

[3]Department of Biology, University of Copenhagen, DK-2100 Copenhagen, Denmark

[4]Center for Permafrost (CENPERM), Department of Geosciences and Natural Resource Management, University of Copenhagen, DK-1350 Copenhagen, Denmark

[5]Lawrence Berkeley National Laboratory, US

[6]Pacific Northwest National Laboratory, US

[7]University Center in Svalbard, UNIS

Supplementary information

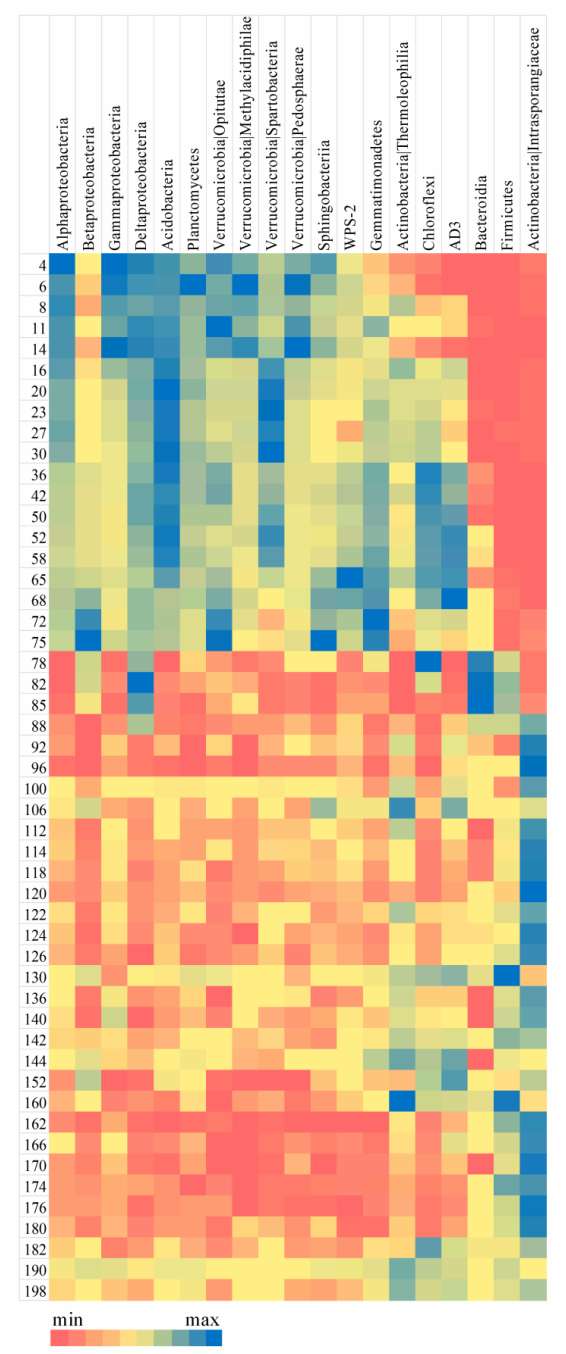

Figure S1: Heat map displaying the highly represented (additive relative abundance >90%) bacterial groups at class level across the permafrost depth profile. Each of the bacterial groups is colored according to its maximum abundance at any depth of the core. The darkest blue illustrates maximum, yellow medium and red lowest abundances.

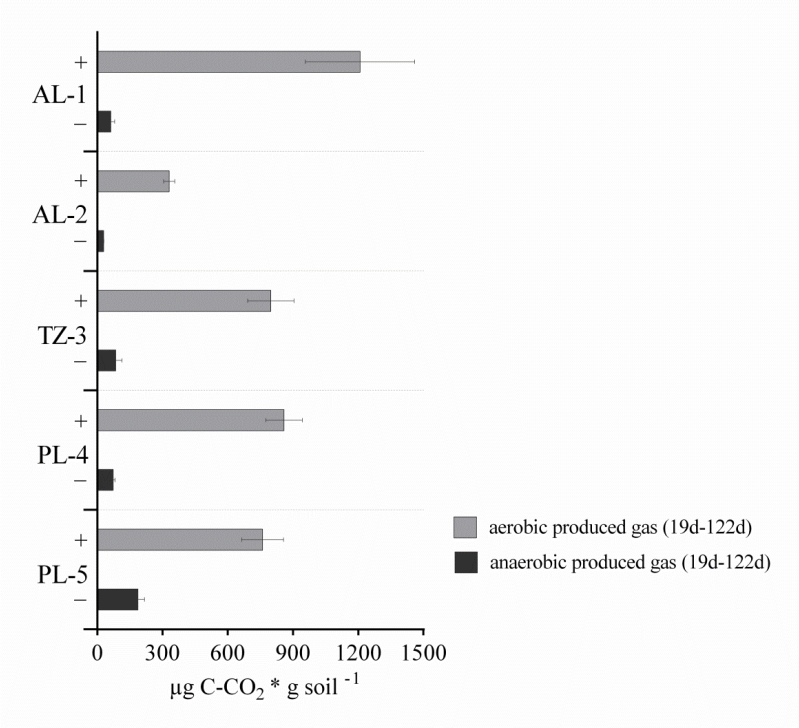

Figure S2: CO_2 emissions over 103 days incubation of permafrost samples, calculated for the period between day 19 and 122. Experiments were performed with 2 g soil samples from 5 segments of core 1 covering the AL, TZ and PL (Table S2). Samples were incubated at 4-6°C under aerobic (+) or anaerobic (-) conditions.

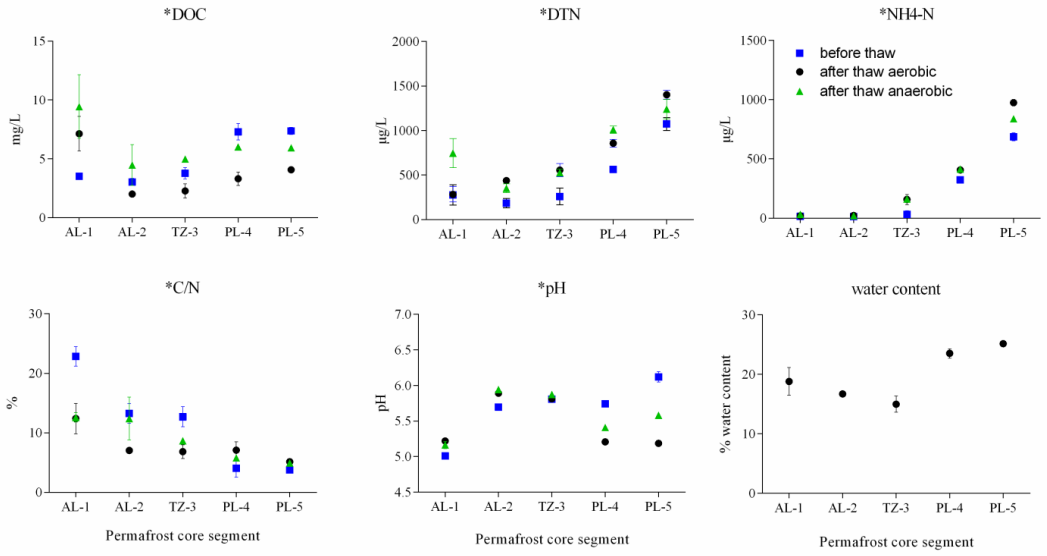

Figure S3: Soil chemistry, including DOC, DTN, NH_4-N, C/N ratio, pH and water content of the permafrost incubations of the five segments from core 1, measured before (black) and after 19 days of incubation under aerobic (blue) and anaerobic (green) conditions.

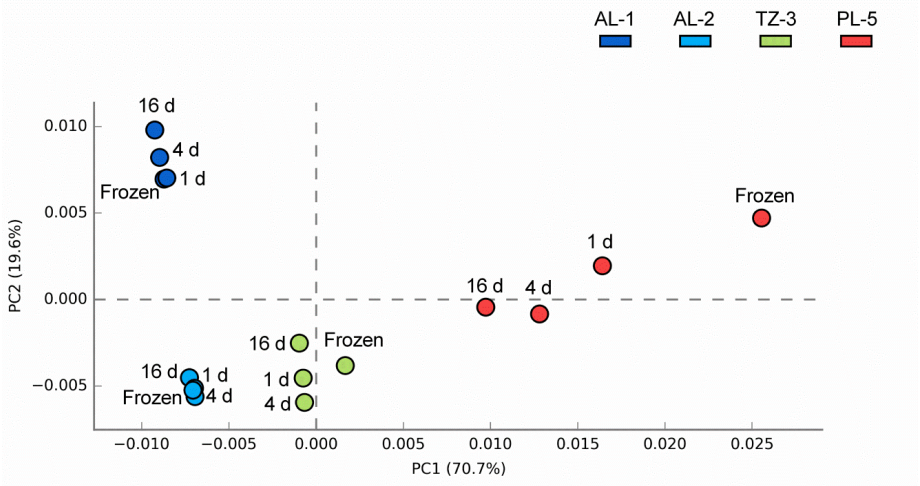

Figure S4: Principal component analysis (PCA) of 16 metagenomes based on frequencies of KEGG annotated read frequency. KEGG reads were normalized to metagenome size and samples are colored according to segments from the incubation experiment. Dark blue = Active Layer 1; Light blue = Active Layer 2; Green = Transition Zone 3; Red = Permafrost Layer 5. The time point of incubation is given by the sample label and only aerobic incubations are included in the analysis.

Table S1: Detailed 16S rRNA sequencing information regarding the number of replicates and sequences before and after processing in Qiime for the entire soil core profile.

Depth in cm	Sample ID	DNA conc. in ng per g soil	16S rRNA sequencing 2012	16S rRNA sequencing 2016	Sequences 2012			Sequences without singletons/unassigned			Sequences 2016			Sequences without singletons/unassigned		
					a	b	c	a	b	c	a	b	c	a	b	c
4	2_1_5	3608.5	x		18339	25765	9022	16862	23455	8453						
6	2_1_4	2541	x		6046	19835	5611	5591	18475	5013						
8	2_1_3	1577.8	x		1743	3729	3452	1610	3421	2866						
11	2_1_2	1663.9	x	x	32629	33563	22476	28755	30346	20186	171055	149955	119299	140922	130176	96050
14	2_1_1	2371.6	x		386	3504	5037	362	3293	4691						
16	2_2_5	1395.1	x		5383	1715	1843	4984	1577	1740						
20	2_2_4	2192.4	x		9477	11919		8796	10939							
23	2_2_3	1228.5	x		14224	8525	9037	13274	7798	8361						
27	2_2_2	1800.4	x		13757	2672	15213	11436	2486	14221						
30	2_2_1	1617	x		55727	90596	11363	50809	85261	10627						
33	2_3_6															
36	2_3_5	1003.3		x							130160	75079	164450	122248	70886	155131
39	2_3_4															
42	2_3_3	672		x							115239	151154	153176	109007	142728	144228
45	2_3_2															
50	2_3_1	416.7		x							157235	103684	130840	147571	97126	122728
52	2_4_5	835.3		x							238117	312342	146174	221041	287317	135086
55	2_4_4															
58	2_4_3	664.7		x							167313	254989	176348	154713	237462	163027
61	2_4_2															
65	2_4_1	1072.7		x							251085	309841	162152	234195	290031	151446
68	2_5_2	841.3		x							98445	129613	170744	93337	121174	161117
72	2_5_1	1230.7		x							89373	46507	65988	86466	45058	62551
75	2_6_3	940.7		x							41600	44458	19180	39923	42705	18600
78	2_6_2	1268		x							435282	286751	113382	410592	270181	107578
82	2_6_1	1126		x							91375	104187	111265	89028	101532	108523
85	2_7_5	803.3		x							92386	57477	156859	88680	54863	150820
88	2_7_4	323.4	x		50763	92017	12140	47872	87381	11272						
92	2_7_3	406	x		118033	111693	61627	111065	103420	56617						
96	2_7_2	330.4	x		101928	114819	101275	93402	107516	93381						
100	2_7_1	379.4	x	x	10228	60107	44768	9752	56594	41407	149053	189616	184934	130619	169363	164458
104	2_8_6															
106	2_8_5	288.7		x							190700	128854		175176	119554	
110	2_8_4															
112	2_8_3	118.3	x		67253	42632	34606	62558	39092	30691						
114	2_8_2	177.8	x		100581	79533	63401	93021	75566	60104						
118	2_8_1	171.5	x		81752	22560	105462	77956	21240	97142						
120	2_9_4	43.4	x		213878	73360	97992	200275	66736	90812						
122	2_9_3	70.7	x		126871	92286		115958	86855							
124	2_9_2	107.6	x		70573	27772	135810	66352	26135	127895						
126	2_9_1	63	x		145651	89626	98530	136234	82973	93021						
128	2_10_6															
130	2_10_5	87.8		x							190851			179238		
134	2_10_4															
136	2_10_3	43.6	x		66653	12953		62760	12192							
140	2_10_2	24.5	x		2333	40272	23365	2174	38234	22128						
142	2_10_1	33.3	x	x	13684	22530	12279	12673	21654	11638	76898	238434	152033	70252	221898	139807
144	2_11_5	66.5		x							191193	156642	254504	176153	144328	234929
148	2_11_4															

152	2_11_3	76.3	x							168233	366032		153895	335792			
156	2_11_2																
160	2_11_1	84	x							128740	172584	187363	119111	158647	173160		
162	2_12_6	44.6	x	28501	63176	50784	27091	60677	47422								
166	2_12_5	45.5	x	116112	22046	54468	108291	20987	51518								
170	2_12_4	67.7	x	40225	12423	12691	37692	11561	12089								
174	2_12_3	57.8	x	136	29717	17457	124	28242	16360								
176	2_12_2	56.9	x	10767	8100	20812	10240	7429	19742								
180	2_12_1	70.5	x	7395	14998	13349	6886	14346	12640								
182	2_13_5	92	x							89265	211421	110251	78385	183880	97865		
186	2_13_4																
190	2_13_3	99.7	x							60180	225524	102941	55665	209863	95893		
194	2_13_2																
198	2_13_1	72.8	x							103497	117303	88951	95124	107910	82326		

Table S2: Overview of permafrost core segments used for the incubation experiments containing the depth and the characteristic layer represented by those segments.

Segment ID	Depth below surface (in cm)		Permafrost zone
	Core 1 2011	Core 2 2014	
AL-1	6-20	20-36	Active layer
AL-2	57-74	57-73	Active layer
TZ-3	74-89	73-83	Transition zone
PL-4	89-107	95-107	Permafrost layer
PL-5	167-187	167-185	Permafrost layer

Table S3: ANOSIM analysis of Euclidean distances between 16S rRNA gene sequencing data from the high resolution soil profile (core 1) and the sequencing data from the five chosen layers used in the incubation experiment from core 1 and core 2. The number indicates the grade of dissimilarity (1=most dissimilar). The best similarity value for each incubation segment of the two cores is highlighted with a light green background.

High resolution profile samples		Incubation samples (all n=1)									
core-2011		core-2011					core-2014				
Layer	Depth in cm	AL-1	AL-2	TZ-3	PL-4	PL-5	AL-1	AL-2	TZ-3	PL-4	PL-5
AL-1 (n=7)	6-20	**-0.08**	0.67	1	1	1	0.65	1	0.89	1	1
AL (n=7)	20-54	0.97	0.10	1	1	1	0.35	1	0.97	1	1
AL-2 (n=5)	57-74	0.4	**0.04**	1	1	1	**0.12**	**0.2**	**-0.12**	1	1
TZ-3 (n=3)	74-89	1	1	**-0.56**	1	1	1	1	1	1	1
PL-4 (n=5)	89-107	1	1	1	**0.08**	0.4	1	1	1	0.68	**0.8**
PL (n=15)	107-167	1	1	1	0.31	**0.38**	1	1.00	1.00	**0.68**	0.80
PL-5 (n=7)	167-187	1	1	1	0.58	0.63	1	1	1	0.92	1

Table S4: Summary of metagenomics sequencing results.

Sample groups	Read length (bp)	No. of reads in Million	No. of contigs (1k) in Million	No. of reads for bin size cutoff		N_{50} (bp)	GC %	Reads mapped against active layer (%)	Reads mapped against transition zone (%)	Reads mapped against permafrost layer (%)
				>5 kb	>10 kb					
Active layer	250	24.67	1.16	3.20%	0.60%	2022	59.94	64.23	29.98	17.85
Transition zone		7.32	0.42	4.93%	1.60%	2498	53.81	36.64	70.24	34.06
Permafrost layer		4.19	0.18	3.72%	0.78%	2100	58.99	49.37	57.53	62.16

Detailed description of the study site, sampling and sample processing

Soil samples were obtained from a characteristic low-centred ice-wedge polygon site in the valley Adventdalen on Svalbard (78.186N, 15.9248E). At our study site in Adventdalen (Svalbard), the maximum AL depth measured by the end of the summer season is less than 100 cm (Christiansen *et al.*, 2010) and the PL below extending to greater than 100 m (Humlum *et al.*, 2003). Adventdalen is a U-shaped, broad valley with braided river floodplain deposits and terraces and the dominant periglacial landforms are pingos and ice wedges (BRYANT, 1982; L. Sørbel & J. Tolgensbakk, 2002). Annual average precipitation is at around 190 mm, making Adventdalen one of the driest parts in Svalbard. Mean annual air temperature is at around -6 °C at Svalbard Airport (1961–1990; (Førland *et al.*, 1997)), 16 km west of the sampling site. The low-centred ice-wedge polygons are typically covered by tall grasses in the troughs and mosses in the central parts (Christiansen, 2005). Overall two separate cores were drilled; the first core was obtained in April 2011 and is referred to as "core 1" and a replicate core which was drilled at the same coordinates in July 2014 ("core 2"). Vegetation was removed along with thawed top soil (4 cm in 2011 and 20 cm in 2014) to drill through the active layer down into the permafrost to a depth of two meter. During drilling, core sections up to 50 cm long were obtained (ø 7.2 cm) and immediately wrapped in aluminum foil, kept frozen and stored at -80 °C, until further analysis. Core 1 was used for the high resolution 16S rRNA gene sequencing. Sub-samples from core 1 and core 2 were used for the incubation experiments to obtain gas flux measurements. Due to experimental restraints, several layers had to be pooled and represent five characteristic different segments of the core profile (Table S2). Similar depths were used to pool material from core 2. These five segments from both cores were as well used for 16S rRNA gene sequencing to confirm firstly, that community structure is comparable in both cores and

secondly that the five segments have a similar community structure at corresponding depths observed from the high resolution sequencing.

Core 1 used for high resolution profile was cut into 1.5 - 2 cm subsections using a diamond blade electric saw, where the sawblade was washed in ethanol prior to the cutting. Core 2 was separated into smaller 4-6 cm subsections using a sterile chisel. To remove potential core surface contaminants, introduced during the drilling procedures, the outermost 2 cm were scraped off with sterile blades. The remaining inner part was kept frozen on dry ice and transferred to a sterile thick plastic bag and homogenized by hammering. Samples for DNA extraction used for the high resolution profile sequencing were collected from core 1 as subsections at 2-4 cm intervals (Table S1). For the incubation experiments soil from several subsections was pooled into 5 larger segments for each core 1 and 2 (Table S2). Characteristic soil properties, such as pH, water content, dissolved organic carbon (DOC), NO_3 and NH^{4+} were measured for most of the subsections of core 1 used for high resolution profile and for all segments from both cores used for the incubation experiments.

Detailed description of chemical analyses and X-ray CT scanning

1 g soil was homogenized and diluted in 10 ml dH_2O and the pH measured on a pH-meter. The water content was calculated based on the difference in weight after the water in 1 g of soil was evaporated at 80 °C for 24 hours. Dissolved organic carbon (DOC) and nitrogen (DTN), including NO_3 and $NH4^+$, were analyzed following a cold water extraction where ~2 g of soil were dissolved in 20 ml of dH_2O and incubated while shaking at 4 °C for 5 hours. The mixtures were centrifuged at 4300 rpm for 10 min and the resulting supernatant was transferred into 30 mL acid washed HDPE bottles. Nitrate and ammonium were measured using flow injection analysis on a FIAstar™ 5000. Samples for DOC measurements were first acidified with 2 M HCl and then analyzed on a TOC-5000A/SSM-5000A.

The core was X-ray CT scanned using a modified Siemens Somatom HiQ medical CT scanner at 133 kV. The scan slice thickness was 2 mm, and scans were performed every centimeter. The voxel dimension for the resulting images was 193 microns x 193 microns x 2000 microns. To obtain bulk density, the CT scanner was calibrated by scanning a number of materials having known density. This technique is fairly good for materials composed mostly of lighter elements, but has larger errors when the scanned soils are high in iron or other heavier elements. The data were analyzed using imageJ (Schindelin *et al.*, 2015). After calibrating the data, a threshold was set such that values between 0.59 and 2.3 g/cm3 were included. Slices having more than 30,000 voxels were considered in assigning axial length values, and slices having more than 50,000 voxels between these values were considered for density measurements. Slices with less

than 50,000 voxels showed unusual values, as they were typically near the core segment ends and perhaps sustained changes from the coring and handling processes.

Detailed description of soil incubations and gas-flux measurements

All preparations for soil incubations were performed in a -20 °C cold room. All incubation experiments included three replicates and covered five different segments (2 from the AL, 1 from the TZ and 2 from the PL) from each of the two permafrost cores. For those segments soil from several subsections was pooled from similar depths for each core 1 and 2 and therefore segments slightly vary between the cores (Table S2). Two gram of soil were added to sterilized glass vials (20 ml) and sealed with butyl rubber stoppers and aluminum crimps. Samples incubated under anaerobic conditions were flushed with nitrogen for 1 min. Three ml of headspace gas were collected from the vials immediately after the incubation was started and at 9 time points (4h, 12h, 24h, 2d, 4d, 6d, 16d, 19d, 122d) during incubation. After each gas collection aerobic or anaerobic conditions were re-established and a positive pressure was applied in bottles by either injecting 3 ml atmospheric gas (aerobic) or 3 ml nitrogen (anaerobic) into the headspace. The gas samples were transferred into 3 ml Exetainer glass vials and analyzed for CO_2, CH_4 and N_2O on a SRI 8610C gas chromatograph. Measurements for CH_4 and N_2O were below the detection limit in all the segments and data therefore not included. All samples were incubated at 4(±1) °C in the dark, over the course of several days and weeks for up to 122 days. Additionally, before the start of the incubation DNA was extracted from the five different segments and 16S rRNA gene sequencing analysis performed as described below.

Detailed description of sequencing and bioinformatic analyses

High-throughput sequencing was performed on a MiSeq platform (Illumina) using the MiSeq Reagent Kit v1 and v2 respectively (Illumina). Sequencing data was processed using different bioinformatic tools incorporated in the Qiime-processing platform using version 1.9.1. (Caporaso *et al.*, 2010). A total of 13,669,151 sequences were retrieved from 151 samples. FASTQ files of paired-end sequences were quality end-trimmed at a phred quality score ≥ 24 using Trimmomatic (Bolger *et al.*, 2014) and merged using PANDAseq (Masella *et al.*, 2012), while all reads <200bp were removed. Prokaryotic OTUs were selected at a sequence similarity threshold of 97% using a de novo uclust (Edgar, 2010) OTU clustering method with default parameters and taxonomy assigned using the Greengenes reference database (DeSantis, 2006). OTUs with a taxonomic identification were assembled to an OTU table providing abundances for each sample excluding singletons and unassigned OTUs. To test for multivariate environmental correlation with the prokaryotic community structure the programs primer-e version 6 (Plymouth, UK) and Canoco 5 (ter Braak and Šmilauer, 2012) were used.

II

III

Bacterial response to permafrost derived organic matter input in an Arctic fjord

Oliver Müller[1*], Lena Seuthe[2], Gunnar Bratbak[1], Maria Lund Paulsen[1]

[1]Department of Microbiology, University of Bergen, 5006 Bergen, Norway

[2]Department of Arctic and Marine Biology, UiT – The Arctic University of Tromsø, 9037 Tromsø, Norway

*Corresponding author: oliver.muller@uib.no

Keywords: dissolved organic matter, Arctic, terrestrial run-off, permafrost, tDOM, Kongsfjorden, microbial community composition, Glaciecola, 16S rRNA sequencing

Abstract:

The warming of the Arctic causes increased riverine discharge, coastal erosion, and the thawing of permafrost. Together, this is leading to an increased wash out of terrestrial dissolved organic matter (tDOM) into the coastal Arctic ecosystems. This tDOM may be anticipated to affect both carbon and nutrient flow in the microbial food web and microbial community composition, but there are few studies detailing this in Arctic marine ecosystems. We tested the effects of tDOM on the bacterial community composition and net-growth by extracting DOM from the active layer of permafrost soil and adding the aged tDOM concentrate to a natural microbial fjord community (Kongsfjorden, NW Svalbard). This resulted in an increased carbon load of 128 µM in the tDOM treatment relative to the control of 83 µM DOC. We observed changes in community composition and activity in incubations already within 12 hours where tDOM was added. Flow cytometry revealed that predominantly large bacteria increased in the tDOM treated incubations. The increase of this group correlated with the increase in relative abundance of the genus *Glaciecola* (Gammaproteobacteria). *Glaciecola* were initially not abundant in the bacterial community (0.6%), but their subsequent increase up to 47% after four days upon tDOM addition compared to 8% in control incubations indicates that they are likely capable of degrading permafrost derived DOM. Further, according to our experimental results we hypothesize that the tDOM addition increased bacterivorous grazing by small protists and thus tDOM might indirectly also effect higher trophic levels of the microbial food web.

Introduction:

The Arctic is experiencing a warming at nearly twice the global rate, with drastic changes for the ecosystem (Trenberth et al. 2007; Screen and Simmonds 2010; Vincent 2010). Higher sea surface temperatures, melting sea ice and increased freshwater input from large Arctic rivers, transporting nutrients and terrestrial organic matter into the ocean, have multiple implications for the marine carbon cycle (Li et al., 2009; Doney et al., 2012; El-Swais et al., 2015; Fichot et al. 2013; Holmes et al., 2013). Higher temperatures are on the one hand responsible for a decreasing sea ice cover, which in turn may enhance primary production and thus the biological carbon pump (CO_2 burial), but on the other hand could also increase the rate of bacterial degradation of phytoplankton derived dissolved organic matter (DOM) (CO_2 production) (Wohlers et al., 2009). This bacterial transformation of phytoplankton derived DOM might lead to the accumulation of more complex humic-like organic matter via the microbial carbon pump (Jiao et al., 2010).

In the Arctic, another source of DOM comes from permafrost soil organic matter and enters the Arctic Ocean via rivers (Feng et al., 2013; Holmes et al., 2012). Estimations show that mobilization of DOM has increased up to 6% from 1985 to 2004 (Feng et al., 2013) and will further increase under the current warming climate (Amon et al., 2012).Yearly, about 3,300 km^3 of freshwater stream into the Arctic Ocean and influence stratification, light absorption, surface temperature, gas exchange, productivity and carbon sequestration (Rachold et al., 2004). This input is often characterized by a high dissolved organic carbon (DOC) concentration, reaching more than 1000 $\mu mol\ kg^{-1}$, compared to open ocean concentrations of around 80 $\mu mol\ kg^{-1}$ (Dittmar and Kattner, 2003; Hansell et al., 2009; Stedmon et al., 2011). The quality of the DOC has in some studies been described to be mainly refractory (Dittmar and Kattner, 2003; Opsahl et al., 1999; Xie et al., 2012), while other studies showed that up to 40% can be degrade within weeks up to months (Hansell, 2004; Holmes et al., 2008; Sipler et al., 2017b; Vonk et al., 2013). Thus, it is still disputed whether Arctic tDOM can represent an important carbon source for marine bacteria, leading to increased CO_2 production and how this may affect the marine trophic network via the microbial loop.

Several studies have examined the ability of bacteria to degrade the seasonally available phytoplankton derived DOM and found that an increase of such carbon sources influences both the structure and the activity of the bacterial community (Pinhassi et al., 2004; Sapp et al., 2007; Teeling et al., 2012). Especially a versatile group of Gammaproteobacteria, belonging to the order *Alteromonadales,* responds immediately both in abundance and activity, when phytoplankton derived DOM becomes available (Beier et al., 2015; Eilers et al., 2000; McCarren et al., 2010; Pedler et al., 2014; von Scheibner et al., 2017). Only few studies have investigated the effects of terrestrial derived DOM on marine microbial community structure and activity (Blanchet et al.; Herlemann et al., 2014, 2017; Traving et al., 2017), of which even less have been conducted in the coastal Arctic (Sipler et al., 2017b). Common for all studies is an observed shift in bacterial community structure due to the addition of tDOM. There is a need to understand how this community shift might affect higher trophic levels in order to better understand climate change impacts on the marine Arctic ecosystem. A higher bacterial activity due to the degradation of tDOM might cause a higher turnover within the microbial loop and therewith increased CO_2 production, but ultimately depends on the bacterial growth efficiency. Increased carbon availability might also enhance the competition between bacteria and phytoplankton for inorganic nutrients and indirectly disadvantage larger phytoplankton (Sipler et

al., 2017a; Thingstad et al., 2008). Thus, high tDOM input may decrease primary production in coastal Arctic areas.

We here studied the impact of permafrost-derived DOM on an Arctic fjord microbial community using 16S rRNA amplicon sequencing and followed the changes over the course of a nine-day incubation experiment. We hypothesized that the increased organic matter input, as a consequence of increased run-off from land, would provide a potential source of organic matter for fjord microbial communities. If bioavailable, this tDOM will stimulate the growth of some fast-responding bacterial groups that were initially underrepresented and increase in abundance over time. In particular, we were interested in answering two questions 1) how tDOM might alter the fjord bacterial community composition and 2) how tDOM might affect the growth and size of bacteria and subsequently protist grazers. This study thus aims to improve our understanding of the implications of a warmer Arctic, influenced by increased run-off from land, on coastal microbial communities.

Material and Methods:

Preparation of aged permafrost-derived tDOM stock solution

Active layer permafrost soil from 50 cm depth, just above the frozen permafrost table, was sampled in Adventdalen, Svalbard (78.19 N, 15.89 E), and mixed with unfiltered water from the nearby Adventfjorden (1m depth) in the ratio 600g soil to 1L water. The mix was stored in the dark for 30 days at 4°C to degrade the predominantly labile compounds, thus producing 'aged tDOM' as has been done in similar studies (Eiler et al., 2003). The rationale behind using an aged tDOM stock was to increase resemblance to the organic matter that reaches the coastal systems, as the most labile compounds will be degraded during its transportation from soil to coastal waters (Lobbes et al. 2000). Before being added to tDOM incubations, the stock solution was filtered through 0.2 µm polycarbonate filters, ensuring that only dissolved organic matter was present in the tDOM stock solution. To test the character of DOM in the tDOM-solution relative to the control, the fluorescent properties were examined during an earlier analysis, performed in 2014. Here five fluorescence components (two humic-like and three amino-like) were described following the method explained in (Stedmon and Markager, 2005). The averaged intensity (given in Raman units) of these components are given in Table S1. The intensity of the humic-like substances was two-fold higher in the tDOM-stock relative to the control (0.2µm filtered Atlantic water) and further one of the amino-like components was 100 times higher in the tDOM stock solution. Since we did not characterize the DOM composition at the end of the experiment, we cannot say what exact compounds were consumed or produced throughout our incubations. The rationale behind measuring the DOM components in the beginning was to ensure that more complex compounds were enriched in the tDOM-solution. The results strongly indicate that the character of the DOM was significantly different in the tDOM treatment compared to the control.

Study site and experimental set-up

Kongsfjorden is a 26 km long fjord, 6 to 14 km wide and includes two tidewater-glaciers, Kronebreen and Kongsvegen (Figure 1A). Water samples for incubations were collected on the 29th of June in 2015 from the centre of the fjord near Kings Bay (78.95°N, 11.93°E) at 40m depth (Figure 1A). The water was filtered through pre-combusted GFC filters (1.2 µm) to reduce the presence of protist. The tDOM-stock solution had a carbon concentration of 190 µM DOC and was mixed in the ratio of 1:2.5 with fjord water (83 µM DOC) and aliquoted into eight 1L air-tight glass bottles (Figure 1B). Filtered (0.2 µm) fjord water was added in the same ratio to the eight control bottles. The final DOC concentration was 1.5 times higher in the tDOM treatment incubations (128 µM) than in the control incubations (83 µM). The elevated DOC concentration in the tDOM treatment reflects ranges of natural, elevated concentrations near the sample site in Kongsfjorden (Zhu et al., 2016). In total, we incubated 16 bottles, representing eight replicated starting conditions to investigate the effect of tDOM addition over time in comparison to eight controls. Incubations were kept dark at 2°C and terminated after 9 days. The responses in terms of bacterial community composition were documented in the treatment and control bottles at eight different time points spanning over nine days in total (0d, 0.5d, 1d, 2d, 3d, 4d, 5d, 9d; Figure 1B), by harvesting one of the eight bottles (ca. 1L), each from the tDOM treatment and control bottles, at every sampling occasion. Samples (6ml) for

measurements of bacterial abundance via flow-cytometry were collected as replicates according to the number of bottles remaining at each respective sampling point (e.g. 8 replicates at t0, 4 at d4 and 1 at d9). Both bacterial abundance and community composition were also analyzed for the untreated 40m fjord sample and 0.2 µm filtered tDOM-stock solution.

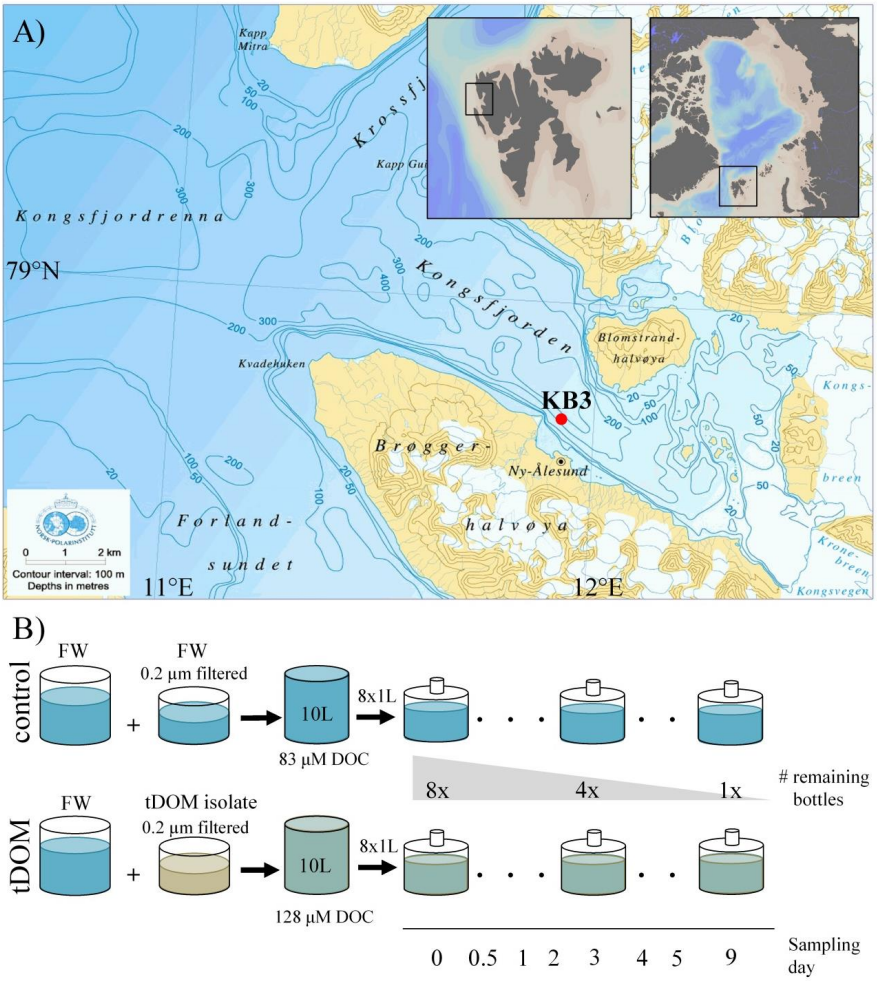

Figure 1: A) Study area in northwest Svalbard (78.95°N, 11.93°E) showing the sampling location in Kongsfjorden (red circle). B) Illustration of the experimental design showing that for both tDOM treatment and control eight bottles with the same starting condition were incubated for different periods (from 12 hours up to 9 days). One bottle was harvested at each sampling point to analyse the bacterial community composition. Bacterial abundance was measured using flow cytometry for samples at the beginning of the experiment, including the fjord water (8.1×10^5 mL^{-1}), the 0.2 µm filtered fjord water (2.8×10^4 mL^{-1}) and the tDOM isolate (3.2×10^4 mL^{-1}) and over the course of the incubation in both treatment and control bottles (number of replicates was dependent on the number of remaining bottles). FW=fjord water; tDOM=solution of terrigenous dissolved organic matter from permafrost; DOC=dissolved organic carbon

Bacterial enumeration using flow cytometry

The abundance of bacteria, virus and heterotrophic nanoflagellates (HNF) were determined on an Attune® Acoustic Focusing Flow Cytometer (Applied Biosystems by Life technologies) with a syringe-based fluidic system and a 20 mW 488 nm (blue) laser. Triplicate samples of 2ml were fixed with glutaraldehyde (0.5% final conc.) at 4°C for a minimum of 30 min, flash frozen in liquid nitrogen and stored at -80°C. Samples were first thawed and diluted x10 with 0.2 µm filtered TE buffer (Tris 10 mM, EDTA 1 mM, pH 8), stained with a green fluorescent nucleic acid dye (SYBR Green I ; Molecular Probes, Eugene, Oregon, USA) and then incubated for 10 min at 80°C in a water bath (Marie et al., 1999). Samples were counted at a low flow rate of 25 µL min^{-1} and a minimum volume of 100 µL. Bacteria were discriminated on a biparametric plot of green florescence (BL1) vs. red florescence (BL3).
Additionally, these plots allowed to distinguish between low nuclear acid (LNA) and high nuclear acid (HNA) bacteria, virus, and a subgroup we here call 'large bacteria'. Heterotrophic nanoflagellates (HNF) were measured at a high flow rate (500 µL min^{-1}) according to (Zubkov et al., 2007). Pico-and nano-sized phytoplankton were counted directly after thawing and the various groups discriminated based on their red fluorescence (BL3) vs. orange fluorescence (BL2) (Paulsen et al., 2016).

DNA extraction, PCR amplification and amplicon sequencing

The bacterial biomass for molecular analysis was collected by filtering ca. 1 L onto 0.22 µm Millipore® Sterivex filters (Merck-Millipore), which were flash frozen in liquid nitrogen and stored at -80°C. DNA and RNA were simultaneously extracted from the Sterivex filters using the AllPrep DNA/RNA Mini Kit (Qiagen, Hilden, Germany) according to the manufacturer's instructions. In this study, only RNA was used in order to investigate changes in the active community. Before PCR amplification, RNA was treated with the DNA-free DNA Removal kit (Invitrogen, CA, USA). Subsequently, 10 ng of DNA-free RNA was reverse transcribed using the SuperScript III First-Strand Synthesis System for RT-PCR (Invitrogen), according to the manufacturer's instructions. Amplification of cDNA (reverse transcribed RNA) targeting the bacterial/archaeal 16S rRNA gene V4 hypervariable region was performed using a two-step nested PCR approach with primers 519F (CAGCMGCCGCGGTAA; Øvreås et al., (1997) and 806R (GGACTACHVGGGTWTCTAAT; Caporaso et al., (2011). In brief, the first PCR step was performed in triplicates. Samples were amplified, comprising 10 ng cDNA, 10 µL HotStarTaq Master Mix (Qiagen), 0.5 µM of each primer and nuclease-free water. PCR reaction conditions were as follows: initial denaturation of 15 min at 95°C, followed by 25 cycles of 95°C for 20 s, 55°C for 30 s and 72°C for 30 s and a final extension step of 72°C for 7 min. After triplicate PCR products were pooled, the DNA Clean & Concentrator-5 kit (Zymo Research Corporation, CA, USA) was used for purification. During the second PCR step, 10 ng of pooled PCR product, 25 µL HotStarTaq Master Mix, 0.5 µM of each nested primer (containing a unique eight-nucleotide barcode) were mixed with nuclease-free water to a reaction volume of 50 µL. PCR reaction conditions were as follows: initial denaturation of 15 min at 95°C, followed by 15 cycles of 95°C for 20 s, 62°C for 30 s, 72°C for 30 s and a final extension step of 72°C for 7 min. Final PCR products were purified using Agencourt AMPure XP Beads (Beckman

Coulter Inc., CA, USA) and pooled in equimolar amounts. Before sequencing, the quality and concentration of the amplicon pool were assessed by agarose gel electrophoresis and a Qubit 3.0 Fluorometer, respectively. The final amplicon library was sequenced at the Norwegian Sequencing Centre (Oslo, Norway) using their MiSeq platform (MiSeq Reagent Kit v2, Illumina, CA, USA). All Illumina sequencing data is available at the European Nucleotide Archive (ENA) under study accession number PRJEB25031.

16S rRNA gene sequence analysis

Illumina Paired-end sequence data was processed using different bioinformatic tools incorporated on a QIIME-processing platform (Caporaso et al., 2011b). In short, FASTQ files were quality end-trimmed at a phred quality score ≥ 24 using Trimmomatic (Bolger et al., 2014) and merged using PANDAseq (Masella et al., 2012), while all reads <200bp were removed. A total of 1,916,574 sequences were retrieved across 18 samples and two sequencing controls. Those sequences were used to select prokaryotic OTUs at a sequence similarity threshold of 97% using a de novo uclust (Edgar, 2010) OTU clustering method and taxonomy assigned using the Silva 111 reference database (Quast et al., 2013). After removal of singletons and unassigned OTUs, sequences were rarefied to 10,000 reads per sample, with a total of 15,513 unique OTUs at 97% sequence identity. Rarefaction curves were calculated using QIIME's alpha rarefaction script and showed that sequencing coverage was sufficiently high, as samples approached an asymptote. The phylogenetic data was then used to calculate relative abundance at different taxonomical levels. When combined with absolute bacterial abundance data from flow cytometer measurements, the absolute abundance of taxa can be calculated. For this the bacterial abundance in cells per ml is multiplied with the relative abundance of the taxa of interest.

Indicator OTU analysis

Calculations to identify indicator OTUs associated with the treatment of tDOM addition were performed using the "indicspecies" package (De Cáceres and Legendre, 2009) included in the statistical software R 3.2.3 (R Core Team 2012) and the script "otu_category_significance.py" within the QIIME-processing platform (Caporaso et al., 2011b). Both tools can be used to assess statistically significant differences between OTU abundances and defined groups. We defined groups according to the experimental strategy in tDOM treatment and control. The analysis included only samples after two days of the experiment when abundances of *Pseudoalteromonas* sequences, an artefact of the experimental set-up, were greatly reduced.

Statistical analysis

Correlations between bacterial abundance and community structure were calculated using the Pearson correlation coefficient (Pearson`s r) and were carried out using GraphPad Prism v 6.01 for Windows (GraphPad Software, CA, USA).

Calculations to estimate bacterial and HNF carbon turnover

Calculations of carbon turnover are based on measurements of abundance and growth efficiency values for bacteria ($_B$) and HNF ($_{HNF}$) from literature. First carbon accumulation (CA) was calculated from the difference in cell abundance over time (ΔA) and values of fixed carbon content per cell for bacteria (0.02 pg C per cell; Lee and Fuhrman 1987) and HNF (3.8 pg C per cell; Børsheim and Bratbak 1987) from literature (1). The release of carbon as CO_2 via respiration (R) is further calculated from the estimated CA values and expected growth efficiency of bacteria (10%; Kritzberg, Duarte, and Wassmann 2010; Middelboe, Glud, and Sejr 2012; Paulsen et al. 2017) and HNF (30%; Fenchel 1982) (2).

$$\mathrm{CA}_B[\mu\mathrm{g\ C}] = \Delta\mathrm{A}_B * 2 * 10^{-8}\mu\mathrm{g\ C} \qquad \mathrm{CA}_{HNF}[\mu\mathrm{g\ C}] = \Delta\mathrm{A}_{HNF} * 3.8 * 10^{-6}\mu\mathrm{g\ C} \qquad (1)$$

$$\mathrm{R}_B[\mu\mathrm{g\ C}_{CO_2}] = \left(\frac{\mathrm{BP}_B}{0.1}\right) * 0.9 \qquad \mathrm{R}_{HNF}[\mu\mathrm{g\ C}_{CO_2}] = \left(\frac{\mathrm{BP}_{HNF}}{0.3}\right) * 0.7 \qquad (2)$$

Results:

tDOM effect on bacterial growth

During the nine-day incubation period the bacterial net-growth was documented (Figure 2). The initial fjord water contained 8.13 x 10^5 bacteria mL^{-1} and when mixed with either the aged tDOM-solution (tDOM treatment) or 0.22 µm filtered fjord water (control), this concentration was diluted to an average abundance of 4.32 x 10^5 or 4.19 x 10^5 mL^{-1}, respectively (Figure 2A). After a lag phase during the first 24 h, we observed net-growth in both treatment and control. The bacterial abundance (BA) increased at twice the rate in the tDOM treatment between day 1 and 4 and the BA was on average 24% higher in the tDOM treatment than in the control during the first 4 days. After day 5, a different pattern emerged. While bacteria continued to grow in the control incubations reaching 4.32 x 10^6 mL^{-1} by day 9, we observed a significant decline of 63% in BA from 1.76 x 10^6 mL^{-1} (5d) to 6.51 x 10^5 mL^{-1} (9d) in the incubations with tDOM addition (Figure 2A).

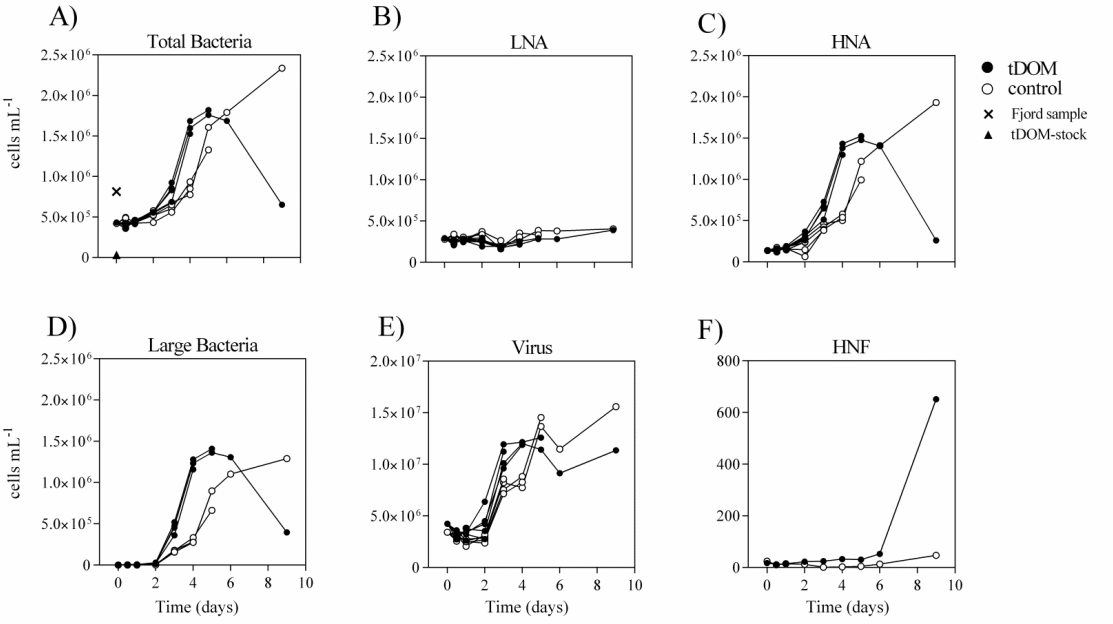

Figure 2: Flow cytometer counts over the course of the experiment in cells mL^{-1} of A) total bacteria; B) low nucleic acid (LNA) containing bacteria; C) high nucleic acid (HNA) containing bacteria; D) a group of large bacteria; E) Virus; F) and heterotrophic nanoflagellates (HNF). Treatment incubations with added tDOM are illustrated as black circles and control incubations as open circles. The bacterial abundance of the untreated fjord sample and of the 0.2 µm filtered tDOM-stock solution is indicated as cross and triangle, respectively. The different lines represent the sample replicates, which declined over the course of the experiment depending on the number of remaining bottles (e.g. eight at t0, four at day 3 and one at day 9).

The group of total bacteria was divided into three subgroups, "LNA", "HNA" and "large bacteria" within the HNA group, to investigate whether a specific group is connected to the increase or decrease in BA (Figure 2 B-F). The LNA group showed no differences in abundance between treatment and control over the nine days and stayed overall stable, ranging between 1.78 x 10^5 and 4.04 x 10^5 mL^{-1} (Figure 2B). In contrary, the HNA group showed significant correlations ($r=0.99$; $p<0.0001$) with the increase in BA, including the same differences between treatment and control described earlier (Figure 2 C). At day 3 we observed a new group on the flow cytometer plots within the HNA group, which we here term "large bacteria" (Figure 3). This group was well-defined in tDOM treatments where it started with low values of 15 x 10^3 mL^{-1} (day 2) and reached up to 1.36 x 10^6 mL^{-1} at day 5, thereby contributing to more than 77% of the BA (Figure 2 D).

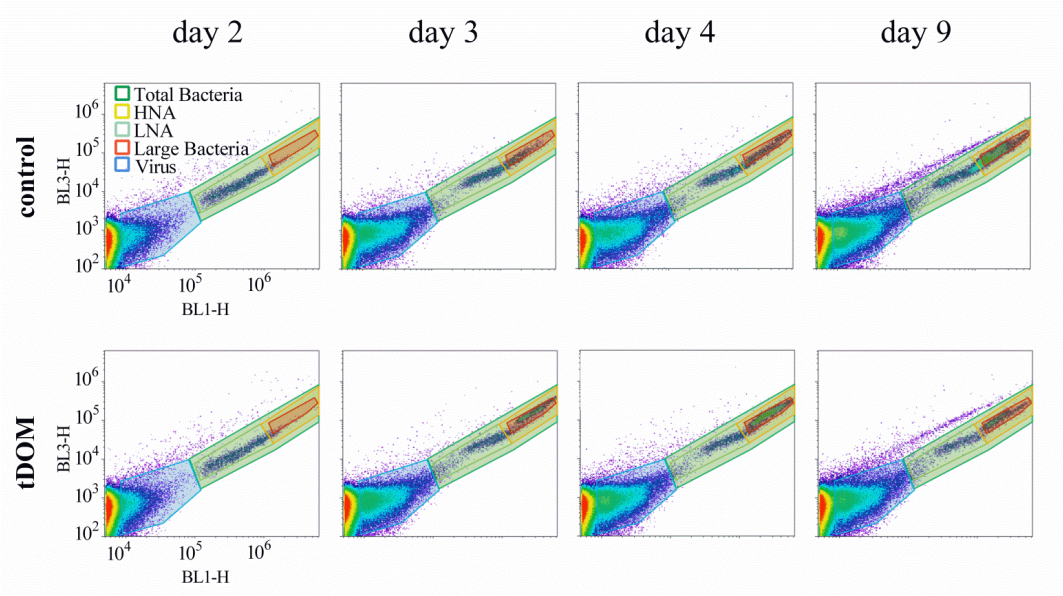

Figure 3: Flow cytometer plots of measurements from day 2-9 showing the changes in bacterial abundance and the subgroups within, illustrating the increase in large bacteria in the tDOM treatment. HNA=High nucleic acid containing bacteria; LNA=Low nucleic acid containing bacteria

Virus abundance was on average one order of magnitude higher than bacteria ranging from 2.58 x 10^6 mL^{-1} to 1.56 x 10^7 mL^{-1} and followed the changes observed for BA in both treatment and control (Figure 2 E). Due to the pre-filtration of the fjord water through 1.2 µm GFC filters, the abundance of small protists was substantially reduced from 600 mL^{-1} in the fjord water to 16±2 mL^{-1} in both treatment and control until day 6 (Figure 2 F). At day 9, the abundance of HNF reached 651 mL^{-1} in the incubation where tDOM was added, while it remained low in the control (47 mL^{-1}). Picophytoplankton were additionally enumerated throughout the incubation period to confirm that autotrophic production did not contribute to the carbon pool. Abundances were reduced from 2,056 mL^{-1} in fjord water to <100 mL^{-1} at the beginning of the experiment and remained low (<150 mL^{-1}).

tDOM effect on community composition

The fjord water used to set up the incubations was taken from 40m depth and was characterized as Atlantic water with a salinity of 34.6 and temperature of 4°C. The analysis of the untreated Atlantic water showed a high abundance of the phylum Proteobacteria (96.5%) (Figure 4A). Gammaproteopbacteria were dominating (±76.2%), followed by Alphaproteobacteria (±14.9%) and Betaproteobacteria (±3.0%). Due to the high diversity within the different Proteobacteria classes, 40% of all sequences at genus level were categorized as "Other" (Figure 4A).

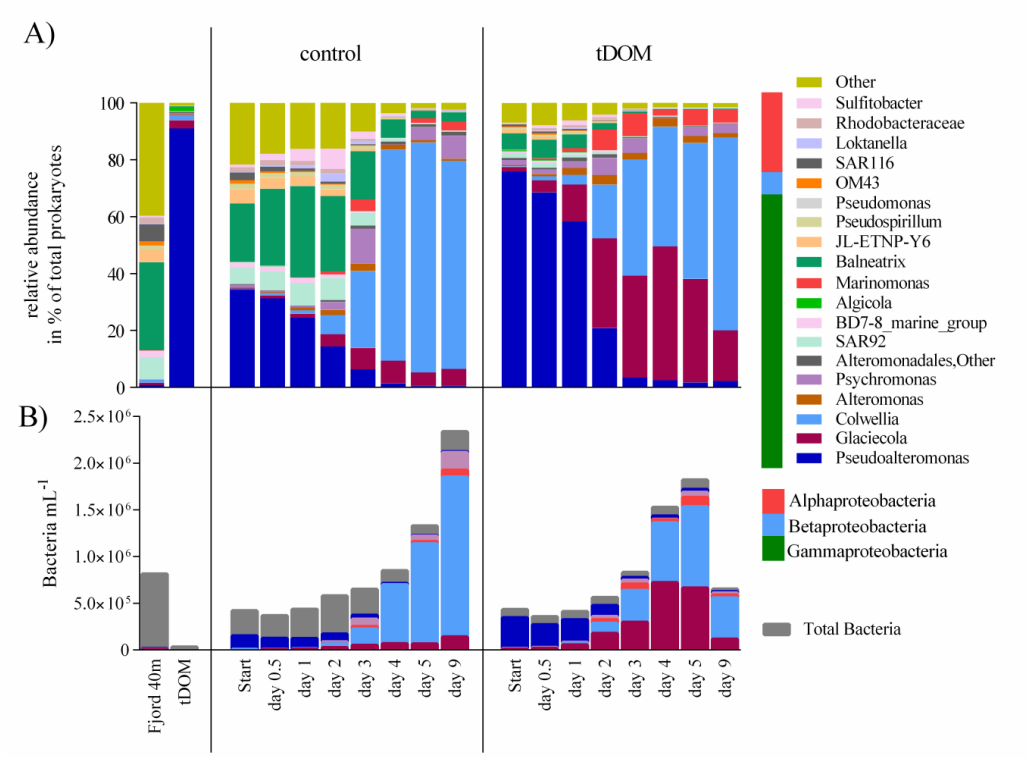

Figure 4: A) A) Bacterial community composition derived from 16S rRNA sequencing data showing the relative abundance of the 20 most abundant taxa at genus level in the fjord sample from 40m depth and during the 9 days of incubation in the control and treatment incubations where tDOM was added. Taxa comprising <1% of the total number of sequences within a sample were summarized as "Other". B) Calculated absolute abundance of the most abundant genera in control and treatment incubations, based on absolute bacterial abundance measured on the flow cytometer and phylogenetic relative abundance.

Community composition at the beginning of the experiment was similar in the control and the tDOM treatment, with around 30-50% of the sequences resembling the *in situ* fjord community and all other sequences belonging to the genus *Pseudoalteromonas*. Sequences belonging to this genus, possibly introduced with the addition of 0.22 µm filtered tDOM solution and 0.22 µm filtered fjord water,

decreased within four days from up to 70% to 4% in the treatment and from 30% to 3% in the control incubations. With increasing incubation time, changes could be attributed to the increase of certain genera. We observed a substantial increase in relative abundance of *Glaciecola, Marinomonas* and *Colwellia* in the treatment experiments. In the control incubations, it was predominantly *Colwellia* that increased in relative abundance and to a lesser extend *Glaciecola*, *Marinomonas* and *Psychromonas*. *Glaciecola* increased from 1.5% to 47.1% on day 5 in the incubations where tDOM was added, while the abundance in the controls increased only up to 7.9%. A Simper analysis showed in agreement, that predominantly the changes in *Glaciecola* relative abundance contributed, with up to 40% (at day 4), for the differences caused by the tDOM addition.

We analyzed the effect of tDOM addition on the community structure by combining the relative abundance of bacterial community composition and absolute abundance of bacterial counts obtained from sequencing data and flow cytometer counts, respectively (Figure 4B). Using this estimation of absolute species abundance, the *Glaciecola* abundance increased two-fold within the first 12 hours and 138-fold after 4 days relative to the beginning (Figure 4B). At day 4, *Glaciecola* abundance was 90.6% higher in tDOM treatment incubations than in control incubations. The abundance of *Marinomonas* increased 92-fold after 5 days and was up to 93.8% higher in incubations with added tDOM than in controls (Figure 4B). Both genera, *Glaciecola* and *Marinomonas*, showed significant ($p=0.006$ and $p=0.018$) responses due to the addition of tDOM. Only in the tDOM treatment incubations *Glaciecola* abundance significantly correlated ($r=0.77$; $p=0.03$) with the abundance of large bacteria (Figure S1). In the control incubations it was only *Colwellia* abundance that correlated significantly ($r=0.83$; $p=0.01$) with the abundance of large bacteria. This genus however showed no significant difference in abundance between treatment and control. In the first days until day 3, the abundance was up to three times higher in the tDOM treatment than the control. This changed on day 4, when abundance in the control incubation was twice as high as in the treatment.

The observed changes for the different genera are based on cumulative abundances of several OTUs which were taxonomically assigned to these genera and grouped accordingly. In order to identify whether all or just some OTUs within each genus are causing the observed changes between treatment and controls, we performed an indicator OTU analysis (Figure 5). This analysis identified the OTUs that significantly contributed to the differences between tDOM treatment and control. Out of the 20 most significant OTUs, seven were significantly more abundant in incubations with tDOM addition and thirteen OTUs had a significant higher abundance in control incubations. Taxonomically, the great majority of OTUs (19/20) belonged to the class of Gammaproteobacteria and within that class to genera including *Glaciecola*, *Marinomonas*, *Colwellia*, *Balneatrix*, *SAR92* and *Psychromonas*. The overall most abundant OTU (33%) belonged to the genus *Glaciecola* and was at day 3 seven times more abundant in the tDOM treatment than the control incubations. Of all genera, *Glaciecola* was the genus with the highest number of OTUs (85%) that were positively associated with incubations where tDOM was added. Other genera, like *Colwellia*, with an overall high abundance had a more equal distribution of OTUs, which were higher in abundance in either treatment or control. 66% of *Colwellia* OTUs were significantly more abundant in control incubations and 33% more abundant in treatment incubations.

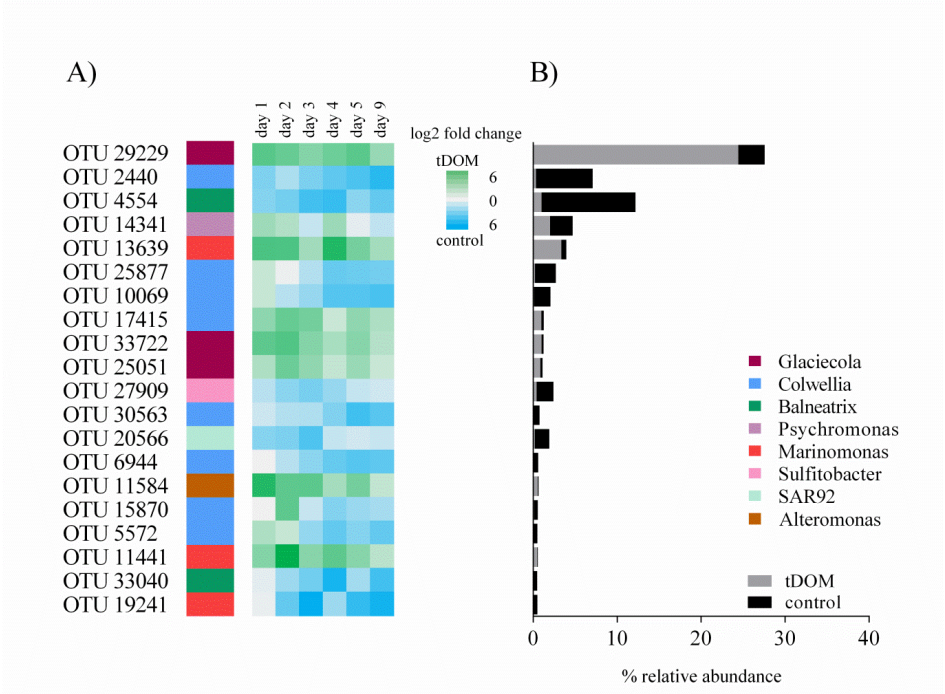

Figure 5: A) The 20 most significant OTUs, identified by an indicator OTU analysis, contributing to the differences in community composition between control and treatment incubations. Relative abundance differences are visualized as two-fold change from day1 until day 9. B) Relative abundance (average values from d1 - d9) of the 20 most significant indicator OTUs visualized in the same order as in (A).

Discussion:

Climate model predictions suggest a 30% increase of terrestrial run-off into the Arctic Ocean by the end of the century (Lehner et al., 2012). The tDOM in this run-off is originating from thawing Arctic soil and is modified during the transport into the Arctic Ocean (Serreze et al. 2000; Lobbes et al. 2000; Fichot et al. 2013; Feng et al. 2013; Holmes et al., 2013). It is uncertain how this will affect the marine microbial life and in particular the coastal communities. Our results indicated increased bacterial abundance (Figure 2), enlarged cell sizes (Figure 3) and changes in the community composition (Figure 4) as an immediate (within 3 days) response to tDOM addition. Together, this suggests that in the future the activity, the physiology and the structure of the fjord microbial community might be affected by increased tDOM rich run-off.

In situ microbial community composition

Environmental conditions in the Arctic are highly affected by seasonality. In accordance, seasonal changes in microbial community composition have been reported for different parts of the Arctic

Oceans, i.e. the increase of *Gammaproteobacteria*, in association to phytoplankton bloom dynamics and increased concentrations of dissolved organic matter, in the summer months (Alonso-Sáez et al., 2008; Buchan et al., 2014; El-Swais et al., 2015; Wilson et al., 2017). The fjord water used for our incubation experiments, taken in June, was indicative for a post-bloom situation, with high relative abundance of the phylum Proteobacteria (96.5%) and in particular the class *Gammaproteobacteria*, with up to 76.1% of all proteobacterial reads (Figure 4), similar to reports from other studies (Piquet et al., 2010; Zeng et al., 2013). The largest contributor was the genus *Balneatrix* (30.9%), known to be associated with phytoplankton blooms and observed in other Arctic fjords (Nikrad et al., 2014; Paulsen et al., 2017). Other dominant taxa within the *Gammaproteobacteria,* such as *SAR92* (10%) and *OM182* (13%), are commonly associated with rather oligotrophic conditions (Cho and Giovannoni, 2004). Surprisingly, Bacteroidetes, commonly found in summer coastal Arctic communities, comprised only 0.3% in our samples (Nikrad et al., 2012; Sipler et al., 2017b). The low abundance of Betaproteobacteria, which comprised, with up to 3%, only a small proportion of all proteobacterial reads is characteristic for Atlantic water masses (Cottrell and Kirchman, 2003; Garneau et al., 2006).

tDOM addition induced changes in bacterial community composition

The large initial relative abundance of *Pseudoalteromonas* was likely an experimental artifact and rapidly decreased in abundance under both experimental conditions. Changes in community composition due to tDOM addition were already measurable after 12 hours of incubation, for example the doubling of *Glaciecola* relative abundance (Figure 4). *Glaciecola* also increased in abundance in control incubations (4171% increase from t0 until d4), confirming both that this taxa is part of the *in situ* microbial community and able to grow using *in situ* carbon sources. The fact that *Glaciecola* grew faster and to a higher abundance in the treatment incubations (10781% increase from t0 until d4) indicates that this genus has the potential to degrade the introduced complex tDOM compounds. Other growth experiments with *Glaciecola* revealed both general phylotypes, capable of degrading a broad range of carbon compounds and specialized phylotypes, capable of degrading only specific carbon sources (Gómez-Consarnau et al., 2012).

Besides *Glaciecola*, *Marinomonas* and *Colwellia*, two taxa known to degrade complex organic matter, also increased in abundance in the tDOM treatment incubations. *Marinomonas* and *Colwellia* had, similar to *Glaciecola*, low starting abundances and increased in both treatment and control incubations, with a stronger response under tDOM addition. It has been shown that a member of the genus *Marinomonas* is capable of catalyzing ring cleavage of aromatic compounds and correlates with lignocellulosic carbon uptake (Chandra et al., 2015; Gontikaki et al., 2015). Also *Colwellia* has been considered to produce extracellular enzymes for the breakdown of high molecular-weight organic compounds (Huston et al., 2004; Methé et al., 2005). *Glaciecola* and *Colwellia* have also recently been shown to increase in abundance under presence of tDOM derived from Arctic rivers (Sipler et al. 2017). Interestingly, it was a different *Glaciecola* OTU that was dominating in their dataset. This OTU was also found in our data set, but is only one of the least abundant *Glaciecola* OTUs. It remains unclear whether this difference is caused by substrate specificity or simply which OTU is most abundant at *in situ* conditions. Sipler and colleagues used seven times higher DOC

concentrations (400-500 µM) than in their control to stimulate a community response, while the DOC concentrations (128 µM) in our study were only 1.5 times higher than in the control incubations. Pulses of tDOM released via Arctic rivers can reach the DOC concentrations used by Sipler and colleagues (Benner et al., 2005), but at our sampling site in Kongsfjorden the DOC concentration is on average 109 µM (Zhu et al., 2016). Despite the relatively small increase in tDOM concentration in our study, we here stimulated faster growth of certain taxa than the change reported by Sipler and colleagues. This might be due to fact that our incubations were conducted in the dark and therefore inhibited phototrophic processes.

OTU specific response to tDOM addition and "the bottle effect"

We detected a significantly stronger increase of the genera *Glaciecola* and *Marinomonas* in incubations where we added tDOM compared to control incubations. The other genus found to increase, *Colwellia*, showed no significant difference between treatment and control. This is reflected in the differential response we observed at the taxonomic level of OTUs (Figure 5). Several OTUs were positively affected by tDOM addition and became more abundant during incubation, whereas other OTUs of the same genus decreased upon tDOM addition (Figure 5). This non-coherent tendency was found for all genera and indicates that strains within the same genus might have different functional roles.

We compared changes in relative OTU abundance between treatment and control to differentiate between potential effects due to the tDOM input and effects caused by the experimental set-up, the so called "bottle effects". The increase of a number of Colwellia OTUs was similar in both control and treatment incubations and is therefore likely to be attributed to the bottle effect, which is a well known inherent concern in incubations studies (Lee and Fuhrman, 1991; Massana et al., 2001; Stewart et al., 2012). Several studies have suggested a combination of factors, including biofilm formation and the binding of nutrients, cells or carbon to the surface of the incubation container, as potential cause of bottle effects (Eilers et al., 2000; Fletcher, 1996; Fogg and Calvario-Martinez, 1989). It appears that the bottle effect predominantly leads to an increase in Gammaproteobacteria taxa, as documented in our and other studies (Dinasquet et al., 2013; Eilers et al., 2000; Herlemann et al., 2014; Stewart et al., 2012). While the bottle effect in the study from Stewart and colleagues and in our study can be attributed to an increase in *Colwelliaceae*, different families, such as *Moraxellaceae* (Herlemann et al., 2014), *Pseudoalteromonadaceae* (Dinasquet et al., 2013) or *Oceanospirillaceae* (Sipler et al., 2017b) were affected in other studies. This suggests that several different types of Gammaproteobacteria can benefit from a bottle effect and that the starting community composition might be the determining factor.

tDOM effects on the coastal microbial food web

The increase of Gammaproteobacteria, in particular of taxa belonging to the order Alteromonadales, including *Glaciecola* and *Colwellia*, has also been observed during marine phytoplankton spring blooms in lower latitudes (Tada et al., 2011; Teeling et al., 2012) and in the Arctic Ocean (Bano and Hollibaugh, 2002; Wilson et al., 2017). This suggests that they can rapidly proliferate in response to new carbon sources, including phytoplankton-derived organic carbon or tDOM as indicated in our

study. A strong grazing pressure by bacterivorous protists has been shown to particularly affect Gammaproteobacteria of the order Alteromonadales (Allers et al., 2007; Beardsley et al., 2003). These studies demonstrated selective grazing on large metabolically active bacteria by heterotrophic flagellate grazers. Size-selective predator-prey interactions have also been shown for *Glaciecola*, that first became abundant upon rapid utilization of phytoplankton derived DOM and subsequently declined in their abundance due to grazing (von Scheibner et al., 2017). It was suggested that once abundant, *Glaciecola* became a target for size selective predation by protists, including heterotrophic nanoflagellates (HNF) due to their above-average cell size.

We also observed an increase in *Glaciecola* abundance upon tDOM addition, which correlated with the appearance of above-average large bacteria measured via flow cytometry (Figure 3 and Figure S1). Towards the end of the experiment, *Glaciecola* abundance declined by 84%, while at the same time the abundance of HNF increased substantially (from 32 to 651 cells mL^{-1}). Interestingly, in the control incubations, where *Glaciecola* abundance stayed low, HNF abundance remained unchanged at a low level and did not increase towards the end. This suggests that after *Glaciecola*, fueled by the tDOM addition, increased in abundance, size-selective HNF caused the decline in *Glaciecola* abundance. The specific predator-prey relation between *Glaciecola* and HNF might be an important link in the microbial food web of Arctic fjord systems, with cascading effects on higher trophic levels, including ciliates, copepods and up to the top level predators.

This link has also consequences for the coastal carbon budget. We calculated carbon turnover assuming a bacterial biomass of 0.02 pg per cell (Lee and Fuhrman, 1987) and a 10% growth efficiency for bacteria (Kritzberg et al., 2010; Middelboe et al., 2012; Paulsen et al., 2017). From day 2 to 4, bacterial growth resulted in the release of 188 µg $C\text{-}CO_2$ L^{-1} in the tDOM treatment compared to 41 µg $C\text{-}CO_2$ L^{-1} in the control. Based on these calculations, 30% of the added tDOM was already processed by the bacteria within 4 days. Since the increase in bacterial abundance after day 4 in the control incubations most likely was caused by the bottle effect, carbon turnover for the later period was not considered as representative for an in situ fjord community carbon turnover. The grazing and subsequent growth of HNF in the tDOM treatment caused a further transition of the bacterial biomass. The carbon turnover by HNF was calculated assuming a biomass of 3.8 pg (Borsheim and Bratbak, 1987) and 30% growth efficiency for HNF (Fenchel, 1982). The increase of HNF from day 5 to day 9 resulted in the incorporation of 2 µg C L^{-1} as biomass and an additional release of 6 µg $C\text{-}CO_2$ L^{-1}. Both the initial growth of *Glaciecola* and the subsequent grazing by HNF will thus affect the carbon turnover in Arctic coastal ecosystems with increased tDOM inputs. Based on our study design, we cannot fully predict such effects, but we can document that the addition of tDOM affected not only bacteria, but indirectly also the organisms grazing on bacteria. To our knowledge we here provide the first results on the effects of permafrost-derived tDOM input on fjord microbial communities and to understand the interactions at higher trophic levels, it is necessary to conduct further experiments with tDOM additions at larger scales, including more members of the marine food web.

Conflict of Interest Statement

The authors declare that the research was conducted in the absence of any commercial or financial relationships that could be construed as a potential conflict of interest.

Author contributions

MLP and OM led the planning of the study. LS collected and OM processed samples. MLP did flow cytometric analysis. OM, GB, LS and MLP analysed data, OM prepared figures and tables and led the writing of the paper. All authors contributed to discussing and interpreting data and writing the paper.

Funding

This study is part of the project "MicroPolar" (RCN 225956) funded by the Norwegian Research Council. Lena Seuthe participated as member of the "Carbon Bridge" project (RCN 226415). Parts of the study was funded by the project "Microorganisms in the Arctic: Major drivers of biogeochemical cycles and climate change" (RCN 227062).

Acknowledgments

We would like to thank all colleagues in the UiB Marine Microbiology group and collaborators abroad who contributed to the research effort. We would like to thank Lise Øvreås for her assistance throughout the sampling. Also thank you Aud Larsen for facilitating the transport of samples and Colin Stedmon for performing the Parafac analysis.

Supplementary:

Table S1: The averaged ± SD (n=8) fluorescent intensity (Raman units) of five fluorescence components of the tDOM-solution and control (0.2 filtered fjord water) illustrated in Figure S2. C1 and C3 are characterized as humic-like fluorescent components and C2, C4 and C5 are characterized as amino-like fluorescent components as in (Stedmon and Markager, 2005).

		tDOM		Control	
		Avg.	SD	Avg.	SD
Humic	C1	0.111	0.004	0.051	0.003
Humic	C3	0.064	0.001	0.028	0.002
Amino	C2	0.081	0.010	0.071	0.004
Amino	C4	0.104	0.007	0.001	0.000
Amino	C5	0.052	0.024	0.063	0.012

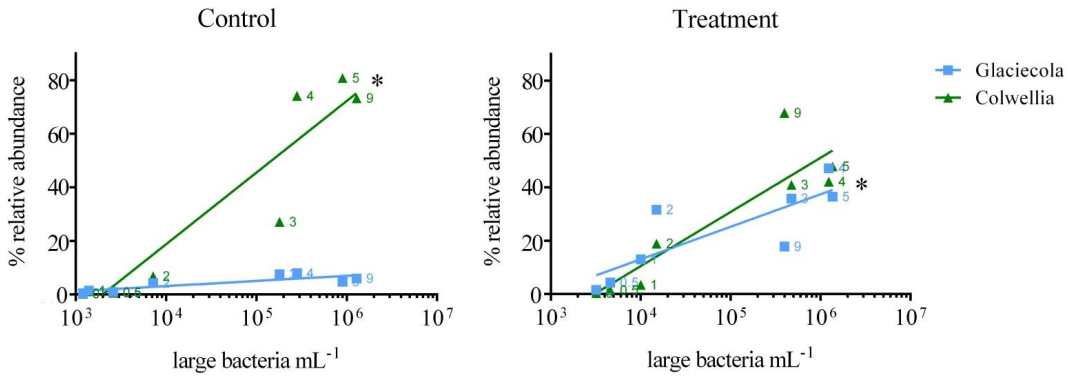

Figure S1: Relative abundance of *Glaciecola* and *Colwellia* from sequencing data plotted against the abundance of large bacteria obtained from flow cytometry for both control and tDOM treatment incubations. Black asterisk indicates significant correlation between relative abundance and large bacteria.

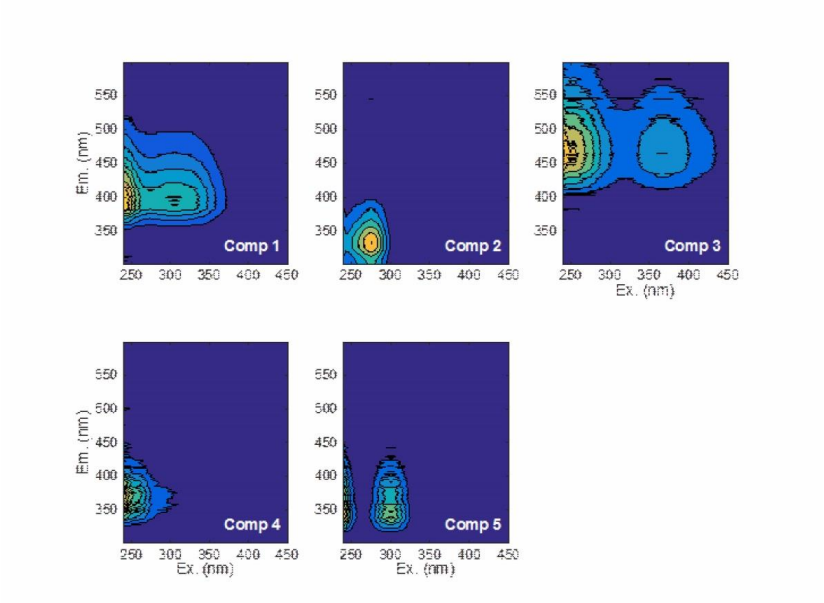

Figure S2: The contour plots show the spectral characteristics of each of the five fluorescence components 1–5 (C1-C5). C1 and C3 are characterized as humic-like fluorescent components and C2, C4 and C5 are characterized as amino-like fluorescent components as in (Stedmon and Markager, 2005).

522 **References:**

523 Allers, E., Gómez-Consarnau, L., Pinhassi, J., Gasol, J. M., Šimek, K., and Pernthaler, J. (2007). Response of
524 Alteromonadaceae and Rhodobacteriaceae to glucose and phosphorus manipulation in marine
525 mesocosms. *Environ. Microbiol.* 9, 2417–2429. doi:10.1111/j.1462-2920.2007.01360.x.

526 Alonso-Sáez, L., Sánchez, O., Gasol, J. M., Balagué, V., and Pedrós-Alio, C. (2008). Winter-to-summer
527 changes in the composition and single-cell activity of near-surface Arctic prokaryotes. *Environ.*
528 *Microbiol.* 10, 2444–2454. doi:10.1111/j.1462-2920.2008.01674.x.

529 Amon, R. M. W., Rinehart, A. J., Duan, S., Louchouarn, P., Prokushkin, A., Guggenberger, G., et al. (2012).
530 Dissolved organic matter sources in large Arctic rivers. *Geochim. Cosmochim. Acta* 94, 217–237.
531 doi:10.1016/j.gca.2012.07.015.

532 Bano, N., and Hollibaugh, J. T. (2002). Phylogenetic composition of bacterioplankton assemblages from the
533 Arctic Ocean. *Appl. Environ. Microbiol.* 68, 505–18. doi:10.1128/AEM.68.2.505-518.2002.

534 Beardsley, C., Pernthaler, J., Wosniok, W., and Amann, R. (2003). Are readily culturable bacteria in coastal
535 North Sea waters suppressed by selective grazing mortality? *Appl. Environ. Microbiol.* 69, 2624–30.
536 doi:10.1128/aem.69.5.2624-2630.2003.

537 Beier, S., Rivers, A. R., Moran, M. A., and Obernosterer, I. (2015). The transcriptional response of
538 prokaryotes to phytoplankton-derived dissolved organic matter in seawater. *Environ. Microbiol.* 17,
539 3466–3480. doi:10.1111/1462-2920.12434.

540 Benner, R., Louchouarn, P., and Amon, R. M. W. (2005). Terrigenous dissolved organic matter in the Arctic
541 Ocean and its transport to surface and deep waters of the North Atlantic. *Global Biogeochem. Cycles* 19,
542 n/a-n/a. doi:10.1029/2004GB002398.

543 Blanchet, M., Pringault, O., Panagiotopoulos, C., Lefèvre, D., Charrière, B., Ghiglione, J.-F., et al. When
544 riverine dissolved organic matter (DOM) meets labile DOM in coastal waters: changes in bacterial
545 community activity and composition. doi:10.1007/s00027-016-0477-0.

546 Bolger, A. M., Lohse, M., and Usadel, B. (2014). Trimmomatic: a flexible trimmer for Illumina sequence data.
547 *Bioinformatics* 30, 2114–20. doi:10.1093/bioinformatics/btu170.

548 Borsheim, K., and Bratbak, G. (1987). Cell volume to cell carbon conversion factors for a bacterivorous
549 Monas sp. enriched from seawater . *Mar. Ecol. Prog. Ser.* 36, 171–175. doi:10.3354/meps036171.

550 Buchan, A., LeCleir, G. R., Gulvik, C. A., and González, J. M. (2014). Master recyclers: features and
551 functions of bacteria associated with phytoplankton blooms. *Nat. Rev. Microbiol.* 12, 686–698.
552 doi:10.1038/nrmicro3326.

553 Caporaso, J. G., Kuczynski, J., Stombaugh, J., Bittinger, K., Bushman, F. D., Costello, E. K., et al. (2011a).
554 NIH Public Access. 7, 335–336. doi:10.1038/nmeth.f.303.QIIME.

555 Caporaso, J. G., Lauber, C. L., Walters, W. A., Berg-Lyons, D., Lozupone, C. A., Turnbaugh, P. J., et al.
556 (2011b). Global patterns of 16S rRNA diversity at a depth of millions of sequences per sample. *Proc.*
557 *Natl. Acad. Sci.* 108, 4516–4522. doi:10.1073/pnas.1000080107.

558 Chandra, R., Chowdhary, P., Ibarra, D., Rencoret, J., Romero, J., Speranza, M., et al. (2015). Properties of
559 bacterial laccases and their application in bioremediation of industrial wastes. *Environ. Sci. Process.*
560 *Impacts* 17, 326–342. doi:10.1039/C4EM00627E.

561 Cho, J.-C., and Giovannoni, S. J. (2004). Cultivation and growth characteristics of a diverse group of
562 oligotrophic marine Gammaproteobacteria. *Appl. Environ. Microbiol.* 70, 432–40.
563 doi:10.1128/AEM.70.1.432-440.2004.

564 Cottrell, M. T., and Kirchman, D. L. (2003). Contribution of major bacterial groups to bacterial biomass
565 production (thymidine and leucine incorporation) in the Delaware estuary. *Limnol. Oceanogr.* 48, 168–
566 178. doi:10.4319/lo.2003.48.1.0168.

567 De Cáceres, M., and Legendre, P. (2009). Associations between species and groups of sites: indices and
568 statistical inference. *Ecology* 90, 3566–74. Available at: http://www.ncbi.nlm.nih.gov/pubmed/20120823
569 [Accessed December 5, 2017].

570 Dinasquet, J., Kragh, T., Schrøter, M.-L., Søndergaard, M., and Riemann, L. (2013). Functional and
571 compositional succession of bacterioplankton in response to a gradient in bioavailable dissolved organic
572 carbon. *Environ. Microbiol.* 15, 2616–2628. doi:10.1111/1462-2920.12178.

573 Dittmar, T., and Kattner, G. (2003). The biogeochemistry of the river and shelf ecosystem of the Arctic Ocean:
574 a review. *Mar. Chem.* 83, 103–120. doi:10.1016/S0304-4203(03)00105-1.

575 Edgar, R. C. (2010). Search and clustering orders of magnitude faster than BLAST. *Bioinformatics* 26, 2460–
576 1. doi:10.1093/bioinformatics/btq461.

577 Eiler, A., Langenheder, S., Bertilsson, S., and Tranvik, L. J. (2003). Heterotrophic bacterial growth efficiency
578 and community structure at different natural organic carbon concentrations. *Appl. Environ. Microbiol.*
579 69, 3701–9. doi:10.1128/AEM.69.7.3701-3709.2003.

580 Eilers, H., Pernthaler, J., and Amann, R. (2000). Succession of pelagic marine bacteria during enrichment: a
581 close look at cultivation-induced shifts. *Appl. Environ. Microbiol.* 66, 4634–40. Available at:
582 http://www.ncbi.nlm.nih.gov/pubmed/11055904 [Accessed December 5, 2017].

583 El-Swais, H., Dunn, K. A., Bielawski, J. P., Li, W. K. W., and Walsh, D. A. (2015). Seasonal assemblages and
584 short-lived blooms in coastal north-west Atlantic Ocean bacterioplankton. *Environ. Microbiol.* 17, 3642–
585 3661. doi:10.1111/1462-2920.12629.

586 Fenchel, T. (1982). Ecology of Heterotrophic Microflagellates. IV Quantitative Occurrence and Importance as
587 Bacterial Consumers. *Mar. Ecol. Prog. Ser.* 9, 35–42. doi:10.3354/meps009035.

588 Feng, X., Vonk, J. E., van Dongen, B. E., Gustafsson, Ö., Semiletov, I. P., Dudarev, O. V, et al. (2013).
589 Differential mobilization of terrestrial carbon pools in Eurasian Arctic river basins. *Proc. Natl. Acad. Sci.*
590 *U. S. A.* 110, 14168–73. doi:10.1073/pnas.1307031110.

591 Fichot, C. G., Kaiser, K., Hooker, S. B., Amon, R. M. W., Babin, M., Bélanger, S., et al. (2013). Pan-Arctic
592 distributions of continental runoff in the Arctic Ocean. *Sci. Rep.* 3, 1053. doi:10.1038/srep01053.

593 Fletcher, M. (1996). *Bacterial Adhesion: Molecular and Ecological Diversity*. Wiley Available at:
594 https://books.google.com/books?hl=en&lr=&id=bYmsjh4ppZYC&pgis=1 [Accessed December 6,
595 2017].

596 Fogg, G. E., and Calvario-Martinez, O. (1989). Effects of bottle size in determinations of primary productivity
597 by phytoplankton. *Hydrobiologia* 173, 89–94. doi:10.1007/BF00015518.

598 Garneau, M., Vincent, W., Alonso-Sáez, L., Gratton, Y., and Lovejoy, C. (2006). Prokaryotic community
599 structure and heterotrophic production in a river-influenced coastal arctic ecosystem. *Aquat. Microb.*
600 *Ecol.* 42, 27–40. doi:10.3354/ame042027.

601 Gómez-Consarnau, L., Lindh, M. V., Gasol, J. M., and Pinhassi, J. (2012). Structuring of bacterioplankton
602 communities by specific dissolved organic carbon compounds. *Environ. Microbiol.* 14, 2361–2378.
603 doi:10.1111/j.1462-2920.2012.02804.x.

604 Gontikaki, E., Thornton, B., Cornulier, T., Witte, U., Cox, M., and Joint, I. (2015). Occurrence of Priming in
605 the Degradation of Lignocellulose in Marine Sediments. *PLoS One* 10, e0143917.
606 doi:10.1371/journal.pone.0143917.

607 Hansell, D. A. (2004). Degradation of Terrigenous Dissolved Organic Carbon in the Western Arctic Ocean.
608 *Science (80-.).* 304, 858–861. doi:10.1126/science.1096175.

609 Hansell, D. A., Carlson, C. A., Repeta, D. J., and Schlitzer, R. (2009). Dissolved organic matter in the ocean -
610 a controversy stimulates new insights. *Oceanography* 22, 202–211.

611 Herlemann, D. P. R., Manecki, M., Dittmar, T., and Jürgens, K. (2017). Differential responses of marine,
612 mesohaline and oligohaline bacterial communities to the addition of terrigenous carbon. *Environ.*
613 *Microbiol.* 19, 3098–3117. doi:10.1111/1462-2920.13784.

614 Herlemann, D. P. R., Manecki, M., Meeske, C., Pollehne, F., Labrenz, M., Schulz-Bull, D., et al. (2014).
615 Uncoupling of bacterial and terrigenous dissolved organic matter dynamics in decomposition
616 experiments. *PLoS One* 9, e93945. doi:10.1371/journal.pone.0093945.

Holmes, R. M., Coe, M. T., Fiske, G. J., Gurtovaya, T., Mcclelland, J. W., Shiklomanov, A. I., et al. (2012). "Climate Change Impacts on the Hydrology and Biogeochemistry of Arctic Rivers," in *Climatic Change and Global Warming of Inland Waters: Impacts and Mitigation for Ecosystems and Societies*, 1–26. doi:10.1002/9781118470596.ch1.

Holmes, R. M., McClelland, J. W., Raymond, P. A., Frazer, B. B., Peterson, B. J., and Stieglitz, M. (2008). Lability of DOC transported by Alaskan rivers to the Arctic Ocean. *Geophys. Res. Lett.* 35, L03402. doi:10.1029/2007GL032837.

Huston, A. L., Methe, B., and Deming, J. W. (2004). Purification, characterization, and sequencing of an extracellular cold-active aminopeptidase produced by marine psychrophile Colwellia psychrerythraea strain 34H. *Appl. Environ. Microbiol.* 70, 3321–3328. doi:10.1128/AEM.70.6.3321-3328.2004.

Jiao, N., Herndl, G. J., Hansell, D. A., Benner, R., Kattner, G., Wilhelm, S. W., et al. (2010). Microbial production of recalcitrant dissolved organic matter: Long-term carbon storage in the global ocean. *Nat. Rev. Microbiol.* 8, 593–599. doi:10.1038/nrmicro2386.

Kritzberg, E. S., Duarte, C. M., and Wassmann, P. (2010). Changes in Arctic marine bacterial carbon metabolism in response to increasing temperature. *Polar Biol.* 33, 1673–1682. doi:10.1007/s00300-010-0799-7.

Lee, S., and Fuhrman, J. a (1987). Relationships between Biovolume and Biomass of Naturally Derived Marine Bacterioplankton. *Appl. Environ. Microbiol.* 53, 1298–1303. doi:10.1016/0198-0254(87)96080-8.

Lee, S., and Fuhrman, J. A. (1991). Species composition shift of confined bacterioplankton studies at the level of community DNA. *Mar Ecol Prog Ser* 79, 195–201. doi:10.3354/meps079195.

Lehner, F., Raible, C. C., Hofer, D., and Stocker, T. F. (2012). The freshwater balance of polar regions in transient simulations from 1500 to 2100 AD using a comprehensive coupled climate model. *Clim. Dyn.* 39, 347–363. doi:10.1007/s00382-011-1199-6.

641 Lobbes, Jörg M; Fitznar, Hans Peter; Kattner, G. (2000). Biogeochemical characteristics of dissolved and
642 particulate organic matter in Russian rivers entering the Arctic Ocean. *T0092 Geochim. Cosmochim. acta*
643 *2000, 64 2973-83 T0092* 64, 2973–2983. Available at:
644 https://people.ucsc.edu/~acr/migrated/BeringResources/Articles of interest/Eurasian Basin/Lobbes et al
645 2000.pdf [Accessed February 14, 2018].

646 Marie, D., Brussaard, C. P. D., Thyrhaug, R., Bratbak, G., and Vaulot, D. (1999). Enumeration of Marine
647 Viruses in Culture and Natural Samples by Flow Cytometry. *Appl. Environ. Microbiol.* 65, 45–52.

648 Masella, A. P., Bartram, A. K., Truszkowski, J. M., Brown, D. G., and Neufeld, J. D. (2012). PANDAseq :
649 PAired-eND Assembler for Illumina sequences. *BMC Bioinformatics* 13, 31. doi:10.1186/1471-2105-13-
650 31.

651 Massana, R., Pedros-Alio, C., Casamayor, E. O., and Gasol, J. M. (2001). Changes in marine bacterioplankton
652 phylogenetic composition during incubations designed to measure biogeochemically significant
653 parameters. *Limnol. Oceanogr.* 46, 1181–1188. doi:10.4319/lo.2001.46.5.1181.

654 McCarren, J., Becker, J. W., Repeta, D. J., Shi, Y., Young, C. R., Malmstrom, R. R., et al. (2010). Microbial
655 community transcriptomes reveal microbes and metabolic pathways associated with dissolved organic
656 matter turnover in the sea. *Proc. Natl. Acad. Sci. U. S. A.* 107, 16420–7. doi:10.1073/pnas.1010732107.

657 Methé, B. A., Nelson, K. E., Deming, J. W., Momen, B., Melamud, E., Zhang, X., et al. (2005). The
658 psychrophilic lifestyle as revealed by the genome sequence of Colwellia psychrerythraea 34H through
659 genomic and proteomic analyses. *Proc. Natl. Acad. Sci. U. S. A.* 102, 10913–8.
660 doi:10.1073/pnas.0504766102.

661 Middelboe, M., Glud, R. N., and Sejr, M. K. (2012). Bacterial carbon cycling in a subarctic fjord: A seasonal
662 study on microbial activity, growth efficiency, and virus-induced mortality in Kobbefjord, Greenland.
663 *Limnol. Oceanogr.* 57, 1732–1742. doi:10.4319/lo.2012.57.6.1732.

664 Nikrad, M. P., Cottrell, M. T., and Kirchman, D. L. (2012). Abundance and single-cell activity of

heterotrophic bacterial groups in the western Arctic Ocean in summer and winter. *Appl. Environ. Microbiol.* 78, 2402–2409. doi:10.1128/AEM.07130-11.

Nikrad, M. P., Cottrell, M. T., and Kirchman, D. L. (2014). Growth activity of gammaproteobacterial subgroups in waters off the west Antarctic Peninsula in summer and fall. *Environ. Microbiol.* 16, 1513–1523. doi:10.1111/1462-2920.12258.

Opsahl, S., Benner, R., and Amon, R. M. W. (1999). Major flux of terrigenous dissolved organic matter through the Arctic Ocean. *Limnol. Oceanogr.* 44, 2017–2023. doi:10.4319/lo.1999.44.8.2017.

Øvreås, L., Forney, L., and Daae, F. L. (1997). Distribution of Bacterioplankton in Meromictic Lake Sælenvannet , as Determined by Denaturing Gradient Gel Electrophoresis of PCR-Amplified Gene Fragments Coding for 16S rRNA. *Appl. Environmantal Microbiol.* 63, 3367–3373.

Paulsen, M. L., Doré, H., Garczarek, L., Seuthe, L., Müller, O., Sandaa, R.-A., et al. (2016). Synechococcus in the Atlantic Gateway to the Arctic Ocean. *Front. Mar. Sci.* 3. doi:10.3389/fmars.2016.00191.

Paulsen, M. L., Nielsen, S. E. B., Müller, O., Møller, E. F., Stedmon, C. A., Juul-Pedersen, T., et al. (2017). Carbon Bioavailability in a High Arctic Fjord Influenced by Glacial Meltwater, NE Greenland. *Front. Mar. Sci.* 4, 176. doi:10.3389/fmars.2017.00176.

Pedler, B. E., Aluwihare, L. I., and Azam, F. (2014). Single bacterial strain capable of significant contribution to carbon cycling in the surface ocean. *Proc. Natl. Acad. Sci. U. S. A.* 111, 7202–7. doi:10.1073/pnas.1401887111.

Pinhassi, J., Sala, M. M., Havskum, H., Peters, F., Guadayol, O., Malits, A., et al. (2004). Changes in bacterioplankton composition under different phytoplankton regimens. *Appl. Environ. Microbiol.* 70, 6753–66. doi:10.1128/AEM.70.11.6753-6766.2004.

Piquet, A. M.-T., Scheepens, J. F., Bolhuis, H., Wiencke, C., and Buma, A. G. J. (2010). Variability of protistan and bacterial communities in two Arctic fjords (Spitsbergen). *Polar Biol.* 33, 1521–1536. doi:10.1007/s00300-010-0841-9.

689 Quast, C., Pruesse, E., Yilmaz, P., Gerken, J., Schweer, T., Glo, F. O., et al. (2013). The SILVA ribosomal
690 RNA gene database project : improved data processing and web-based tools. *nucleic acid Res.* 41, 590–
691 596. doi:10.1093/nar/gks1219.

692 Rachold, V., Eicken, H., Gordeev, V. V., Grigoriev, M. N., Hubberten, H.-W., Lisitzin, A. P., et al. (2004).
693 "Modern Terrigenous Organic Carbon Input to the Arctic Ocean," in *The Organic Carbon Cycle in the*
694 *Arctic Ocean* (Berlin, Heidelberg: Springer Berlin Heidelberg), 33–55. doi:10.1007/978-3-642-18912-
695 8_2.

696 Sapp, M., Wichels, A., Wiltshire, K. H., and Gerdts, G. (2007). Bacterial community dynamics during the
697 winterâ€"spring transition in the North Sea. *FEMS Microbiol. Ecol.* 59, 622–637. doi:10.1111/j.1574-
698 6941.2006.00238.x.

699 Serreze, M., Walsh, J., and Iii, F. C. (2000). Observational evidence of recent change in the northern high-
700 latitude environment. *Clim. Change*, 159–207.

701 Sipler, R. E., Baer, S. E., Connelly, T. L., Frischer, M. E., Roberts, Q. N., Yager, P. L., et al. (2017a).
702 Chemical and photophysiological impact of terrestrially-derived dissolved organic matter on nitrate
703 uptake in the coastal western Arctic. *Limnol. Oceanogr.* 62, 1881–1894. doi:10.1002/lno.10541.

704 Sipler, Kellogg, C. T. E., Connelly, T. L., Roberts, Q. N., Yager, P. L., and Bronk, D. A. (2017b). Microbial
705 community response to terrestrially derived dissolved organic matter in the coastal Arctic. *Front.*
706 *Microbiol.* 8, 1018. doi:10.3389/fmicb.2017.01018.

707 Stedmon, C. a., Amon, R. M. W., Rinehart, a. J., and Walker, S. a. (2011). The supply and characteristics of
708 colored dissolved organic matter (CDOM) in the Arctic Ocean: Pan Arctic trends and differences. *Mar.*
709 *Chem.* 124, 108–118. doi:10.1016/j.marchem.2010.12.007.

710 Stedmon, C. A., and Markager, S. (2005). Resolving the variability in dissolved organic matter fluorescence in
711 a temperate estuary and its catchment using PARAFAC analysis. *Limnol. Oceanogr.* 50, 686–697.
712 doi:10.4319/lo.2005.50.2.0686.

713 Stewart, F. J., Dalsgaard, T., Young, C. R., Thamdrup, B., Revsbech, N. P., Ulloa, O., et al. (2012).
714 Experimental Incubations Elicit Profound Changes in Community Transcription in OMZ
715 Bacterioplankton. *PLoS One* 7, e37118. doi:10.1371/journal.pone.0037118.

716 Tada, Y., Taniguchi, A., Nagao, I., Miki, T., Uematsu, M., Tsuda, A., et al. (2011). Differing growth responses
717 of major phylogenetic groups of marine bacteria to natural phytoplankton blooms in the western North
718 Pacific Ocean. *Appl. Environ. Microbiol.* 77, 4055–65. doi:10.1128/AEM.02952-10.

719 Tamocai, C., Canadell, J. G., Schuur, E. A. G., Kuhry, P., Mazhitova, G., and Zimov, S. (2009). Soil organic
720 carbon pools in the northern circumpolar permafrost region. *Global Biogeochem. Cycles* 23, n/a-n/a.
721 doi:10.1029/2008GB003327.

722 Teeling, H., Fuchs, B. M., Becher, D., Klockow, C., Gardebrecht, A., Bennke, C. M., et al. (2012). Substrate-
723 Controlled Succession of Marine Bacterioplankton Populations Induced by a Phytoplankton Bloom.
724 *Science (80-.).* 336. Available at: http://science.sciencemag.org/content/336/6081/608 [Accessed
725 December 5, 2017].

726 Thingstad, T. F., Bellerby, R. G. J., Bratbak, G., Børsheim, K. Y., Egge, J. K., Heldal, M., et al. (2008).
727 Counterintuitive carbon-to-nutrient coupling in an Arctic pelagic ecosystem. *Nature* 455, 387–390.
728 doi:10.1038/nature07235.

729 Traving, S. J., Rowe, O., Jakobsen, N. M., Sørensen, H., Dinasquet, J., Stedmon, C. A., et al. (2017). The
730 Effect of Increased Loads of Dissolved Organic Matter on Estuarine Microbial Community Composition
731 and Function. *Front. Microbiol.* 8, 351. doi:10.3389/fmicb.2017.00351.

732 von Scheibner, M., Sommer, U., and Jürgens, K. (2017). Tight Coupling of Glaciecola spp. and Diatoms
733 during Cold-Water Phytoplankton Spring Blooms. *Front. Microbiol.* 8, 27.
734 doi:10.3389/fmicb.2017.00027.

735 Vonk, J. E., Mann, P. J., Davydov, S., Davydova, A., Spencer, R. G. M., Schade, J., et al. (2013). High
736 biolability of ancient permafrost carbon upon thaw. *Geophys. Res. Lett.* 40, 2689–2693.

737 doi:10.1002/grl.50348.

738 Wilson, B., Müller, O., Nordmann, E.-L., Seuthe, L., Bratbak, G., and Øvreås, L. (2017). Changes in Marine
739 Prokaryote Composition with Season and Depth Over an Arctic Polar Year. *Front. Mar. Sci.* 4.
740 doi:10.3389/fmars.2017.00095.

741 Wohlers, J., Engel, A., Zöllner, E., Breithaupt, P., Jürgens, K., Hoppe, H.-G., et al. (2009). Changes in
742 biogenic carbon flow in response to sea surface warming. *Proc. Natl. Acad. Sci. U. S. A.* 106, 7067–72.
743 doi:10.1073/pnas.0812743106.

744 Xie, H., Bélanger, S., Song, G., Benner, R., Taalba, A., Blais, M., et al. (2012). Photoproduction of
745 ammonium in the southeastern Beaufort Sea and its biogeochemical implications. *Biogeosciences* 9,
746 3047–3061. doi:10.5194/bg-9-3047-2012.

747 Zeng, Y.-X., Zhang, F., He, J.-F., Lee, S. H., Qiao, Z.-Y., Yu, Y., et al. (2013). Bacterioplankton community
748 structure in the Arctic waters as revealed by pyrosequencing of 16S rRNA genes. *Antonie Van*
749 *Leeuwenhoek* 103, 1309–1319. doi:10.1007/s10482-013-9912-6.

750 Zhu, Z.-Y., Wu, Y., Liu, S.-M., Wenger, F., Hu, J., Zhang, J., et al. (2016). Organic carbon flux and
751 particulate organic matter composition in Arctic valley glaciers: examples from the Bayelva River and
752 adjacent Kongsfjorden. *Biogeosciences* 13, 975–987. doi:10.5194/bg-13-975-2016.

753 Zubkov, M. V, Burkill, P. H., and Topping, J. N. (2007). Flow cytometric enumeration of DNA-stained
754 oceanic planktonic protists. *J. Plankton Res.* 29, 79–86. doi:10.1093/plankt/fbl059.

755

IV

frontiers in Marine Science

ORIGINAL RESEARCH
published: 13 April 2017
doi: 10.3389/fmars.2017.00095

Changes in Marine Prokaryote Composition with Season and Depth Over an Arctic Polar Year

Bryan Wilson[1], Oliver Müller[1], Eva-Lena Nordmann[1], Lena Seuthe[2], Gunnar Bratbak[1] and Lise Øvreås[1]*

[1] Marine Microbiology Research Group, University of Bergen, Bergen, Norway, [2] Department of Arctic and Marine Biology, UiT - The Arctic University of Norway, Tromsø, Norway

As the global climate changes, the higher latitudes are seen to be warming significantly faster. It is likely that the Arctic biome will experience considerable shifts in ice melt season length, leading to changes in photoirradiance and in the freshwater inputs to the marine environment. The exchange of nutrients between Arctic surface and deep waters and their cycling throughout the water column is driven by seasonal change. The impacts, however, of the current global climate transition period on the biodiversity of the Arctic Ocean and its activity are not yet known. To determine seasonal variation in the microbial communities in the deep water column, samples were collected from a profile (1-1000 m depth) in the waters around the Svalbard archipelago throughout an annual cycle encompassing both the polar night and day. High-throughput sequencing of 16S rRNA gene amplicons was used to monitor prokaryote diversity. In epipelagic surface waters (<200 m depth), seasonal diversity varied significantly, with light and the corresponding annual phytoplankton bloom pattern being the primary drivers of change during the late spring and summer months. In the permanently dark mesopelagic ocean depths (>200 m), seasonality subsequently had much less effect on community composition. In summer, phytoplankton-associated Gammaproteobacteria and Flavobacteriia dominated surface waters, whilst in low light conditions (surface waters in winter months and deeper waters all year round), the Thaumarchaeota and *Chloroflexi*-type SAR202 predominated. Alpha-diversity generally increased in epipelagic waters as seasonal light availability decreased; OTU richness also consistently increased down through the water column, with the deepest darkest waters containing the greatest diversity. Beta-diversity analyses confirmed that seasonality and depth also primarily drove community composition. The relative abundance of the eleven predominant taxa showed significant changes in surface waters in summer months and varied with season depending on the phytoplankton bloom stage; corresponding populations in deeper waters however, remained relatively unchanged. Given the significance of the annual phytoplankton bloom pattern on prokaryote diversity in Arctic waters, any changes to bloom dynamics resulting from accelerated global warming will likely have major impacts on surface marine microbial communities, those impacts inevitably trickling down into deeper waters.

Keywords: Arctic, marine microbiology, seasonality, nutrient cycling, depth, climate change, phytoplankton bloom, mesopelagic

OPEN ACCESS

Edited by:
Connie Lovejoy,
Laval University, Canada

Reviewed by:
Nico Salmaso,
Fondazione Edmund Mach, Italy
Dolors Vaque,
Consejo Superior de Investigaciones Científicas, Spain

****Correspondence:***
Bryan Wilson
bryan.wilson@uib.no

Specialty section:
This article was submitted to Aquatic Microbiology, a section of the journal Frontiers in Marine Science

Received: *01 October 2016*
Accepted: *20 March 2017*
Published: *13 April 2017*

Citation:
Wilson B, Müller O, Nordmann E-L, Seuthe L, Bratbak G and Øvreås L (2017) Changes in Marine Prokaryote Composition with Season and Depth Over an Arctic Polar Year. Front. Mar. Sci. 4:95. doi: 10.3389/fmars.2017.00095

1. INTRODUCTION

Polar regions are vulnerable and most sensitive to global climate change. Therefore, there is an increasing research focus needed on these high latitude environments. During the annual cycle, the poles undergo some of the most extreme environmental changes on the planet, from that of the subzero permanently dark winter to the relative warmth and perpetual daylight of the summer. The extensive biodiversity of these regions is understandably well-adapted to these periodic shifts but accelerated atmospheric warming is irrefutably altering conditions here and therefore needs to be studied in detail. The Arctic is warming three times faster than the global mean warming rate (Trenberth et al., 2007) and the extent and thickness of sea ice in the polar oceans is steadily decreasing (Chen et al., 2009), at a rate of up to ten percent per year (Comiso et al., 2008). Recent decades have also seen the summer melt season increase in length (Markus et al., 2009) and the percentage of thin first-year ice increase as compared with thicker multiyear ice (MYI) (Comiso, 2012), such that the late summer Arctic Ocean may be ice-free before the end of the twenty-first century (Boe et al., 2009) or sooner still (Kerr, 2012). Some of these striking environmental changes occurring in the Arctic are related to the inflow of Atlantic water to the Arctic Ocean. The West Spitsbergen Current passing through the eastern Fram Strait is the most significant inflow to the Arctic Ocean and it has intensified over the last decades (Schauer et al., 2004). Increased inflow of the warm and highly saline Atlantic Water affects water column stability and is also probably one of the main drivers of the recent sea ice loss north of Svalbard (Onarheim et al., 2014; Randelhoff et al., 2015). The cumulative consequence of these effects has been the exposure of polar seas to increasing levels of solar radiation (Perovich et al., 2007). Furthermore, enhanced permafrost thawing (Romanovsky et al., 2010) in concert with the profound influence of several large river systems (an hydrology peculiar to the Arctic) (Anderson, 2002) and a greater erosion of exposed coastlines (Lantuit et al., 2012), is leading to an increased terrigenous input of carbon to the Arctic Ocean (Frey and McClelland, 2009). All of which has the potential to radically impact the primary production and successive trophic levels of the polar marine environment (Anderson and Macdonald, 2015).

The greater part of high latitude research has been carried out in the Arctic (predominantly due to the relative logistical ease of working in the region when compared with Antarctica) and the Svalbard archipelago in particular has become a key site for Arctic marine studies, particularly with regards to its being the confluence of both the Arctic and Atlantic Oceans (Hop et al., 2002, 2006; Svendsen et al., 2002). The ocean around the Western coastline of Svalbard is a sea ice-associated pelagic ecosystem (Svendsen et al., 2002) and as with other high latitude locations, seasonal variations in light (and thus in primary production) are more pronounced here than elsewhere. The extreme seasonality of these environmental drivers has revealed a number of trends particular to the polar regions. A single major spring bloom along the retreating ice edge accounts for >50% of the annual primary production around Svalbard and in the Northern Barents Sea (Sakshaug, 2004). By late summer, this develops into a successional post-bloom stage, comprising different phytoplankton populations (Sherr et al., 2003) and it follows, their different associated successional heterotrophic prokaryote consortia, in particular the Flavobacteriia and Gammaproteobacteria classes (Alonso-Sáez et al., 2008; Teeling et al., 2012). This phenomenon of the polar phytoplankton blooms (Williams et al., 2013) followed by the heterotrophic bacterial populations also seemingly drives the annual disappearance of the chemolithoautotrophic marine Archaea from surface waters (Kalanetra et al., 2009; Alonso-Sáez et al., 2012; Pedneault et al., 2014) and the subsequent seasonal fluctuations in prokaryote diversity (Murray et al., 1998; Ghiglione and Murray, 2012; Grzymski et al., 2012; Ladau et al., 2013).

A significant fraction of the phytoplankton primary production sinks out of these surface waters (Reigstad et al., 2008), contributing a single annual major input of organic carbon and energy to the microbial communities residing in dark mesopelagic and deep waters. This subsurface realm dominates the global ocean biome and whereas the Arctic Ocean is the shallowest of the five major oceanic divisions, still its average depth is >1000 m deep. These aphotic zones are characterized by higher pressures, lower temperatures and higher inorganic nutrient concentrations than the photic surface waters above (Arístegui et al., 2009; Orcutt et al., 2011). Yet it is these physicochemical factors, in addition to their remoteness from the surface wind effects and solar irradiation that affect the upper layers so, that also determines their characteristic stability (Orcutt et al., 2011). The waters at these depths contain the largest pool of microbes in aquatic systems (Whitman et al., 1998) and play a major role in ocean biogeochemistry, comprising extraordinarily high genetic and metabolic diversity (Arístegui et al., 2009). The marine snow (primarily dissolved and particulate organic matter) produced by the spring and summer phytoplankton blooms in the stratified epipelagic zone is transported down during winter into the mesopelagic zone by convective mixing and subduction after cooling of the sea surface (Arístegui et al., 2009; Grzymski et al., 2012). Chemolithoautotrophic processes (such as archaeal ammonia oxidation) then come into play during the dark winter months (Grzymski et al., 2012) and the resulting nitrate buildup fuels the subsequent phytoplankton spring bloom (Connelly et al., 2014). However, should suggested models of a freshening Arctic be correct (Comeau et al., 2011), surface Arctic basin waters in a warming world may become increasingly stratified, such that the vertical flux of nutrients between deeper waters and the epipelagic zone may be reduced; primary productivity would consequently be lessened and this annual biogeochemical cycle, so essential for Arctic Ocean productivity, would inevitably be disrupted (Tremblay et al., 2008).

As the majority of Arctic studies of marine microbial communities have either been carried out in the more amenable spring and summer seasons or in shallow waters, the primary objective of the present study was to expand upon these data. More specifically, we wished to identify the key mediators of the prokaryotic microbial community in the Atlantic water inflow to the Arctic Ocean during the light-driven summers vs. the dark

winter night, seasons characterized by the massive variation in availability of fresh photosynthesis-derived carbon. Additionally, we intended to compare the cold, deep and dark mesopelagic ocean with the cold, shallow and dark surface waters above, to gain more insight into the driving mechanisms resulting from such environmental conditions. High-throughput sequencing technologies have previously highlighted the extreme microbial seasonality of the polar regions (Kirchman et al., 2010; Christman et al., 2011; Connelly et al., 2014). In this study we implement the same technologies to sequence reverse-transcribed total RNA (with its significantly shorter life span than DNA) to provide a timely snapshot of the more metabolically-active fraction of the marine microbial community.

2. MATERIALS AND EXPERIMENTAL METHODS

2.1. Sampling

Samples were taken from various transects bisecting the West Spitsbergen Current along the coast of Svalbard, a Norwegian archipelago in the Arctic Ocean (**Figure 1**) from the research vessels RV Lance and RV Helmer Hanssen, operating under either the MicroPolar and Carbon Bridge projects (**Table 1**). Samples (25–50 L) representative of the water column profile were collected from a range of water masses (defined in Paulsen et al., 2016) between 1m and 1000 m (**Table 1**) using Niskin bottles mounted on a rosette deployed from the vessels. Water samples were filtered through 0.22 μm Sterivex Filter Units (Merck-Millipore, MA, USA) via a peristaltic pump and frozen at −80°C immediately.

2.2. Chlorophyll *a* Measurement

The concentration of chlorophyll (chl) *a* was determined fluorometrically (Parson et al., 1984). Sample water was filtered onto triplicate Whatman GF/F glass-fiber filters (Sigma-Aldrich, MO, USA). The chl *a* on the filters was immediately extracted in 5 mL methanol (>99.8% v/v) at 4°C in the dark for 12 h without grinding. The fluorescence of the extracts was measured with a fluorometer (Model 10-AU, Turner Designs, CA, USA), calibrated with pure chl *a* (Sigma-Aldrich).

2.3. RNA Extraction

RNA were extracted directly from filters with the AllPrep DNA/RNA Mini Kit (Qiagen, CA, USA) using a protocol modified from the manufacturer's instructions. Briefly, filters were thawed on ice and an extraction buffer (comprising 990 μL Buffer RLT Plus and 10 μL β-mercaptoethanol per filter) prepared. Extraction buffer (1 mL) was added to each filter and filters vortexed vertically for 2 min, inverted and vortexed for a further 2 min. Lysate was removed from the filter using a 10 mL syringe and transferred to a 1.5 mL microfuge tube. Lysate (700 μL) was loaded on to an AllPrep DNA spin column and centrifuged for 30 s at 8000 × *g*, saving the flow-through for subsequent RNA extraction. Centrifugation steps were repeated for any remaining lysate volume, as necessary.

One volume 70% (v/v) ethanol was added to the flow-through, mixed by pipetting and 700 μL transferred to an RNeasy spin column in a 2 mL microfuge tube, before centrifugation for 15 s at 8000 × *g*. Centrifugation was repeated for the remaining liquid volume as necessary, discarding the flow-through each time. Buffer RW1 (700 μL) was added to the RNeasy spin column and the tube centrifuged again for 15 s at 8000 × *g* and the flow-through discarded. Buffer RPE (500 μL) was added to the RNeasy spin column and the tube centrifuged for 15 s at 8000 × *g*, discarding the flow-through. Buffer RPE (500 μL) was again added to the RNeasy spin column and the tube centrifuged for 2 min at 8000 × *g*. The RNeasy spin column was placed in a fresh 2 mL microfuge tube and centrifuged for 1 min at full speed. The RNeasy spin column was placed in a fresh 1.5 mL microfuge tube and 50 μL RNase-free water added to the spin column, before centrifugation for 1 min at 8000 × *g*. RNase-free water (50 μL) was added to the spin column again and the centrifugation repeated. The eluate (100 μL) was stored at −20°C.

The quantity and quality of RNA were assessed using a Qubit 3.0 Fluorometer (Thermo Fisher Scientific Inc., MA, USA) and by agarose gel electrophoresis.

2.4. Reverse Transcription and PCR for High-Throughput Sequencing (HTS) Library Construction

RNA (10 ng) was treated with the DNA-free DNA Removal kit (Invitrogen, CA, USA), prior to reverse transcription using the SuperScript III First-Strand Synthesis System for RT-PCR (Invitrogen), as per the manufacturer's instructions. The V4 region of the 16S rRNA gene was amplified from cDNA using a two-step nested PCR approach. In the first step, triplicate samples were amplified using primers 519F (5′-CAGCMGCCGCGGTAA-3′) (Øvreås et al., 1997) and 806R (5′-GGACTACHVGGGTWTCTAAT-3′) (Caporaso et al., 2011). The reaction mixture consisted of 10 μL HotStarTaq Master Mix (Qiagen), 500 nM of each primer, 10 ng of cDNA and nuclease-free water to bring the total volume to 20 μL. Reactions were initially denatured for 15 min at 95°C, followed by 25 cycles of denaturation at 95°C for 20 s, primer annealing at 55°C for 30 s and extension at 72°C for 30 s, followed by a final extension step of 72°C for 7 min. Triplicate amplicons were pooled and purified using the DNA Clean & Concentrator-5 kit (Zymo Research Corporation, CA, USA), as per the manufacturer's instructions, and quantified using a Qubit 3.0 Fluorometer.

In the second step, pooled amplicons were amplified by nested PCR using MID-tagged primers 519F and 806R in a reaction mixture comprising 25 μL HotStarTaq Master Mix, 500 nM of each primer, 50 ng of pooled DNA, and nuclease-free water to bring the total volume to 50 μL. Reactions were initially denatured for 15 min at 95°C, followed by 15 cycles of denaturation at 95°C for 20 s, primer annealing at 62°C for 30 s and extension at 72°C for 30 s. This was followed by a final extension step of 72°C for 7 min. The quantity and quality of RNA was assessed by agarose gel electrophoresis. Amplicons were purified using Agencourt AMPure XP Beads (Beckman Coulter Inc., CA, USA) and quantified again using a Qubit 3.0 Fluorometer and by agarose gel electrophoresis. MID-tagged

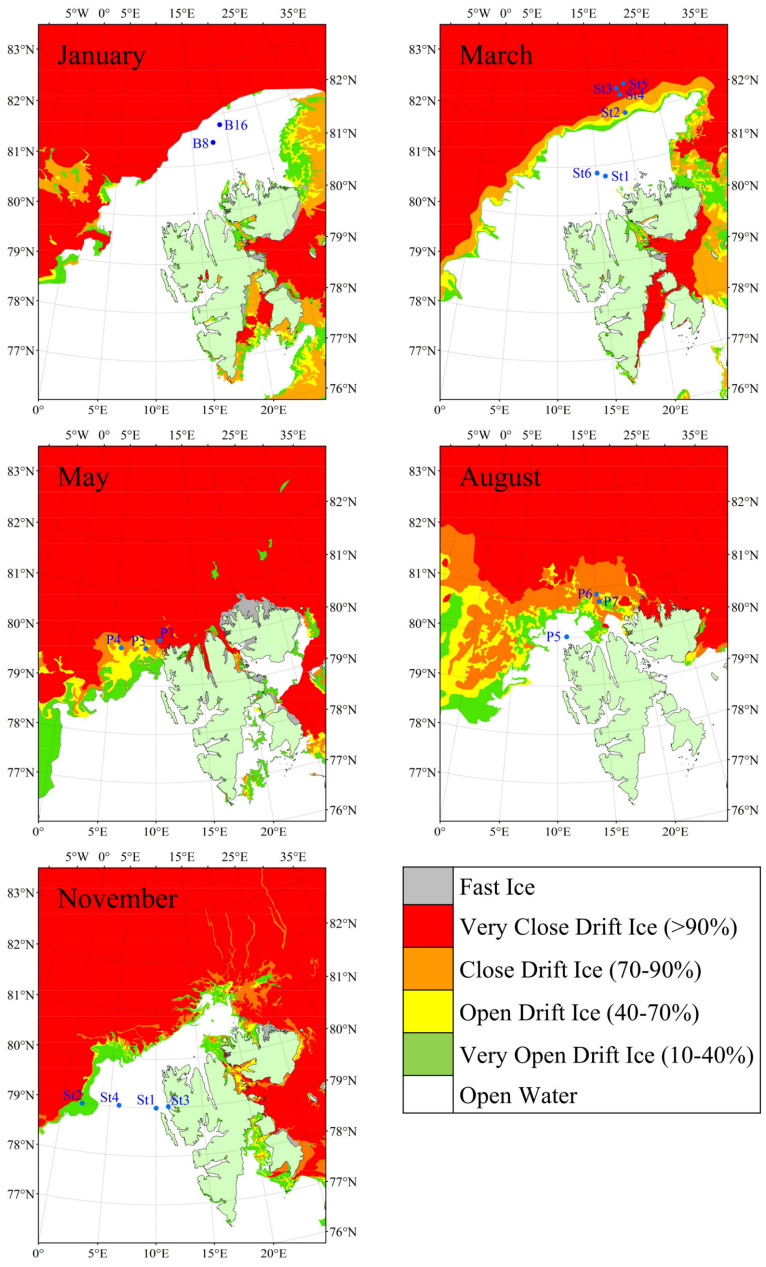

FIGURE 1 | Map showing sampling locations and sea ice extent around the Svalbard Archipelago. Maps were generated using the Global Self-consistent Hierarchical High-resolution Geography (GSHHG) data from the National Geospatial-Intelligence Agency (NGA), distributed under the GNU Lesser General Public License (LGPL). Ice data were provided by the Norwegian Ice Service (MET Norway) for the following dates; January 10, March 7, May 23, August 12, and November 7, 2014.

amplicons were then pooled in equimolar amounts for library construction.

Libraries were sent to the Norwegian Sequencing Centre (Oslo, Norway) for HTS on a MiSeq platform (Illumina, CA, USA) using the MiSeq Reagent Kit v2 (Illumina).

2.5. Bioinformatic Analyses

16S rRNA gene sequences were processed using a custom BioPython (Cock et al., 2009) script incorporating various bioinformatic tools, along with the QIIME pipeline (Version 1.8.0) (Caporaso et al., 2010b). Briefly, FASTQ files were quality end-trimmed at a phred quality score ≥20 using Sickle (Version 1.33) (Joshi and Fass, 2011) and PhiX contaminants and adapters removed using Bowtie 2 (Langmead and Salzberg, 2012) and cutadapt (Martin, 2011), respectively. Paired-end reads were merged using PANDAseq (Masella et al., 2012) and all reads <200 bp removed. The remaining sequence reads were checked for chimeras with the *identify chimeric seqs* and *filter fasta* scripts in QIIME, using usearch61 (Edgar, 2010) and the ChimeraSlayer (Haas et al., 2011) reference database (Gold.fa) found in the Broad Microbiome Utilities suite (http://microbiomeutil.sourceforge.net/). The *pick de novo otus* script in QIIME (using default parameters) was used for *de novo* OTU picking (using uclust (Edgar, 2010) and a sequence similarity threshold of 97%), taxonomy assignment (using PyNAST, Caporaso et al., 2010a) at 90% sequence similarity against the Greengenes core reference alignment database (Release 13_8) (DeSantis et al., 2006), and finally, the assembly of a table of OTU abundances with taxonomic identifiers for each OTU. OTUs were grouped by different taxonomic levels using the *summarize taxa* and *plot taxa summary* QIIME scripts. Rarefaction curves and Chao1 values were calculated using QIIME's *alpha rarefaction* script, whilst principal coordinate analysis plots used the *beta diversity through plots* script. All statistical figures were produced using the R Software Environment (R Core Team, 2013). High-throughput sequencing data were submitted to the European Nucleotide Archive (ENA) under Accession Number PRJEB19605.

3. RESULTS

3.1. Environmental Data

The dataset comprised fifty two samples in total, with the numbers of samples taken on each cruise (**Table 1**) varying with prevailing conditions and ship access time. Summer and winter conditions in the Arctic Ocean around Svalbard are very different (**Figure 1**) and much of the archipelago is ice-bound during the year, with the dark polar night persisting for almost three months. The study area (**Table 1**) is hydrographically characterized by Atlantic water masses, either as pure Atlantic water [AW; T (temperature) > 2°C and S (salinity) > 34.92; (Walczowski, 2013) and references therein], or as modified colder water masses, such as cold Atlantic Water (cAW) with 0 < T < 2°C (S > 34.9) and Intermediate Water (IW) T < 0°C (S > 3 4.9) (de Steur et al., 2014). Arctic water (ArW) was found at some stations and depths. Not all water classified here as ArW necessarily originated from the central Arctic Ocean. This may instead have been water that had undergone freshening and cooling processes, and hence had a density ρ_θ > 27.7 kg m^{-3} and S <34.92 (or 34.9 when cooler than 2°C). These are also the physical characteristics for ArW in the central Arctic Ocean. Cold surface water (SW; ρ_θ > 27.7 kg m^{-3} and S < 34.92) was encountered at stations within the marginal ice zone, created by sea ice melt. Sea ice extended furthest North during the winter months, and furthest South during May and August, prohibiting sampling north of Svalbard during the summer months. Consequently, most stations sampled in May and August were covered by ice, while all stations sampled during March and November were situated in open waters.

Concentration of chl *a* (a proxy for phytoplankton biomass) showed a clear seasonal cycle in phytoplankton, with lower concentrations throughout the water column during the dark winter months and March, higher concentrations in surface waters in May, and intermediate concentrations in August (**Table 1**). Detailed investigations of the phytoplankton showed a major shift from communities dominated by smaller-celled zooplankton during winter and March, to spring bloom communities dominated by large-celled phytoplankton, such as diatoms and *Phaeocystis* colonies in May (M. Reigstad, Personal Communication). In August, the phytoplankton communities were diverse and dominated again by smaller cells. The community shift from May to August reflects the general shift from nitrate-based phytoplankton communities in May to phytoplankton communities based on regenerated production in August (M. Reigstad, Personal Communication). In the deep mesopelagic waters, there was much less variation in biological and chemical properties than surface waters over the course of the year.

3.2. Prokaryote Diversity

After quality trimming and chimera removal, the complete 16S rRNA dataset (targeting the V4 region) comprised 7 902 016 sequence reads from 52 samples, with on average 127 452 reads per sample, totalling 470 567 OTUs (75.7% of these [356 512 OTUs] were singletons). Prokaryote communities were dominated by taxa typical of marine environments, including the bacterial classes Alphaproteobacteria, Gammaproteobacteria and *Chloroflexi*-type SAR202 and the archaeal class Thaumarchaeota (**Figure 2**). The relative abundances of these major classes were seen to vary significantly with season and depth. The Thaumarchaeota, *Chloroflexi*-type SAR202, AB16 (Marine Group A, originally SAR406) and Deltaproteobacteria were only observed to predominate in waters where light availability was low (in surface waters during the winter months and in deeper waters the year round). Representation of the Gammaproteobacteria and Flavobacteriia however was greatest when light availability and phytoplankton levels were highest (in epipelagic waters in the summer months). In the darker months (January, March and November), the relative abundances of the Alphaproteobacteria were recorded at similar levels irrespective of sample depth. In May however, levels were substantially higher in deeper waters, whilst August saw an abrupt shift to similarly high levels in surface waters.

Principal coordinate analyses (PCoA) on unweighted UniFrac distances (**Figure 3**) indicated that light availability and depth

TABLE 1 | Chemical and biological parameters for samples taken from the Arctic Ocean around the Svalbard Archipelago in 2014.

Month[a]	Station	Latitude (°North)	Longitude (°East)	Depth (m)	Temperature (°C)	Water mass[b]	Chl *a* (μg L^{-1})
January[c]	B16	81.77	19.16	1	−1.85	SW	0.02
				20	−1.85	SW	0.02
				500	+0.95	cAW	0.00
				1,000	−0.27	ArW	0.00
	B8	81.43	17.88	1	+2.20	AW	NA
				20	+2.19	AW	0.03
				500	+2.28	AW	0.01
				1,000	−0.25	IW	0.01
March[m]	St1	80.77	16.12	20	+3.13	AW	NA
	St2	81.99	20.02	1	−1.80	SW	0.05
				320	+2.00	cAW	0.01
				1,000	−0.10	IW	0.00
	St3	82.51	19.39	1	−1.80	SW	0.05
				20	−1.50	SW	NA
	St4	82.38	19.87	1	−1.78	ArW	0.07
				20	−1.70	ArW	0.04
	St5	82.55	21.03	20	−1.70	ArW	0.06
				120	+0.80	ArW	0.04
				320	+2.10	AW	NA
				1,000	−0.45	IW	NA
	St6	80.86	15.08	20	+3.20	AW	0.02
				1,000	−0.40	IW	NA
May[c]	P1	79.97	10.69	1	+1.01	SW	11.56
				10	+1.87	ArW	8.34
				365	+2.30	cAW	0.82
	P3	79.73	9.35	1	−0.34	SW	13.46
				10	−0.19	SW	14.49
				375	+2.37	cAW	0.27
	P4	79.78	6.17	1	−0.97	SW	5.54
				20	+1.05	SW	8.98
				500	+2.70	AW	0.04
				1,000	−0.81	IW	0.01
August[c]	P5	79.97	10.75	1	+6.03	SW	3.31
				20	+5.79	SW	2.44
				200	+4.20	AW	0.17
	P6	80.86	15.02	1	−1.00	SW	0.00
				25	+3.01	SW	0.20
				500	+2.16	AW	0.35
				1,000	−0.46	IW	0.33
	P7	80.69	15.28	1	+0.11	SW	0.01
				25	+4.98	AW	0.18
				500	+3.40	AW	1.23
				1,000	−0.24	IW	0.47
November[m]	St1	78.99	10.00	20	+3.30	ArW	0.21
	St2	79.01	1.97	750	+0.50	cAW	0.01
	St3	79.02	11.33	20	+2.30	SW	0.08
				300	+3.63	AW	0.07
	St4	79.03	6.01	5	+3.66	AW	0.11
				20	+3.67	AW	0.10
				200	+3.69	AW	0.07
				500	+1.87	cAW	0.02
				1,000	−0.39	IW	0.04

[a]Research Cruise, c, Carbon Bridge; m, MicroPolar; [b]SW, Surface Water; ArW, Arctic Water; AW, Atlantic Water; cAW, Cold Atlantic Water; IW, Intermediate Water; NA, Not Available; c Carbon Bridge; m MicroPolar.

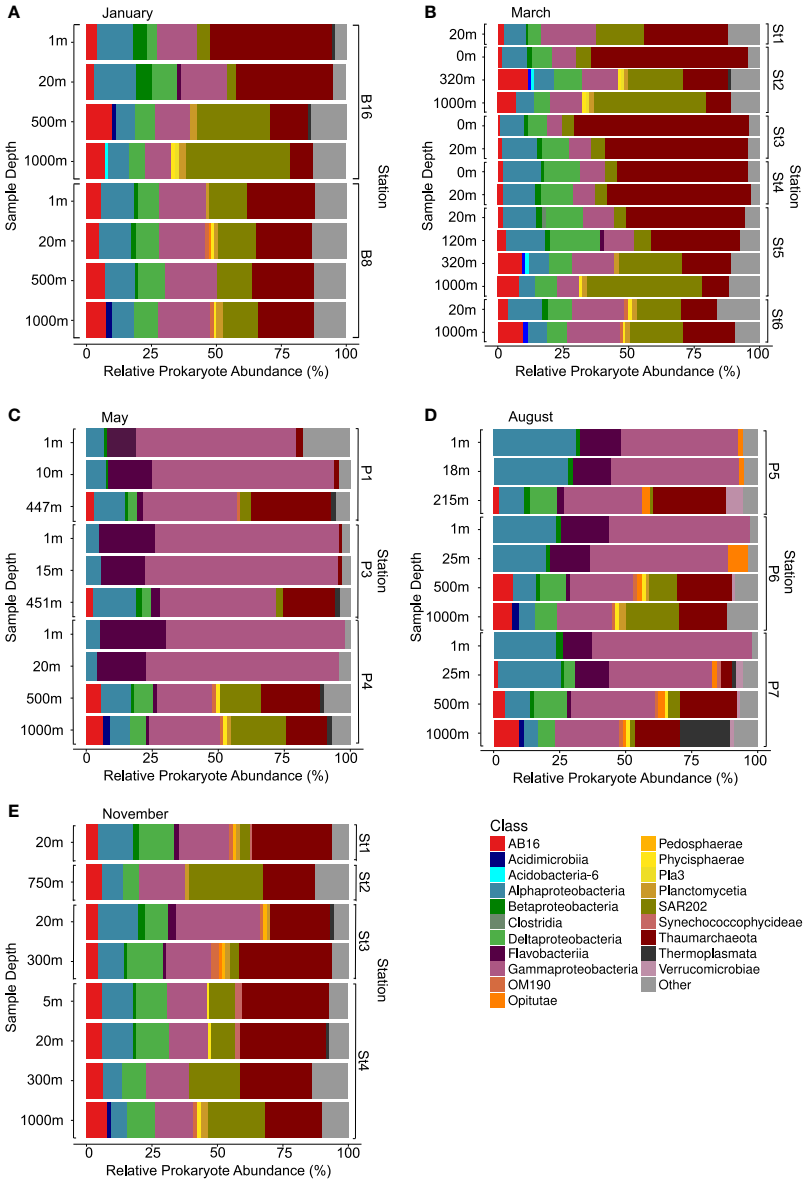

FIGURE 2 | Taxonomic diversity and relative abundance at the class level of prokaryotes from samples collected from the Arctic Ocean at different times, locations and depths. Sequences were taxonomically assigned to the Greengenes database (DeSantis et al., 2006) using QIIME (Caporaso et al., 2010b). For clarity of presentation, unassigned sequences and classes comprising <1% of the total number of sequences within a sample were simply classified as "Other" (gray), whilst sequences affiliated with phylum Cyanobacteria class Chloroplast were removed. **(A)** January, **(B)** March, **(C)** May, **(D)** August, and **(E)** November.

(of which light availability is a factor) primarily drove the phylogenetic beta-diversity across prokaryote communities, with three clearly separated clusters; one cluster (**Figure 3A**) containing communities from deep and dark mesopelagic waters, predominantly those samples collected from January, March and November; a second cluster (**Figure 3B**) comprising

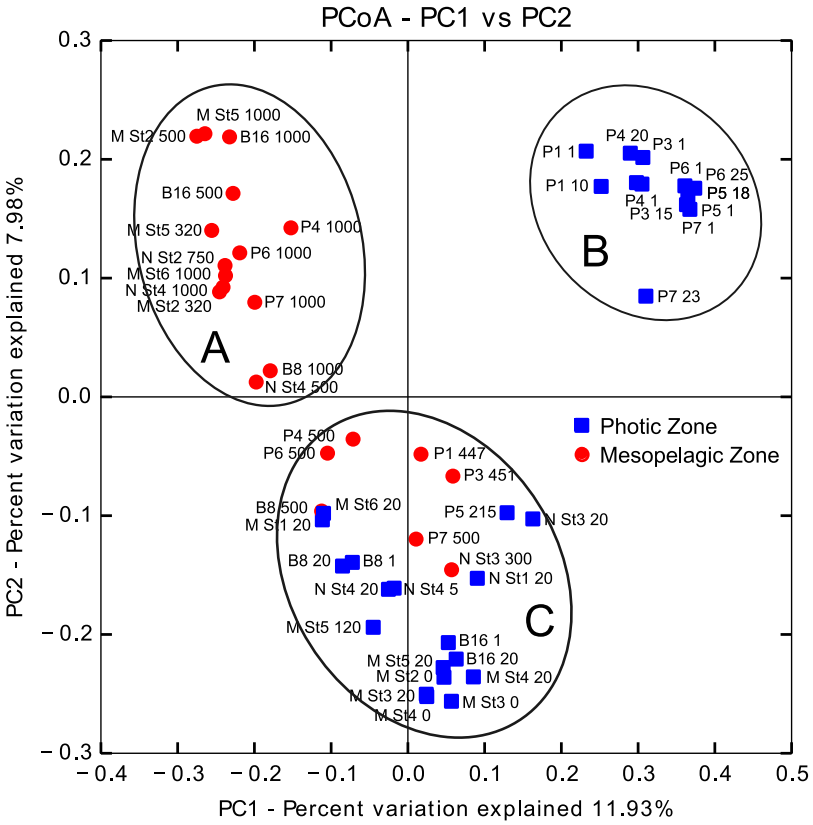

FIGURE 3 | Principal Coordinate Analysis (PCoA) of unweighted UniFrac distances of prokaryote 16S OTUs in putative Epipelagic (<200 m depth; blue squares) and Mesopelagic (200–1000 m depth; red circles) Zones of the Arctic Ocean. Text in the figure at each point refers to sampling station and depth; B8–16 (January), M St1–6 (March), P1–4 (May), P5–7 (August), and N St1–4 (November). PC, principal coordinate. Ellipses around the clusters labeled **(A–C)** were added to the figure manually for descriptive purposes only.

communities from samples collected from shallow and light epipelagic waters in May and August only; and a third cluster (**Figure 3C**), an admixture of communities from shallow and dark epipelagic waters in January, March and November and mesopelagic waters from May and August. Prokaryote alpha-diversity generally decreased as light availability increased to a maximum in the summer (**Figure 4** and Figure S1). Within each sampling period, Chao-1 estimates of OTU richness increased with increasing depth, with deeper waters containing a greater richness than surface waters, with maximum richness over the year observed in the deepest January samples. In surface waters, richness decreased until a minimum in August, before increasing again as light availability decreased during the late autumn.

The seasonal and depth variation in the relative abundance of eleven major prokaryote taxa (**Figure 5**) confirmed the impact of increased light availability and the resulting phytoplankton blooms on Arctic marine microbial populations in epipelagic waters. Generally, the dominant taxa in surface waters were seen to exhibit either a significant positive or negative population change in the summer months, whilst corresponding populations in deeper waters remained relatively unchanged. The relative abundance of 16S rRNAs derived from chloroplasts reached a maximum in May (**Figure 5**) and this was reflected by maxima in the Oceanospirillaceae, Alteromonadaceae and Flavobacteriaceae and minima in the archaeal family Cenarchaeaceae, Rhodospirillaceae, Nitrospinaceae and OM27, moving from March into May - in all these taxa, relative abundance increased substantially with the transition into the darker winter months. The family AEGEAN185 were unusual in that there was sharp decrease in the May relative abundance in deeper waters, as were the group SAR324 which saw concurrent minima in both surface and deeper waters.

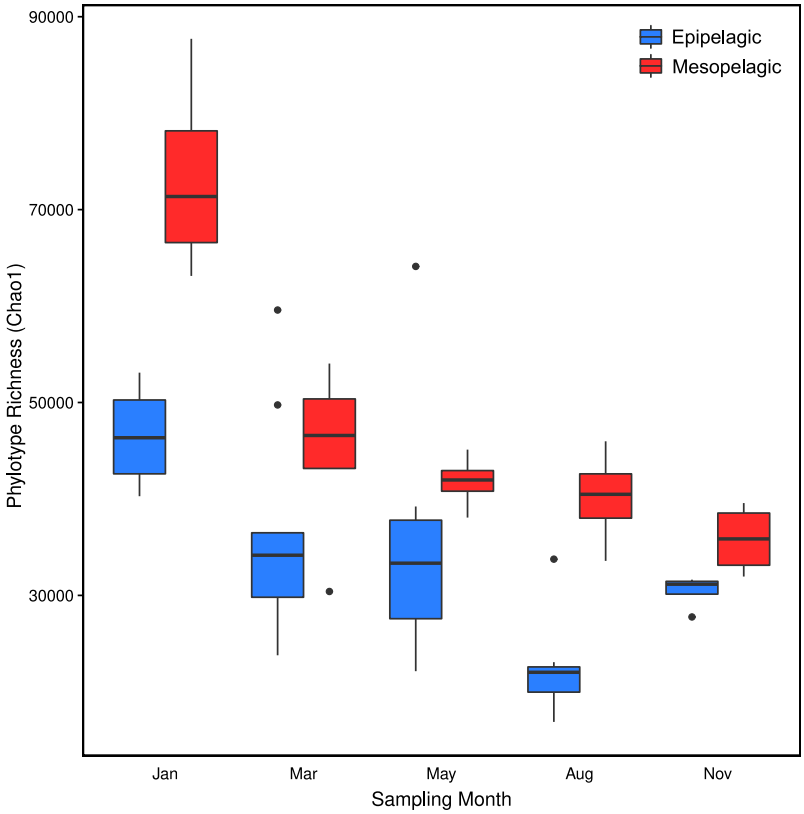

FIGURE 4 | Chao1 estimates of prokaryote 16S OTU richness in putative Epipelagic (<200 m depth) and Mesopelagic (200–1000m depth) Zones of the Arctic Ocean. The ends of the box represent the 25th and 75th percentiles, the whiskers represent minimum and maximum range, the band inside each box represents the median and the black circles represent outliers.

The second bloom in August, characterized by a different phytoplankton community to the earlier May one (E. S. Egge, Personal Communication), saw maxima in both the families Halomonadaceae and Rhodobacteraceae.

4. DISCUSSION

Recent advances in high-throughput sequencing technologies and software development for data management and processing have helped to shed light on the composition and seasonal dynamics of marine microbial communities, suggesting that many follow cyclical and predictable patterns (Fuhrman et al., 2006, 2015). Our study collected water samples in the seas around Svalbard from nominal depths ranging from 1 to 1000 m throughout the year, spanning the whole spectrum of environmental light conditions from the total darkness of the polar night to the perpetual illumination of the polar day. Our analysis of prokaryote 16S ribosomal RNA diversity using high-throughput sequencing confirmed that the microbial communities of Arctic waters during the polar winter and summer varied significantly. Additionally, this data suggested that seasonal and depth-related light availability and sea conditions and the associated phytoplankton blooms are the primary drivers for successional changes in community composition in these waters. Phylogenetic diversity increased with decreasing illumination, with regards to both seasonality and water depth, with the greatest richness to be found in the deepest and darkest water samples. The phytoplankton bloom and post-bloom stages dominated surface water communities in May and August, respectively, and saw corresponding increases in the relative abundance of bloom-associated copiotrophic organisms related to the Gammaproteobacteria and Flavobacteriia. The chemolithotrophic Thaumarchaeota

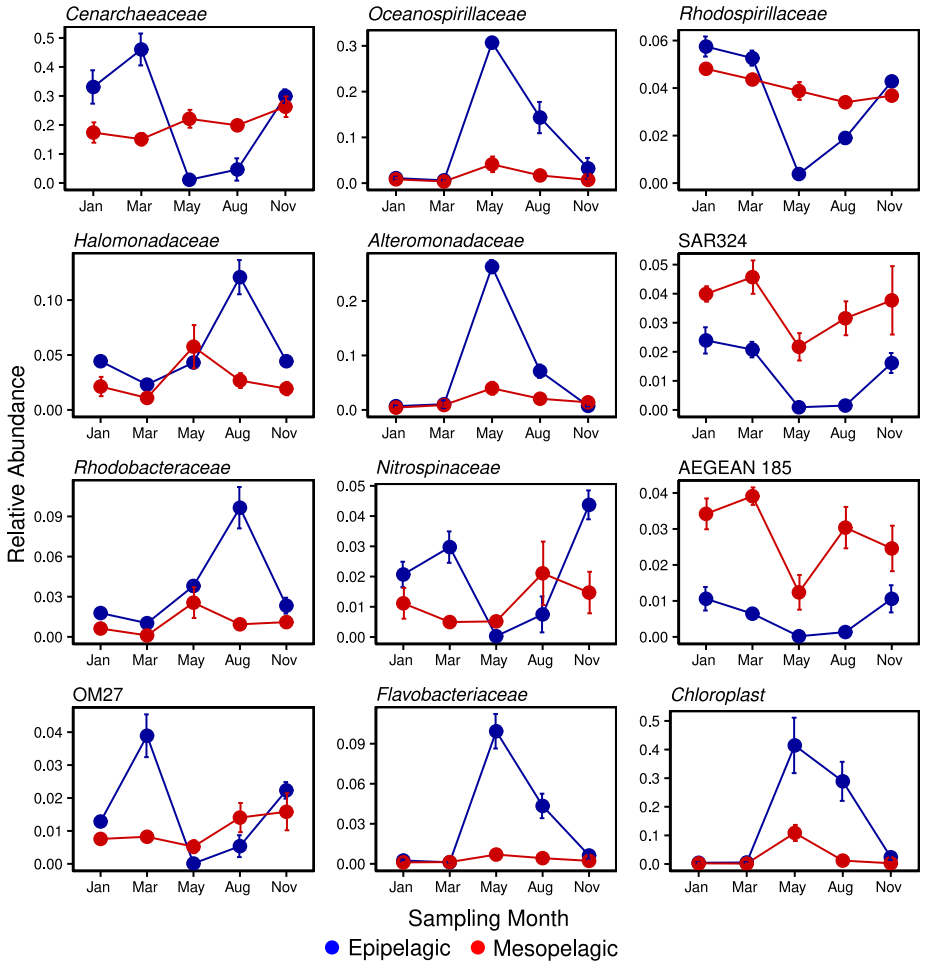

FIGURE 5 | Temporal variability of selected strong indicator prokaryote 16S phylotypes (at the family level) in putative Epipelagic (<200 m depth) and Mesopelagic (200–1000 m depth) Zones of the Arctic Ocean.

and *Chloroflexi*-type SAR202 dominated deep aphotic waters all year round but varied significantly in surface waters with varying light levels, proliferating in the dark winter months and diminishing in the well-lit summer months. Whether these taxa were responding directly to the changes in light availability or nutrient composition, or were outcompeted by the resulting phytoplankton blooms and successional prokaryotes is not known. The objectives of this research were to assess these microbial communities in time and space and investigate how these organisms respond down through the water column to the extreme variations in surface environmental conditions during the polar year.

We observed distinct seasonal fluctuations in prokaryote diversity, comprising high richness in the darker autumn and winter months and lower richness in the late spring and summer (Gilbert et al., 2012; El-Swais et al., 2015), similar to other surveys of surface waters in high latitude marine ecosystems (Murray et al., 1998; Murray and Grzymski, 2007; Ghiglione and Murray, 2012; Grzymski et al., 2012; Ladau et al., 2013). Phylotype richness peaked in January and then decreased through the year (**Figure 4**) until the annual minimum in August, coincident with the late summer phytoplankton post-bloom, before increasing again in the late autumn. Cyclic annual patterns of prokaryote community structure have been observed in waters off the

Antarctic Peninsula (Murray et al., 1998; Church et al., 2003; Murray and Grzymski, 2007) and had sampling in our study persisted, we predict that phylotype richness would likely have peaked again in January (Fuhrman et al., 2015). Rarefaction curves (Figure S1) also indicated that there was a distinct change in the number of unique phylotypes with season, which contrasts with seasonal pyrosequencing data for the Western Arctic (Kirchman et al., 2010). However, the authors do concede that the depth of their sequencing efforts may not have captured the complete diversity of these communities. Samples in the current study were rarified to 62500 sequences (tenfold higher than that of Kirchman et al., 2010) and this was sufficient to illustrate seasonal differences in community diversity. Whilst rarefaction curves for the May and August surface samples approached an asymptote, showing that coverage by these libraries was high, sequencing efforts for the winter months were typically undersaturated, as evidenced by the continued upwards curve of the January samples even at 170 000 reads (data not shown).

There was a clear trend in the variation in relative proportions of the two prokaryote domains in surface waters over the annual cycle, with the Archaea increasing to maxima in the winter months and decreasing to almost undetectable levels in the summer months (**Figure 5**). This was reflected in reverse by the Bacteria, mirroring seasonal observations of near-surface prokaryote communities in the Western Arctic (Alonso-Sáez et al., 2008). In our study, the Proteobacteria were the most abundant bacterial phylum throughout the year and of these, it was the class Gammaproteobacteria that predominated, particularly in the summer months, along with class Flavobacteriia of the phylum Bacteroidetes (**Figure 2**). The high relative abundance of these taxa in coastal waters around Svalbard (Zeng et al., 2013) has been associated with the release of dissolved organic matter following a phytoplankton bloom (Ghiglione and Murray, 2012; De Corte et al., 2013; Buchan et al., 2014; El-Swais et al., 2015) and they are seen to dominate Arctic MYI communities (Bowman et al., 2012). The Gammaproteobacteria are typically seen to increase toward the summer months (Alonso-Sáez et al., 2008) and of the strong indicator phylotypes determined during the study year, three of the top five (Oceanospirillaceae, Halomondaceae and Alteromonadaceae) were members of this class (**Figure 5**). Members of both the Oceanospirillaceae and Alteromonadaceae are known to be *r*-strategist, broad substrate generalists and are frequently seen to be closely-associated with phytoplankton blooms (Teeling et al., 2012; Buchan et al., 2014; El-Swais et al., 2015). However, in comparison with the abundance of physiological and genomic studies of bloom-associated Bacteroidetes and Alphaproteobacteria strains, there is a relative paucity of data regarding the Gammaproteobacteria (Buchan et al., 2014).

Recent whole genome analyses of various members of the Bacteroidetes have confirmed long-held assumptions of a preference for and selective advantage of the phylum when growing on complex organic matter (Abell and Bowman, 2005; Teeling et al., 2012; Fernández-Gómez et al., 2013; Williams et al., 2013), such as that typically produced by marine phytoplankton (Passow, 2002). Consequently, Bacteroidetes and phytoplankton are often found in close association in polar waters (Grossart et al., 2005; Piquet et al., 2011; Williams et al., 2013) with the relative abundance of the former significantly correlated with the emergence of the late spring blooms (Alonso-Sáez et al., 2008). During May of 2014, the Flavobacteriaceae were notable by their prolific increase in relative abundance from negligible levels in March, congruent with the spike in chloroplast 16S rRNA abundance (**Figure 5**) and chl *a* maxima (**Table 1**). Secondary bacterial production is typically correlated with chl *a* concentration (Buchan et al., 2014). The Flavobacteriaceae are one of the most commonly found groups in polar ecosystems (Abell and Bowman, 2005), particularly in the summer months (Grzymski et al., 2012; Williams et al., 2012), frequently comprising the majority of Bacteroidetes sequences in these environments (Ghiglione and Murray, 2012; Williams et al., 2013) and amongst the first groups to respond to phytoplankton blooms (Williams et al., 2013). Previously, the Flavobacteriia have been found at peak abundance during the decay phase of a bloom (Riemann et al., 2000; Pinhassi et al., 2004) but this was not the case in our post-bloom August samples (**Figure 2**). Proteorhodopsins, which support photoheterotrophic growth, have however been found in flavobacterial isolates (Gómez-Consarnau et al., 2007) previously and this may explain the peak abundance observed during the higher photoirradiance conditions of May. It has been suggested that increased numbers of Bacteroidetes would be found in the water column during spring and summer as a consequence of increased melting sea ice, either by seeding, as persistent members of sea ice biota (Bowman et al., 2012; Lo Giudice et al., 2012) or as a result of growth on organic matter released by the thawing (Piquet et al., 2011). As an abundance of Flavobacteriial proteins involved in oxidative stress protection have also been recovered from Antarctic metaproteomes, this suggests that the group may also exhibit a higher tolerance to the high solar irradiance found in polar spring and summer waters (Williams et al., 2013) and may indeed come to play a more dominant role in the surface layers of an ice-free Arctic.

A notable outcome immediately apparent from the 16S rRNA phylogenetic diversity data was the glaring disparity in the relative abundance of Alphaproteobacteria, when compared with previously published studies which saw them dominate polar waters (Alonso-Sáez et al., 2008; Manganelli et al., 2009; Bowman et al., 2012; Williams et al., 2013; Zeng et al., 2013). Closer examination revealed that the ubiquitous SAR11 were notable by their unusually low representation in the dataset, with their relative abundance no higher than 2.5% during the entirety of the study. The SAR11 typically comprise the greater part of observed Alphaproteobacteria in global marine communities (Morris et al., 2002), and more pertinently in the Arctic (Alonso-Sáez et al., 2008; Kirchman et al., 2010; Bowman et al., 2012). In a previous study in Svalbard coastal waters (De Corte et al., 2013), SAR11 were only detected at the 16S rDNA level, none being detected in the 16S rRNA; in the present investigation however, similarly low levels of SAR11 were discerned in both 16S rDNA and rRNA (data not shown). *In silico* analysis of the universal prokaryotic primer set 519F-806R (Øvreås et al., 1997; Caporaso et al., 2011) used in this study suggested a low-binding efficiency

of the reverse primer with the SAR11 cluster, an inherent flaw of the primers confirmed in recent studies (Apprill et al., 2015; Parada et al., 2016). Preliminary shotgun metagenomic data for this same polar time-series did reveal a significantly higher abundance of SAR11 (up to 28% of total prokaryote abundance; data not shown) and so, we can assume that the SAR11 are likely underrepresented in this 16S tag amplicon data set.

Members of the Alphaproteobacterial families Rhodospirillaceae and Rhodobacteraceae were however highly abundant in Arctic waters over the year, with both taxa appearing to be significantly correlated (negatively and positively, respectively) with different phytoplankton bloom stages (**Figure 5**). The Rhodobacteraceae were the most abundant OTUs recorded in late summer seas off Svalbard (Zeng et al., 2013) and the genus *Roseobacter* within this family has been seen to peak with chl *a* maximum in the Western Arctic (Alonso-Sáez et al., 2008), which is assumed to relate to this taxon's common association with phytoplankton blooms (González et al., 2000; Pinhassi et al., 2004; West et al., 2008; Buchan et al., 2014). In the current study however, *Roseobacter* species were not detected at the Genus level using the Greengenes database (DeSantis et al., 2006) but comparison of unassigned Rhodobacteraceae OTUs with BLAST confirms that they were present, albeit not at the levels seen in similar studies during the polar summer (Grzymski et al., 2012).

The Arctic Ocean has the greatest freshwater input of any ocean (Carmack, 2007) and so as might be expected, the Betaproteobacteria, one of the most prevalent groups in freshwaters, were present in the surface marine samples all year round (**Figure 2**) albeit at low levels; it is the corresponding absence of rivers in Antarctica which supports their recorded low levels in Southern Oceans (Ghiglione et al., 2012). Interestingly, we observed that the relative abundance of Betaproteobacteria in surface water samples decreased as a function of distance either from the coast or from the pack ice. A number of large glacial fjords flow into the Western coastal waters off Svalbard (**Figure 1**) and the Betaproteobacteria have been retrieved from Kongsfjorden there (Zeng et al., 2009, 2013; Piquet et al., 2010). The group have also been seen to predominate in Arctic pack ice summer melt pools (Brinkmeyer et al., 2004), which might further seed ocean waters upon thawing. In more temperate latitudes, the abundance of Betaproteobacteria decreases with increasing salinity (Garneau et al., 2009) but in the colder waters of the Arctic, they may persist further offshore (Pedrós-Alió et al., 2015). With climate change bringing with it increased freshwater inputs to the Arctic Ocean, we may also see the relative abundance of the Betaproteobacteria in marine microbial communities rise.

The lower diversity of surface waters during summer appears to be related to both taxonomic and methodological factors; whilst the spike in carbon and nutrient concentrations following a phytoplankton bloom inevitably leads to the proliferation of a few specific bacterial groups (Buchan et al., 2014), the elevated levels of phytoplankton in surface waters can often overwhelm efforts to sample representatively. Indeed, during this study, filters were frequently blocked by phytoplankton cell debris and consequently, without preventative measures, chloroplast 16S rRNAs would routinely comprise >90% of amplicon tag sequences, thereby reducing the sequencing coverage of targetted prokaryotes. Accordingly, prokaryote richness in surface waters during the winter months (and in deeper waters year round) was considerably higher, potentially also due to the more complex composition of the dissolved organic carbon pool (Alonso-Sáez et al., 2008) in darker waters not dominated by just a few bloom-related taxa.

Whilst light availability is thought to be the main driving factor in the epipelagic zone (Giovannoni and Stingl, 2005), conditions within deep dark waters are far from homogenous (Hewson et al., 2006; Teira et al., 2006; Galand et al., 2010). The oceans comprise regional water masses, defined by their distinct temperature and salinity properties, and these circulate around the globe at different spatial scales. Our sampling area off the west coast of Svalbard is notable as being the confluence of North Atlantic and Arctic waters and depending on sample season, location and depth, the deep water column may comprise a number of different water masses (**Table 1**). A study of the deep Arctic Ocean suggested that these water masses may act as physical barriers to microbial dispersal and that communities within these water masses may therefore have a distinct biogeography (Galand et al., 2010). Preliminary analyses of our data however did not seem to suggest a relationship between water mass and community composition (data not shown), with the effect of light and depth being much more significant (**Figure 3**).

Microbial life in the mesopelagic zone is quite different from that of the epipelagic zone (Orcutt et al., 2011) and whilst the absence of light is the most obvious difference, the deep oceans are also typically colder and at a higher pressure (increasing by approximately 10 MPa km^{-1} depth) than surface waters. Within each seasonal sample in our study, there was a clear difference in prokaryote composition between epipelagic and mesopelagic communities (**Figure 2**) and as might be expected, these differences were much more pronounced during the lighter months of May and August, driven by the massive change in surface communities during the phytoplankton blooms. In the darker months, communities were much more similar with depth and were dominated throughout the water column by the Thaumarchaeota and *Chloroflexi*-type SAR202. Seasonal changes had little effect on mesopelagic communities, with the moderate variations in prokaryote diversity congruent with the relatively unchanging nature of the deep marine environment. However, we do see a significant difference in phylotype richness in mesopelagic waters between January and the other months and one reason for this might very well be January's placing in the polar year, in the middle of the dark Arctic winter. The phytoplankton bloom results in a single annual pulse of nutrients and in the successional development of mesozooplankton and heterotrophic prokaryotes, the bulk of the simple compounds will be degraded relatively rapidly in the photic surface waters. What is left sinks as marine snow, which continues to be metabolized by the prokaryote community on its way down through the water column. By the time much of this matter reaches the mesopelagic depths, several months after the initial deposition from surface waters, what remains

is likely to be diverse relcalcitrant compounds. The primary factor differentiating the deep ocean from surface waters is that metabolic reactions are based only on chemical redox reactions (rather than photosynthetic processes) and much more variably coupled temporally, spatially and functionally (Orcutt et al., 2011). The more diverse chemical processes ongoing in the deep ocean will therefore likely require more functionally (and phylogenetically) diverse organisms than in surface waters, the richness of which seemingly peaks in the winter months.

Unmitigated atmospheric warming will undoubtedly affect gross changes in the marine environment and its phytoplankton populations through increased photoirradiation and nutrients made available by thawing sea ice and permafrost (Li et al., 2009; Doney et al., 2012; El-Swais et al., 2015), respectively. Whilst the phytoplankton blooms are restricted to the well-lit upper layers of the ocean, the effects of their prolific but short-lived activity are seen throughout the deep ocean beneath. As these summer blooms are inextricably linked to the deep and dark activities of the winter blooms of chemolithoautotrophic organisms, a change in one system will inevitably be manifested in the other, potentially via more subtle effects on specific taxonomic or functional prokaryote groups. As major contributors to the marine nitrogen cycle (Nicol and Schleper, 2006) and the dominant chemolithoautotrophs in polar waters, the role of the Thaumarchaeota (previously classified as members of the phylum Crenarchaeota Brochier-Armanet et al., 2008) is well-established (Fuhrman et al., 1992; DeLong et al., 1994; Karner et al., 2001). More recently, the cyclical rise (during winter) and decline (in summer) of the group in the surface waters of polar regions has received some attention (Murray et al., 1998, 1999; Church et al., 2003; Alonso-Sáez et al., 2008, 2012; Grzymski et al., 2012; Williams et al., 2012) and indeed, our data confirmed these findings. The almost total disappearance of the Thaumarchaeota from the photic zone during the summer months (**Figure 5**) is therefore suggestive of photoinhibition of ammonia oxidation (Guerrero and Jones, 1996; Murray et al., 1998; Mincer et al., 2007; Schleper and Nicol, 2010; Merbt et al., 2012), or has been more recently posited, a sensitivity to reactive oxygen species produced as a result of photosynthesis (Tolar et al., 2016). The reasons may however be multifactorial and it is thought that the Archaea may also be outcompeted by phytoplankton (Murray et al., 1998; Ward, 2000, 2005; Church et al., 2003; Herfort et al., 2007; Smith et al., 2014) and Bacteria (which are much more active in the uptake of the labile bloom-produced substrates Alonso-Sáez et al., 2008; Kalanetra et al., 2009), or even subjected to selective viral infection (Labonté et al., 2015). The proportional abundance of Thaumarchaeota has been correlated with ammonium concentrations (Herfort et al., 2007; Kirchman et al., 2007) and their peak abundance in winter surface waters has been hypothesized to result from mixing with deep water masses in Antarctic seas (Kalanetra et al., 2009; Grzymski et al., 2012); however, in areas of the Arctic Ocean where the water column tends to remain stratified during the winter (Forest et al., 2011), recent data suggests that the increase is in fact due to growth and proliferation of surface water Thaumarchaeota populations *in situ* (Alonso-Sáez et al., 2012). As the polar winter precludes photosynthesis and consequently, a source of labile organic matter, the autotrophic Thaumarchaeota are ideally adapted to bloom in these otherwise limiting conditions (Pedrós-Alió et al., 2015). Interestingly, in both Arctic (Alonso-Sáez et al., 2012) and Antarctic (Kalanetra et al., 2009; Grzymski et al., 2012) winter surface waters, a single Thaumarchaeotal OTU was seen to dominate archaeal 16S rRNA and ammonia monooxygenase *amoA* gene libraries and we saw a similar dominance in Arctic winter surface waters; however, as we continued down through the water profile, this dominant OTU gradually yields to another Thaumarchaeotal OTU, which ultimately dominates deeper waters. These shallow and deep cladal differences have been described in ammonia-oxidizing Archaea (AOA) previously, based primarily in differences in their *amoA* genes (Francis et al., 2005; Sintes et al., 2013; Pedneault et al., 2014; among others) but also other metabolic genes (Sintes et al., 2013; Luo et al., 2014; Villanueva et al., 2015).

Any change in Thaumarchaeota populations may have significant impacts on certain of the phytoplankton populations. In unlit surface waters, the Thaumarchaeota oxidize ammonium to nitrate, which in turn promotes phytoplankton growth come the lighter months; however, as the larger diatoms are thought to outcompete picophytoplankton for nitrate (Stolte and Riegman, 1995), diatom populations may be proportionally more affected by a loss of Thaumarchaeota (Comeau et al., 2011). Conversely, a warming freshening Arctic will be increasingly stratified and there will be less mixing with the nutrient-rich depths, potentially favoring smaller picophytoplankton (Li et al., 2009).

Taxa showing similar seasonal dynamics to the chemolithotrophic Thaumarchaeota in surface waters were the Deltaproteobacteria-affiliated SAR324, Nitrospinaceae and OM27 (**Figure 5**), all of which saw drops in relative abundance during the summer months. The nitrite-oxidizing genus *Nitrospina* has been observed in winter-only samples from both Antarctic (Grzymski et al., 2012) and Arctic (Alonso-Sáez et al., 2010) waters, as well as in temperate waters (El-Swais et al., 2015) and has also been correlated with *amoA*-containing Thaumarchaeota in Monterey Bay (Mincer et al., 2007). Whilst we recorded generally higher levels of all three taxa in winter surface and year-round deeper waters, active populations were still detected in surface waters in summer months, albeit at much lower levels. The *Chloroflexi*-type SAR202 cluster is also typical and highly abundant in mesopelagic waters (Morris et al., 2004; Varela et al., 2008; Arístegui et al., 2009; Dobal-Amador et al., 2016). Recent studies have shown the *Chloroflexi* to be well adapted to deeper oligotrophic waters and to efficiently utilize recalcitrant organic compounds uptake, such as those found in the mesopelagic zone (Yilmaz et al., 2016).

5. CONCLUSIONS

This high-throughput sequencing study of a polar year in the Arctic Ocean revealed the driving force of light and

phytoplankton blooms on the marine prokaryote community, and in particular the Thaumarchaeota, in both surface and deep ocean waters. Investigations such as this one and others discussed in the text are fundamentally important as a historic record of the current microbial state of the polar oceans and an indicator of the ongoing rate of change (Ducklow et al., 2009). Additionally, we believe that it is crucial to consider the deeper water column in these studies, as part of a whole, dynamic and interconnected marine system. As a complement to this study, we are also investigating shotgun metagenomic and metatranscriptomic data for these same seasonal samples, which will greatly improve the resolution of these preliminary results. We suggest that the future progress of the field would benefit greatly from repeated longer-term investigations, in concert with the continued improvement of omics tools and in this manner, we hope that these data may be used to support the overwhelming physical evidence of our changing global climate.

AUTHOR CONTRIBUTIONS

BW analyzed data, prepared figures and tables, and wrote the paper. OM, EN, LS, GB, and LØ collected, optimized, and processed samples. OM, LS, GB, and LØ were involved in project description, design of experiment, discussion, and interpreting data.

FUNDING

The MicroPolar project (also responsible for the cruises during March and November) was funded by the Research Council of Norway (RCN 225956). We would also like to thank the Carbon Bridge project (RCN 226415) for allowing us to participate during their cruises in January, May, and August. LØ is also affiliated with the University Centre in Svalbard (UNIS) and was funded, along with OM, by "Microorganisms in the Arctic: Major drivers of biogeochemical cycles and climate change" (RCN 227062). LS was funded through the Carbon Bridge project (RCN 226415).

ACKNOWLEDGMENTS

We would like to thank crew members of the Norwegian Research Vessels RV Helmer Hanssen and RV Lance for their assistance in sampling expeditions and all colleagues in the UiB Marine Microbiology group and collaborators abroad who contributed to the research effort.

SUPPLEMENTARY MATERIAL

The Supplementary Material for this article can be found online at: http://journal.frontiersin.org/article/10.3389/fmars.2017.00095/full#supplementary-material

REFERENCES

Abell, G. C. J., and Bowman, J. P. (2005). Ecological and biogeographic relationships of class Flavobacteria in the Southern Ocean. *FEMS Microbiol. Ecol.* 51, 265–277. doi: 10.1016/j.femsec.2004.09.001

Alonso-Sáez, L., Galand, P. E., Casamayor, E. O., Pedrós-Alió, C., and Bertilsson, S. (2010). High bicarbonate assimilation in the dark by Arctic bacteria. *ISME J.* 4, 1581–1590. doi: 10.1038/ismej.2010.69

Alonso-Sáez, L., Sánchez, O., Gasol, J. M., Balagué, V., and Pedrós-Alió, C. (2008). Winter-to-summer changes in the composition and single-cell activity of near-surface Arctic prokaryotes. *Environ. Microbiol.* 10, 2444–2454. doi: 10.1111/j.1462-2920.2008.01674.x

Alonso-Sáez, L., Waller, A. S., Mende, D. R., Bakker, K., Farnelid, H., Yager, P. L., et al. (2012). Role for urea in nitrification by polar marine Archaea. *Proc. Natl. Acad. Sci. U.S.A.* 109, 17989–17994. doi: 10.1073/pnas.1201914109

Anderson, L. G., and Macdonald, R. W. (2015). Observing the Arctic Ocean carbon cycle in a changing environment. *Polar Res.* 34:26891. doi: 10.3402/polar.v34.26891

Anderson, L. G. (2002). "DOC in the Arctic Ocean," in *Biogeochemistry of Marine Dissolved Organic Matter*, eds D. A. Hansell and C. A. Carlson (New York, NY: Elsevier), 665–683.

Apprill, A., McNally, S. P., Parsons, R., and Weber, L. (2015). Minor revision to V4 region SSU rRNA 806R gene primer greatly increases detection of SAR11 bacterioplankton. *Aquat. Microb. Ecol.* 75, 129–137. doi: 10.3354/ame01753

Arístegui, J., Gasol, J. M., Duarte, C. M., and Herndl, G. J. (2009). Microbial oceanography of the dark ocean's pelagic realm. *Limnol. Oceanogr.* 54, 1501–1529. doi: 10.4319/lo.2009.54.5.1501

Boe, J., Hall, A., and Qu, X. (2009). September sea-ice cover in the Arctic Ocean projected to vanish by 2100. *Nat. Geosci.* 2, 341–343. doi: 10.1038/ngeo467

Bowman, J. S., Rasmussen, S., Blom, N., Deming, J. W., Rysgaard, S., and Sicheritz-Ponten, T. (2012). Microbial community structure of Arctic multiyear sea ice and surface seawater by 454 sequencing of the 16S RNA gene. *ISME J.* 6, 11–20. doi: 10.1038/ismej.2011.76

Brinkmeyer, R., Glöckner, F. O., Helmke, E., and Amann, R. (2004). Predominance of β-proteobacteria in summer melt pools on Arctic pack ice. *Limnol. Oceanogr.* 49, 1013–1021. doi: 10.4319/lo.2004.49.4.1013

Brochier-Armanet, C., Boussau, B., Gribaldo, S., and Forterre, P. (2008). Mesophilic crenarchaeota: proposal for a third archaeal phylum, the Thaumarchaeota. *Nat. Rev. Microbiol.* 6, 245–252. doi: 10.1038/nrmicro1852

Buchan, A., LeCleir, G. R., Gulvik, C. A., and González, J. M. (2014). Master recyclers: features and functions of bacteria associated with phytoplankton blooms. *Nat. Rev. Micro.* 12, 686–698. doi: 10.1038/nrmicro3326

Caporaso, J. G., Bittinger, K., Bushman, F. D., DeSantis, T. Z., Andersen, G. L., and Knight, R. (2010a). PyNAST: a flexible tool for aligning sequences to a template alignment. *Bioinformatics* 26, 266–267. doi: 10.1093/bioinformatics/btp636

Caporaso, J. G., Kuczynski, J., Stombaugh, J., Bittinger, K., Bushman, F. D., Costello, E. K., et al. (2010b). QIIME allows analysis of high-throughput community sequencing data. *Nat. Methods* 7, 335–336. doi: 10.1038/nmeth.f.303

Caporaso, J. G., Lauber, C., Walters, W. A., Berg-Lyons, D., Lozupone, C. A., Turnbaugh, P. J., et al. (2011). Global patterns of 16S rRNA diversity at a depth of millions of sequences per sample. *Proc. Natl. Acad. Sci. U.S.A.* 108, 4516–4522. doi: 10.1073/pnas.1000080107

Carmack, E. (2007). The alpha/beta ocean distinction: a perspective on freshwater fluxes, convection, nutrients and productivity in high-latitude seas. *Deep-Sea Res. II* 54, 2578–2598. doi: 10.1016/j.dsr2.2007.08.018

Chen, J. L., Wilson, C. R., Blankenship, D., and Tapley, B. D. (2009). Accelerated Antarctic ice loss from satellite gravity measurements. *Nat. Geosci.* 2, 859–862. doi: 10.1038/ngeo694

Christman, G. D., Cottrell, M. T., Popp, B. N., Gier, E., and Kirchman, D. L. (2011). Abundance, diversity, and activity of ammonia-oxidizing prokaryotes in the coastal Arctic Ocean in summer and winter. *Appl. Environ. Microb.* 77, 2026–2034. doi: 10.1128/AEM.01907-10

Church, M. J., Delong, E. F., Ducklow, H. W., Karner, M. B., Preston, C. M., and Karl, D. M. (2003). Abundance and distribution of planktonic *Archaea* and *Bacteria* in the waters west of the Antarctic Peninsula. *Limnol. Oceanogr.* 48, 1893–1902. doi: 10.4319/lo.2003.48.5.1893

Cock, P. J. A., Antao, T., Chang, J. T., Chapman, B. A., Cox, C. J., Dalke, A., et al. (2009). Biopython: freely available Python tools for computational molecular biology and bioinformatics. *Bioinformatics* 25, 1422–1423. doi: 10.1093/bioinformatics/btp163

Comeau, A. M., Li, W. K. W., Tremblay, J.-E., Carmack, E. C., and Lovejoy, C. (2011). Arctic Ocean microbial community structure before and after the 2007 record sea ice minimum. *PLoS ONE* 6:e27492. doi: 10.1371/journal.pone.0027492

Comiso, J. C. (2012). Large decadal decline of the Arctic multiyear ice cover. *J. Clim.* 25, 1176–1193. doi: 10.1175/JCLI-D-11-00113.1

Comiso, J. C., Parkinson, C. L., Gersten, R., and Stock, L. (2008). Accelerated decline in the Arctic sea ice cover. *Geophys. Res. Lett.* 35:L01703. doi: 10.1029/2007GL031972

Connelly, T. L., Baer, S. E., Cooper, J. T., Bronk, D. A., and Wawrik, B. (2014). Urea uptake and carbon fixation by marine pelagic bacteria and archaea during the Arctic summer and winter seasons. *Appl. Environ. Microb.* 80, 6013–6022. doi: 10.1128/AEM.01431-14

De Corte, D., Sintes, E., Yokokawa, T., and Herndl, G. J. (2013). Comparison between MICRO-CARD-FISH and 16S rRNA gene clone libraries to assess the active versus total bacterial community in the coastal Arctic. *Environ. Microbiol. Rep.* 5, 272–281. doi: 10.1111/1758-2229.12013

de Steur, L., Hansen, E., Mauritzen, C., Beszczynska-Möller, A., and Fahrbach, E. (2014). Impact of recirculation on the East Greenland current in fram strait: results from moored current meter measurements between 1997 and 2009. *Deep-Sea Res. I* 92, 26–40. doi: 10.1016/j.dsr.2014.05.018

DeLong, E. F., Wu, K. Y., Prézelin, B. B., and Jovine, R. V. M. (1994). High abundance of archaea in antarctic marine picoplankton. *Nature* 371, 695–697. doi: 10.1038/371695a0

DeSantis, T. Z., Hugenholtz, P., Larsen, N., Rojas, M., Brodie, E. L., Keller, K., et al. (2006). Greengenes, a chimera-checked 16S rRNA gene database and workbench compatible with ARB. *Appl. Environ. Microb.* 72, 5069–5072. doi: 10.1128/AEM.03006-05

Dobal-Amador, V., Nieto-Cid, M., Guerrero-Feijoo, E., Hernando-Morales, V., Teira, E., and Varela, M. M. (2016). Vertical stratification of bacterial communities driven by multiple environmental factors in the waters (0-5000 m) off the Galician coast (NW Iberian margin). *Deep-Sea Res. I* 114, 1–11. doi: 10.1016/j.dsr.2016.04.009

Doney, S. C., Ruckelshaus, M., Duffy, J. E., Barry, J. P., Chan, F., English, C. A., et al. (2012). Climate change impacts on marine ecosystems. *Ann. Rev. Mar. Sci.* 4, 11–37. doi: 10.1146/annurev-marine-041911-111611

Ducklow, H. W., Doney, S. C., and Steinberg, D. K. (2009). Contributions of long-term research and time-series observations to marine ecology and biogeochemistry. *Ann. Rev. Mar. Sci.* 1, 279–302. doi: 10.1146/annurev.marine.010908.163801

Edgar, R. C. (2010). Search and clustering orders of magnitude faster than BLAST. *Bioinformatics* 26, 2460–2461. doi: 10.1093/bioinformatics/btq461

El-Swais, H., Dunn, K. A., Bielawski, J. P., Li, W. K. W., and Walsh, D. A. (2015). Seasonal assemblages and short-lived blooms in coastal north-west Atlantic Ocean bacterioplankton. *Environ. Microbiol.* 17, 3642–3661. doi: 10.1111/1462-2920.12629

Fernández-Gómez, B., Richter, M., Schüler, M., Pinhassi, J., Acinas, S. G., González, J. M., et al. (2013). Ecology of marine bacteroidetes: a comparative genomics approach. *ISME J.* 7, 1026–1037. doi: 10.1038/ismej.2012.169

Forest, A., Tremblay, J.-E., Gratton, Y., Martin, J., Gagnon, J., Darnis, G., et al. (2011). Biogenic carbon flows through the planktonic food web of the Amundsen Gulf (Arctic Ocean): a synthesis of field measurements and inverse modeling analyses. *Prog. Oceanogr.* 91, 410–436. doi: 10.1016/j.pocean.2011.05.002

Francis, C. A., Roberts, K. J., Beman, J. M., Santoro, A. E., and Oakley, B. B. (2005). Ubiquity and diversity of ammonia-oxidizing archaea in water columns and sediments of the ocean. *Proc. Natl. Acad. Sci. U.S.A.* 102, 14683–14688. doi: 10.1073/pnas.0506625102

Frey, K. E. and McClelland, J. W. (2009). Impacts of permafrost degradation on arctic river biogeochemistry. *Hydrol. Process* 23, 169–182. doi: 10.1002/hyp.7196

Fuhrman, J. A., Cram, J. A., and Needham, D. M. (2015). Marine microbial community dynamics and their ecological interpretation. *Nat. Rev. Micro.* 13, 133–146. . doi: 10.1038/nrmicro3417

Fuhrman, J. A., Hewson, I., Schwalbach, M. S., Steele, J. A., Brown, M. V., and Naeem, S. (2006). Annually reoccurring bacterial communities are predictable from ocean conditions. *Proc. Natl. Acad. Sci. U.S.A.* 103, 13104–13109. doi: 10.1073/pnas.0602399103

Fuhrman, J. A., McCallum, K., and Davis, A. A. (1992). Novel major archaeabacterial group from marine plankton. *Nature* 356, 148–149. doi: 10.1038/356148a0

Galand, P. E., Potvin, M., Casamayor, E. O., and Lovejoy, C. (2010). Hydrography shapes bacterial biogeography of the deep Arctic Ocean. *ISME J.* 4, 564–576. doi: 10.1038/ismej.2009.134

Garneau, M.-E., Vincent, W. F., Terrado, R., and Lovejoy, C. (2009). Importance of particle-associated bacterial heterotrophy in a coastal Arctic ecosystem. *J. Mar. Syst.* 75, 185–197. doi: 10.1016/j.jmarsys.2008.09.002

Ghiglione, J.-F., Galand, P. E., Pommier, T., Pedrós-Alió, C., Maas, E. W., Bakker, K., et al. (2012). Pole-to-pole biogeography of surface and deep marine bacterial communities. *Proc. Natl. Acad. Sci. U.S.A.* 109, 17633–17638. doi: 10.1073/pnas.1208160109

Ghiglione, J. F. and Murray, A. E. (2012). Pronounced summer to winter differences and higher wintertime richness in coastal Antarctic marine bacterioplankton. *Environ. Microbiol.* 14, 617–629. doi: 10.1111/j.1462-2920.2011.02601.x

Gilbert, J. A., Steele, J. A., Caporaso, J. G., Steinbruck, L., Reeder, J., Temperton, B., et al. (2012). Defining seasonal marine microbial community dynamics. *ISME J.* 6, 298–308. doi: 10.1038/ismej.2011.107

Giovannoni, S. J., and Stingl, U. (2005). Molecular diversity and ecology of microbial plankton. *Nature* 437, 343–348. doi: 10.1038/nature04158

Gómez-Consarnau, L., González, J. M., Coll-Lladó, M., Gourdon, P., Pascher, T., Neutze, R., et al. (2007). Light stimulates growth of proteorhodopsin-containing marine Flavobacteria. *Nature* 445, 210–213. doi: 10.1038/nature05381

González, J. M., Simó, R., Massana, R., Covert, J. S., Casamayor, E. O., Pedrós-Alió, C., et al. (2000). Bacterial community structure associated with a dimethylsulfoniopropionate-producing North Atlantic algal bloom. *Appl. Environ. Microb.* 66, 4237–4246. doi: 10.1128/AEM.66.10.4237-4246.2000

Grossart, H.-P., Levold, F., Allgaier, M., Simon, M., and Brinkhoff, T. (2005). Marine diatom species harbour distinct bacterial communities. *Environ. Microbiol.* 7, 860–873. doi: 10.1111/j.1462-2920.2005.00759.x

Grzymski, J. J., Riesenfeld, C. S., Williams, T. J., Dussaq, A. M., Ducklow, H., Erickson, M., et al. (2012). A metagenomic assessment of winter and summer bacterioplankton from Antarctica Peninsula coastal surface waters. *ISME J.* 6, 1901–1915. doi: 10.1038/ismej.2012.31

Guerrero, M. A. and Jones, R. D. (1996). Photoinhibition of marine nitrifying bacteria. 1. Wavelength-dependent response. *Mar. Ecol. Prog. Ser.* 141, 183–192. doi: 10.3354/meps141183

Haas, B. J., Gevers, D., Earl, A. M., Feldgarden, M., Ward, D. V., Giannoukos, G., et al. (2011). Chimeric 16s rRNA sequence formation and detection in Sanger and 454-pyrosequenced PCR amplicons. *Genome Res.* 21, 494–504. doi: 10.1101/gr.112730.110

Herfort, L., Schouten, S., Abbas, B., Veldhuis, M. J. W., Coolen, M. J. L., Wuchter, C., et al. (2007). Variations in spatial and temporal distribution of Archaea in the North Sea in relation to environmental variables. *FEMS Microbiol. Ecol.* 62, 242–257. doi: 10.1111/j.1574-6941.2007.00397.x

Hewson, I., Steele, J. A., Capone, D. G., and Fuhrman, J. A. (2006). Remarkable heterogeneity in meso- and bathypelagic bacterioplankton assemblage composition. *Limnol. Oceanogr.* 51, 1274–1283. doi: 10.4319/lo.2006.51.3.1274

Hop, H., Falk-Petersen, S., Svendsen, H., Kwasniewski, S., Pavlov, V., Pavlova, O., et al. (2006). Physical and biological characteristics of the pelagic system across Fram Strait to Kongsfjorden. *Prog. Oceanogr.* 71, 182–231. doi: 10.1016/j.pocean.2006.09.007

Hop, H., Pearson, T., Hegseth, E. N., Kovacs, K., Wiencke, C., Kwasniewski, S., et al. (2002). The marine ecosystem of Kongsfjorden, Svalbard. *Polar Res.* 21, 167–208. doi: 10.1111/j.1751-8369.2002.tb00073.x

Joshi, N. A. and Fass, J. N. (2011). *Sickle: A Sliding-Window, Adaptive, Quality-Based Trimming Tool for FastQ Files.* Available online at: https://github.com/najoshi/sickle

Kalanetra, K. M., Bano, N., and Hollibaugh, J. T. (2009). Ammonia-oxidizing *Archaea* in the Arctic Ocean and Antarctic coastal waters. *Environ. Microbiol.* 11, 2434–2445. doi: 10.1111/j.1462-2920.2009.01974.x

Karner, M. B., DeLong, E. F., and Karl, D. M. (2001). Archaeal dominance in the mesopelagic zone of the Pacific Ocean. *Nature* 409, 507–510. doi: 10.1038/35054051

Kerr, R. A. (2012). Ice-Free Arctic Sea may be years, not decades, a way. *Science* 337:1591. doi: 10.1126/science.337.6102.1591

Kirchman, D. L., Cottrell, M. T., and Lovejoy, C. (2010). The structure of bacterial communities in the western Arctic Ocean as revealed by pyrosequencing of 16S rRNA genes. *Environ. Microbiol.* 12, 1132–1143. doi: 10.1111/j.1462-2920.2010.02154.x

Kirchman, D. L., Elifantz, H., Dittel, A. I., Malmstrom, R. R., and Cottrell, M. T. (2007). Standing stocks and activity of Archaea and bacteria in the western Arctic Ocean. *Limnol. Oceanogr.* 52, 495–507. doi: 10.4319/lo.2007.52.2.0495

Labonté, J. M., Swan, B. K., Poulos, B., Luo, H., Koren, S., Hallam, S. J., et al. (2015). Single-cell genomics-based analysis of virus-host interactions in marine surface bacterioplankton. *ISME J.* 9, 2386–2399. doi: 10.1038/ismej.2015.48

Ladau, J., Sharpton, T. J., Finucane, M. M., Jospin, G., Kembel, S. W., O'Dwyer, J., et al. (2013). Global marine bacterial diversity peaks at high latitudes in winter. *ISME J.* 7, 1669–1677. doi: 10.1038/ismej.2013.37

Langmead, B. and Salzberg, S. L. (2012). Fast gapped-read alignment with Bowtie 2. *Nat. Methods* 9, 357–359. doi: 10.1038/nmeth.1923

Lantuit, H., Overduin, P. P., Couture, N., Wetterich, S., Aré, F., Atkinson, D., et al. (2012). The Arctic coastal dynamics database: a new classification scheme and statistics on Arctic permafrost coastlines. *Estuar. Coast* 35, 383–400. doi: 10.1007/s12237-010-9362-6

Li, W. K. W., McLaughlin, F. A., Lovejoy, C., and Carmack, E. C. (2009). Smallest Algae Thrive As the Arctic Ocean Freshens. *Science* 326:539. doi: 10.1126/science.1179798

Lo Giudice, A., Caruso, C., Mangano, S., Bruni, V., De Domenico, M., and Michaud, L. (2012). Marine bacterioplankton diversity and community composition in an Antarctic Coastal environment. *Microb. Ecol.* 63, 210–223. doi: 10.1007/s00248-011-9904-x

Luo, H., Tolar, B. B., Swan, B. K., Zhang, C. L., Stepanauskas, R., Ann Moran, M., et al. (2014). Single-cell genomics shedding light on marine Thaumarchaeota diversification. *ISME J.* 8, 732–736. doi: 10.1038/ismej.2013.202

Manganelli, M., Malfatti, F., Samo, T. J., Mitchell, B. G., Wang, H., and Azam, F. (2009). Major role of microbes in carbon fluxes during austral winter in the southern drake passage. *PLoS ONE* 4:e6941. doi: 10.1371/journal.pone.0006941

Markus, T., Stroeve, J. C., and Miller, J. (2009). Recent changes in Arctic sea ice melt onset, freezeup, and melt season length. *J. Geophys. Res. Oceans* 114:C12024. doi: 10.1029/2009JC005436

Martin, M. (2011). Cutadapt removes adapter sequences from high-throughput sequencing reads. *EMBnet J.* 17, 10–12. doi: 10.14806/ej.17.1.200

Masella, A. P., Bartram, A. K., Truszkowski, J. M., Brown, D. G., and Neufeld, J. D. (2012). PANDAseq: PAired-eND assembler for illumina sequences. *BMC Bioinformatics* 13:31. doi: 10.1186/1471-2105-13-31

Merbt, S. N., Stahl, D. A., Casamayor, E. O., Martí, E., Nicol, G. W., and Prosser, J. I. (2012). Differential photoinhibition of bacterial and archaeal ammonia oxidation. *FEMS Microbiol. Lett.* 327, 41–46. doi: 10.1111/j.1574-6968.2011.02457.x

Mincer, T. J., Church, M. J., Taylor, L. T., Preston, C., Karl, D. M., and DeLong, E. F. (2007). Quantitative distribution of presumptive archaeal and bacterial nitrifiers in monterey bay and the North Pacific Subtropical Gyre. *Environ. Microbiol.* 9, 1162–1175. doi: 10.1111/j.1462-2920.2007.01239.x

Morris, R. M., Rappé, M. S., Connon, S. A., Vergin, K. L., Siebold, W. A., Carlson, C. A., et al. (2002). SAR11 clade dominates ocean surface bacterioplankton communities. *Nature* 420, 806–810. doi: 10.1038/nature01240

Morris, R. M., Rappé, M. S., Urbach, E., Connon, S. A., and Giovannoni, S. J. (2004). Prevalence of the *Chloroflexi*-related SAR202 bacterioplankton cluster throughout the mesopelagic zone and deep ocean. *Appl. Environ. Micro.* 70, 2836–2842. doi: 10.1128/AEM.70.5.2836-2842.2004

Murray, A. E. and Grzymski, J. J. (2007). Diversity and genomics of Antarctic marine micro-organisms. *Philos. Trans. R. Soc. Lond. B. Biol. Sci.* 362, 2259–2271. doi: 10.1098/rstb.2006.1944

Murray, A. E., Preston, C. M., Massana, R., Taylor, L. T., Blakis, A., Wu, K., et al. (1998). Seasonal and spatial variability of bacterial and archaeal assemblages in the coastal waters near anvers island, antarctica. *Appl. Environ. Microb.* 64, 2585–2595.

Murray, A. E., Wu, K., Moyer, C., Karl, D. M., and DeLong, E. F. (1999). Evidence for circumpolar distribution of planktonic Archaea in the Southern Ocean. *Aquat. Microb. Ecol.* 18, 263–273. doi: 10.3354/ame018263

Nicol, G. W. and Schleper, C. (2006). Ammonia-oxidising Crenarchaeota: important players in the nitrogen cycle? *Trends Microbiol.* 14, 207–212. doi: 10.1016/j.tim.2006.03.004

Onarheim, I. H., Smedsrud, L. H., Ingvaldsen, R. B., and Nilsen, F. (2014). Loss of sea ice during winter north of Svalbard. *Tellus A* 66:23933. doi: 10.3402/tellusa.v66.23933

Orcutt, B. N., Sylvan, J. B., Knab, N. J., and Edwards, K. J. (2011). Microbial ecology of the dark ocean above, at, and below the seafloor. *Microbiol. Mol. Biol. Rev.* 75, 361–422. doi: 10.1128/MMBR.00039-10

Øvreås, L., Forney, L., Daae, F. L., and Torsvik, V. (1997). Distribution of bacterioplankton in meromictic lake saelenvannet, as determined by denaturing gradient gel electrophoresis of PCR-amplified gene fragments coding for 16S rRNA. *Appl. Environ. Microb.* 63, 3367–3373.

Parada, A. E., Needham, D. M., and Fuhrman, J. A. (2016). Every base matters: assessing small subunit rRNA primers for marine microbiomes with mock communities, time series and global field samples. *Environ. Microbiol.* 18, 1403–1414. doi: 10.1111/1462-2920.13023

Parson, T. R., Maita, Y., and Lalli, C. M. (1984). "4.3 - fluorometric determination of chlorophylls," in *A Manual of Chemical and Biological Methods for Seawater Analysis*, eds T. R. Parson, Y. Maita, and C. M. Lalli (Amsterdam: Pergamon), 107–109.

Passow, U. (2002). Transparent exopolymer particles (TEP) in aquatic environments. *Progr. Oceanogr.* 55, 287–333. doi: 10.1016/S0079-6611(02)00138-6

Paulsen, M., Doré, H., Garczarek, L., Seuthe, L., Müller, O., Sandaa, R.-A., et al. (2016). *Synechococcus* in the Atlantic gateway to the Arctic Ocean. *Front. Mar. Sci.* 3:191. doi: 10.3389/fmars.2016.00191

Pedneault, E., Galand, P., Potvin, M., Tremblay, J.-E., and Lovejoy, C. (2014). Archaeal *amoA* and *ureC* genes and their transcriptional activity in the Arctic Ocean. *Sci. Rep.* 4:4661. doi: 10.1038/srep04661

Pedrós-Alió, C., Potvin, M., and Lovejoy, C. (2015). Diversity of planktonic microorganisms in the Arctic Ocean. *Progr. Oceanogr.* 139, 233–243. doi: 10.1016/j.pocean.2015.07.009

Perovich, D. K., Light, B., Eicken, H., Jones, K. F., Runciman, K., and Nghiem, S. V. (2007). Increasing solar heating of the Arctic Ocean and adjacent seas, 1979-2005: attribution and role in the ice-albedo feedback. *Geophys. Res. Lett.* 34:L19505. doi: 10.1029/2007GL031480

Pinhassi, J., Sala, M. M., Havskum, H., Peters, F., Guadayol, O., Malits, A., and Marrasé, C. (2004). Changes in bacterioplankton composition under different phytoplankton regimens. *Appl. Environ. Microb.* 70, 6753–6766. doi: 10.1128/AEM.70.11.6753-6766.2004

Piquet, A. M.-T., Bolhuis, H., Meredith, M. P., and Buma, A. G. (2011). Shifts in coastal Antarctic marine microbial communities during and after melt water-related surface stratification. *FEMS Microbiol. Ecol.* 76, 413–427. doi: 10.1111/j.1574-6941.2011.01062.x

Piquet, A. M.-T., Scheepens, J. F., Bolhuis, H., Wiencke, C., and Buma, A. G. J. (2010). Variability of protistan and bacterial communities in two Arctic fjords (Spitsbergen). *Polar Biol.* 33, 1521–1536. doi: 10.1007/s00300-010-0841-9

R Core Team (2013). *R: A Language and Environment for Statistical Computing*. Vienna: R Foundation for Statistical Computing.

Randelhoff, A., Sundfjord, A., and Reigstad, M. (2015). Seasonal variability and fluxes of nitrate in the surface waters over the Arctic shelf slope. *Geophys. Res. Lett.* 42, 3442–3449. doi: 10.1002/2015GL063655

Reigstad, M., Riser, C. W., Wassmann, P., and Ratkova, T. (2008). Vertical export of particulate organic carbon: attenuation, composition and loss rates in the northern Barents sea. *Deep-Sea Res. II* 55, 2308–2319. doi: 10.1016/j.dsr2.2008.05.007

Riemann, L., Steward, G. F., and Azam, F. (2000). Dynamics of bacterial community composition and activity during a mesocosm diatom bloom. *Appl. Environ. Microb.* 66, 578–587. doi: 10.1128/AEM.66.2.578-587.2000

Romanovsky, V. E., Smith, S. L., and Christiansen, H. H. (2010). Permafrost thermal state in the polar Northern Hemisphere during the international polar year 2007-2009: a synthesis. *Permafrost Periglac* 21, 106–116. doi: 10.1002/ppp.689

Sakshaug, E. (2004). "Primary and secondary production in the Arctic seas," in *The Organic Carbon Cycle in the Arctic Ocean*, eds R. Stein and R. W. MacDonald (Berlin; Heidelberg:Springer), 57–81.

Schauer, U., Fahrbach, E., Osterhus, S., and Rohardt, G. (2004). Arctic warming through the fram strait: oceanic heat transport from 3 years of measurements. *J. Geophys. Res. Oceans* 109:C06026. doi: 10.1029/2003JC001823

Schleper, C. and Nicol, G. W. (2010). "Ammonia-oxidising archaea physiology, ecology and evolution," in *Advances in Microbial Physiology*, Vol. 57, ed R. K. Poole (Cambridge: Academic Press), 1–41.

Sherr, E. B., Sherr, B. F., Wheeler, P. A., and Thompson, K. (2003). Temporal and spatial variation in stocks of autotrophic and heterotrophic microbes in the upper water column of the central Arctic Ocean. *Deep-Sea Res. I* 50, 557–571. doi: 10.1016/S0967-0637(03)00031-1

Sintes, E., Bergauer, K., De Corte, D., Yokokawa, T., and Herndl, G. J. (2013). Archaeal *amoA* gene diversity points to distinct biogeography of ammonia-oxidizing *Crenarchaeota* in the ocean. *Environ. Microbiol.* 15, 1647–1658. doi: 10.1111/j.1462-2920.2012.02801.x

Smith, J. M., Chavez, F. P., and Francis, C. A. (2014). Ammonium uptake by phytoplankton regulates nitrification in the sunlit ocean. *PLoS ONE* 9:e108173. doi: 10.1371/journal.pone.0108173

Stolte, W. and Riegman, R. (1995). Effect of phytoplankton cell size on transient-state nitrate and ammonium uptake kinetics. *Microbiology* 141, 1221–1229. doi: 10.1099/13500872-141-5-1221

Svendsen, H., Beszczynska-Møller, A., Hagen, J., Lefauconnier, B., Tverberg, V., Gerland, S., et al. (2002). The physical environment of kongsfjorden-krossfjorden, an Arctic fjord system in Svalbard. *Polar Res.* 21, 133–166. doi: 10.1111/j.1751-8369.2002.tb00072.x

Teeling, H., Fuchs, B. M., Becher, D., Klockow, C., Gardebrecht, A., Bennke, C. M., et al. (2012). Substrate-controlled succession of marine bacterioplankton populations induced by a phytoplankton bloom. *Science* 336, 608–611. doi: 10.1126/science.1218344

Teira, E., Lebaron, P., van Aken, H., and Herndl, G. J. (2006). Distribution and activity of Bacteria and Archaea in the deep water masses of the North Atlantic. *Limnol. Oceanogr.* 51, 2131–2144. doi: 10.4319/lo.2006.51.5.2131

Tolar, B. B., Powers, L. C., Miller, W. L., Wallsgrove, N. J., Popp, B. N., and Hollibaugh, J. T. (2016). Ammonia oxidation in the ocean can be inhibited by nanomolar concentrations of hydrogen peroxide. *Front. Mar. Sci.* 3:237. doi: 10.3389/fmars.2016.00237

Tremblay, J.-É., Simpson, K., Martin, J., Miller, L., Gratton, Y., Barber, D., et al. (2008). Vertical stability and the annual dynamics of nutrients and chlorophyll fluorescence in the coastal, southeast Beaufort sea. *J Geophys. Res. Oceans* 113:C07S90. doi: 10.1029/2007JC004547

Trenberth, K. E., Jones, P. D., Amenhem, P., Bojariu, R., Easterling, D., Tank, A. K., et al. (2007). "Observations: atmospheric surface and climate change," in *Climate Change 2007: The Physical Science Basis. Contribution of Working Group I to the Fourth Assessment Report of the Intergovernmental Panel on Climate Change*, eds S. Solomon, D. Qin, M. Manning, Z. Chen, M. Marquis, K. B. Avery, M. Tignor, and H. L. Miller (Cambridge, UK: Cambridge University Press), 235–336.

Varela, M. M., Van Aken, H. M., and Herndl, G. J. (2008). Abundance and activity of *Chloroflexi*-type SAR202 bacterioplankton in the meso- and bathypelagic waters of the (sub)tropical Atlantic. *Environ. Microbiol.* 10, 1903–1911. doi: 10.1111/j.1462-2920.2008.01627.x

Villanueva, L., Schouten, S., and Sinninghe Damsté, J. S. (2015). Depth-related distribution of a key gene of the tetraether lipid biosynthetic pathway in marine Thaumarchaeota. *Environ. Microbiol.* 17, 3527–3539. doi: 10.1111/1462-2920.12508

Walczowski, W. (2013). Frontal structures in the West Spitsbergen current margins. *Ocean Sci.* 9, 957–975. doi: 10.5194/os-9-957-2013

Ward, B. B. (2000). "Nitrification and the marine nitrogen cycle," in *Microbial Ecology of the Oceans*, ed D. L. Kirchman (New York, NY: Wiley-Liss), 427–453.

Ward, B. B. (2005). Temporal variability in nitrification rates and related biogeochemical factors in monterey bay, california, U.S.A. *Mar. Ecol. Prog. Ser.* 292, 97–109. doi: 10.3354/meps292097

West, N. J., Obernosterer, I., Zemb, O., and Lebaron, P. (2008). Major differences of bacterial diversity and activity inside and outside of a natural iron-fertilized phytoplankton bloom in the Southern Ocean. *Environ. Microbiol.* 10, 738–756. doi: 10.1111/j.1462-2920.2007.01497.x

Whitman, W. B., Coleman, D. C., and Wiebe, W. J. (1998). Prokaryotes: the unseen majority. *Proc. Natl. Acad. Sci. U.S.A.* 95, 6578–6583. doi: 10.1073/pnas.95.12.6578

Williams, T. J., Long, E., Evans, F., DeMaere, M. Z., Lauro, F. M., Raftery, M. J., et al. (2012). A metaproteomic assessment of winter and summer bacterioplankton from Antarctic Peninsula coastal surface waters. *ISME J.* 6, 1883–1900. doi: 10.1038/ismej.2012.28

Williams, T. J., Wilkins, D., Long, E., Evans, F., DeMaere, M. Z., Raftery, M. J., et al. (2013). The role of planktonic *Flavobacteria* in processing algal organic matter in coastal East Antarctica revealed using metagenomics and metaproteomics. *Environ. Microbiol.* 15, 1302–1317. doi: 10.1111/1462-2920.12017

Yilmaz, P., Yarza, P., Rapp, J. Z., and Glöckner, F. O. (2016). Expanding the world of marine bacterial and archaeal clades. *Front. Microbiol.* 6:1524. doi: 10.3389/fmicb.2015.01524

Zeng, Y., Zheng, T., and Li, H. (2009). Community composition of the marine bacterioplankton in Kongsfjorden (Spitsbergen) as revealed by 16S rRNA gene analysis. *Polar Biol.* 32, 1447–1460. doi: 10.1007/s00300-009-0641-2

Zeng, Y.-X., Zhang, F., He, J.-F., Lee, S. H., Qiao, Z.-Y., Yu, Y., et al. (2013). Bacterioplankton community structure in the Arctic waters as revealed by pyrosequencing of 16S rRNA genes. *Antonie Van Leeuwenhoek* 103, 1309–1319. doi: 10.1007/s10482-013-9912-6

Conflict of Interest Statement: The authors declare that the research was conducted in the absence of any commercial or financial relationships that could be construed as a potential conflict of interest.

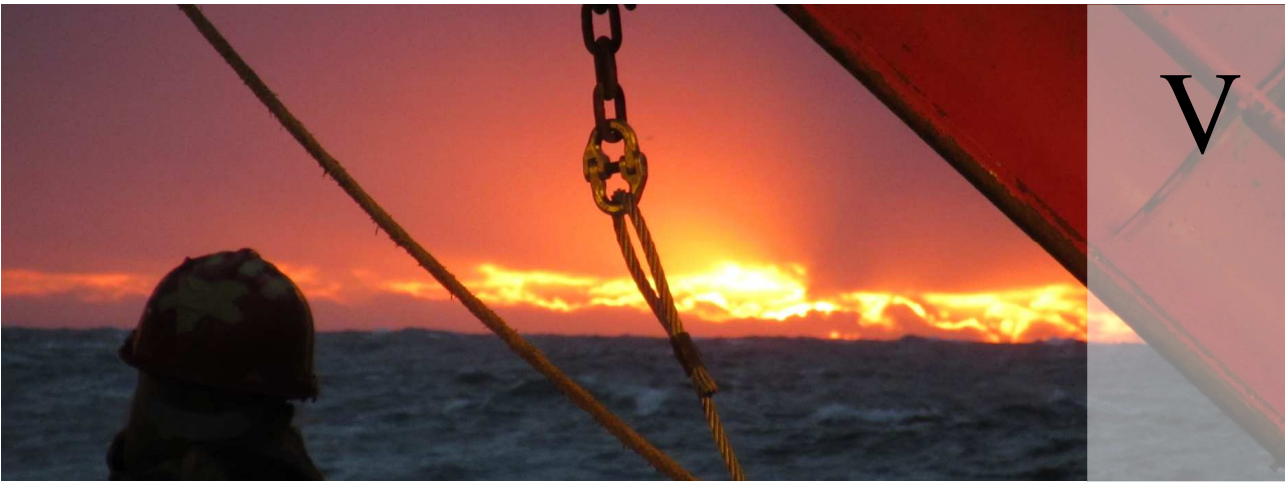

V

frontiers in Microbiology

ORIGINAL RESEARCH
published: 23 January 2018
doi: 10.3389/fmicb.2018.00024

Spatiotemporal Dynamics of Ammonia-Oxidizing Thaumarchaeota in Distinct Arctic Water Masses

Oliver Müller[1]*, *Bryan Wilson*[1], *Maria L. Paulsen*[1], *Agnieszka Rumińska*[1], *Hilde R. Armo*[1], *Gunnar Bratbak*[1] and *Lise Øvreås*[1,2]

[1] Department of Microbiology, University of Bergen, Bergen, Norway, [2] University Center in Svalbard (UNIS), Longyearbyen, Norway

One of the most abundant archaeal groups on Earth is the Thaumarchaeota. They are recognized as major contributors to marine ammonia oxidation, a crucial step in the biogeochemical cycling of nitrogen. Their universal success is attributed to a high genomic flexibility and niche adaptability. Based on differences in the gene coding for ammonia monooxygenase subunit A (amoA), two different ecotypes with distinct distribution patterns in the water column have been identified. We used high-throughput sequencing of 16S rRNA genes combined with archaeal *amoA* functional gene clone libraries to investigate which environmental factors are driving the distribution of Thaumarchaeota ecotypes in the Atlantic gateway to the Arctic Ocean through an annual cycle in 2014. We observed the characteristic vertical pattern of Thaumarchaeota abundance with high values in the mesopelagic (>200 m) water throughout the entire year, but also in the epipelagic (<200 m) water during the dark winter months (January, March and November). The Thaumarchaeota community was dominated by three OTUs which on average comprised 76% ± 11 and varied in relative abundance according to water mass characteristics and not to depth or ammonium concentration, as suggested in previous studies. The ratios of the abundance of the different OTU types were similar to that of the functional *amoA* water cluster types. Together, this suggests a strong selection of ecotypes within different water masses, supporting the general idea of water mass characteristics as an important factor in defining microbial community structure. If indeed, as suggested in this study, Thaumarchaeota population dynamics are controlled by a set of factors, described here as water mass characteristics and not just depth alone, then changes in water mass flow will inevitably affect the distribution of the different ecotypes.

Keywords: thaumarchaeota, ammonia-oxidation, Arctic Ocean, water mass, ecotype, *amoA*, 16S rRNA gene sequencing

OPEN ACCESS

Edited by:
Stanley Chun Kwan Lau,
Hong Kong University of Science and Technology, Hong Kong

Reviewed by:
Anne Bernhard,
Connecticut College, United States
Yu Zhang,
Shanghai Jiao Tong University, China

***Correspondence:**
Oliver Müller
oliver.muller@uib.no

Specialty section:
This article was submitted to Aquatic Microbiology, a section of the journal Frontiers in Microbiology

Received: *09 October 2017*
Accepted: *08 January 2018*
Published: *23 January 2018*

Citation:
Müller O, Wilson B, Paulsen ML, Rumińska A, Armo HR, Bratbak G and Øvreås L (2018) Spatiotemporal Dynamics of Ammonia-Oxidizing Thaumarchaeota in Distinct Arctic Water Masses. Front. Microbiol. 9:24. doi: 10.3389/fmicb.2018.00024

INTRODUCTION

The discovery of the high abundance of marine planktonic Archaea in 1992 was a revelation (DeLong, 1992; Fuhrman et al., 1992). Since then, numerous studies have confirmed both their high proportions and population dynamics, especially in deeper waters and from both polar oceans (Massana et al., 1998; Murray et al., 1998). In later studies the marine Archaea have been

found to play important roles in many biogeochemical processes (Ouverney and Fuhrman, 2000; Offre et al., 2013). When Craig Venter and colleagues discovered genes encoding for ammonia monooxygenase subunit A (amoA) in their metagenome analyses from the Sargasso Sea, new information regarding these processes was provided, leading to a particular interest in the marine Thaumarchaeota (Venter et al., 2004). This interest was further strengthened with the cultivation and characterization of the first marine archaeal isolate (*Candidatus Nitrosopumilus maritimus* SCM1) capable of ammonia oxidation (Könneke et al., 2005). Today, chemoautotrophic ammonia oxidizing Archaea (AOA) are recognized as the major contributors to marine microbial ammonia oxidation and thus driving nitrification processes, dominating these relative to their bacterial ammonia oxidizing (AOB) counterparts (Wuchter et al., 2006; Valentine, 2007).

Thaumarchaeota are widely distributed and may make up a significant part of marine microbial communities (Karner et al., 2001; Agogué et al., 2008; Beman et al., 2008). In the surface waters of polar regions there seem to be temporal changes in the relative abundance of Thaumarchaeota with an increase during winter and decline in summer (Massana et al., 1998; Murray et al., 1998; Church et al., 2003; Alonso-Sáez et al., 2008; Grzymski et al., 2012). Photoinhibition of ammonia oxidation has been hypothesized as an underlying cause for the seasonal disappearance of AOA (Guerrero and Jones, 1996; Murray et al., 1998; Mincer et al., 2007; Merbt et al., 2012). However, other factors, such as competition with an increasing abundance of phytoplankton and associated bacterial blooms (Massana et al., 1998; Church et al., 2003; Herfort et al., 2007) or nutrient limitations, including ammonium (Wuchter et al., 2006; Herfort et al., 2007; Kirchman et al., 2007), may also play important roles. Physical aspects such as deep water mixing have been suggested to resolve the winter increase of Thaumarchaeota abundance in the Southern Oceans (Kalanetra et al., 2009; Grzymski et al., 2012), but this could not explain the same trends in the Arctic, where the ocean remains relatively stratified during winter (Forest et al., 2011). Recent data have suggested that the increase in AOA is due to *in situ* growth at the surface and not to mixing with deeper water masses (Alonso-Sáez et al., 2012).

The surface Thaumarchaeota populations comprise predominantly one type of AOA, while the deep ocean is dominated by another type of AOA and have thus far, based on differences in their *amoA* genes, been divided into a surface (WCA) and a deep (WCB) type (Francis et al., 2005; Hallam et al., 2006; Beman et al., 2008; Sintes et al., 2013). Their depth-dependent distribution has been demonstrated in many different regions, including the Gulf of California (Beman et al., 2008), the Gulf of Mexico (Tolar et al., 2013), the Arctic Ocean (Pedneault et al., 2014), Monterey Bay (Smith et al., 2014) and throughout the entire Atlantic Ocean (Sintes et al., 2016). Taxonomically, *amoA* sequences can be divided into six main subclusters all branching to the *N. maritimus* cluster (Pester et al., 2012; Sintes et al., 2016). Two subclusters include only WCA sequences and the other four subclusters include exclusively WCB sequences.

The abundance of the different AOA types has also been correlated with ammonium concentrations and this has led to the introduction of high and low ammonium concentration AOA (HAC-AOA and LAC-AOA, respectively) (Herfort et al., 2007; Kirchman et al., 2007; Sintes et al., 2013). HAC-AOA dominate at depths with high ammonium concentrations while LAC-AOA are in higher abundance in deeper ocean regions where the ammonium concentration is low (Sintes et al., 2013). Overall, LAC-AOA corresponded taxonomically to WCB-types and HAC-AOA with WCA types. Ammonium concentrations (Woodward and Rees, 2001; Varela et al., 2007; Clark et al., 2008) measured for different oceanic regions could also support an observed macroecological AOA distribution in the Atlantic Ocean (Sintes et al., 2016). However, other environmental factors such as depth, temperature, dissolved oxygen, nitrite, and salinity have been previously identified as influences on the abundance and diversity of AOA (Francis et al., 2005; Herfort et al., 2007; Abell et al., 2010; Santoro et al., 2010; Biller et al., 2012; Pester et al., 2012; Sintes et al., 2015). Overall, the niche specification of the two ecotypes is best explained by depth in combination with geographic region and to a lesser extent with environmental factors, including ammonium concentration. However, it remains unclear whether these taxonomic definitions, both WCA/WCB and HAC/LAC, can be used to associate observed abundances with distinct biogeochemical niches, like water masses.

We have recently reported the high relative abundance and seasonal variation of Thaumarchaeota in waters around the western coast of Svalbard (Wilson et al., 2017). Here we extend the studies and investigate the Thaumarchaeota community in five different water masses, dominated by Atlantic and Arctic Water, using high throughput 16S rRNA gene sequencing aiming to identify different Thaumarchaeota populations and using *amoA* gene abundance to elucidate functional capabilities that may influence their distribution and dynamics.

MATERIALS AND METHODS

Study Site and Sampling

Samples were collected as part of the MicroPolar project (in cooperation with the project "CarbonBridge") during five cruises in 2014 north-west of Svalbard, following several transects along the West Spitsbergen Current (WSC) at the eastern part of the Fram Strait up to the Arctic Ocean (**Figure 1**). This area is hydrographically characterized by three Atlantic water masses, including Atlantic Water (AW), cold Atlantic Water (cAW) and Intermediate Water (IW), having salinity >34.9 and temperatures >2°C, 0–2°C and <0°C, respectively; and also, by two Arctic water masses, Surface Water (SW) and Arctic Water (ArW), having salinity <34.92 and density (σ_t) <27.7 and >27.7 respectively (Cokelet et al., 2008; de Steur et al., 2014; Randelhoff et al., 2015). An overview of the water mass characteristics is listed in Supplementary Table S3. The WSC at the eastern part of the Fram Strait transports Atlantic water into the Arctic Ocean. This Atlantic water can also be found in deeper mesopelagic zones as cAW and IW. The water masses classified as Arctic Water do not necessarily originate from the Arctic Ocean interior, but have undergone similar freshening and cooling processes and have the same physical characteristics as Arctic Ocean water masses.

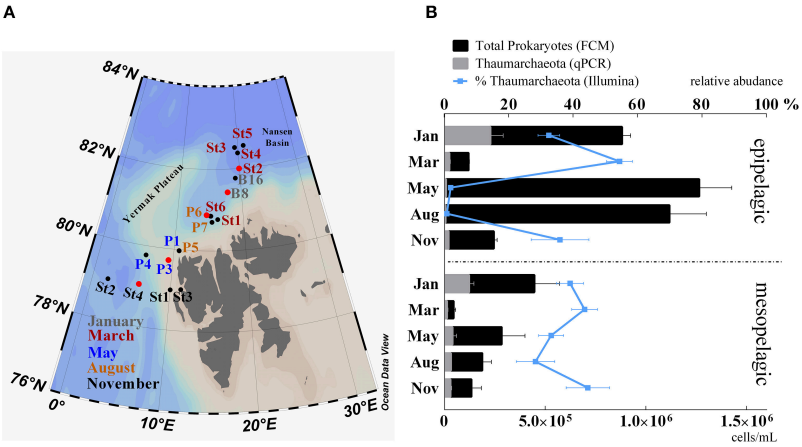

FIGURE 1 | (A) Study area Northwest of Svalbard. Stations are colored according to their time of sampling: gray, January; red, March; blue, May; yellow, August; black, November. Stations marked with a red circle were selected for *amoA* functional gene analyses. **(B)** Abundance of prokaryotes counted by flow cytometry (black bars) and superimposed abundance of Thaumarchaeota (gray bars) determined by qPCR of 16S rRNA genes. Relative abundance of Thaumarchaeota in relation to the total of 16S rRNA genes from Illumina sequencing data is shown by the blue line. Samples were grouped in epipelagic (0–200 m; $n = 28$) and mesopelagic (200–1,000 m; $n = 22$) zones and according to their sampling month. Standard errors were calculated for average values and are indicated as error bars.

Sampling periods extended over an entire polar year with cruises in January (06.01–15.01), March (05.03–10.03), May (15.05–02.06), August (07.08–18.08), and November (03.11–10.11). Depth profiles of temperature, salinity and fluorescence were recorded using a SBE 911plus CTD system (Sea-Bird Scientific, WA, USA) and used to identify water masses and to collect water for downstream analyses. Samples (25-50 L) for molecular analyses were taken between depths of 1 and 1,000 m (Supplementary Table S1), filtered onto 0.22 µm pore size Millipore® Sterivex filters (Merck-Millipore, MA, USA) and immediately frozen at −80°C. In total 50 samples (epipelagic zone; 0–200 m; $n = 28$ and mesopelagic zone; 200–1,000 m; $n = 22$) were used for molecular analysis. Further cruise and sampling details are described in Paulsen et al. (2016) and Wilson et al. (2017), respectively.

Flow Cytometry

The abundance of prokaryotes was detected from samples collected at 18 stations from 11 depths (1, 5, 10, 20, 30, 50, 100, 200, 500, 750, and 1,000 m) during 5 cruises using an Attune® Acoustic Focusing Flow Cytometer (Applied Biosystems by Life technologies, CA, USA) with a syringe-based fluidic system and a 20 mW 488 nm (blue) laser. First, samples were fixed with glutaraldehyde (0.5% final conc.) and incubated at 4°C for a minimum of 30 min, frozen in liquid nitrogen and stored at −80°C. For analysis, samples were diluted with 0.2 µm filtered TE buffer (Tris 10 mM, EDTA 1 mM, pH 8), stained with a green fluorescent nucleic acid dye (SYBR Green I; Molecular Probes, Eugene, Oregon, USA) and kept for 10 min at 80°C in a water bath (Marie et al., 1999). A minimum of 100 µL was counted at a low flow rate of 25 µL min^{-1} and prokaryotes were discriminated on a biparametric plot of green florescence vs. red florescence.

Ammonium Measurements

Concentrations of NH_4^+ were determined fluorometrically from frozen samples (4 mL) using orthophthadialdehyde according to the protocol by Holmes (1999). The method was adapted for microplate readings following (Poulin and Pelletier, 2007) and samples were analyzed on a 2300 EnSpire™ Multilabel Plate Reader (PerkinElmer, Finland). A 0.1 M ammonium chloride stock solution was used to prepare standard curves (0.1, 0.3, 0.6, 1, 2 µM) with correlation coefficients ≥0.986.

Nucleic Acids Extraction and Amplification for Amplicon Sequencing

DNA and RNA from Sterivex filters were extracted using the AllPrep DNA/RNA Mini Kit (Qiagen, Hilden, Germany). Details regarding RNA processing can be found in Wilson et al. (2017). In short, 10 ng RNA was treated with the DNA-free DNA Removal kit (Invitrogen, CA, USA) and subsequently reverse transcribed using the SuperScript III First-Strand Synthesis System for RT-PCR (Invitrogen), following the manufacturer's instructions. DNA was amplified using a two-step nested PCR approach with primers 519F and 806R (Supplementary Table S2) targeting both the archaeal and the bacterial 16S rRNA gene V4 hypervariable region. During the first step, triplicate samples were amplified in reaction volumes of 20 µL, comprising 10 ng DNA, 10 µL HotStarTaq Master Mix (Qiagen), 0.5 µM of each primer and nuclease-free water. PCR reaction conditions were as follows: initial denaturation of 15 min at 95°C, followed by 25 cycles of 95°C for 20 s, 55°C for 30 s and 72°C for 30 s and a final extension

step of 72°C for 7 min. Triplicate PCR products were pooled and purified using the DNA Clean & Concentrator-5 kit (Zymo Research Corporation, CA, USA). 10 ng of pooled PCR product was used for the second PCR step, in a reaction volume of 50 μL together with 25 μL HotStarTaq Master Mix, 0.5 μM of each nested primer (containing a unique eight-nucleotide barcode) and nuclease-free water. PCR reaction conditions were as follows: initial denaturation of 15 min at 95°C, followed by 15 cycles of 95°C for 20 s, 62°C for 30 s, 72°C for 30 s and a final extension step of 72°C for 7 min. Final PCR products were purified using Agencourt AMPure XP Beads (Beckman Coulter Inc., CA, USA) and prepared for sequencing by pooling the samples in equimolar amounts. The quality and concentration of the amplicon pool were assessed by agarose gel electrophoresis and a Qubit 3.0 Fluorometer, respectively. Libraries were sequenced at the Norwegian Sequencing Centre (Oslo, Norway) using their Illumina MiSeq platform (MiSeq Reagent Kit v2, Illumina, CA, USA). Sequencing data are available at the European Nucleotide Archive (ENA) under study accession number PRJEB23129. The primers (519F-806R) used in this study have been shown to have a low affinity for the SAR11 cluster, which can result in overestimation of other prokaryotic groups (Apprill et al., 2015).

16s rRNA Gene Sequence Analysis

Paired-end sequences were processed using various bioinformatic tools incorporated in the QIIME software environment (Caporaso et al., 2011), as described in Paulsen et al. (2016). Briefly, FASTQ files were quality end-trimmed, merged and prokaryotic OTUs were selected at a sequence similarity threshold of 97% and taxonomy assigned using the Silva 111 reference database (Quast et al., 2013). A total of 5,995,334 sequences were retrieved from high-throughput sequencing of the 16S rRNA gene V4 hypervariable region from DNA across fifty samples from five cruises. After removal of singletons, unassigned OTUs and chloroplast reads, sequences were rarefied to 10,000 reads per sample, with a total of 24,723 unique OTUs (63.1% singletons) at 97% sequence similarity. Bray–Curtis resemblance and ANOSIM statistical analysis were performed using PRIMER-E (Version 6; Quest Research Limited, Auckland, NZ).

Quantitative Real-Time PCR (qPCR)

All qPCR assays were run in triplicates on a C1000 Thermocycler (BioRad, CA, USA). The following qPCR reaction mixture was used: 10 μl Fast EvaGreen® qPCR Master Mix (Biotium, Inc., Hayward, CA, USA), 0.5 μM final concentration of each primer, 1 μL template DNA (corresponding to 1 ng of environmental DNA) and water were added to a final volume of 20 μL. All qPCR reactions were performed in white 96 well plates (BioRad). Thaumarchaeota 16S rRNA genes were quantified using the Thaumarchaeota specific forward primer Thaum-494F (Hong et al., 2015) and an archaeal universal primer ARC917R (Loy et al., 2002). This primer pair was suggested to better target the Thaumarchaeota and showed a higher affinity (96%) *in silico* to Marine Group I Archaea than previously used primer pairs (Hong et al., 2015). qPCR reaction conditions were as follows: initial activation for 2 min at 95°C, followed by 35 cycles of amplification, including denaturation at 95°C for 30 s, annealing at 55°C for 30 s, extension at 72°C for 30 s and a final extension step of 10 min at 72°C. The fluorescence was measured at the end of each cycle and a melting curve obtained from 65 to 95°C, with increments of 0.2°C. Ten-fold dilutions ranging from 1.1×10^8 to 1.1×10^3 copies of environmental Thaumarchaeota 16S rRNA gene were used as a quantification standard. Efficiencies for all qPCR reactions ranged from 83 to 84% with constant R^2-values of 0.998. To calculate gene copies per mL, the copy number per ng was multiplied by the DNA concentration per mL (based on flow cytometer counts and the assumption that one prokaryote contains 3 fg of DNA; Fuhrman and Azam, 1982; Jeffrey et al., 1996).

Phylogenetic Analysis of amoA and 16s rDNA Clone Libraries

A total of 10 MicroPolar samples from five stations representative of all five water masses were selected for *amoA* functional gene amplification. Each time point comprised both a surface and deep sample, excluding surface samples from the summer season (May and August), due to very low *amoA* abundances. Overall, eight DNA and two RNA samples were used for this analysis. The two RNA samples were from the same depths as the DNA samples from the November cruise and are included as an indicator of the active transcription of *amoA* mRNA. Amplification was performed using archaeal *amoA* primers (Supplementary Table S2) targeting a 635 bp gene fragment using the protocol of Francis et al. (2005) and 30 amplification cycles (iCycler, Bio-Rad, CA, USA). These primers have been widely used, but have been shown to underestimate *amoA* abundance in surface water samples (Tolar et al., 2013). PCR products were purified using the ExoSap-IT kit (Applied Biosystems) and subsequently cloned with the Qiagen PCR Cloning Kit (Qiagen) following manufacturer instructions. A total of 242 clones from all 10 samples were selected, and sequenced in-house at the sequencing facility of the University of Bergen (http://www.uib.no/en/seqlab). In order to obtain the 16S rRNA gene fragments for phylogenetic analysis, the same steps were followed as for the *amoA* genes; amplification was performed using an Archaea-specific forward primer in combination with a universal prokaryotic reverse primer resulting in amplicons of 1481 bp length (Supplementary Table S2). PCR reaction conditions were similar to those described before, with the exception of the annealing temperature, which was adjusted to 52°C. All *amoA* gene sequences from this study have been deposited at ENA under study accession number PRJEB23151. The three full length sequences of the 16S rRNA gene have been deposited at NCBI under GenBank accession numbers MG238502-MG238504.

Sequencing of *amoA* clones resulted in a total of 230 high quality sequences. This dataset was combined with an additional 254 *amoA* sequences (220 bp gene fragment) from a recent study on archaeal ammonia oxidizing ecotypes in the Atlantic Ocean (Sintes et al., 2016). This combined dataset was used to define OTUs at 97% sequence similarity using the *de novo* uclust (Edgar, 2010) OTU clustering method in QIIME, using

default parameters. In total, 189 OTUs were identified and used for phylogenetic analysis based on multiple alignments of *amoA* OTUs using MUSCLE (Edgar, 2004) with default parameters. The phylogenetic tree was inferred using the neighbor–joining method (Saitou and Nei, 1987) with 1000 bootstrap replicates. The retrieved tree was viewed using Evolview v2 (He et al., 2016).

The same strategy was implemented for Thaumarchaeota16S rRNA gene sequences. In order to include the Illumina amplicon reads, all sequences used (clonal or otherwise) for the phylogenetic analysis were trimmed to a size of 268 bp. A total of 1256 Thaumarchaeota sequences, including the three most abundant Thaumarchaeota OTUs from our amplicon data set, three full length 16S rRNA Sanger-sequenced reads and 1242 environmental sequences from the Arctic Ocean, the Atlantic Ocean, the Northeast Pacific, the North Sea and Gulf of Mexico were used to define OTUs at 97% similarity (Agogué et al., 2008; Bale et al., 2013; Tolar et al., 2013; Wright, 2013; Ijichi and Hamasaki unpublished). The resulting 23 OTUs were used for phylogenetic analysis as described above. We calculated the relative abundance of these OTUs in sets of samples from depths below or above 100 m.

RESULTS

Hydrography and Seasonal Thaumarchaeota Abundance

We used 16S rRNA gene sequencing and qPCR analyses to determine the relative and absolute abundance of Thaumarchaeota in samples taken during five cruises throughout the year in the Arctic Ocean off the western coast of Svalbard (**Figure 1**). Throughout the sampling period, Thaumarchaeota represented up to 73% (62% by qPCR) of the prokaryotic community. The relative abundance of Thaumarchaeota varied with both depth and season. Surface samples from the epipelagic (1–200 m) zone showed clear seasonal changes in Thaumarchaeota relative abundance. During the winter months relative abundance was high (44% ±15), while it was low during the summer season (1.4% ±1.4). In contrast, Thaumarchaeota relative abundance in the deep mesopelagic samples (200–1,000 m) was relatively high (38% ±11) throughout the entire year (**Figure 1B**).

Although total prokaryote abundance strongly increased during the summer months, absolute Thaumarchaeota abundance of up to 3.8×10^5 cells mL^{-1} (January, 1 m, station B8) was highest during the winter months (**Figures 1B**, **2**). Relative Thaumarchaeota abundance values from 16S rRNA gene sequencing and calculated values from qPCR were comparable, while the Illumina derived relative abundance was on average 14% higher (Supplementary Figure S3). We identified the three most abundant OTUs, which constituted on average 76% ±11 of the total Thaumarchaeota community in all samples. The same three OTUs were identified from 16S rRNA sequencing of reverse-transcribed total RNA, suggesting an active role in the prokaryotic community (Wilson et al., 2017).

Phylogenetic analysis of 16S rRNA genes, which included the three OTUs, and 1,242 environmental sequences from the Arctic Ocean, the Atlantic Ocean, the Northeast Pacific, the North Sea and Gulf of Mexico, showed that the three most abundant OTUs from our study are also represented in other environments. The OTUs representing our three most abundant Thaumarchaeota types comprise 92% of all sequences included in the analysis. The phylogenetic tree shows that all OTUs are related to the cultured strain *Nitrosopulimus maritimus* SCM1 and that they divide into two subgroups representing predominantly samples of either epipelagic or mesopelagic origin (Supplementary Figure S1). While OTUs affiliated to the surface group can be found in samples from both the epipelagic and mesopelagic zones, OTUs from the deep group were exclusively from mesopelagic samples indicating a depth-dependent distribution pattern as documented before.

Thaumarchaeota Abundance Patterns Correlated with Specific Water Masses

The profiles in **Figures 2A–D** illustrate the differences in abundance of Thaumarchaeota OTUs for the five cruises and in contrasting stations with varying water masses. Overall, similar presence/absence patterns of the three most abundant OTUs can be observed throughout all cruises, which are partly connected to depth (**Figure 2**). This includes OTU 81053 and OTU 201889 being most abundant in the surface and deep waters, respectively. In order to identify a distribution pattern for these OTUs, we separated all samples, according to their depth in epipelagic and mesopelagic groups, as has been done previously (**Figure 4A**). The OTU abundance pattern between the two water zones was significantly different, as shown by an ANOSIM analysis ($R = 0.32$; $p = 0.001$). Whilst OTU 81053 was most abundant in epipelagic waters (62–88%), it was found to be highly variable in samples from the mesopelagic zone (9.8–71%), thus referred to as "surface OTU". In contrast, OTU 201889 was barely detectable in epipelagic samples (<0.5%) and of varying abundance (0.2–51%) in mesopelagic samples, hence was referred to as "deep OTU". The third most abundant OTU (0.2–19%) was detected in variable abundance in both epipelagic and mesopelagic waters and is referred to as "middle OTU". All other Thaumarchaeota OTUs were grouped into those three OTU types, according to their abundance pattern.

In order to identify Thaumarchaeota distribution patterns throughout the entire sample set, a cluster analysis using Bray-Curtis similarities was performed (**Figure 3** and Supplementary Figure S4). The cluster analysis shows five groups, which are in co-occurrence with the five physical water masses observed in the study area (exceptions marked in red). This co-occurrence pattern was observed over the entire sampling period and the Thaumarchaeota abundance pattern in January in AW samples was highly similar to AW samples from March, May August and November (**Figure 3**). Therefore grouping the samples into the water mass groups revealed a more distinct distribution pattern of the three most abundant OTUs, shown to be significantly different by an ANOSIM analysis ($R = 0.63$; $p = 0.001$) (**Figure 4B**). The different water mass groups include samples from varying depths and some from both epipelagic and mesopelagic zones, as indicated in **Figure 4B**.

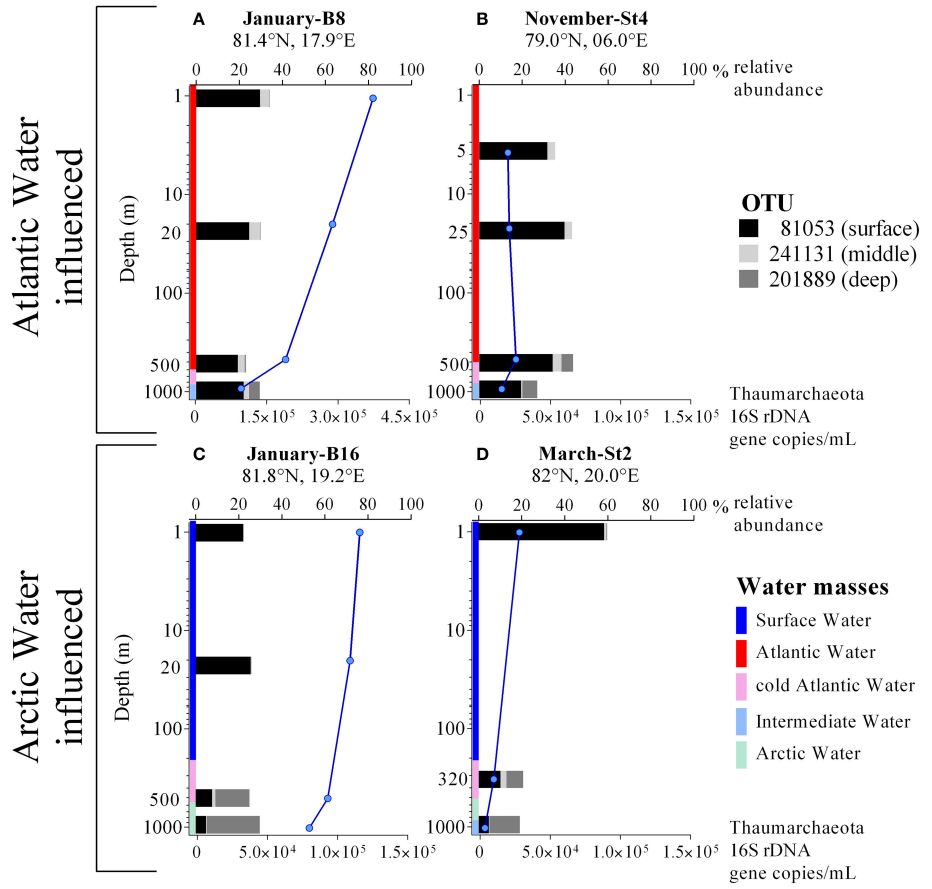

FIGURE 2 | (A–D) Profiles of Thaumarchaeota abundance (blue lines) determined by qPCR of 16S rRNA genes and Thaumarchaeota relative abundance (black, gray, light gray bars; in % of total 16S rRNA Illumina amplicons) from four different stations, where either Atlantic or Arctic water masses were dominating. Notice different scales on the x-axis (lower x-axis for qPCR derived Thaumarchaeota gene copies per mL; upper x-axis for Thaumarchaeota relative abundance from Illumina sequencing data). Colors indicate the water mass profile. Note that the y-axis is in logarithmic scale.

The influence between water mass and Thaumarchaeota OTU abundance was particularly noticeable at the two stations in January (**Figures 2A,C**). Only 43 km apart, the two stations showed very different Thaumarchaeota abundance patterns at comparable depths, connected to the discriminating water masses observed at the stations. These OTU abundance patterns seen in January were also observed at other stations during other sampling months. Over the entire sampling period, the three OTUs showed distinctive changes in abundance in the five water masses. The surface OTU showed highest abundance in SW (84% ± 3.1) and declined in the other water masses down to 14% ± 3.6 in ArW. An opposite trend was observed for the deep OTU with highest abundance in ArW (40%±10) declining in IW (23% ± 4.7), cAW (9.2% ± 2.5), AW (1.5% ± 1.7), and lowest in SW (0.2% ± 0.2). The highest abundance of the middle OTU was found in AW (11% ± 4.0) and declining in the other modified Atlantic water masses (cAW: 6.3% ± 0.2; IW: 4.0% ± 2.8). In the SW and ArW the middle OTU was underrepresented (1.7% ± 1.4; 1.3% ± 1.4).

We tested whether the changes in relative abundance of the three OTUs were significantly correlated with the different water masses and other environmental factors. The best fit for linear regressions was achieved when Thaumarchaeota abundance was plotted against water mass and not depth. All three OTUs showed distinct seasonally reoccurring abundance patterns that correlate with the distinct water masses in the area. OTU abundance either

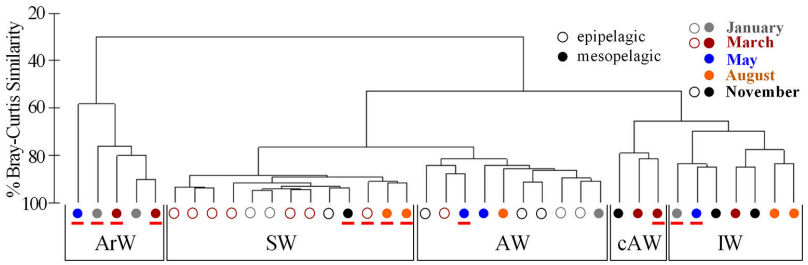

FIGURE 3 | Hierarchical cluster analysis of Bray-Curtis similarities, based on the diversity of Thaumarchaeota sequences from Illumina amplicon sequencing of 16S rRNA genes, illustrating the distribution of samples into five groups. These five groups are labeled according to water mass specificities of the samples within the groups (ArW, Arctic Water; SW, Surface Water; AW, Atlantic Water; cAW, cold Atlantic Water; IW, Intermediate Water). Samples with a mismatch between their associated water mass group and the physical water mass of their sampling origin are marked with a red line. The sampling month is given by colors. Samples were further distinguished according to depth, with open circles for epipelagic samples (0–200 m; $n = 16$) and filled circles for mesopelagic samples (200–1,000 m; $n = 22$).

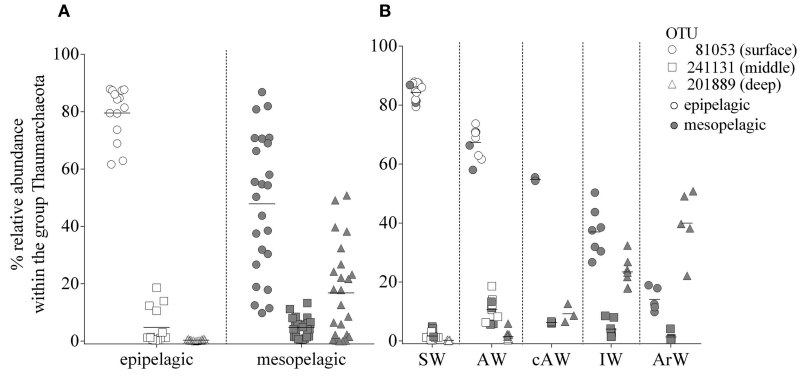

FIGURE 4 | (A) Relative abundance of the three most abundant Thaumarchaeota OTUs. Samples were divided according to their sampling origin in epipelagic (open symbols; 0–200 m; $n = 16$) and mesopelagic (filled symbols; 200–1,000 m; $n = 22$) zones. **(B)** Same data as in **(A)**, grouped according to assigned water masses based on sample similarities illustrated in **Figure 3**. ArW, Arctic Water; SW, Surface Water; AW, Atlantic Water; cAW, cold Atlantic Water; IW, Intermediate Water.

decreased (surface and middle OTU, $R^2 = 0.96$; $p < 0.0001$ and $R^2 = 0.6$; $p < 0.0001$) or increased (deep OTU, $R^2 = 0.84$; $p < 0.0001$) from SW or AW toward deeper water masses, such as cAW, IW, and ArW (**Figure 4B**). Environmental factors were correlated with some OTUs but not all three together. For example, both the middle OTU and surface OTU were positively (Pearson's r, $r = 0.51$; $p < 0.0014$) or negatively (Pearson's r, $r = -0.51$; $p < 0.0012$) correlated respectively to salinity, whilst the deep OTU was not correlated at all. Temperature was also correlated with abundance of the middle OTU (Pearson's r, $r = 0.69$; $p < 0.0001$), but not the other OTUs. None of the three OTUs was correlated with ammonium concentration or sampling month.

Analysis of amoA Gene Phylogeny

To answer whether there was a similar Thaumarchaeota distribution pattern on the functional gene level, we analyzed the distribution of the gene encoding for amoA. A single station for each sampling month (comprising both a surface and deep sampling point) was chosen, excluding summer season surface samples with the low Thaumarchaeota abundance. These eight samples represented all different water masses encountered during the five cruises and resulted in 230 *amoA* sequences. The genetic diversity of these MicroPolar sequences, combined with published sequences from the entire Atlantic, is illustrated in Supplementary Figure S2 and revealed the six main subclusters previously reported (Sintes et al., 2016). A simplified version of this phylogenetic tree is shown in **Figure 5**. MicroPolar sequences can be found both in subclusters 1 and 2 (representing sequences from WCA) and 3–6 (excluding 4; representing sequences from WCB). In total 15 (5 with >1 sequence) new *amoA* OTUs representing 50 MicroPolar sequences were identified. The majority of our Arctic *amoA* sequences affiliated to subclusters 2 and 6. The deep subcluster 6 represented sequences mostly from mesopelagic samples, while sequences from subcluster 2 were from both epipelagic and mesopelagic MicroPolar samples. The

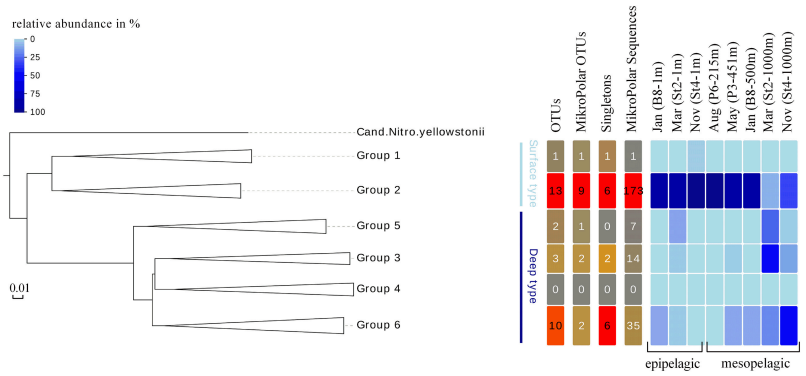

FIGURE 5 | Left panel Phylogenetic tree of 189 *amoA* OTUs at 97% sequence identity, representative of the genetic diversity of *amoA* clades 1-6 in reference samples (254 sequences) and in 10 MicroPolar samples (230 sequences). The colored lines indicates the grouping of the six *amoA* clusters in surface (light blue) and deep (dark blue) type. **Right panel** Distribution of OTUs, OTUs which only consist of MicroPolar sequences, OTUs that only consist of one sequence and MicroPolar sequences within the six *amoA* clusters. Heat map, in shades of blue, displaying the relative abundance of OTUs at each analyzed station and grouped by sampling depth.

heat map (illustrating the relative abundance pattern both of the WCA and WCB *amoA* sequences) shows only two samples (Mar-St2-1,000 m and Nov-St4-1,000 m) where *amoA* OTUs were more abundant in the deep WCB group than the surface WCA group (**Figure 5**). Other mesopelagic samples from January, May and August comprised mainly sequences from the WCA group. We compared the 10 samples from the *amoA* data set with our 16S rRNA gene Illumina amplicon data as we observed a similar pattern between the deep and surface OTU types (**Figure 6**). The different ratio of contrasting 16S rRNA gene surface/deep types was highly similar to *amoA* gene WCA/WCB types in all samples. For both genes the observed pattern was co-occurring with different water masses.

DISCUSSION

Thaumarchaeota are ubiquitous in marine environments, but a temporal pattern, where abundances decrease significantly during summer seasons, has been described for the polar regions (Massana et al., 1998; Murray et al., 1998; Church et al., 2003; Alonso-Sáez et al., 2008; Christman et al., 2011). We detected high Thaumarchaeota abundances in winter surface waters, contributing up to 38% to the total prokaryotic community. High Thaumarchaeota abundance in surface waters have been reported before, with maximum values of 64% in the Antarctic (Kalanetra et al., 2009) or up to 40% in the Northern Gulf of Mexico (Tolar et al., 2013). Measurements of absolute Thaumarchaeota abundance in other parts of the Arctic Ocean (Amundsen Gulf region) showed similar high gene copy numbers (10^5 16S rRNA gene copies mL^{-1}) in winter surface water as observed in our study. Our data confirmed a cyclical shift in Thaumarchaeota abundance in surface waters, showing a strong increase in winter months and a decline in summer months (**Figure 1B**). At the taxonomic level of OTUs, we observed a distinct distribution of different Thaumarchaeota ecotypes that were not directly correlated with their epipelagic or mesopelagic sampling origin. These ecotypes rather seemed to occur according to different water masses, representing a possibly important (yet often neglected) environmental factor as the main driver of Thaumarchaeota distribution. This study better defines how water masses may influence the abundance of Thaumarchaeota in the ocean. Water masses combine by definition a set of measurable environmental parameters, extending the three, including salinity, density and temperature used to define them, as well as factors like origin and history. Due to this complexity it remains unclear which environmental parameter is driving the distribution of Thaumarchaeota OTUs. However, the results of this study point toward a more complex mechanism of Thaumarchaeota distribution than, as previously reported, depth or ammonium concentration could explain.

Thaumarchaeota Abundance Patterns Correlated with Specific Water Masses

The 16S rRNA gene sequence data showed that the surface Thaumarchaeota group is dominated by a single OTU, which has previously been found both in the Arctic and Antarctic Oceans (Arctic 70%: Alonso-Sáez et al., 2012; Antarctic 83%: Kalanetra et al., 2009; Grzymski et al., 2012). The most abundant OTU in our data set was predominantly identified in surface samples, comprising up to 88% of the Thaumarchaeota population and sharing 98% identity with the same OTU from the Arctic and Antarctic studies. As a result of the repeated sampling campaigns of depth profiles over the entire polar year, we detected the reoccurrence of this OTU in the winter surface waters and decreasing abundance with depth. Interestingly, another single OTU outcompeted the surface OTU and was dominant in our

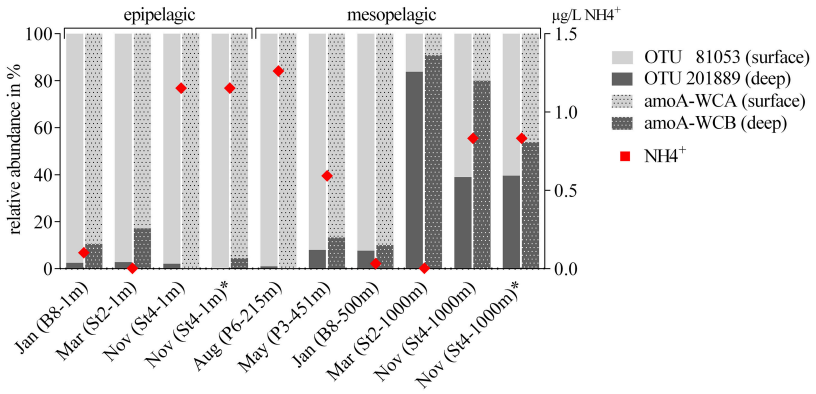

FIGURE 6 | Comparison of the relative abundance of Thaumarchaeota OTUs (16S rRNA gene) and the functional gene for ammonia oxidation (*amoA*). Thaumarchaeota OTUs are divided into the two most abundant sequences (OTU 81053 and OTU 201889), with highest relative abundance at the surface or the deep, respectively. *amoA* OTUs were divided into the two depth depending clusters WCA (surface) and WCB (deep). One station for each sampling month with a surface and deep sampling point were chosen (note, due to very low abundances, summer surface samples are not included), including all five water masses encountered during the five cruises. Ammonium concentrations at each sampling point are visualized as red diamonds (0 = below the detection limit).

mesopelagic samples. However, depth alone could not explain the abundance pattern. Our data indicates a clear distribution and hence niche diversification of Thaumarchaeota ecotypes according to discriminating water masses in this area (**Figure 4**). A distinct biogeography for Thaumarchaeota in the ocean has been described before, but abundance patterns of different Thaumarchaeota groups were only connected to depth-specific water profile characteristics (Francis et al., 2005; Beman et al., 2008; Sintes et al., 2013, 2016). However, there have been studies where shifts in marine microbial community composition were correlated to differences in physicochemical water mass parameters (Agogué et al., 2008; Galand et al., 2009; Baltar et al., 2016).

For the first time, we have made a causal link between the abundance patterns of different Thaumarchaeota ecotypes to water masses entering the Arctic Ocean. Thaumarchaeota OTUs group primarily into three clusters, with each group having one OTU being most abundant. These three OTUs, putatively defined as surface, middle and deep OTUs, seemingly exhibit a certain niche specificity, as they vary in abundance best explained by water mass distribution and not, as otherwise suggested, depth or ammonium concentration. By applying this principle to our data, twelve out of thirty-eight samples were revised with regard to their physicochemical water mass definition. These revisions however, can be used to explain the hydrographical system in our study area in a more concise way.

For example, according to the physicochemical water mass information, 1,000 m samples taken from stations in the Nansen Basin were different, either assigned to ArW or IW. However, the Thaumarchaeota abundance pattern was highly similar suggesting that they all originated from ArW, which is different from other deep water masses. Based on the molecular data, we therefore conclude that the water mass at 1,000 m throughout the Nansen Basin is ArW. We did not see this Thaumarchaeota pattern in all of our 1,000 m samples, but only from the stations closest to the deep Nansen Basin, indicating that this OTU was not depth-specific, but rather water mass-specific. Additionally, the absence of the surface OTU is indicative that this water mass did not result from mixing of SW or incoming AW, but rather originated from the deep central Arctic Ocean. Another, co-occurrence between an OTU abundance pattern and water mass was found for AW. By following the changes in abundance of the middle OTU (which correlated with higher salinity and warmer sea temperatures) in particular, we could trace the inflow and modification of AW. The surface OTU on the other hand had highest abundances in SW samples, which is influenced by ice melt. This suggests that the microbial assemblage can provide information on the origin of the water masses, in addition to the physical parameters. It further highlights the possibility that water mass definition can go beyond pure physical parameters and by including molecular microbiological data, such as OTU distribution patterns, presented in this study, explain better the origin and development of water masses (Fuhrman and Steele, 2008; Galand et al., 2009; Djurhuus et al., 2017).

The differences in Thaumarchaeota OTU abundance also reveal that water masses act as clearly separated boundaries for the distribution of marine prokaryotes, while we also defined water masses which seemed to be the result of mixing or dilution processes. On the one hand water masses can be considered barriers to microbial dispersal and on the other hand influencing community composition by physical processes like mixing (Agogué et al., 2011; Acha et al., 2015; Djurhuus et al., 2017). This was especially apparent in January, where two stations, just 43 km apart, showed a totally different abundance pattern for the three defined Thaumarchaeota ecotypes throughout the depth profile down to 1,000 m, while overall Thaumarchaeota abundance was

comparable at both stations (**Figures 2A,C**). This is similar to a phenomenon observed at the Subtropical Frontal zone, where community composition of surface water samples was highly different for samples taken only 7 km apart at an oceanic front (Baltar et al., 2016).

Oceanic frontal zones and ocean currents have been considered to be barriers of dispersal (Srivastava and Kratina, 2013). This affects to a high degree the biogeography of microbial communities and is adding a new element in contrast to the idea of strong regional environmental factors structuring the marine communities (Carr et al., 2003). Our data suggests a dual role of water masses in shaping Thaumarchaeota community composition. They both limit and facilitate dispersal of Thaumarchaeota OTUs, which dominate in specific water masses and are distributed when water mass are mixed.

16s rRNA and amoA Gene Phylogeny and Global Relevance

In our study, the deep OTU was highly abundant in samples up to 500 m, but not in shallower depths (**Figure 4**). The 16S rRNA gene sequence was the most abundant sequence (68%) of samples taken below 100 m, in a global dataset of 1256 marine Thaumarchaeota sequences (Supplementary Figure S1). The deep OTU sequence was not found in any samples collected above 100 m, whilst the middle OTU (phylogenetically in the same cluster as the deep OTU) was found both in epipelagic and mesopelagic samples. The surface OTU was found in highest abundance in the Arctic surface water in our data set. This same OTU has been recorded in high abundance in surface waters globally and seems to be universally successful under different conditions, having been found both at the Equator and in the Arctic. In fact, none of the three most abundant OTUs in our data set was Arctic-specific and all have been found in marine waters around the globe. Whether those three OTUs are indeed universally successful remains unclear, as the 16S rRNA gene with an OTU definition of 97% similarity might not be suitable to reveal functional ecotype variation.

The distribution of different *amoA* genes was investigated to see if we could identify a similar water mass-dependent pattern as for the 16S rRNA gene data. The relative distribution of the two AOA groups, WCA (surface) and WCB (deep), was found to correspond with the distribution of surface and deep OTUs based on 16S rRNA gene data. By using independent PCR approaches it is however not possible to directly associate the 16S rRNA and *amoA* genotypes, but their observed grouping, co-occurring with different water masses may indicate that the ecotypes defined by the 16S rRNA gene sequence could be functionally different. One hypothesis for this functional difference is the presence of urease genes (*ureC*) in the deep WCB clusters (Swan et al., 2011; Alonso-Sáez et al., 2012; Qin et al., 2014; Tolar et al., 2016). We did not measure the abundance of *ureC* genes in our samples, but it has been shown that Thaumarchaeota ecotypes from Arctic deep waters have a higher abundance of the *ureC* gene than surface groups (Alonso-Sáez et al., 2012). The genomic differences we observe between the surface and deep *amoA* types might be an indicator for evolutionarily different physiological strategies, including the utilization of urea by the deep WCB (**Figure 5**).

Identifying environmental drivers, which might explain the proportional abundances seen in this study as well as several other studies, will ultimately help understand the ecological role of the different AOA types. Our data indicated a distribution which corresponds to water masses rather than strict depth dependencies. We measured ammonium concentrations at the sampled stations and did not see a correlation between ammonium availability and WCA to WCB (HAC- to LAC-*amoA*) ratio, despite previous reports (Kirchman et al., 2007; Christman et al., 2011; Sintes et al., 2013, 2015, 2016; Santoro et al., 2017). Environmental parameters such as salinity (Francis et al., 2005; Abell et al., 2010), nitrite (Herfort et al., 2007), dissolved oxygen (Santoro et al., 2008), light (Mincer et al., 2007; Merbt et al., 2012), reactive oxygen species (Tolar et al., 2016), and temperature (Biller et al., 2012) have been suggested to regulate Thaumarchaeota community composition. It was further speculated that depth (Biller et al., 2012; Sintes et al., 2013, 2015), which is often correlated with Thaumarchaeota distribution, is a collection of other environmental factors following a gradient (Santoro et al., 2017). We expand that idea by highlighting that water masses, being by definition a set of several environmental parameters, are important for the distribution of Thaumarchaeota OTUs. Ultimately, it is therefore a challenge to comprehensively identify a single primary driver of AOA distribution.

CONCLUSION

We observed a co-occurrence of the three dominant Thaumarchaeota OTUs with water masses at the inflow to the Arctic Ocean. This supports the theory that water mass history to a great extent defines the mesopelagic microbial community structure (Galand et al., 2009; Reinthaler et al., 2010). The Thaumarchaeota pattern we observed was possibly a combination of several factors; water mass characteristics seemed to be a significant factor, influencing the distribution of the three most abundant OTUs; additionally, physical mixing or dilution of water masses might be another important factor explaining the differences in abundance of the three Thaumarchaeota ecotypes. Our study highlights the importance of water masses in influencing Thaumarchaeota population distributions. As water mass distributions will change in a future Arctic Ocean, due to processes such as increased sea ice melting (Comeau et al., 2011) or "Atlantification" (Polyakov et al., 2005; Holland et al., 2006; Walczowski and Piechura, 2006), so will the Thaumarchaeota distribution change. Further research is needed to investigate possible ecological implications of such scenarios.

AUTHOR CONTRIBUTIONS

LØ and GB: led the planning of the study; OM, HA, AR, and LØ: collected and processed samples; In addition, BW: assisted on designing bioinformatic analysis strategies and helped improving the language and grammar of the manuscript; MP: performed

flow cytometric analysis; OM, BW, AR and LØ: analyzed data, OM prepared figures and tables and wrote the paper; All authors contributed to discussion and interpretation of the data and writing the paper.

FUNDING

This study is part of the project "MicroPolar" (RCN 225956) funded by the Norwegian Research Council, which organized the cruises in March and November. The "CarbonBridge" project (RCN 226415) organized the cruises in January, May, and August where thankfully we could participate. Parts of the study were funded by the project "Microorganisms in the Arctic: Major drivers of biogeochemical cycles and climate change" (RCN 227062).

ACKNOWLEDGMENTS

We would like to thank crew members of the Norwegian Research Vessels RV Helmer Hanssen and RV Lance for their assistance in sampling expeditions and all colleagues in the UiB Marine Microbiology group and collaborators abroad who contributed to the research effort. A special thanks to Jean-Éric Tremblay for providing ammonium measurements.

SUPPLEMENTARY MATERIAL

The Supplementary Material for this article can be found online at: https://www.frontiersin.org/articles/10.3389/fmicb.2018.00024/full#supplementary-material

REFERENCES

Abell, G. C., Revill, A. T., Smith, C., Bissett, A. P., Volkman, J. K., and Robert, S. S. (2010). Archaeal ammonia oxidizers and nirS-type denitrifiers dominate sediment nitrifying and denitrifying populations in a subtropical macrotidal estuary. *ISME J.* 4, 286–300. doi: 10.1038/ismej.2009.105

Acha, E. M., Piola, A., Iribarne, O, and Mianzan, H. (2015). *Biology of Fronts*. Cham: Springer.

Agogué, H., Brink, M., Dinasquet, J., and Herndl, G. J. (2008). Major gradients in putatively nitrifying and non-nitrifying archaea in the deep North Atlantic. *Nature* 456, 788–791. doi: 10.1038/nature07535

Agogué, H., Lamy, D., Neal, P. R., Sogin, M. L., and Herndl, G. J. (2011). Water mass-specificity of bacterial communities in the North Atlantic revealed by massively parallel sequencing. *Mol. Ecol.* 20, 258–274. doi: 10.1111/j.1365-294X.2010.04932.x

Alonso-Sáez, L., Sánchez, O., Gasol, J. M., Balagué, V., and Pedrós-Alio, C. (2008). Winter-to-summer changes in the composition and single-cell activity of near-surface Arctic prokaryotes. *Environ. Microbiol.* 10, 2444–2454. doi: 10.1111/j.1462-2920.2008.01674.x

Alonso-Sáez, L., Waller, A. S., Mende, D. R., Bakker, K., Farnelid, H., Yager, P. L., et al. (2012). Role for urea in nitrification by Polar Marine *Archaea*. *Proc. Natl. Acad. Sci. U.S.A.* 109, 17989–17994. doi: 10.1073/pnas.1201914109

Apprill, A., McNally, S., Parsons, R., and Weber, L. (2015). Minor revision to V4 REgion SSU rRNA 806R gene primer greatly increases detection of SAR11 bacterioplankton. *Aq. Microb. Ecol.* 75, 129–137. doi: 10.3354/ame01753

Bale, N. J., Villanueva, L., Hopmans, E. C., Schouten, S., and Sinninghe Damsté, J. S. (2013). Different seasonality of pelagic and benthic thaumarchaeota in the North Sea. *Biogeosciences* 10, 7195–7206. doi: 10.5194/bg-10-7195-2013

Baltar, F., Currie, K., Stuck, E., Roosa, S., and Morales, S. E. (2016). Oceanic fronts: transition zones for bacterioplankton community composition. *Environ. Microbiol. Rep.* 8, 132–138. doi: 10.1111/1758-2229.12362

Beman, J. M., Popp, B. N., and Francis, C. A. (2008). Molecular and Biogeochemical evidence for ammonia oxidation by marine crenarchaeota in the gulf of California. *ISME J.* 2, 429–441. doi: 10.1038/ismej.2007.118

Biller, S. J., Mosier, A. C., Wells, G. F., and Francis, C. A. (2012). Global biodiversity of aquatic ammonia-oxidizing archaea is partitioned by habitat. *Front. Microbiol.* 3:252. doi: 10.3389/fmicb.2012.00252

Caporaso, J. G., Lauber, C. L., Walters, W. A., Berg-Lyons, D., Lozupone, C. A., and Turnbaugh, P. J., et al. (2011). Global patterns of 16S rRNA diversity at a depth of millions of sequences per sample. *Proc. Natl. Acad. Sci. U.S.A.* 108(Suppl. 1), 4516–4522. doi: 10.1073/pnas.1000080107

Carr, M. H., Neigel, J. E., Estes, J. A., Andelman, S., Warner, R. R., and Largier, J. L. (2003). Comparing marine and terrestrial ecosystems: implications for the design of coastal marine reserves. *Ecol. Appl.* 13, 90–107. doi: 10.1890/1051-0761(2003)013[0090:CMATEI]2.0.CO;2

Christman, G. D, Cottrell, M. T., Popp, B. N., Gier, E,., and Kirchman, D. L. (2011). Abundance, diversity, and activity of ammonia-oxidizing prokaryotes in the coastal Arctic Ocean in summer and winter. *Appl. Environ. Microbiol.* 77, 2026–2034. doi: 10.1128/AEM.01907-10

Church, M. J., DeLong, E. F., Ducklow, H. W., Karner, M. B., Preston, C. M., and Karl, D. M. (2003). Abundance and distribution of planktonic *Archaea* and *Bacteria* in the waters West of the Antarctic Peninsula. *Limnol. Oceanogr.* 48, 1893–1902. doi: 10.4319/lo.2003.48.5.1893

Clark, D. R., Rees, A. P., and Joint, I. (2008). Ammonium regeneration and nitrification rates in the oligotrophic Atlantic Ocean: implications for new production estimates. *Limnol. Oceanogr.* 53, 52–62. doi: 10.4319/lo.2008.53.1.0052

Cokelet, E. D., Tervalon, N., and Bellingham, J. G. (2008). Hydrography of the West spitsbergen current, svalbard branch: autumn 2001. *J. Geophys. Res.* 113, C01006. doi: 10.1029/2007JC004150

Comeau, A. M., Li, W. K. W., Tremblay, J.-É., Carmack, E. C., and Lovejoy, C. (2011). Arctic ocean microbial community structure before and after the 2007 record sea ice minimum. edited by jack anthony gilbert. *PLoS ONE* 6:e27492. doi: 10.1371/journal.pone.0027492

DeLong, E. F. (1992). *Archaea* in coastal marine environments. *Proc. Natl. Acad. Sci. U.S.A.* 89, 5685–5689. doi: 10.1073/pnas.89.12.5685

de Steur, L., Hansen, E., Mauritzen, C., Beszczynska-Möller, A., and Fahrbach, E. (2014). Impact of Recirculation on the east greenland current in fram strait: results from moored current meter measurements between 1997 and 2009. *Deep Sea Res.* 92, 26–40. doi: 10.1016/j.dsr.2014.05.018

Djurhuus, A., Boersch-Supan, P. H., Mikalsen, S.-O., and Rogers. A. D. (2017). Microbe biogeography tracks water masses in a dynamic oceanic frontal system. *Open Sci.* 4:170033. doi: 10.1098/rsos.170033.

Edgar, R. C. (2004). MUSCLE: multiple sequence alignment with high accuracy and high throughput. *Nucleic Acids Res.* 32, 1792–1797. doi: 10.1093/nar/gkh340

Edgar, R. C. (2010). Search and clustering orders of magnitude faster than BLAST. *Bioinformatics* 26, 2460–2461. doi: 10.1093/bioinformatics/btq461

Forest, A., Tremblay, J.-É., Gratton, Y., Martin, J., Gagnon, J., Darnis, G., et al. (2011). Biogenic Carbon flows through the planktonic food web of the amundsen gulf (Arctic Ocean): a synthesis of field measurements and inverse modeling analyses. *Prog. Oceanogr.* 91, 410–436. doi: 10.1016/j.pocean.2011.05.002

Francis, C. A., Roberts, K. J., Beman, J. M., Santoro, A. E., and Oakley, B. B. (2005). Ubiquity and diversity of ammonia-oxidizing *Archaea* in water columns and sediments of the Ocean. *Proc. Natl. Acad. Sci. U.S.A.* 102, 14683–14688. doi: 10.1073/pnas.0506625102

Fuhrman, J. A., and Azam, F. (1982). Thymidine incorporation as a measure of heterotrophic bacterioplankton production in marine surface waters: evaluation and field results. *Mar. Biol.* 66, 109–120. doi: 10.1007/BF00397184

Fuhrman, J. A., McCallum, K., and Davis, A. A. (1992). Novel major archaebacterial group from marine plankton. *Nature* 356, 148–149. doi: 10.1038/356148a0

Fuhrman, J. A., and Steele, J. A. (2008). Community structure of marine bacterioplankton: patterns, networks, and relationships to function. *Aq. Microb. Ecol.* 53, 69–81. doi: 10.3354/ame01222

Galand, P. E., Potvin,M., Casamayor, E. O., and Lovejoy, C. (2009). Hydrography shapes bacterial biogeography of the deep Arctic Ocean. *ISME J.* 4, 564–576. doi: 10.1038/ismej.2009.134

Grzymski, J. J, Riesenfeld, C. S., Williams, T. J., Dussaq, A. M., Ducklow, H., Erickson, M.,et al. (2012). A metagenomic assessment of winter and summer bacterioplankton from Antarctica peninsula coastal surface waters. *ISME J.* 6, 1901–1915. doi: 10.1038/ismej.2012.31

Guerrero, M. A., and Jones, R. D. (1996). Photoinhibition of marine nitrifying bacteria. I. Wavelength-dependent response. *Mar. Ecol. Prog. Ser.* 141, 183–192. doi: 10.3354/meps141183

Hallam, S. J, Mincer, T. J., Schleper, C., Preston, C. M., Roberts, K., Richardson, P. M., et al. (2006). Pathways of carbon assimilation and ammonia oxidation suggested by environmental genomic analyses of marine crenarchaeota. *PLoS Biol.* 4:e95. doi: 10.1371/journal.pbio.0040095

He, Z., Zhang, H., Gao, S., Lercher, M. J., Chen, W.-H., and Hu, S. (2016). Evolview v2: an online visualization and management tool for customized and annotated phylogenetic trees. *Nucleic Acids Res.* 44, W236–W241. doi: 10.1093/nar/gkw370

Herfort, L., Schouten, S., Abbas, B., Veldhuis, M. J. W., Coolen, M. J. L., Wuchter, C., et al. (2007). Variations in spatial and temporal distribution of archaea in the north sea in relation to environmental variables. *FEMS Microbiol. Ecol.* 62, 242–257. doi: 10.1111/j.1574-6941.2007.00397.x

Holland, M. M., Finnis, J., Serreze, M. C., Holland, M. M., Finnis, J., and Serreze, M. C. (2006). Simulated Arctic Ocean freshwater budgets in the twentieth and twenty-first centuries. *J. Clim.* 19, 6221–6242. doi: 10.1175/JCLI3967.1

Holmes, R. M. (1999). A simple and precise method for measuring ammonium in marine and freshwater ecosystems. *Can. J. Fish. Aquat. Sci.* 56, 1801–1808. doi: 10.1139/f99-128

Hong, J.-K., Cho, J.-C., Offre, P., Zumbragel, S., Haider, S., and Rychlik, N. (2015). Environmental variables shaping the ecological niche of thaumarchaeota in soil: direct and indirect causal effects. *PLoS ONE* 10:e0133763. doi: 10.1371/journal.pone.0133763

Jeffrey, W. H., Von Haven, R., Hoch, M. P., and Coffin, R. B. (1996). Bacterioplankton RNA, DNA, protein content and relationships to rates of thymidine and leucine incorporation. *Aq. Microb. Ecol.* 10, 87–95. doi: 10.3354/ame010087

Kalanetra, K. M., Bano, N., and Hollibaugh, J. T. (2009). Ammonia-Oxidizing *Archaea* in the Arctic Ocean and Antarctic coastal waters. *Environ. Microbiol.* 11, 2434–2445. doi: 10.1111/j.1462-2920.2009.01974.x

Karner, M. B., DeLong, E. F., and Karl, D. M. (2001). Archaeal dominance in the mesopelagic zone of the Pacific Ocean. *Nature* 409, 507–510. doi: 10.1038/35054051

Kirchman, D. L, Elifantz, H., Dittel, A. I., Malmstrom, R. R., and Cottrell, M. T. (2007). Standing stocks and activity of *Archaea* and bacteria in the western arctic ocean. *Limnol. Oceanogr.* 52, 495–507. doi: 10.4319/lo.2007.52.2.0495

Könneke, M., Bernhard, A. E., De La Torre, J. R., Walker, C. B., Waterbury, J. B., and Stahl, D. A. (2005). Isolation of an autotrophic ammonia-oxidizing marine Archaeon. *Nature* 437, 543–546. doi: 10.1038/nature03911

Loy, A., Lehner, A., Lee, N., Adamczyk, J., Meier, H., Ernst, J., et al. (2002). Oligonucleotide microarray for 16S rRNA gene-based detection of all recognized lineages of sulfate-reducing prokaryotes in the environment. *Appl. Environ. Microbiol.* 68, 5064–5081. doi: 10.1128/AEM.68.10.5064-5081.2002

Marie, D., Brussaard, C. P. D., Thyrhaug, R., Bratbak,G., , and Vaulot, D. (1999). Enumeration of marine viruses in culture and natural samples by flow cytometry. *Appl. Environ. Microbiol.* 65, 45–52.

Massana, R., Taylor, L. T., Murray, A. E., Wu, K. Y., Jeffrey, W. H., and DeLong, E. F. (1998). Vertical distribution and temporal variation of marine planktonic *Archaea* in the gerlache strait, Antarctica, during early spring. *Limnol. Oceanogr.* 43, 607–617. doi: 10.4319/lo.1998.43.4.0607

Merbt, S. N., Stahl, D. A., Casamayor, E. O., Martí, E., Nicol, G. W., and Prosser, J. I. (2012). Differential photoinhibition of bacterial and Archaeal ammonia oxidation. *FEMS Microbiol. Lett.* 327, 41–46. doi: 10.1111/j.1574-6968.2011.02457.x

Mincer, T. J., Church, M. J., Taylor, L. T., Preston, C., Karl, D. M., and DeLong, E. F. (2007). Quantitative distribution of presumptive archaeal and bacterial nitrifiers in monterey bay and the north pacific subtropical gyre. *Environ. Microbiol.* 9, 1162–1175. doi: 10.1111/j.1462-2920.2007.01239.x

Murray, A. E., Preston, C. M., Massana, R., Taylor, L. T., Blakis, A., Wu, K., et al. (1998). Seasonal and spatial variability of bacterial and archaeal assemblages in the coastal waters near Anvers Island, Antarctica. *Appl. Environ. Microbiol.* 64, 2585–2595.

Offre, P., Spang, A., and Schleper, C. (2013). *Archaea* in biogeochemical cycles. *Annu. Rev. Microbiol.* 67, 437–457. doi: 10.1146/annurev-micro-092412-155614

Ouverney, C. C., and Fuhrman, J. A. (2000). Marine planktonic *Archaea* take up amino acids. *Appl. Environ. Microbiol.* 66, 4829–4833. doi: 10.1128/AEM.66.11.4829-4833.2000

Paulsen, M., Doré, H., Garczarek, L., Seuthe, L., and Müller, O. (2016). Synechococcus in the Atlantic gateway to the Arctic Ocean. *Front. Mar. Sci.* 3:191. doi: 10.3389/fmars.2016.00191

Pedneault, E., Galand, P. E., Potvin, M., Tremblay, J.-É., and Lovejoy, C. (2014). Archaeal amoA and ureC genes and their transcriptional activity in the Arctic Ocean. *Sci. Rep.* 4:4661. doi: 10.1038/srep04661

Pester, M., Rattei, T., Flechl, S., Gröngröft, A., Richter, A., Overmann, J., et al. (2012). amoA-based consensus phylogeny of ammonia-oxidizing *Archaea* and deep sequencing of amoa genes from soils of four different geographic regions. *Environ. Microbiol.* 14, 525–539. doi: 10.1111/j.1462-2920.2011.02666.x

Polyakov, I. V., Beszczynska, A., Carmack, E. C., Dmitrenko, I. A., Fahrbach, E., Frolov, I. E., et al. (2005). One more step toward a warmer Arctic. *Geophys. Res. Lett.* 32:L17605. doi: 10.1029/2005GL023740

Poulin, P., and Pelletier, E. (2007). Determination of ammonium using a microplate-based fluorometric technique. *Talanta* 71, 1500–1506. doi: 10.1016/j.talanta.2006.07.024

Qin, W., Amin, S. A., Martens-Habbena, W., Walker, C. B., Urakawa, H., Devol, A. H., et al. (2014). Marine ammonia-oxidizing archaeal isolates display obligate mixotrophy and wide ecotypic variation. *Proc. Natl. Acad. Sci. U.S.A.* 111, 12504–12509. doi: 10.1073/pnas.1324115111

Quast, C., Pruesse, E., Yilmaz, P., Gerken, J., Schweer, T., Glo, F. O., et al. (2013). The SILVA Ribosomal RNA gene database project : improved data processing and web-based tools. *Nucleic Acid Res.* 41, 590–596. doi: 10.1093/nar/gks1219

Randelhoff, A., Sundfjord, A., and Reigstad, M. (2015). Seasonal variability and fluxes of nitrate in the surface waters over the Arctic shelf slope. *Geophys. Res. Lett.* 42, 3442–3449. doi: 10.1002/2015GL063655

Reinthaler, T., van Aken, H. M., and Herndl, G. J. (2010). Major contribution of autotrophy to microbial carbon cycling in the deep north Atlantic's interior. *Deep Sea Res.* 57, 1572–1580. doi: 10.1016/j.dsr2.2010.02.023

Saitou, N., and Nei, M. (1987). The neighbor-joining method: a new method for reconstructing phylogenetic trees. *Mol. Biol. Evol.* 4, 406–425.

Santoro, A. E., Casciotti, K. L., and Francis, C. A. (2010). Activity, abundance and diversity of nitrifying *Archaea* and *Bacteria* in the central California current. *Environ. Microbiol.* 12, 1989–2006. doi: 10.1111/j.1462-2920.2010.02205.x

Santoro, A. E., Francis, C. A., de Sieyes, N. R., and Boehm, A. B. (2008). Shifts in the relative abundance of ammonia-oxidizing *Bacteria* and *Archaea* across physicochemical gradients in a subterranean estuary. *Environ. Microbiol.* 10, 1068–1079. doi: 10.1111/j.1462-2920.2007.01547.x

Santoro, A. E., Saito, M. A., Goepfert, T. J., Lamborg, C. H., Dupont, C. L., and DiTullio, G. R. (2017). Thaumarchaeal ecotype distributions across the equatorial pacific Ocean and their potential roles in nitrification and sinking flux attenuation. *Limnol. Oceanogr.* 62, 1984–2003. doi: 10.1002/lno.10547

Sintes, E., Bergauer, K,., De Corte, D., Yokokawa, T., and Herndl, G. J. (2013). Archaeal *Amo* a gene diversity points to distinct biogeography of ammonia-oxidizing *Crenarchaeota* in the Ocean. *Environ. Microbiol.* 15, 1647–1658. doi: 10.1111/j.1462-2920.2012.02801.x

Sintes, E., De Corte, D., Haberleitner, E., and Herndl, G. J. (2016). Geographic distribution of archaeal ammonia oxidizing ecotypes in the Atlantic Ocean. *Front. Microbiol.* 7:77. doi: 10.3389/fmicb.2016.00077

Sintes, E., De Corte, D., Ouillon, N., and Herndl, G. J. (2015). Macroecological patterns of archaeal ammonia oxidizers in the Atlantic Ocean. *Mol. Ecol.* 24, 4931–4942. doi: 10.1111/mec.13365

Smith, J. M., Casciotti, K. L., Chavez, F. P., and Francis, C. A. (2014). Differential contributions of archaeal ammonia oxidizer ecotypes to nitrification in coastal surface waters. *ISME J.* 8, 1704–1714. doi: 10.1038/ismej.2014.11

Srivastava, D. S., and Kratina, P. (2013). Is dispersal limitation more prevalent in the ocean? *Oikos* 122, 298–300. doi: 10.1111/j.1600-0706.2012.21042.x

Swan, B. K., Martinez-Garcia, M., Preston, C. M., Sczyrba, A., Woyke, T., Lamy, D., et al. (2011). Potential for chemolithoautotrophy among ubiquitous bacteria lineages in the dark ocean. *Science* 333, 1296–1300. doi: 10.1126/science.1203690

Tolar, B. B., King, G. M., and Hollibaugh, J. T. (2013). An analysis of thaumarchaeota populations from the northern gulf of Mexico. *Front. Microbiol.* 4:72. doi: 10.3389/fmicb.2013.00072

Tolar, B. B., Powers, L. C., Miller, W. L., Wallsgrove, N. J., Popp, B. N., and Hollibaugh, J. T. (2016). Ammonia oxidation in the ocean can be inhibited by nanomolar concentrations of hydrogen peroxide. *Front. Mar. Sci.* 3:237. doi: 10.3389/fmars.2016.00237

Valentine, D. L. (2007). Adaptations to energy stress dictate the ecology and evolution of the *Archaea*. *Nat. Rev. Microbiol.* 5, 316–323. doi: 10.1038/nrmicro1619

Varela, M. M., van Aken, H. M., Sintes, E., and Herndl, G. J. (2007). Latitudinal trends of crenarchaeota and bacteria in the meso- and bathypelagic water masses of the Eastern North Atlantic. *Environ. Microbiol.* 10, 110–24. doi: 10.1111/j.1462-2920.2007.01437.x

Venter, J. C., Remington, K., Heidelberg, J. F., Halpern, A. L., Rusch, D., Eisen, J. A., et al. (2004). Environmental genome shotgun sequencing of the sargasso sea. *Science* 304, 66–74. doi: 10.1126/science.1093857

Walczowski, W., and Piechura, J. (2006). New evidence of warming propagating toward the Arctic Ocean. *Geophys. Res. Lett.* 33, L12601. doi: 10.1029/2006GL025872

Wilson, B., Müller, O., Nordmann, E.-L., Seuthe, L., Bratbak, G., and Øvreås, L. (2017). Changes in marine prokaryote composition with season and depth over an arctic polar year. *Front. Mar. Sci.* 4:95. doi: 10.3389/fmars.2017.00095

Woodward, E. M. S., and Rees, A. P. (2001). Nutrient distributions in an anticyclonic eddy in the Northeast Atlantic Ocean, with reference to nanomolar ammonium concentrations. *Deep Sea Res. Part II. Topical Stud. Oceanogr.* 48, 775–793. doi: 10.1016/S0967-0645(00)00097-7

Wright, J. J. (2013). *Microbial Community Structure and Ecology of Marine Group A Bacteria in the Oxygen Minimum Zone of the Northeast Subarctic Pacific Ocean, January*. Vancouver, BC: University of British Columbia.

Wuchter, C., Abbas, B., Coolen, M. J. L., Herfort, L., van Bleijswijk, J., Timmers, P., et al. (2006). Archaeal nitrification in the ocean. *Proc. Natl. Acad. Sci. U.S.A.* 103, 12317–12322. doi: 10.1073/pnas.0600756103

Conflict of Interest Statement: The authors declare that the research was conducted in the absence of any commercial or financial relationships that could be construed as a potential conflict of interest.

Graphic design: Communication Division, UiB / Print: Skipnes Kommunikasjon AS

uib.no

ISBN: 978-82-308-3711-5